MESENCHYMAL STEM CELLS AS VECTORS FOR ANTI-TUMOUR THERAPY

Michael Richard Loebinger

A thesis submitted to UCL for the degree of Doctor of Philosophy

DECLARATION

I, Michael Richard Loebinger, confirm that the work presented in this thesis is my own. Where information has been derived from other sources, I confirm that this has been indicated in the thesis.

ABSTRACT

Cancer is a leading cause of mortality throughout the world and new treatments are urgently needed. Recent studies suggest that bone marrow-derived mesenchymal stem cells (MSCs) home to and incorporate within tumour tissue. This property can be utilised to deliver targeted anticancer therapies. This thesis describes the production of MSCs engineered to express TNF-related apoptosis-inducing ligand (TRAIL), a transmembrane protein that causes selective apoptosis of tumour cells.

Human MSCs were transduced with TRAIL and the IRES-GFP reporter gene using a lentiviral vector, under the control of a tetracycline promoter. Transduced and activated MSCs caused lung, breast, squamous, and cervical cancer cell apoptosis in vitro. In vivo, the cells were able to specifically home to tumours and both significantly reduce tumour growth, and eliminate metastatic disease.

The data included in this thesis demonstrates for the first time a significant reduction in metastatic tumour burden with frequent eradication of metastases using inducible TRAIL-expressing MSCs. This has a wide potential therapeutic role, which includes the treatment of both primary tumours and their metastases, possibly as an adjuvant therapy in clearing micrometastatic disease following primary tumour resection.

ACKNOWLEDGEMENTS

I would like to thank the Medical Research Council (UK) for funding this project through a clinical training fellowship.

In addition, there are many people that helped significantly during the course of this project. Firstly, I would like to thank my supervisor, Sam Janes. He has been a source of inspiration throughout the project. I was his first PhD student, and could not think of a better, more approachable supervisor. His calmness in the face of adversity has been a lesson in life as well as research.

Professor Geoff Laurent, my second supervisor, and the Director of the Centre for Respiratory Research (CRR), has been a constant source of encouragement throughout the project, and was instrumental in making me feel an important part of the laboratory. I would also like to thank Professor Rachel Chambers, who has strongly supported me throughout.

Everybody in the CRR has made this experience extremely enjoyable. I would particularly like to thank Danielle, Iona, Livia, Nicola, and Sylwia for their support and friendship, and for listening to my moans and worries.

At Cancer Research UK, London Research Institute, I would like to thank Susana, in addition to Derek, Ayad and the rest of the flow cytometry laboratory.

As always, my parents and sister have supported me unconditionally throughout.

Finally, I would like to acknowledge my beautiful wife and son. Sarah and Ben are my life, and this thesis is dedicated to them both.

TABLE OF CONTENTS

TITLE PAGE 1
DECLARATION 2
ABSTRACT 3
ACKNOWLEDGEMENTS 4
TABLE OF CONTENTS 5
LIST OF FIGURES 11
LIST OF TABLES 14
LIST OF ABBREVIATIONS 15

CHAPTER 1. INTRODUCTION 19

1.1 BACKGROUND 19
1.2 APOPTOSIS 19
1.3 TRAIL 22
1.3.1 Cellular Effects of TRAIL 24
1.3.2 Tumour sensitivity 27
1.3.3 Physiological functions of TRAIL 29
1.3.4 Uses of TRAIL as an antitumour therapy 31
1.3.4.1 In vitro studies 31
1.3.4.2 In vivo studies 32
1.3.4.3 Combinations of TRAIL with other agents 34
1.3.4.4 Translational studies 35
1.3.5 The need for a better TRAIL vector 36
1.4 STEM CELLS 37
1.4.1 Contribution of bone marrow stem cells to extracellular matrix 39
1.4.1.1 Tissue stroma 39
1.4.1.2 Tumour stroma 40
1.5 MESENCHYMAL STEM CELLS 43
1.5.1 Homing mediators 43
1.5.2 Use of MSCs as delivery vectors 47
1.5.2.1 Cancer 47

1.5.2.2 Non-cancer 48
1.5.3 Effects of MSCs themselves *50*
1.5.3.1 Non-cancer 50
1.5.3.2 Cancer 52
1.6 THE COMBINATION OF TRAIL AND MSCS 54
1.7 SUMMARY 55
1.8 HYPOTHESIS 55
1.9 AIMS 56
CHAPTER 2. MATERIALS AND METHODS 57
2.1 GENERAL CHEMICALS, SOLVENTS AND PLASTIC WARE 57
2.2 CELL CULTURE 57
2.3 MESENCHYMAL STEM CELLS 58
2.3.1 Differentiation *58*
2.3.2 Colony forming ability *59*
2.4 SIDE POPULATION CELLS 59
2.4.1 Side population identification and sorting *59*
2.4.2 Colony-forming assays *60*
2.5 PRODUCTION OF PLASMID CONSTRUCTS 61
2.5.1 Production of TRAIL DNA for plasmid *61*
2.5.1.1 PCR conditions 62
2.5.2 Production of lentiviral backbone for plasmid *65*
2.5.2.1 Restriction enzyme digestion 68
2.5.3 Production of the flTRAIL, sTRAIL, and empty Tet-inducible plasmid. *69*
2.6 PLASMID INTRODUCTION INTO CELLS 73
2.6.1 Transient transfection *73*
2.6.2 Stable transduction *74*
2.6.2.1 Production of lentivirus 74
2.6.2.2 Titration of lentivirus 75
2.6.2.3 Stable transduction of MSCs 75
2.7 IN VITRO TRAIL TRANSGENE EXPRESSION 76
2.7.1 Antibodies *76*
2.7.2 Flow cytometry *76*
2.7.3 Western blots *77*

2.7.3.1 Sample collection and preparation 77
2.7.3.2 BCA protein assay 77
2.7.3.3 Western blotting procedures 78
2.7.4 ELISA assay *79*
2.8 IN VITRO TRAIL TRANSGENE FUNCTIONAL ASSESSMENT 79
2.8.1 Agonists and antibodies *79*
2.8.2 Coculture experiments *79*
2.8.2.1 Apoptosis assessment 80
2.8.2.2 Production of dominant negative FADD cancer cells 81
2.8.3 Colony forming ability in coculture *82*
2.9 IN VITRO ASSESSMENT OF MSC HOMING TO TUMOURS 82
2.9.1 Antagonists *82*
2.9.2 Cell migration assay *82*
2.9.3 Human cytokine array kit *83*
2.10 IN VIVO MODELS 84
2.10.1 Animals *84*
2.10.2 Models *84*
2.10.2.1 Subcutaneous model 84
2.10.2.2 Lung cancer model 85
2.10.2.3 Metastatic model 85
2.10.3 Use of TRAIL-transduced MSCs *85*
2.11 TISSUE PREPARATION 86
2.11.1 Histological processing *86*
2.11.2 Preparation of ex-vivo tumour cells *86*
2.11.3 Tissue homogenisation *87*
2.12 IMMUNOHISTOCHEMISTRY 87
2.12.1 Antibodies *87*
2.12.2 Immunoperoxidase technique *87*
2.12.3 Immunofluorescence *88*
2.12.4 TUNEL staining *89*
2.13 REAL-TIME RT-PCR ANALYSIS 89
2.13.1 RNA extraction *90*
2.13.2 cDNA synthesis *91*
2.13.3 Primer design *91*

2.13.4 Real time RTPCR *92*
2.14 METASTASES QUANTIFICATION 94
2.15 STATISTICS 94

CHAPTER 3. RESULTS I - MSCS ENGINEERED TO EXPRESS INDUCIBLE TRAIL 95

3.1 MESENCHYMAL STEM CELL PROPERTIES 96
3.2 EXPRESSION OF TRAIL IN TRANSDUCED CELLS 97
3.2.1 Transient transfection *97*
3.2.2 Stable transduction *99*
3.2.2.1 Full length, membrane-bound TRAIL 100
3.2.2.2 Soluble TRAIL 103
3.2.3 Control of TRAIL expression with doxycycline *106*
3.3 FUNCTION OF TRAIL IN TRANSDUCED CELLS 108
3.3.1 Coculture experiments *108*
3.3.2 Specific death of cancer cells *111*
3.3.3 Dose dependent effect *112*
3.3.4 Mechanism of MSCFLT-induced cancer cell death *112*
3.3.4.1 Death of cancer cells by TRAIL expression 112
3.3.4.2 Death of cancer cells by extrinsic apoptosis pathway 113
3.4 SUMMARY 115

CHAPTER 4. RESULTS II – HOMING OF MSCS TO CANCER 116

4.1 CANCER MODELS 117
4.1.1 Nude mice *117*
4.1.2 NOD/SCID mice *118*
4.2 MSC MIGRATION TO TUMOURS 120
4.2.1 In vitro *120*
4.2.2 In vivo *122*
4.2.2.1 Coinjection 122
4.2.2.2 Systemic introduction 123
4.2.3 Tumour cell lines produce multiple cytokines and chemokines *126*
4.2.4 Ex-vivo tumours produce multiple cytokines and chemokines *126*
4.2.5 In vitro cytokine neutralisation *128*

4.2.6 Future migration work *131*
4.3 SUMMARY 132

CHAPTER 5. RESULTS III – IN VIVO TUMOUR EFFECTS OF TRAIL-EXPRESSING MSCS 133

5.1 SUBCUTANEOUS TUMOUR MODEL 134
5.1.1 Coinjection *134*
5.1.2 Intratumour Delivery *138*
5.1.3 Systemic Delivery *138*
5.2 METASTATIC TUMOUR MODEL 141
5.2.1 Systemic Delivery *141*
5.2.2 Early, prophylactic delivery *143*
5.3 PHYSIOLOGICAL METASTATIC TUMOUR MODEL 145
5.4 SUMMARY 148

CHAPTER 6. RESULTS IV – CANCER STEM CELLS AND THE SIDE POPULATION 149

6.1 INTRODUCTION 149
6.1.1 Cancer Stem Cells *149*
6.1.2 Side Population *149*
6.2 RESULTS 151
6.2.1 Squamous and lung cancer cell lines contain an ABC transporter side population *151*
6.2.2 The SP cells exhibit stem-like characteristics in vitro *153*
6.2.3 The SP cells exhibit stem-like characteristics in vivo *153*
6.2.4 The SP cells are chemoresistant *154*
6.2.5 The SP cells can be killed by TRAIL-expressing MSCs *156*
6.2.6 The addition of TRAIL-expressing MSCs to mitoxantrone treatment causes additional cancer cell killing *160*
6.3 DISCUSSION 161
6.4 SUMMARY 163

CHAPTER 7. DISCUSSION 164

7.1 OVERVIEW 164
7.2 MESENCHYMAL STEM CELLS 165

7.3 VIRAL TRANSDUCTION 166
7.4 TRAIL TRANSGENE 168
7.4.1 Tetracycline inducible 169
7.5 IN VITRO CELL DEATH 170
7.6 MIGRATION 172
7.7 IN VIVO MODELS 174
7.8 TRANSLATION 177

CHAPTER 8. SUMMARY AND FUTURE DIRECTIONS 180

CHAPTER 9. REFERENCES 183

PUBLICATIONS RELATED TO THESIS 220
AWARDS RELATED TO THESIS 221
APPENDIX. COPIES OF 1ST AUTHOR ORIGINAL PAPERS 222

LIST OF FIGURES

Figure 1.1 The extrinsic and intrinsic apoptosis pathways. 20

Figure 1.2 The TRAIL receptors..... 24

Figure 1.3 The cellular effects of TRAIL 26

Figure 1.4 Cancer cells are specifically sensitive to TRAIL-induced apoptosis. 29

Figure 1.5 MSCs migrate towards tumours 49

Figure 2.1 The sequence of full length TRAIL containing the restriction enzymes Mlu1 and BstB1 64

Figure 2.2 Production of plasmid constructs. 67

Figure 2.3 Xba1 digestion distinguishes the TRAIL lentivirus plasmid from the intermediate DKK lentivirus plasmid. 71

Figure 3.1 Characterisation of MSCs. 96

Figure 3.2 Transient transfection of 293T cells 98

Figure 3.3 Transiently transduced 293T cells produce TRAIL. 99

Figure 3.4 Full length TRAIL lentivirus titrated with 293T cells. 101

Figure 3.5 Hela cells are killed by transduction with the full length TRAIL lentivirus and activation with doxycycline. 102

Figure 3.6 MSCs transduced with full length TRAIL lentivirus express GFP and TRAIL under doxycycline control. 104

Figure 3.7 293T and Hela cells transduced with soluble TRAIL lentivirus express GFP but are not killed. 105

Figure 3.8 Timescale of full length TRAIL transgene activation with doxycycline. 107

Figure 3.9 TRAIL-expressing MSCs cause cancer cell apoptosis in vitro. 109

Figure 3.10 The supernatant of TRAIL-expressing MSCs contains functional TRAIL. 110

Figure 3.11 The cancer cells are specifically killed in coculture with TRAIL-expressing MSCs..... 111

Figure 3.12 TRAIL-expressing MSCs induce cancer cell apoptosis at low MSC to cancer cell ratios via the extrinsic apoptotic pathway..... 114

Figure 4.1 Tumour models. 119

Figure 4.2 MSCs migrate to some cancer cells in vitro and transduction does not affect this migration 121

Figure 4.3 Incorporation of MSCs into subcutaneous tumours when directly injected. 122

Figure 4.4 MSCs migrate to metastases in vivo..... 124

Figure 4.5 MSCs migrate to subcutaneous tumours, and have negligible incorporation into normal organs 125

Figure 4.6 Cancer cells produce multiple cytokines and chemokines in vitro and in vivo..... 129

Figure 4.7 MSC migration to cancer cells is not reduced by IL-6 or IL-8 inhibitors. 130

Figure 5.1 TRAIL-expressing MSCs reduce the growth of subcutaneous tumours. 136

Figure 5.2 TRAIL-expressing MSCs reduce the growth of subcutaneous tumours. 137

Figure 5.3 Intratumour delivery of TRAIL-expressing MSCs does not reduce the growth of established subcutaneous tumours. 139

Figure 5.4 Systemic delivery of TRAIL-expressing MSCs does not reduce the growth of subcutaneous tumours. 140

Figure 5.5 TRAIL-expressing MSCs reduce the growth of lung metastases. 142

Figure 5.6 TRAIL and GFP can be detected in the lung metastases following intravenous delivery of TRAIL-expressing MSCs. 144

Figure 5.7 Early systemic delivery of TRAIL-expressing MSCs does not prevent the development of metastases. 146

Figure 5.8 TRAIL-expressing MSCs reduce the growth of physiological lung metastases. 147

Figure 6.1 Squamous cancer and lung cancer cell lines contain a side population. 152

Figure 6.2 The SP cells are tumorigenic in vivo. 154

Figure 6.3 The SP cells have an increased resistance to mitoxantrone. 155

Figure 6.4 TRAIL-expressing MSCs lead to death and apoptosis of H357 SP and non-SP cells. 157

Figure 6.5 TRAIL-expressing MSCs lead to death and apoptosis of A549 SP and non-SP cells. 158

Figure 6.6 TRAIL-expressing MSCs reduce the clonigenic potential of H357 SP and non-SP cells. 159

Figure 6.7 TRAIL-expressing MSCs produce additional SP cancer cell killing to mitoxantrone treatment. 160

LIST OF TABLES

Table 1.1 Definitions of cell types 40

Table 2.1 Primers used to flank full length (fl) and soluble (s) TRAIL with Mlu1 and BstB1 restriction enzymes. 63

Table 2.2 Primers used to flank DKK with Sal1 and BamH1 restriction enzymes to allow entry into the pENTR1A plasmid adjacent to IRES-GFP 65

Table 2.3 Primers used to flank DKK-IRES-GFP with Mlu1 and EcoRV restriction enzymes to allow entry into the Tet-inducible lentiviral plasmid. 66

Table 2.4 Primers used to flank IRES-GFP with Mlu1 and EcoRV restriction enzymes to allow entry into the Tet-inducible lentiviral plasmid. 72

Table 2.5 Primers used for real time RTPCR of TRAIL and the housekeeping gene 18S. 92

LIST OF ABBREVIATIONS

ABC	ATP binding cassette
AP	ammonium persulphate
APAF	apoptotic protease-activating factor
ATP	adenosine triphosphate
BCA	bicinchoninic acid
bFGF	basic fibroblast growth factor
BMSC	bone marrow-derived stem cell
BSA	bovine serum albumin
cDNA	complementary DNA
cFLIP	cellular FLICE-like inhibitory protein
CNTF	ciliary neurotrophic factor
CR	complete response
CRAd	conditional replicative adenovirus
DAB	3,3-diaminobenzidine
DAPI	4,6-diamidino-2-phenylindole
DcR	decoy receptor
dH_2O	distilled and deionised water
DIABLO	direct IAP binding protein with low PI
DiI	1,1-dioctadecyl-3,3,3,3-tetramethylindocarbocyanine perchlorate
DISC	death inducing signalling complex
DKK	dickkopf
DMEM	Dulbecco's modified Eagle's medium
DMSO	dimethyl sulfoxide
DNA	deoxyribonucleic acid
DNase	deoxyribonucleic acid endonuclease
dNTP	deoxynucleotide triphosphate
dox	doxycycline
DR	death receptor
ECL	enhanced chemiluminescence
EDTA	ethyldiaminotetraacetic acid

EGF	epidermal growth factor
ELISA	enzyme-linked immunosorbent assay
EMT	epithelial to mesenchymal transition
FVIII	factor VIII
g	G-force
GFP	green fluorescent protein
GvHD	graft versus host disease
ERK	extracellular signal-regulated kinase
FACS	fluorescence activated cell sorting
(dn)FADD	(dominant negative) fas associated death domain
FAK	focal adhesion kinase
Fas-L	fas-ligand
FBS	fetal bovine serum
flTRAIL	full length TRAIL
GM-CSF	granulocyte macrophage colony-stimulating factor
H&E	haematoxylin and eosin
HDAC	histone deacetylase
HLA	human leukocyte antigen
HRP	horseradish peroxidase
HSC	haematopoietic stem cell
IAP	inhibitor of apoptosis
ICAM	intercellular adhesion molecule
IFN	interferon
IGF	insulin-like growth factor
IκB	inhibitor of NFκB
IKK	IκB kinase
IL	interleukin
IP_3	inositol 1-, 4-, 5-, triphosphate
IRES	internal ribosome entry site
JNK	Jun N-terminal kinase
kDa	kilo Dalton
KS	Kaposi's sarcoma
LB	Luria-Bertani

LTR	long terminal repeat
MAPK	mitogen-activated protein kinase
MHC	major histocompatibility complex
MIF	macrophage migration inhibitory factor
MMP	matrix metalloproteinase
MOI	multiplicity of infection
MSC	mesenchymal stem cell
MSCFLT	mesenchymal stem cell transduced with the flTRAIL transgene
mRNA	messenger RNA
nd	no doxycycline
NEMO	NFkB essential modulator
NFkB	nuclear factor kB
NHL	non-Hodgkin's lymphoma
NK	natural killer
NOD/SCID	non-obese diabetic/severe combined immunodeficiency
NSCLC	non-small cell lung cancer
OPG	osteoprotegerin
PBS	phosphate-buffered saline
PCR	polymerase chain reaction
PDGF	platelet-derived growth factor
PECAM	platelet/endothelial adhesion molecule
PEI	polyethylenimine
PFA	paraformaldehyde
PI	propidium iodide
PI3K	phosphatidylinositol 3-kinase
PR	partial response
RANK	receptor activator of nuclear κB
RIP	receptor interacting protein
RNA	ribonucleic acid
RNase	ribonucleic acid endonuclease
rRNA	ribosomal RNA
RTPCR	reverse transcriptase PCR
SD	stable disease

SDF1α	stromal derived factor 1α (aka CXCL12)
SDS	sodium dodecyl sulphate
SMAC	second mitochondrial activator of caspases
SP	side population
STAT	signal transducer and activator of transcription
sTRAIL	soluble TRAIL
TBS	Tris-buffered saline
TBST	TBS/Tween
TE	Tris-EDTA buffer
TEMED	tetramethylethylenediamine
TGF	transforming growth factor
TIMP	tissue inhibitor of MMPs
TNF	tumour necrosis factor
TRADD	FADD/TNF receptor associated death domain
TRAF	FADD/TNF receptor associated factor
TRAIL	TNF-related apoptosis-inducing ligand
TUNEL	TdT-mediated dUTP-X nick end labelling
VCAM	vascular cell adhesion molecule
VEGF	vascular endothelial growth factor
VLA	very late antigen
VSV-G	vesicular stomatitis G protein
zVAD	zVADfmk

CHAPTER 1. INTRODUCTION

1.1 Background

Cancer remains one of the leading causes of mortality and morbidity throughout the world (Jemal et al., 2007). Present therapy focuses on the combination of surgery, chemotherapy and radiation treatment. Despite healthcare improvements and treatment advances, many tumours are unresponsive to conventional therapy and a new modality of treatment is urgently needed.

Cancer cells acquire the ability for unlimited cell proliferation, with self-sufficiency of growth signals and insensitivity to anti-growth signals. They also gain angiogenic, metastatic and invasion abilities and are able to successfully avoid apoptosis (Hanahan & Weinberg, 2000). These hallmarks of cancer cells, which set them apart from normal human cells, must be reversed for successful treatment of many cancers.

1.2 Apoptosis

Apoptosis is the process of programmed cell death. It is a tightly regulated process important both in normal development and cell homeostasis in addition to the removal of damaged cells. Apoptosis is achieved by activation of either the intrinsic or extrinsic apoptotic pathway (Figure 1.1). Both pathways lead to the activation of a number of caspases. The caspases are cysteine-aspartate-proteases that are synthesized as inactive precursors. The initiator caspases (2,8,9) are activated by proximity-induced dimerisation, and they are then able to activate the effector caspases (3,6,7) by proteolytic cleavage. These effector caspases cleave DNA and intracellular structures, leading to successful apoptosis characterised by condensation of chromatin, fragmentation of DNA, and cell shrinkage (Motadi et al., 2007).

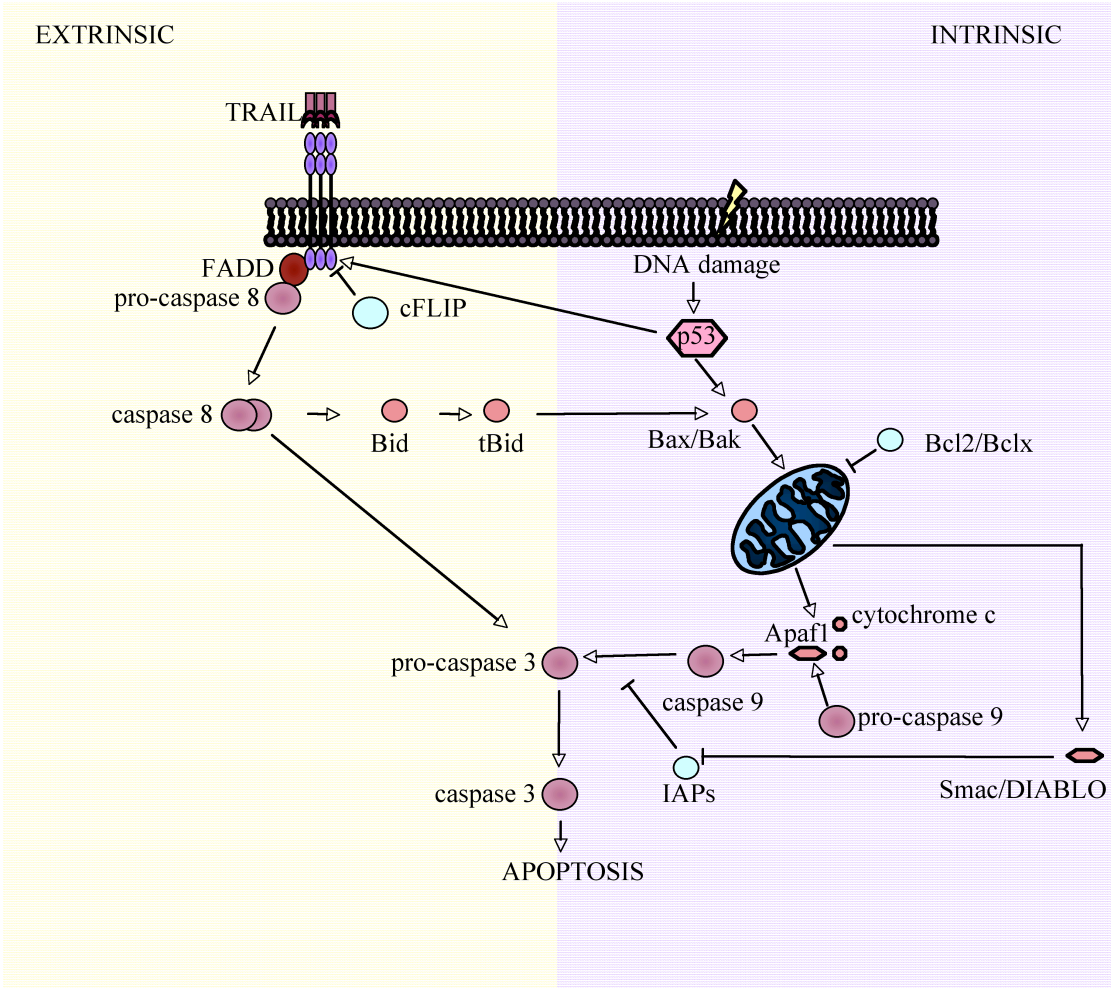

Figure 1.1 The extrinsic and intrinsic apoptosis pathways.
The extrinsic apoptosis pathway is instigated by the binding of a death ligand to a specific receptor. This leads to recruitment of Fas associated death domain (FADD) and caspase 8 and a resulting caspase cascade. Traditional cancer therapeutics work via the intrinsic apoptosis pathway, which centres on DNA damage, the activation of the proapoptotic members of the Bcl-2 family, Bax and Bak, and the release of cytochrome c from the mitochodria. Cytochrome c forms an apoptosome with caspase 9 and apoptotic protease-activating factor 1 (Apaf 1), leading to activation of the effector caspases and apoptosis. The pathways are interlinked as demonstrated and are heavily regulated with multiple activators (represented by arrows) including Smac/DIABLO and inhibitors (represented by headless arrows) such as inhibitors of apoptosis (IAPs), and cellular FLICE-like inhibitory protein (cFLIP).

One of the main aims of cancer therapy is to cause increased apoptosis of the transformed cells. Most chemotherapeutic agents and radiotherapy treatments attempt to produce apoptosis of cancer cells by causing DNA damage and the activation of the intrinsic apoptotic pathway. This mechanism is reliant on the function of the p53 tumour suppressor gene, which causes the activation of the Bcl-2 family member Bax, causing mitochondrial instability and release of cytochrome c into the cytosol (Levine, 1997). This then forms a complex with apoptotic protease-activating factor 1 (Apaf 1), ATP and procaspase 9 to form an apoptosome, leading to caspase 9 activation, and in turn the activation of the effector caspases. The mitochondria also release second mitochondrial activator of caspases/direct IAP binding protein with low PI (Smac/DIABLO), which are also proapoptotic, neutralising the caspase-inhibiting activity of the inhibitor of apoptosis proteins (IAPs). However, the majority of human tumours acquire mutations of p53, leading to the development of resistance to the intrinsic apoptosis pathway and conventional oncological therapies (Ashkenazi et al., 1999).

Death inducing ligands are able to cause apoptosis of cells by an independent mechanism, activating the extrinsic apoptotic pathway, and are thus attractive as anti-tumour agents. The death ligands are members of the tumour necrosis factor (TNF) superfamily. These include TNF, Fas-ligand (Fas-L), and Tumour necrosis factor related apoptosis inducing ligand (TRAIL). On binding the corresponding death ligand, the receptors trimerise and form death inducing signalling complexes (DISC) with Fas-associated death domain (FADD) and the initiator caspases 8 and 10. The initiator caspases are activated, leading to activation of the effector caspases (3,6,7) and the cleavage of a large number of cellular targets and apoptosis. Activation of the initiator caspases at the DISC can be inhibited by the cellular FLICE-like inhibitory protein (cFLIP), which has homology to caspase 8 and prevents its activation.

There is some crosstalk between the extrinsic and intrinsic pathways by death ligand-induced activation of Bid, another Bcl family member. Bid is cleaved by caspase 8 and translocates to the mitochondria, interacting with the proapoptotic Bcl proteins, Bax and Bak, to cause outer mitochondrial membrane pores and release cytochrome c causing apoptosis via the intrinsic pathway. In some cells (Type II), this cross-talk

and concurrent activation of the intrinsic pathway is necessary for death ligand-induced apoptosis. However activation of only the extrinsic pathway is sufficient in other cells (Type I), which are thought to produce larger amounts of activated caspase 8 in the DISC (Ozoren & El-Deiry, 2002; Scaffidi et al., 1998). Conversely, the activation of the intrinsic death pathway has also been shown to lead to a sensitisation of cells to death ligands. Specifically, chemotherapeutic drugs, and irradiation have been shown to cause an upregulation of TRAIL receptors via p53 dependent (Burns et al., 2001; Nimmanapalli et al., 2001; Wen et al., 2000; Wu et al., 2003b) and independent mechanisms (Wen et al., 2000).

Within the TNF family of death ligands, the expression of TNF and Fas-L ligands are extremely tightly controlled, being transiently expressed on some activated cells, and these molecules have been shown to damage normal tissues in addition to their proapoptotic effect on transformed cells (Ashkenazi & Dixit, 1998). This translates to the limited clinical use of overexpression of these ligands in cancer therapy. TNF has many actions in addition to the induction of apoptosis. It primarily activates the proinflammatory and prosurvival nuclear factor κB (NFκB), and this action causes a large inflammatory response and hypotension if TNF is used clinically. Fas–L also has limited clinical use as it causes apoptosis in hepatocytes (Ashkenazi et al., 1999; Ogasawara et al., 1993). Conversely, TRAIL is able to selectively induce apoptosis in transformed cells, but not in most normal cells (Ashkenazi et al., 1999; Walczak et al., 1999; Wiley et al., 1995), making it a promising candidate for tumour therapy.

1.3 TRAIL

TRAIL was originally described in 1995 having been cloned based on its homology to other members of the TNF family (Pitti et al., 1996; Wiley et al., 1995). TRAIL is a type 2 transmembrane protein, which can be proteolytically cleaved from the membrane to produce a soluble molecule. This novel ligand was found to cause apoptosis on binding to specific receptors in a similar way to TNF and Fas-L.

To date, five receptors have been described for TRAIL (Figure 1.2). Two of these receptors are found on the cell surface and contain active cytoplasmic death domains, leading to apoptosis on binding by the ligand; death receptor 4 (DR4) and death receptor 5 (DR5). These receptors are type 1 transmembrane proteins consisting of cysteine rich domains. DR5 has 58% overall homology to DR4, with particular similarity in the intracellular death domain region. They are expressed on activated lymphocytes, in addition to a wide range of tissues (Kimberley & Screaton, 2004). Two further receptors are also located on the cell surface, but are unable to form cytoplasmic death domains; decoy receptor 1 (DcR1) and decoy receptor 2 (DcR2). DcR1 lacks an intracellular region and is attached to the cell membrane by a glycophospholipid. It is expressed on peripheral blood lymphocytes, but is generally expressed much less widely than the other TRAIL receptors (Kimberley & Screaton, 2004). DcR2 has a shortened and inactive cytosolic portion but 58-70% homology with the other TRAIL receptors. It is also widely expressed (Kimberley & Screaton, 2004). The fifth receptor, osteoprotegerin (OPG), is a soluble receptor of the TNF receptor family. It is heavily glycosylated and exists primarily as a disulphide linked dimer. The importance of osteoprotegerin as a decoy receptor in TRAIL has not been fully established. Osteoprotegerin is primarily involved in the regulation of bone turnover and particularly the maturation and activity of osteoclasts by binding to the receptor activator of nuclear kappa beta ligand (RANKL) inhibiting its ability to bind to the RANK receptor and stimulate osteoclastogenesis (Holen & Shipman, 2006). Furthermore, studies have demonstrated a poor binding of TRAIL to OPG at body temperatures (Truneh et al., 2000). In the mouse only one death-inducing receptor with homology to DR5 has been discovered, in addition to two decoy receptors (mDcTrailr1, msDcTrailr2) (Lawrence et al., 2001).

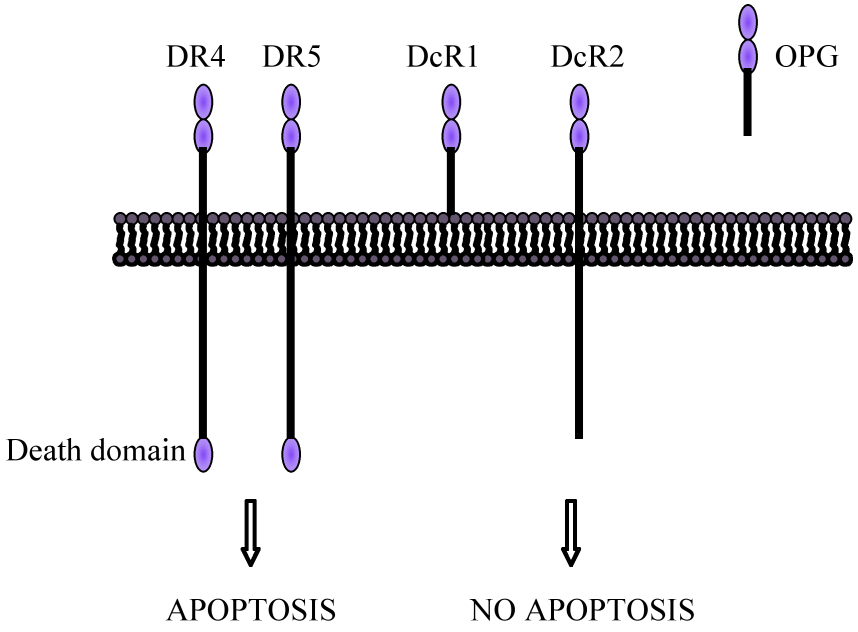

Figure 1.2 The TRAIL receptors
TRAIL has 5 receptors. DR4 and DR5 contain active cytoplasmic death domains, leading to apoptosis. The decoy receptors DcR1 and DcR2 lack active death domains; DcR1 lacks an intracellular region and is attached to the cell membrane by a glycophospholipid, DcR2 has a shortened and inactive cytosolic portion. Osteoprotegerin (OPG) is a soluble receptor, its role as a decoy receptor in TRAIL has not been fully established.

1.3.1 Cellular Effects of TRAIL

The primary cellular effect of TRAIL is the initiation of apoptosis. Apoptosis is signalled after TRAIL binds as a homotrimer to DR4 or DR5. This results in trimerisation of the receptors and activation of the extrinsic apoptosis pathway, as described above.

In addition to apoptosis, TRAIL has also been shown to act via other signalling pathways including NFκB, mitogen activated protein kinases (MAPKs), phosphoinositide 3-kinase (PIK3) and Akt (Figure 1.3). This stimulation is much less potent and rapid than with TNF (Varfolomeev et al., 2005). The molecular

determinants of the activation of these kinases have been investigated with co-immunoprecipitation experiments. These have suggested the involvement of complexes of secondary signalling molecules in addition to the formation of the apoptosis-inducing DISC (Varfolomeev et al., 2005). Suggested components of these secondary signalling complexes include receptor interacting protein 1 (RIP1), TNF receptor associated factor 2 (TRAF2), NFκB essential modulator/IκB kinase γ (NEMO/IKKγ), FADD/TNF receptor associated death domain (TRADD), and caspase 8. RIP1 and TRAF2 are thought to lead to JUN N-terminal kinase (JNK) activation and the expression of cell proliferation genes, whereas NFκB activation is stimulated by the recruitment of NEMO and IκB kinase α/β (IKK α/β), which phosphorylate inhibitors of κB (IκB), leading to IκB degradation and NFκB activation (Falschlehner et al., 2007). However, the mechanisms underlying kinase pathway stimulation by TRAIL remain poorly understood, with studies demonstrating both a caspase-dependent (Varfolomeev et al., 2005) and a caspase-independent (Ehrhardt et al., 2003) mechanism. In addition, the exact role and importance of TRAIL activation of these kinase pathways is uncertain. Many studies suggest a predominantly anti-apoptotic or proliferative effect (Ehrhardt et al., 2003; Romagnoli et al., 2007; Weldon et al., 2004), and it has been demonstrated that inhibition of the NFκB (Romagnoli et al., 2007), and p38 MAPK (Weldon et al., 2004) signalling pathways can lead to sensitisation of cancer cells to TRAIL-induced apoptosis. The importance of these kinase signalling pathways may be increased in apoptosis resistant cells, where TRAIL has been shown to lead to an NFκB-mediated increase in proliferation and invasion of tumours in vitro (Ehrhardt et al., 2003; Ishimura et al., 2006). In addition, some studies have demonstrated the activation of NFκB by the decoy receptor DcR2 (Degli-Esposti et al., 1997a), but this was not a universal finding (Meng et al., 2000).

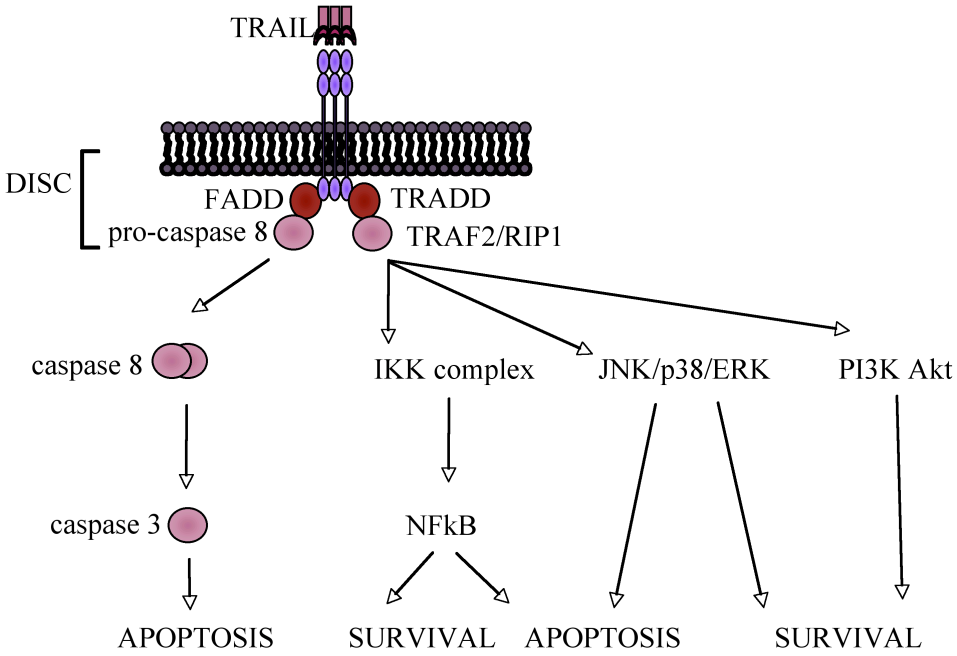

Figure 1.3 The cellular effects of TRAIL
The predominant effect of TRAIL receptor activation is apoptosis via the extrinsic apoptotic pathway. TRAIL has also been shown to activate additional signalling pathways such as nuclear factor κB (NFκB), mitogen activated protein kinases (MAPKs); extracellular signal-regulated kinase (ERK), JUN N-terminal kinase (JNK), and p38 and phosphoinositide 3-kinase (PIK3) and Akt. The signalling events downstream of receptor activation have not been determined but are thought to involve molecules such as receptor interacting protein 1 (RIP1), TNF receptor associated factor 2 (TRAF2), NFκB essential modulator/IκB kinase γ (NEMO/IKKγ), and FADD/TNF receptor associated death domain (TRADD). The functional significance of these pathways is also unknown with studies demonstrating both a prosurvival and apoptotic effect.

However, these signalling pathways are complex, and, depending on the subunit composition of NFκB, either a proapoptotic or antiapoptotic outcome may result (Johnstone et al., 2008). Similarly, activation of extracellular signal-regulated kinase (ERK) (Frese et al., 2003), JNK (Sah et al., 2003), and p38 (Ohtsuka et al., 2003) have also been shown to sensitise cancer cells to TRAIL-mediated apoptosis, and other groups have suggested a supporting role of these kinase pathways in apoptosis with the increase of cytokines interleukin-8 (IL-8) and CCL2 leading to macrophage attraction and the engulfment of apoptotic cells (Varfolomeev et al., 2005). At present, the studies investigating the role and importance of these kinase signalling pathways are rather contradictory, and the effects may be cell-specific.

1.3.2 Tumour sensitivity

TRAIL appears to be able to induce apoptosis selectively in tumour cells, sparing normal cells. The mechanism underlying this selectivity is not fully understood, although it is likely to be multifactorial (Figure 1.4). The presence of decoy receptors was initially thought to explain the difference in sensitivity between tumour cells and normal cells to TRAIL-induced apoptosis. The decoy receptors have been shown to afford some protection to cells against the activities of TRAIL. Transient transfection experiments using DcR1 and DcR2 have demonstrated its ability to inhibit TRAIL-induced apoptosis (Degli-Esposti et al., 1997a; Degli-Esposti et al., 1997b). The mechanism of this effect has yet to be fully elucidated with suggested theories including simple competitive inhibition and the formation of ineffective mixed receptor complexes (Kimberley & Screaton, 2004). Interestingly, DcR2 receptors lacking their intracellular domain do not protect cells from apoptosis suggesting that some intracellular mechanism is necessary for the decoy effect (Meng et al., 2000). Despite the initial hypothesis that TRAIL sensitivity of a cell was directly related to its balance of TRAIL receptors and TRAIL decoy receptors, most studies have failed to show a correlation between the expression of these receptors and susceptibility to TRAIL-induced apoptosis (Kimberley & Screaton, 2004) and experiments with receptor specific monoclonal antibodies have also suggested that decoy receptor expression does not explain the relative sensitivity of a cell (Griffith et al., 1999). Indeed, even the relative importance of DR4 and DR5 to the apoptosis of individual cells appears to differ between cell types and cannot be determined by the receptor expression. B chronic lymphocytic leukaemia cells rely predominantly on DR4 to transmit the apoptotic signal, however have DR5 more abundantly expressed (MacFarlane et al., 2005).

The regulation of sensitivity appears to be far more complicated than receptor number and type. Recent data suggest that post-translational modification of DR4 and DR5 may be important in determining the sensitivity of a cell to TRAIL-mediated apoptosis. Tumours may over-express O-glycosyltransferase which leads to O-glycosylation of TRAIL receptors, enhancing ligand-mediated receptor clustering, DISC formation and caspase 8 activation (Wagner et al., 2007). Cells sensitive to TRAIL-mediated apoptosis have O-glycosylation of DR4 and DR5,

whereas inhibition of this post-translational modification suppressed apoptosis (Wagner et al., 2007). The association of TRAIL receptors with lipid rafts may also be important. Lipid rafts are cholesterol and sphingolipid rich areas in the cell membranes that concentrate signalling molecules and provide specific and distinct signalling, which may be different to the actions of the same proteins in different subcellular locations. It has recently been demonstrated that TRAIL receptors not associated with lipid rafts may preferentially activate the non-apoptotic signalling pathways in response to TRAIL, such as NFκB and ERK (Song et al., 2007).

The relative activation of these alternative non-apoptotic TRAIL signalling pathways may also offer some explanation for the differential sensitivity of cells. Inhibition of NFκB activity has been shown to sensitise some cells to TRAIL-induced apoptosis (Romagnoli et al., 2007), and cancer cells with activating PI3K mutations are relatively resistant to apoptosis by TRAIL (Samuels et al., 2005).

Whatever the actual mechanism responsible for the selectivity of tumour cells to TRAIL, it is clear that cancer cells contain multiple molecular abnormalities, which normally lead to their death by apoptosis. The cells that evade these normal safety mechanisms are nevertheless primed for apoptosis and hence may be more sensitive to death ligand targeting.

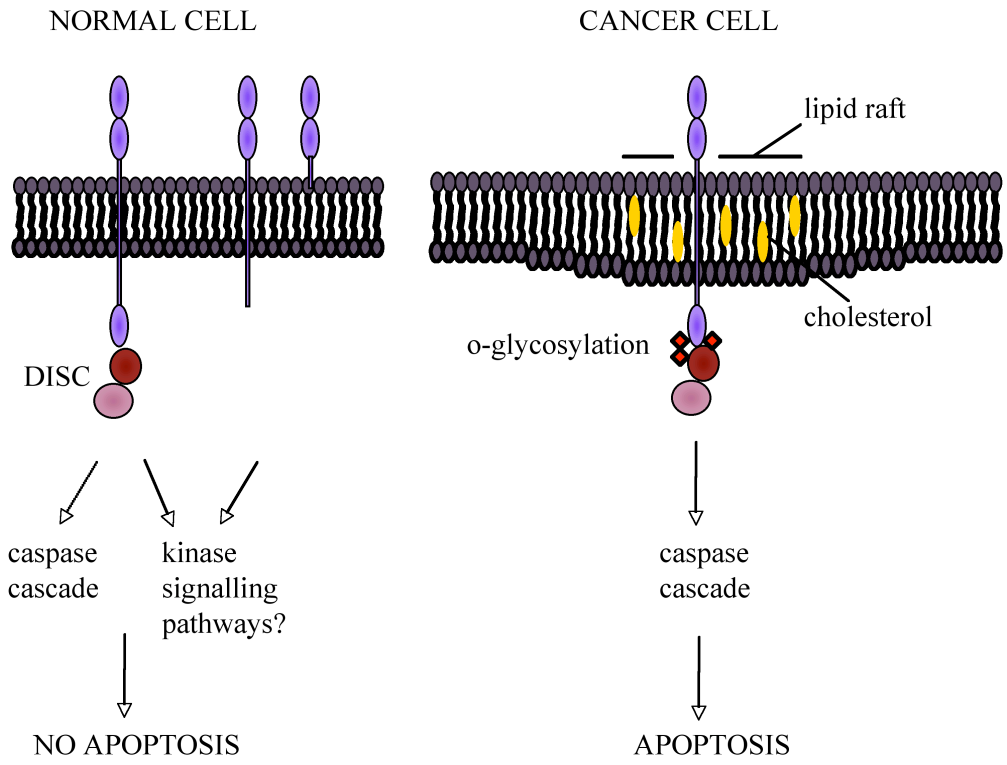

Figure 1.4 Cancer cells are specifically sensitive to TRAIL-induced apoptosis.
Possible mechanisms to explain the selective apoptosis of cancer cell to TRAIL include 1) increase in decoy receptors in normal cells which may activate anti-apoptotic kinase signalling pathways, 2) O-glycosylation of receptors and 3) their location in lipid rafts enhancing death inducing signalling complex (DISC) formation.

1.3.3 Physiological functions of TRAIL

Although TRAIL mRNA is found in a variety of cells and tissues in the body, the protein is mainly detected in cells of the immune system giving a hint as to the physiological role of this molecule. TRAIL has been proposed to have a role in the regulation of haematopoiesis (Secchiero & Zauli, 2008) and as an important mediator for the development of the immune system and particularly the negative selection of immature thymocytes (Lamhamedi-Cherradi et al., 2003). However, this hypothesis has been questioned by in vitro data demonstrating a lack of effect of soluble TRAIL receptors in negative selection (Simon et al., 2001), and no lymphoid

or myeloid abnormalities in TRAIL-deficient mice (Cretney et al., 2003; Sedger et al., 2002). TRAIL does however appear to have a role in immunoregulation with the modulation of T-cell activation, survival, and the production of memory T-cells (Janssen et al., 2005). TRAIL-knockout mice have been shown to have a failure to induce apoptosis of activated T-cells and an increased autoimmunity (Lamhamedi-Cherradi et al., 2003).

The predominant effect of TRAIL is thought to be its physiological role in the immune surveillance against tumours. Natural killer (NK) cells, T-cells, monocytes, neutrophils, and dendritic cells have all been shown to express TRAIL physiologically and have TRAIL dependent anti-tumour effects (Cassatella, 2006; Kayagaki et al., 1999a; Kayagaki et al., 1999b). TRAIL (in addition to perforin 1 and FasL) is known to partly mediate the NK cell-induced cytotoxicity of TRAIL-sensitive tumour lines in vitro and the anti-metastatic NK function in vivo in a mouse liver metastatic model (Takeda et al., 2001). These responses were found to be dependent on interferon γ (IFNγ). In a murine, allogenic bone marrow transplant (BMT), TRAIL expression on donor T-cells was also shown to be necessary for optimal graft-versus-tumour effects, but had no effects on graft-versus-host, again highlighting the tumour specificity of TRAIL (Schmaltz et al., 2002).

Administration of a neutralising anti-TRAIL antibody or the use of TRAIL-knockout mice demonstrated the increased susceptibility of TRAIL-deficient mice to TRAIL-sensitive tumours following subcutaneous application of the carcinogen methylcholanthrene (MCA) (Cretney et al., 2002; Takeda et al., 2002). Furthermore, $p53^{+/-}$ mice that were treated with the same neutralising antibody developed an increased incidence of spontaneous, TRAIL-sensitive tumours (Takeda et al., 2002). The incidence of spontaneous haematological malignancies has also been shown to be increased in TRAIL-deficient mice (Zerafa et al., 2005).

The physiological importance of TRAIL in tumour surveillance is also suggested by genetic lesions in some human cancers. The TRAIL receptor genes can be mapped to 8p21-22 on the human chromosome, a site of frequent allelic loss in cancers (Johnstone et al., 2008). DR5 mutations have been identified in up to 20% of human

cancers, including breast (Shin et al., 2001) and lung (Lee et al., 1999) cancer and a rare DR4 allele has been found more frequently in leukaemias and urogenital malignancies (Wolf et al., 2006). There are also defined mutations in human malignancies in the genes downstream from TRAIL, in the extrinsic apoptotic pathway, such as caspase 8 and cFLIP, however these are part of a common pathway and do not define a specific role for TRAIL (Johnstone et al., 2008).

In addition to a role in tumour surveillance, TRAIL is also thought to be involved in the elimination of virus-infected cells. Normal colonic epithelial cells and fibroblasts were shown to be resistant to TRAIL-induced apoptosis. Infection of these cells with cytomegalovirus or adenovirus led to an upregulation of TRAIL receptors and sensitised the cells to TRAIL (Sedger et al., 1999; Strater et al., 2002). A separate study demonstrated an upregulation of TRAIL expression in the lungs and on NK and T cells in influenza virus-infected mice, suggesting a role of TRAIL in the innate immunity against viral infection (Ishikawa et al., 2005).

1.3.4 Uses of TRAIL as an antitumour therapy

1.3.4.1 In vitro studies

The selective sensitivity of cancer cells to recombinant TRAIL has been shown in a number of studies in vitro. 39 different cell lines from tumours of the lung, breast, colon, central nervous system, kidney and skin were tested with recombinant soluble TRAIL, with evidence of cytostatic or cytotoxic effects on cell growth assays evident in 32 of the tested lines. Conversely, similar tests on normal human cell types including lung fibroblasts, breast, renal and prostate epithelial cells, colon smooth muscle cells, and astrocytes showed no evidence of cytotoxicity (Ashkenazi et al., 1999). These results have been repeated in several similar assays with both multiple cell lines and primary human cell cultures (Mitsiades et al., 2001) and a dose dependent effect of recombinant TRAIL has also been demonstrated in viability assays with glioma cells (Kock et al., 2007). In addition to the use of recombinant TRAIL, monoclonal agonist antibodies against the active TRAIL receptors (DR4, DR5) have also been produced and shown to cause apoptosis in a variety of cancer

cell lines (Motoki et al., 2005; Pukac et al., 2005). Cell lines have also been directly transduced to express both membrane-bound and soluble forms of TRAIL to cause apoptosis of cancer cells. An increase in apoptosis, measured by flow cytometry and cell viability assays, was demonstrated in lung cancer (A549, H460) and colon cancer (DLD-1, Lovo) cell lines transduced with adenoviruses expressing TRAIL (Lin et al., 2002). Cancer cells transduced to express TRAIL were shown not only to become apoptotic themselves but also to cause death of neighbouring cancer cells by a 'bystander effect' (Kagawa et al., 2001).

1.3.4.2 In vivo studies

There have been some concerns as to the toxicity of recombinant soluble TRAIL preparations with some studies demonstrating in vitro sensitivity of normal human hepatocytes, brain tissues, neutrophils, and some epithelial cells (Jo et al., 2000; Nitsch et al., 2000; Renshaw et al., 2003). Such toxicity had limited earlier trials on other death ligands. Injection of Fas-L led to massive hepatic necrosis and haemorrhage and death of mice, whereas use of TRAIL was without systemic effects (Walczak et al., 1999). This pattern was repeated in cynomolgus monkeys, where TNF caused severe toxicities but TRAIL was well tolerated (Ashkenazi et al., 1999). In addition to the apparent lack of toxicity, the repeated intravenous injections of recombinant TRAIL led to an increase in tumour cell apoptosis, a reduction in tumour growth, and an increase in survival in colon (Ashkenazi et al., 1999), pancreatic (Hylander et al., 2005), lung (Jin et al., 2004), myeloma (Mitsiades et al., 2001), glioma (Pollack et al., 2001), and breast (Walczak et al., 1999) cancer xenograft models. It is now thought that much of the in vitro toxicity was related to the tagged histidine or leucine segments of the recombinant TRAIL formations (Ganten et al., 2006; Lawrence et al., 2001; Meurette et al., 2006).

TRAIL monoclonal antibodies with agonist activity have also shown the ability to destroy cancer cells in vivo. An intravenous monoclonal antibody directed against DR4 caused a reduction in tumour growth in colonic, non small cell lung and renal tumours implanted subcutaneously (Pukac et al., 2005). Similar results were also obtained with intraperitoneal treatment of a subcutaneous colon cancer model with a

monoclonal antibody to DR5 (Motoki et al., 2005). An added advantage of monoclonal antibody therapy is that in addition to binding to the death ligand receptor, the antibodies may also provoke immunological anti-tumour effects via the Fc fragment of the antibody. This was suggested by a study which demonstrated the antibody isotype was important in the efficacy of a DR4 antibody treatment in a mouse colon cancer model (Chuntharapai et al., 2001). The Fc fragment can cause the recruitment of Fc receptor-expressing innate immune cells and cause antibody-dependent cell-mediated cytotoxicity, or complement-dependent cytotoxicity.

Other TRAIL-delivery systems, such as gene therapy, have also been used. Adenoviruses have been used to express TRAIL. Such adenoviruses have been directly injected into tumours, causing a reduction in tumour growth in several in vivo xenograft models including subcutaneous prostate (Griffith & Broghammer, 2001) and colon (Lin et al., 2002) cancer models, a breast peritoneal carcinomatosis model (Lee et al., 2002), and an orthotopic glioblastoma model (Lee et al., 2002). Adenovirus vectors can cause tissue damage secondary to the innate and cellular immune responses to the virus and as such, less immunogenic recombinant adeno-associated viruses have also been used in similar models (Mohr et al., 2004). In addition to the direct injection of TRAIL-expressing adenoviruses into tumours, cells resistant to the effects of TRAIL have been transduced to express the death ligand and then used for injection into tumours to cause apoptosis with their bystander effects (Ucur et al., 2003).

The transduction of cells to express TRAIL in the in vitro and in vivo systems described above produced predominantly membrane-bound TRAIL. Most investigators could find no evidence of soluble TRAIL in the supernatant of transduced cells by ELISA, and the apoptosis of cancer cells was not reproduced by the use of the supernatant (Kagawa et al., 2001; Ucur et al., 2003), although this was not a universal finding (Wei et al., 2001). Some authors have specifically attempted to produce soluble TRAIL by virally transducing cells with just the extracellular portion of TRAIL (Kim et al., 2006; Kim et al., 2004; Ma et al., 2005; Shi et al., 2005; Wu et al., 2001; Wu & Hui, 2004). There is some evidence that this leads to an increased apoptotic effect in some in vivo systems (Kim et al., 2006). Conversely, there is also evidence to suggest that whereas DR4 will be activated by soluble or

membrane-bound TRAIL, DR5 requires membrane-bound or cross-linked TRAIL for activation, and that some cells which are not sensitive to soluble TRAIL apoptose when the TRAIL is tethered to a cell membrane (Carlo-Stella et al., 2006; Muhlenbeck et al., 2000; Wajant et al., 2001).

1.3.4.3 Combinations of TRAIL with other agents

To increase cancer cell killing, TRAIL can be used in combination with other agents. Logically, the use of standard anticancer therapies, which cause cancer cell death by the intrinsic apoptosis pathway, would combine well with TRAIL therapy, which utilises the extrinsic pathway. There is however an increased synergism of such a combined approach, greater than the sum of its parts, due to the cross-talk between the intrinsic and extrinsic pathways, such that chemotherapeutic agents and radiotherapy are able to increase the apoptotic effects of TRAIL, even in cancer cells previously resistant. This synergism has been demonstrated with both in vitro and in vivo xenograft studies. There are a variety of possible mechanisms postulated for the synergism of the standard anti-cancer therapies including the upregulation of TRAIL receptors (shown in prostate and bladder cancer cells with ionising radiation (Shankar et al., 2004) and a range chemotherapy drugs including paclitaxel, vincristine, vinblastine, etoposide, and doxorubicin (Shankar et al., 2005)), the clustering of the receptors into lipid rafts (shown in leukaemic B-cells with doxorubicin (Dumitru et al., 2007)), the downregulation of apoptotic pathway inhibitors (c-FLIP down regulation demonstrated in prostate cancer cells with doxorubicin (El-Zawahry et al., 2005)), or the enhanced cleavage of caspases (demonstrated in mesothelioma with cisplatin (Belyanskaya et al., 2007) and etoposide (Broaddus et al., 2005)).

In addition to the combination with chemo- and radiotherapy, as the mechanism of TRAIL-induced apoptosis has become elucidated, this has also led to the rational combination of TRAIL therapy with other agents to specifically sensitise tumour cells to TRAIL-induced apoptosis. These include blocking inhibitors of the apoptosis cascades such as c-FLIP, Bcl-2 (Kock et al., 2007), and IAP inhibitors (Li et al., 2004) and blocking the pro-survival pathways with PI3K (Martelli et al., 2003)

and NFκB inhibitors (Khanbolooki et al., 2006), the latter of which was shown to overcome TRAIL resistance in pancreatic cancer cells both in vitro and in vivo. Histone deacetylase (HDAC) inhibitors have been shown to increase TRAIL receptor expression and localisation to lipid rafts (Vanoosten et al., 2005), and proapoptotic genes, while reducing the apoptotic inhibitors c-FLIP and the IAPs (Bolden et al., 2006) making it a promising candidate for combination therapy, and this was demonstrated in vivo with the eradication of murine breast tumours (Frew et al., 2008).

As described above, a potential advantage of TRAIL monoclonal antibodies is the immunological recruitment. Some authors have investigated the prospect of augmenting this further to enhance the production of tumour-specific cytotoxic T lymphocytes. One approach was the combination of the DR5 agonist monoclonal antibody with agonists to CD40 and CD137, to stimulate antigen presenting cells or costimulating T-cells respectively. This combination treatment was able to cause regression of tumours comprising 90% breast cells engineered to be TRAIL-resistant (Uno et al., 2006).

It is important to bear in mind that the increased sensitivity of cancer cells to TRAIL with combination therapies may also increase the sensitivity of normal cells to this therapy. There is some evidence of chemotherapy (Meurette et al., 2006) and HDAC inhibitors sensitising normal hepatocytes to TRAIL, and hence it would be important to consider the possible increased toxicity of combination therapy.

1.3.4.4 Translational studies

The promise of TRAIL as an oncological treatment from in vitro and in vivo work has led to its development for translational work. Recombinant TRAIL (AMG951, Amgen, CA, US) has been used in Phase 1 studies for advanced solid tumours or non-Hodgkin's lymphoma (NHL). No drug related dose limiting toxicities were reported. Consistent with preclinical work (Ashkenazi et al., 1999), the half-life of the recombinant TRAIL was 36 minutes. Out of the 51 trial patients, 1 partial response (PR - defined by Response Evaluation Criteria in Solid Tumours (RECIST))

and 13 with stable disease (SD) were reported. Further Phase 1b studies of AMG951 in combination with other agents have been performed in relapsed, low-grade NHL and non small cell lung cancer (NSCLC) with good tolerability and tumour response rates (NHL- 11 patients, 3 complete responses (CR), 3PR; NSCLC- 18 patients 1CR, 9PRs). These studies are now in Phase 2 clinical trials (Ashkenazi, 2008; Johnstone et al., 2008).

There has also been the development of human monoclonal antibodies to DR5 (HGS-ETR2 (mapatumumab, Human Genome Sciences, MD, USA)) and DR4 (HGS-ETR1 (lexatumumab, Human Genome Sciences)). Two Phase 1 trials using intravenous humanised mapatumumab as a monotherapy for advanced solid malignancies have been performed. Stable disease was reported in 19/49 and 12/41 patients in these trails, with the agent being well tolerated (Hotte et al., 2008). This product was also used in combination with chemotherapy agents yielding PRs in 4/28 patients. Phase 2 trials have also been reported with mapatumumab in NHL and NSCLC (NHL- 40 patients, 1CR, 2PR, 12SD; NSCLC- 32 patients, 9SD) (Greco et al., 2008). Clinical trials with lexatumumab for solid malignancies demonstrated stable disease in 22/68 cumulative patients from two Phase 1 trials, with 1 patient reported to have asymptomatic liver enzyme derangement. Further DR5 monoclonal antibodies (HGS-TR2J (Human Genome Sciences), AMG655 (Amgen), Apomab (Genentech, CA, US), LBY-135 (Novartis, NJ, US), CS1008 (Daiichi Sankyo Co., Tokyo, Japan)) have also recently begun clinical testing (Ashkenazi, 2008; Johnstone et al., 2008).

1.3.5 The need for a better TRAIL vector

The use of intravenous recombinant TRAIL or monoclonal antibodies, and the direct injection of TRAIL expressing cells into tumours have both shown promise as possible treatments for cancer. The intravenous use of recombinant TRAIL has several problems. The nature of its delivery means that there is no specific targeting of the active compound. In addition, the pharmacokinetic half-life of recombinant TRAIL was shown to be 32 minutes in the plasma of the experimental monkey (Ashkenazi et al., 1999) and 36 minutes in the recent human Phase 1 clinical trial,

necessitating frequent and high doses to produce the desired effect. Monoclonal antibodies against TRAIL receptors have the advantages of specific and high affinity binding with a prolonged half-life in comparison to the recombinant TRAIL. However, with the uncertainty surrounding the biological importance of decoy receptors, there is a possibility that this specific binding to active receptors may cause increased toxicity to normal cells. In addition, not all cells express both DR4 and DR5 and even when both receptors are present on the cell surface, they may not activate the apoptosis cascade equally. This is exemplified by colon and breast cancer cell lines, which express both types of TRAIL receptor, but only transduce the apoptotic signal with DR5 ligand binding (Kelley et al., 2005). Conversely, only binding to DR4 promotes apoptosis in chronic lymphocytic leukaemia cells, despite the expression of both DR4 and DR5 on the cell surface (MacFarlane et al., 2005). The majority of monoclonal antibodies being produced at present for clinical trials are agonists to DR5 (see above), however this is likely to be a reflection of the relatively increased expression of DR5 on tumour cells rather than on functional studies (Johnstone et al., 2008).

An improved treatment will involve the direct targeting of tumour cells and their micrometastases by cells expressing TRAIL in a long term, controllable manner. For this delivery, adult stem cells and especially mesenchymal stem cells from the adult bone marrow are a promising source of vectors to realise the full potential of TRAIL therapy.

1.4 Stem Cells

Stem cells are cells that have unlimited self-renewal properties with the ability to divide asymmetrically, both renewing themselves and producing more differentiated progenitors (Table 1.1). Stem cells are characteristically divided into embryonic and adult stem cells. Embryonic stem cells are derived from the inner cell mass of the blastocyst of a developing embryo and are able to produce progeny of all cell lineages (ectoderm, mesoderm, endoderm). In contrast to the pluripotency of embryonic stem cells, the progeny of adult stem cells are classically thought to be

lineage restricted. Adult stem cells are found in discrete niches within adult tissues and are thought to divide infrequently in the steady state, but have the potential to repair damaged tissues by replacing specific, specialised cells. The best characterised and most accessible adult stem cells are bone marrow derived stem cells (BMSCs). Bone marrow derived stem cells consist of haematopoietic stem cells (HSCs) which produce progenitors for all types of mature blood cells and mesenchymal stem cells (MSCs) which differentiate into mature cells of the stromal tissue including fat, bone, and cartilage (Bonnet, 2003).

Many adult organs have limited regenerative capacity, and the initial research with stem cells focused on attempts to harness the potential for the reparative and unlimited survival properties of stem cells to mediate epithelial repair in injured organs. The primitive nature and pluripotent potential of embryonic stem cells would appear to make them the best candidate for such reparative therapies with the potential to produce any differentiated cell necessary. The limited potency of adult stem cells would seem to restrict them to repair of cells of a specific lineage, for example the restoration of the immune system after bone marrow transplantation. Interestingly, several studies over the last decade have pointed towards the potential of adult stem cells, and bone marrow stem cells in particular, to be able to produce differentiated cells not restricted to their lineage, with cells from the adult bone marrow producing a variety of non-haematopoietic cells both in vitro and in vivo (Anjos-Afonso et al., 2004; Ishizawa et al., 2004; Kotton et al., 2001; Krause et al., 2001; Yamada et al., 2004). This ability of adult cells to produce progeny crossing lineage barriers, adopting the phenotypes of other tissues, is defined as 'plasticity'. Initial experiments suggested that following transplantation, a single bone marrow stem cell had the potential to engraft as epithelial cells in many organs, including 20% of type 2 pneumocytes in the lung (Krause et al., 2001). Further studies demonstrated a reduction in injury following bone marrow stem cell administration (Ortiz et al., 2003; Rojas et al., 2005). However the last few years has seen a re-evaluation, and there is an appreciation that the significant contribution of bone marrow cells to epithelial repair is probably a function of methodological flaws and artefacts (Loebinger et al., 2008; Loebinger & Janes, 2007).

The ability of the stem cell to differentiate in multiple lineages is not the primary consideration for this thesis. The aim is the utilisation of the ability of these cells to migrate to tumours, and for this adult bone marrow derived cells have several advantages. The use of embryonic cells is likely to involve the destruction of an embryo and research in this field has met with moral, ethical and political objections. Embryonic stem cells have a greater tumorigenic potential than adult stem cells and there are inherent risks associated with the immune rejection of these cells (Orkin & Morrison, 2002). Conversely, adult stem cells can be manipulated ex-vivo and the cells used can be autologous, thus reducing the risk of immune rejection. Many of the ethical objections with embryonic cells are also not valid with the use of these cells.

1.4.1 Contribution of bone marrow stem cells to extracellular matrix

1.4.1.1 Tissue stroma

Despite the reassessment of the contribution of bone marrow derived cells to epithelial repair in damage models, there remains strong evidence for their participation in areas of both physiological and pathological extracellular matrix deposition, including wound healing, tissue stroma, and organ fibrosis. The fibroblasts that enter and proliferate within fibrotic lesions were classically thought to be of resident tissue origin. Models describing the pathophysiology of fibrosis have developed to include other contributions to the fibroblast and myofibroblast communities within these fibrotic lesions. These include the possibility of epithelial to mesenchymal transition (EMT) and the significant contribution of fibroblasts and myofibroblasts from the bone marrow (McAnulty, 2007). Circulating fibrocytes originating from the bone marrow were described and shown to be important in both physiological and pathological repair (Abe et al., 2001; Bucala et al., 1994; Phillips et al., 2004; Schmidt et al., 2003). Chimeric mice with transplanted, labelled bone marrow were used to demonstrate greater than 30% bone marrow contribution to the fibroblasts in a skin wound healing model (Direkze et al., 2003; Ishii et al., 2005). In a bleomycin mouse model of lung fibrosis, 80% of type 1 collagen-expressing fibroblasts at the sites of lung fibrosis were shown to be of bone marrow origin

(Hashimoto et al., 2004; Ishii et al., 2005), and similar results were found with paracetamol induced lung injury (Direkze et al., 2003). MSCs have been shown to be preferentially attracted to and retained in infarcted myocardium (Barbash et al., 2003), cerebral ischaemia (Chen et al., 2001), areas of allograft rejection (Wu et al., 2003a), and lung fibrosis (Epperly et al., 2003; Ortiz et al., 2003).

Cell type	Definition
Stem cell	Cells with unlimited self renewal, dividing asymmetrically to produce an identical daughter cells and a more differentiated progenitor.
Bone marrow stem cell	Comprises haematopoietic and mesenchymal stem cells.
Haematopoietic stem cell	Stem cell able to form all cells of the blood lineage.
Mesenchymal stem cell	Stromal stem cell able to produce supporting cells including bone, fat, and cartilage.
Fibroblast	Main mature cell type involved in the production of the extracellular matrix and collagen of tissues.
Myofibroblast	Fibroblasts can be activated (e.g. by transforming growth factor β (TGFβ) to form these cells, which produce extracellular matrix but also have the ability to contract.
Fibrocytes	Circulating peripheral cells of bone marrow origin. Often described as blood-derived fibroblasts. Express a characteristic pattern of markers including the leukocyte common antigen CD45, the haematopoietic marker CD34, and collagen 1.

Table 1.1 Definitions of cell types

1.4.1.2 Tumour stroma

The tumour stroma is very important in determining cancer spread and growth. The tumour stroma is composed of fibroblasts and myofibroblasts which produce extracellular matrix and the 'desmoplastic reaction', endothelial cells involved in angiogenesis, and inflammatory cells (De Wever & Mareel, 2003; Desmouliere et al.,

2004; Direkze & Alison, 2006). Contrary to acting solely as a supporting structure, the tumour stroma is integral to the behaviour of the tumour (Bhowmick et al., 2004). Tumours have been compared to unresolved wounds that produce a continuous source of inflammatory mediators (Dvorak, 1986). Myofibroblasts in the tumour stroma can secrete growth factors and proteolytic enzymes that influence the invasion and progression of tumours (Orimo et al., 2005). In some situations the presence of a tumour capsule has been shown to be protective, leading to a increased prognosis in human hepatocellular carcinoma (Ng et al., 1992). Conversely, increased stroma and myofibroblast numbers were associated with a worse prognosis in other cancers (Barth et al., 2002a; Barth et al., 2002b; Barth et al., 2002c; Cardone et al., 1997), and the proliferative activity of stromal fibroblasts was shown to correlate to breast cancer metastasis (Hasebe et al., 2000). Tumour-stromal cell contact has been shown to upregulate the expression of stromal matrix metalloproteinases and promote the invasion of human cervical cancer cells (Sato et al., 2004). Furthermore, myofibroblasts and fibroblasts, activated by irradiation, led to an increased invasiveness of pancreatic cancer cells in coculture experiments (Ohuchida et al., 2004).

As with repair and fibrosis, in addition to the tissue origin of stromal cells, bone marrow derived stem cells contribute to this desmoplastic response in the form of myofibroblasts and fibroblasts, as well as participating in tumour neovasculogenesis. Experiments tracking the fate of labelled, bone marrow-derived cells following bone marrow transplant have shown myofibroblasts and endothelial cells originating from the bone marrow in a murine xenograft pancreatic tumour model (Ishii et al., 2003), and an endogenous murine pancreatic cancer model where up to 25% of the myofibroblasts were bone marrow derived (Direkze et al., 2004). These results have been repeated in a range of xenograft tumour models, with the amount of tumour stroma and bone marrow-derived cell contribution related to both the tumour cell and the site of implantation (Sangai et al., 2005). Furthermore, these bone marrow derived cells appear to be functional with the demonstration of collagen production (Direkze et al., 2006).

Tumour neovasculogenesis is one of the hallmarks of cancer, and a contribution of bone marrow derived stem cells to the angiogenesis of tumours has also been

demonstrated (Lyden et al., 2001). Bone marrow cells (Sca^{1+}) labelled and injected intravenously were shown to incorporate as endothelial like cells into the periphery of a glioma (Anderson et al., 2005). The importance of this contribution was illustrated by a decrease in tumour size and an increase in apoptosis when these bone marrow cells were transduced with the suicide gene (HSV-*tk*) (Ferrari et al., 2003). In contrast, other studies have only shown a minimal contribution of bone marrow cells to the newly formed tumour endothelium (Dwenger et al., 2004).

Sex mismatched bone marrow transplants in humans have also been utilised to determine the contribution of bone marrow derived cells to tumours. Colorectal adenomas diagnosed 2 months after bone marrow transplantation were found to consist of 1-4% bone marrow derived cells which displayed features of neoplastic colonic adenoma cells. A similar pattern, with up to 20% of the neoplastic cells of bone marrow origin was found in a patient who developed lung cancer four years post bone marrow transplant (Cogle et al., 2007). A contribution to the tumour vasculature has also been demonstrated (Peters et al., 2005).

In addition to the incorporation of bone marrow-derived cells following whole bone marrow transplantation, mesenchymal stem cells have also been shown to have an ability to specifically target tumour tissue. In vitro migration studies have demonstrated a enhanced migration of MSCs towards tumour cells and the conditioned medium from tumour cells (Menon et al., 2007; Nakamizo et al., 2005; Xin et al., 2007), in addition to platelet-derived growth factor (PDGF), epidermal growth factor (EGF), and CXCL12 (SDF1 α) (Nakamizo et al., 2005). A variety of tumour models have also shown the ability of MSCs to incorporate into and proliferate within tumour stroma in vivo. Kaposi's sarcoma (Khakoo et al., 2006), colorectal cancer (Menon et al., 2007), glioma (Nakamizo et al., 2005), breast metastases (Studeny et al., 2004) and melanoma metastases (Studeny et al., 2002; Studeny et al., 2004; Xin et al., 2007) have all been used and showed consistent MSC incorporation when MSCs were delivered systemically. MSCs have also been shown to migrate to tumours when delivered intraperitoneally in an ovarian cancer model (Komarova et al., 2006), and cerebrally in a glioma model (Nakamizo et al., 2005). The incorporation of MSCs has been shown both into established tumours and when delivered concurrently to the tumour cells (Khakoo et al., 2006). However,

some authors have suggested that established tumours are necessary for the development of the neovascularisation and the stromal-derived cytokines and growth factors that are essential to attract the circulating MSCs (Djouad et al., 2003).

1.5 Mesenchymal Stem Cells

MSCs are a subgroup of the adult bone marrow stem cells, which play an important role in supporting haematopoiesis and supplying differentiated stromal tissue. They can be isolated by their ability to adhere to plastic in culture, and expanded easily. There are no specific cell markers that can be used to categorically define an MSC and present identification relies upon a combination of their ability to differentiate in vitro into fat, bone, and cartilage, the expression of CD73, CD90, and CD105, and the lack of expression of haematopoietic cell markers (CD11b, CD14, CD19, CD34, CD45, CD79α, HLA-DR) on the cell surface (Dominici et al., 2006). MSCs have several properties in addition to their tumour homing capabilities, which lend them towards a role as a vector for cancer therapy. MSCs can be relatively easily transduced and expanded in culture for many passages, whilst retaining their growth and multi-lineage potential (Giordano et al., 2007; Lee et al., 2001; Marx et al., 1999). They also seem to be relatively immunoprivileged due to their expression of major histocompatibility complex (MHC)1, but lack of MHC2, and the costimulatory molecules CD80, CD86, CD40 (Javazon et al., 2004). This property may allow the delivery of allogenic MSCs without prior immunomodulation, opening up the possibility of their clinical use as a cell therapy.

1.5.1 Homing mediators

It is likely that the mechanism responsible for the homing of adult bone marrow stem cells to tumours involves chemokine ligands and receptors in a similar fashion to the recruitment of leukocytes to areas of inflammation. The importance of the chemokine CXCL12 and its receptor CXCR4 has been well established for haematopoietic stem cells (Chute, 2006; Peled et al., 1999). The chemokines

responsible for homing and migration of mesenchymal stem cells are however less well characterised. Chemokines are a family of small glycoproteins that regulate chemotaxis in addition to effects on proliferation and differentiation. There are approximately 50 human chemokines that are divided in XC, CC, CXC, and CX_3C families, based on the position of the cysteine residues within the primary amino acid sequence. They bind to seven-transmembrane, G-protein coupled receptors. Multiple authors have attempted to describe a definitive account of the functional chemokine receptors that are present on human MSCs and the cytokines and chemokines that have the greatest influence on MSC migration (Honczarenko et al., 2006; Ponte et al., 2007; Ringe et al., 2007; Sordi et al., 2005; Von Luttichau et al., 2005). One study demonstrated that MSCs expressed three CC chemokine receptors (CCR1,7,9) and CXC chemokine receptors (CXCR4,5,6), and one CX_3C chemokine receptor (CX_3CL1) by RTPCR and flow cytometry. The use of chemokine ligands for these receptors stimulated signalling pathways, with the phosphorylation of MAPKs, activation of signal transducer and activator of transcription (STATs; CXCL12 activating STAT-5, CCL5 activating STAT-1), and focal adhesion kinase signalling pathways (FAKs). The chemokine ligands also stimulated chemotaxis in vitro, and CXCL12 induced F-actin polymerisation (Honczarenko et al., 2006). A slightly different panel of chemokine receptors (CCR2,3,4,5; CXCR4,5) was suggested in a further study by flow cytometry and Western blot. This study demonstrated, by functional migration experiments, that the growth factors PDGF and insulin-like growth factor-1 (IGF-1) were the most potent chemotaxis agents to MSCs, with only three (CCL5, CXCL12, CCL22) of nine tested chemokines having a significant effect on migration. The stimulation of MSCs with tumour necrosis factor α (TNFα) however, significantly increased the chemokine-induced migration, suggesting that both the systemic and local inflammatory state may be important in MSC homing (Ponte et al., 2007). Growth factors were also deemed important in MSC migration in a further study in which basic fibroblast growth factor (bFGF) had the most potent effect (Schmidt et al., 2006). MSCs isolated from multiple donors were used to demonstrate the mRNA expression of a large panel of chemokine receptors, however immunochemistry only confirmed protein expression in a subgroup of these. Furthermore, the expression of some chemokine receptors (particularly the CC group) varied between donors, whereas other chemokine

receptors were expressed universally (CXCRs, CCR8,9) (Ringe et al., 2007). Other multiple reports have suggested alternative expression patterns and functional importance of different chemokines and their receptors in MSC migration including CCR1,4,7,10, CXCR5 (Von Luttichau et al., 2005), and CCR1,7, CXCR4,6, CX_3CR1 (Sordi et al., 2005).

Of the chemokines, the contribution of CXCL12 to the recruitment of MSCs is of particular interest. This chemokine is critical for haematopoietic stem cell migration, and knockouts of either the ligand or receptor CXCR4 are universally fatal in utero, with the chemokine involved in the migration of HSCs from the liver to the bone marrow. Similarly, the migration of bone marrow-derived stem cells to fibrotic lung is reduced with CXCL12 neutralisation (Phillips et al., 2004; Xu et al., 2007a). The importance of this chemokine in MSC migration is suggested by studies demonstrating an increased migration of MSCs, tranduced to overexpress CXCR4, to the infarcted myocardium (Cheng et al., 2008), and the in vivo migration of MSCs to the brain after exogenous CXCL12 injection (Ji et al., 2004). CXCL12 may also be an important mediator of MSC recruitment to tumours. The stroma surrounding breast cancer was shown to be a rich source of this chemokine (Orimo et al., 2005) and whole tumour explants were also shown to secrete this cytokine (Dwyer et al., 2007). A further in vitro study examined the differences in gene expression profiles between MSCs exposed to conditioned medium from tumours cells and bone marrow cells. The authors concluded that the CXCL12/CXCR4 axis was important, but that the MSCs produced the chemokine which then acted in an autocrine manner (Menon et al., 2007). Other studies however have failed to confirm the importance of CXCR4 for MSC migration. Blockade of CXCR4 did not affect MSC migration in a myocardial infarct model (Ip et al., 2007) and some groups have not shown expression of this receptor on MSCs (Von Luttichau et al., 2005).

Based on the established literature for leukocyte migration, other possible important candidates for MSC chemotaxis include the receptors CXCR1,2 and CCR3, neutralisation of which has been shown to decrease leukocyte migration (Luster et al., 2005; Spaeth et al., 2008), and CCR2 important in macrophage trafficking (Sekido et al., 1993). Indeed, CCL2 was shown to be secreted by breast cancer cells in vivo and the use of a neutralising antibody reduced the homing of MSCs (Dwyer et al.,

2007). The same study also demonstrated an increased serum level of CCL2 in post-menopausal breast cancer patients compared to controls.

MSCs are also believed to use adhesion molecules and integrins to enable extravasation in a similar fashion to leukocytes (Ruster et al., 2006). P-selectin is important in the initial endothelial contact and rolling of leukocytes, and neutralising antibodies against the endothelially expressed P-selectin also resulted in fewer endothelial cell-bound MSCs in vitro (Ruster et al., 2006). The very late antigen-4 (VLA-4) and its counterpart adhesion molecule vascular cell adhesion molecule-1 (VCAM-1) are critical for leukocyte arrest on activated endothelium, and antibodies to either resulted in a decreased MSC adherence to the endothelium (Ruster et al., 2006). Furthermore, the migration of MSCs to ischaemic myocardium was reduced by blocking MSC β1-integrin, a component of VLA-4 (Ip et al., 2007). Despite the similarities, there are however likely to be differences between leukocyte and MSC extravasation, for example platelet/endothelial cell adhesion molecule-1 (PECAM-1), which is involved in leukocyte transmigration, is not expressed on MSCs (Karp & Leng Teo, 2009).

The large variability between the reports of the chemokines and cytokines relevant to MSC migration may be partly explained by the heterogeneity of the cell population. This includes the extraction and identification of the cells, the culture conditions and the possibility of cell activation either in vivo or ex vivo. The ability of MSCs to home and migrate appears to decrease during in vitro expansion in relation to their loss of surface expression of chemokine receptors (Honczarenko et al., 2006; Rombouts & Ploemacher, 2003). Culture confluence has also been shown to impact on MSC homing with increased confluency increasing the production of the tissue inhibitor of matrix metalloproteinase-3 (TIMP-3) and inhibiting transendothelial migration (De Becker et al., 2007). Conversely, hypoxic culture conditions increase matrix metalloproteinases (MMPs) and MSC migration (Annabi et al., 2003). Despite the variability, the general consensus is that MSCs do express a number of chemokine receptors which are likely to be involved in their homing capabilities (Chamberlain et al., 2007), often with combination of cytokines and chemokines necessary for the maximal effect (Ozaki et al., 2007).

1.5.2 Use of MSCs as delivery vectors

1.5.2.1 Cancer

The ability of MSCs to specifically home to a wide range of tumours has led several groups to investigate these cells in delivering anticancer agents (Figure 1.5). Human MSCs, engineered to express IFNβ by transduction with adenovirus, have been used to provide targeted delivery of this potent antiproliferative and proapoptotic agent to gliomas (Nakamizo et al., 2005) and metastatic breast (Studeny et al., 2004), melanoma (Studeny et al., 2002; Studeny et al., 2004), and prostate (Ren et al., 2008b) cancer models. The use of MSC-delivered IFNβ, which suppresses tumour cell growth by induction of differentiation, S-phase accumulation and apoptosis, resulted in an increased survival and/or reduced tumour burden in all these models. IFNα-expressing MSCs have also been used for the immunostimulatory, apoptosis-inducing, and anti-angiogenic effects of IFNα with similar results in a metastatic melanoma model (Ren et al., 2008a). MSCs have also been adenovirus-transduced to express IL-12, with the rationale of improving the anti-cancer immune surveillance by activating cytotoxic lymphocytes, natural killer cells, and producing IFNγ. In this model, the intravenously delivered IL-12-expressing MSCs reduced metastases from subcutaneous tumours (Chen et al., 2008). In addition, if delivered intraperitonealy, one-week prior to tumour inoculation, the MSCs were able to prevent the development of the subcutaneous tumours (Chen et al., 2006). A similar approach of immunostimulation with tumour-targeted chemokines was used to deliver the chemokine CX_3CL1 (fractalkine), which is able to activate T-cells and NK cells. This therapy reduced the metastastic load caused by the intravenous delivery of melanoma and colon cancer cell lines (Xin et al., 2007). MSCs have also been produced to deliver IFNγ which stimulated apoptosis and inhibited leukaemic cell proliferation in vitro (Li et al., 2006), and the immunomodulatory cytokine IL-2 with a reduction in tumour growth and improved survival when directly injected into murine gliomas (Nakamura et al., 2004).

In addition to the delivery of growth factors, cytokines, and chemokines, MSCs have also been engineered to deliver conditional replicative adenoviruses (CRAds) to reduce tumour growth and spread in vivo. These viruses are able to destroy tumour cells by viral replication, and following oncolysis, further newly produced virus is

then released to the surrounding tumour tissue. This therapy improved survival in a murine ovarian cancer model (Komarova et al., 2006), orthotopic breast and lung tumour models (Hakkarainen et al., 2007), and a lung metastasis model (Stoff-Khalili et al., 2007).

MSCs have also been used to serve as vehicles for targeted chemotherapy with an enzyme prodrug conversion approach. One study combined MSCs that produced herpes simplex virus-thymidine kinase (HSV-*tk*) retroviral vectors in the proximity of tumours, with the prodrug ganciclovir, leading to glioma cell death in vitro and in vivo (Uchibori et al., 2009). In different studies, MSCs expressed the cytosine deaminase enzyme, which converts the substrate 5-fluorocytosine (5-FC) to the highly toxic 5-fluorouracil (5-FU), which they delivered to the tumour cells resulting in a reduction of melanoma (Kucerova et al., 2008) and colon cancer (Kucerova et al., 2007) subcutaneous tumours. However, these approaches are limited by the toxicity of the treatment to the delivery MSC.

1.5.2.2 Non-cancer

In addition to homing to tumours, MSCs also home to areas of damage and repair. As a result, studies have also investigated their use as delivery vectors in other pathologies. Endotoxin-mediated acute lung injury was reduced with the use of MSCs expressing angiopoietin-1, a critical factor for endothelial survival (Mei et al., 2007). Mesenchymal stem cells transduced with endothelial nitric oxide synthase (eNOS) could also improve monocrotaline-induced pulmonary arterial hypertension in rats (Kanki-Horimoto et al., 2006). Vascular endothelial growth factor (VEGF) expressing MSCs were also shown to improve cardiac function in a myocardial infarction model (Matsumoto et al., 2005). Significant improvements were also recorded in an experimental autoimmune encephalomyelitis model with the use of intravenous MSCs transduced to express human ciliary neurotrophic factor (CNTF), a factor known to promote myelogenesis and reduce inflammation (Lu et al., 2009), and a collagen induced arthritis model with IL-10 overexpressing MSCs, suppressing the immune response and regulating cytokine production (Choi et al., 2008).

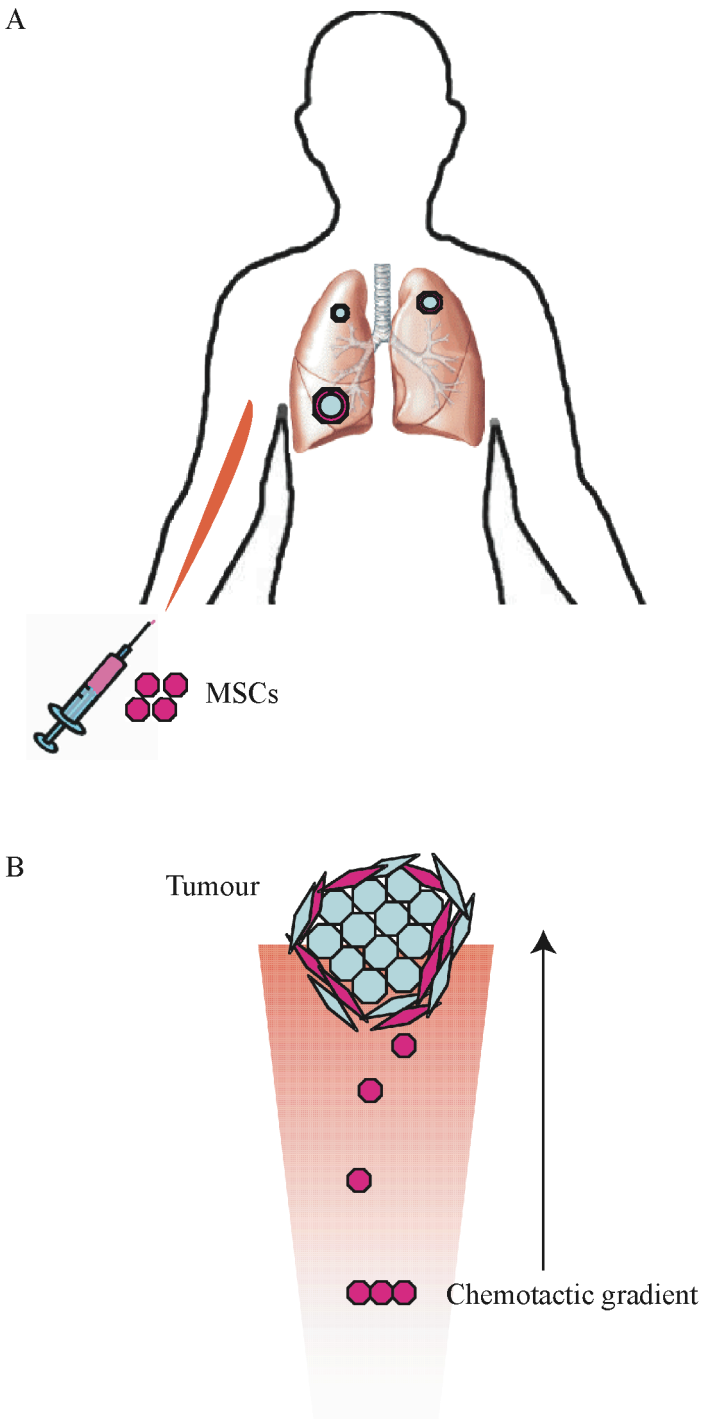

Figure 1.5 MSCs migrate towards tumours
A) Intravenously injected MSC are able to specifically migrate towards multiple lung metastases. B) The tumour produces a chemotactic gradient attracting MSCs, which are able to incorporate into the tumour architecture.

MSCs can also be used to deliver genes to 'replace' mutant genes in genetic deficiencies. Animal and small clinical studies have shown potential in osteogenesis imperfecta (Horwitz et al., 1999; Horwitz et al., 2001) and lysosomal storage diseases (Koc et al., 2002).

Other bone marrow derived progenitor cells have also been used as vectors. Endothelial progenitor cells transduced with eNOS have been used in a similar pulmonary hypertension model (Zhao et al., 2005) and this has led to the development of the PHACeT clinical trial in humans, which is currently enrolling patients.

1.5.3 Effects of MSCs themselves

1.5.3.1 Non-cancer

It is important not to regard MSCs simply as inert vectors but as active cells with possible effects on both physiological and pathological processes. In particular, it is known that MSCs have profound immunosuppressive effects. T-cells cultured with MSCs do not proliferate with antigenic or mitogenic stimuli. This may be due to the arrest of the T-cell in the G0/G1 phase with consequent prevention of S phase entry and inhibition of cell division (Glennie et al., 2005). Similar effects have been demonstrated on B-cells (Corcione et al., 2006) and dendritic cells (Ramasamy et al., 2007a), leading to a reduction in plasma cell maturation and antibody production, and antigen presentation respectively. In addition to direct T-cell inhibition, MSCs also induce $CD4^{+}CD25^{+}FoxP3^{+}$ regulatory T-cells (Treg), which further limit the activation of CD4 and CD8 subsets, B-cells, and NK cells (Wolf & Wolf, 2008). MSCs affect immune cells by several mechanisms including direct cell contact and the release of many soluble factors, including nitric oxide (Sato et al., 2007).

The immunosuppressive effects of MSCs have been harnessed in the treatment of graft versus host disease (GvHD) following bone marrow transplantation. A multicentre, Phase 2 clinical trial for MSCs in severe, steroid-resistant GvHD, demonstrated a complete response in 30 patients and partial response in a further 9

out of 55 treated patients. Interestingly, there was no difference in response or adverse effects between patients receiving cells from matched or unmatched donors (Le Blanc et al., 2008). A Phase 2 study utilising the immunosuppressive effects of the MSCs is also ongoing in Crohn's disease (Weiss et al., 2008), and there is also encouraging in vivo data for experimental collagen-induced arthritis (Augello et al., 2007) and autoimmune encephalomyelitis (Zappia et al., 2005), suggesting further potential clinical applications in other autoimmune diseases.

In addition, MSCs are thought to be able to reduce damage in several injury systems by both stimulating repair and exerting anti-inflammatory effects. This has been utilised in clinical trials in cardiology (Assmus et al., 2006; Hare & Chaparro, 2008; Lunde et al., 2006; Schachinger et al., 2006), whereby MSCs have been infused acutely following myocardial infarction and in chronic ischaemic heart failure, with an improvement in cardiac function, infarct size, and remodelling (Hare & Chaparro, 2008). In the lung, systemic MSC administration following bleomycin-induced pulmonary fibrosis led to decreased inflammation, and reduced fibrosis and collagen deposition in murine models (Ortiz et al., 2003; Rojas et al., 2005). Expression of IL-1 receptor antagonist by MSCs and the subsequent reduction of the proinflammatory cytokines TNFα and IL-1 have been postulated as central to this effect. Similarly, MSCs were shown to regulate the inflammatory signals from lung cells injured by either intratracheal (Gupta et al., 2007) or intraperitoneal (Xu et al., 2007b) endotoxin, with a reduction in lung injury. Phase 2 clinical trials are presently being performed to investigate whether the anti-inflammatory and reparative function of MSCs may benefit patients with moderate to severe chronic obstructive lung disease. The paracrine effects of MSCs on tissue protection and repair, with the secretion of trophic factors, have also been proposed for the improvements in other organ damage models including fulminant hepatic failure (Parekkadan et al., 2007), stroke (Li et al., 2002), and acute kidney injury (Togel et al., 2007). MSCs have also been shown to produce proangiogenic cytokines including VEGF and bFGF, and this property has been used to enhance blood vessel growth in chronic limb ischaemia (Kinnaird et al., 2004).

1.5.3.2 Cancer

It is especially important to consider the role of the MSC in cancer in the context of these immunosuppressive, reparative, and angiogenic properties. Subcutaneously delivered, allogenic, melanoma cells only produced tumours in mice with the co-administration of MSCs, and immunosuppression was thought to be a pivotal factor for this observation (Djouad et al., 2003). The same group also demonstrated an earlier development of tumours when syngeneic Renca kidney cancer cells were implanted with MSCs. MSCs however did not alter the cancer cell growth in vitro, supporting an immunosuppressive role for the in vivo differences. The kinetics of tumour growth and metastases were not affected in these experiments (Djouad et al., 2006).

The production of trophic factors by MSCs has also been implicated in enhancing tumour growth and spread. MSCs enhanced the in vivo growth of Burkitt's lymphoma cells by a mechanism dependent on the VEGF pathway (Kyriakou et al., 2006). MSCs have also been shown to secrete the chemokine CCL5, which promoted an increase in the motility, invasion, and metastasis of breast cancer cells in a mouse subcutaneous xenograft model (Karnoub et al., 2007). The production of IL-6 by MSCs was also implicated in the increased growth of breast cancer cells by STAT-3 phosphorylation and signalling (Sasser et al., 2007).

Further tumour-enhancing effects of MSCs have also been demonstrated with colonic cancer (Zhu et al., 2006) and chronic myeloid leukaemia cell lines. In the latter experiment the MSCs increased in vivo tumour proliferation, but reduced the cancer cell proliferation in vitro. In order to resolve the discrepancy, the authors suggested MSCs were able to downregulate cyclin D2 and arrest cancer cells at G0/G1, preserving their proliferative capacity and reducing apoptosis (Ramasamy et al., 2007b).

In contrast, MSCs have also been shown to have intrinsic antineoplastic properties. MSCs were also shown to arrest hepatoma, lymphoma, and insulinoma cells at G0/G1, but this reduced proliferation was accompanied by an increase in cancer cell apoptosis and a reduction in malignant ascites when hepatoma cells were injected

intraperitoneally (Lu et al., 2008). An improvement in other cancer models has also been demonstrated with the use of MSCs. Intratumoural injection of MSCs led to the inhibition of tumour growth and increased survival of rats with glioma (Nakamura et al., 2004), and both intratumoural or intravenous injection of MSCs led to the reduction in growth and metastases of a breast cancer model, with the increase of apoptotic markers (Sun et al., 2009).

Furthermore, intravenously delivered MSCs were able to inhibit the growth of Kaposi's sarcoma (KS) in a mouse model, in a dose dependent manner. The mechanism was due to the inhibition of Akt activity within KS cells, and cell-cell contact was necessary (Khakoo et al., 2006). The release of soluble factors by MSCs has also been shown to reduce tumour growth and progression in glioma (Nakamura et al., 2004), melanoma and lung carcinoma models (Maestroni et al., 1999). The MSC-induced cancer cell inhibition was preserved with the separation of the cells across a transwell membrane. The nature of the soluble factor was not determined, however the effect was not neutralised by IFNα/β, TNFα, or TGFβ antibodies (Maestroni et al., 1999). Conditioned media from MSCs has however also been shown to lead to the downregulation of NFκB and the phosphorylation of inhibitor κBα (p-IκBα) in hepatoma and breast cancer cells, leading to a decrease in their in vitro proliferation (Qiao et al., 2008b). The same group also delineated a further mechanism in a separate study, with the secretion of dickkopf proteins (DKK-1) by MSCs leading to the downregulation of the Wnt signalling pathway in breast cancer cells and a reduction in their proliferation (Qiao et al., 2008a).

In addition to affecting the behaviour of cancer cells, there is some concern that the stem cells may themselves become malignant. Stem cells have the capacity for unlimited proliferation, making them attractive candidates for malignant change. In vitro passaging of human MSCs has demonstrated the potential for the development of karyotype abnormalities (Rubio et al., 2005; Wang et al., 2005), and systemically delivered murine MSCs have produced sarcomas (Tolar et al., 2007) and osteosarcomas (Aguilar et al., 2007). Malignant change of bone marrow-derived cells has also been implicated in a murine gastric carcinoma model. *Helicobacter felis* was used to create a chronic gastric injury, within which a carcinoma developed

from bone marrow-derived cells (Houghton et al., 2004). However, a recent study performed to assess the potential susceptibility of human bone marrow-derived MSCs to malignant transformation demonstrated no features consistent with this, with stable karyotypes and shortening teleomeres over the 44-week culture period, and concluded that MSCs remained suitable for cell therapies after in vitro expansion (Bernardo et al., 2007).

Despite the concerns, Phase 1 and 2 clinical trials have now been performed, or are ongoing, with exogenous MSCs for the promotion of haematopoietic recovery (Koc et al., 2000), and GvHD (Le Blanc et al., 2008) following BMT, osteogenesis imperfecta (Horwitz et al., 2002), ischaemic cardiac disease (Hare & Chaparro, 2008), Crohn's disease (Weiss et al., 2008), and chronic obstructive pulmonary disease (COPD) (Iyer et al., 2009), and so far neither acute nor long term adverse effects have been reported following their infusion.

1.6 The combination of TRAIL and MSCs

The use of MSCs to deliver TRAIL combines cells with the ability to seek out tumours with a protein that is able to specifically kill them. This combination is particularly attractive. TRAIL has advantages over some of the other anti-cancer MSC delivery systems described above, as there appear to be very limited effects on non-cancerous tissues. Furthermore, the targeted delivery of TRAIL with MSCs overcomes some of the problems encountered with recombinant TRAIL or TRAIL monoclonal antibodies. MSC-targeted TRAIL is more physiological than the monoclonal antibodies, which rely on the effects of a specific active receptor, and has a much better half life and increased delivery across the blood-brain barrier than recombinant TRAIL. In addition the MSCs deliver TRAIL directly to the tumours.

Such is the promise of this technique, recent studies have now investigated the combination of TRAIL with bone marrow derived cells. In one study, mice underwent a bone marrow transplant with constitutively TRAIL-overexpressing donor marrow. The aim of this study was not specific tumour targeting of TRAIL,

however it did show a lack of toxicity of normal cells and a reduction of syngeneic tumour growth in vivo (Song et al., 2006). Another group used adenoviruses to produce transient expression of TRAIL in $CD34^+$ bone marrow cells. These cells were selected because of their ability to interact with endothelial cells and demonstrated an improved survival in lympho-haematopoietic tumours (Carlo-Stella et al., 2006). Some very recent work has also looked at combining MSCs with TRAIL. These studies demonstrated a decreased tumour growth following administration of TRAIL-expressing MSCs in glioma (Kim et al., 2008; Sasportas et al., 2009) and subcutaneous tumour models (Mohr et al., 2008), however all of these studies used direct intratumoural MSC administration to demonstrate the effect. The ideal goal would be to use systemic MSC therapy for multiple tumours to fully utilise the homing ability of the MSC. The one study looking at systemic TRAIL-expressing MSCs showed no effect on a subcutaneous colon cancer model (Luetzkendorf et al., 2009).

1.7 Summary

The possible use of mesenchymal stem cells as a cellular therapy in cancer is exciting. TRAIL is a new molecule with the potential to become a mainstay of cancer therapy. This thesis combines two exciting and developing fields by engineering mesenchymal stem cells to express TRAIL in a controlled manner, and utilises their ability to incorporate into different tumour models.

1.8 Hypothesis

Mesenchymal stem cells will home to cancer. These cells can be engineered to produce TRAIL, under the control of doxycycline, which will cause cancer cell apoptosis. This will allow control of tumour growth and metastasis in vivo.

1.9 Aims

1. Engineer MSCs to express doxycycline-inducible TRAIL.
2. Produce suitable tumour models and establish MSC incorporation into tumours.
3. Reduce cancer growth and metastasis with the use of MSC expression of TRAIL.

CHAPTER 2. MATERIALS AND METHODS

2.1 General chemicals, solvents and plastic ware

All chemicals were of analytical grade or above and were obtained from Sigma Aldrich (Poole, UK) unless otherwise stated. All water used for the preparation of buffers was distilled and deionised (dH_2O), using a Millipore water purification system (Milipore R010 followed by Millipore Q plus; Millipore Ltd., MA, US). Polypropylene centrifuge tubes and pipettes were obtained from Becton Dickenson (Oxford, UK).

2.2 Cell Culture

All sterile tissue culture media, sterile tissue culture grade trypsin/EDTA, tissue culture antibiotics and fetal bovine serum (FBS) were purchased from Invitrogen (Paisley, UK) unless otherwise stated. Sterile tissue culture flasks and plates were obtained from Nunc (Roskilde, Denmark) unless otherwise stated.

All cells were cultured in Dulbecco's modified Eagle's medium (DMEM) with 4mM L-Glutamine, 50U/ml penicillin and 50μg/ml streptomycin and 10% (v/v) fetal bovine serum (FBS) and incubated at 37°C in a humidified, 5% CO_2 atmosphere, unless otherwise stated. The serum for all cells transduced with the Tet-on plasmids was replaced by Tet-system approved FBS (Clontech, Paris, France).

Hela, A549, 293T H357 and MDAMB231 cells were obtained from Cancer Research UK, London Research Institute (CRUK, London, UK). Normal primary human adult lung fibroblasts were a kind gift from Dr. Robin McAnulty in the host laboratory and were cultured in a 10% CO_2 atmosphere. Human adult mesenchymal

stem cells were provided through the Tulane Centre for Gene Therapy, MSC cell distribution center (LA, US) and cultured in αMEM with 4mM L-Glutamine, 50 U/ml penicillin and 50μg/ml streptomycin, and 16% (v/v) fetal bovine serum (FBS). H357 cells were cultured in a 1:3 mix of Hams F12 medium and DMEM. In addition to FBS, L-Glutamine, and antibiotics, this medium was supplemented with 10^{-10}M cholera enterotoxin (ICN Pharmaceuticals Ltd., Oxon, UK), 0.5g/ml hydrocortisone, 10ng/ml epidermal growth factor, and 5μg/ml insulin.

Media was changed every 3 days. Cells were grown until approximately 80% confluent and then mobilised by washing with autoclaved phosphate-buffered saline (PBS) followed by 18μl/cm^2 of 0.05% trypsin in EDTA. The H357 cells would not detach efficiently using this technique and hence they were washed and then incubated in Versene for 5 minutes at 37°C before trypsinisation as above. After detachment, cells were passaged into 175 cm^2 tissue culture flasks at ratios of 1:3 to 1:8 every 3 – 10 days depending on rate of proliferation. Human adult mesenchymal stem cells were plated at 50-100 cells/cm^2 following passage. All cells were stored in liquid nitrogen, in 50% (v/v) medium, 40% (v/v) FBS and 10% (v/v) DMSO, except human adult mesenchymal stem cells, which were stored in 65% medium, 30% FBS, and 5% DMSO.

2.3 Mesenchymal stem cells

The human adult mesenchymal stem cells provided from the Tulane Centre for Gene Therapy were fully characterised at source. Nevertheless, key MSC properties were reassessed.

2.3.1 Differentiation

Human adult mesenchymal stem cells were differentiated according to previously described methods (Pittenger et al., 1999). The cells were plated in 6-well plates until they reached 100% confluency. The cell culture medium was then removed,

the cells washed with PBS, and bone (cell culture medium containing 10nM dexamethasone, 20mM β-glycerolphosphate, 50μM L-Ascorbic acid 2-phosphate) or fat (cell culture medium containing 0.5μM dexamethasone, 0.5μM isobutylmethylxanthine, 50μM indomethacin) differentiation media was added to the wells as required. The cells were washed with PBS and the medium changed every 3 days for 21 days. At the end of 21 days, the cells were washed in PBS and fixed in neutral buffered formalin. The bone differentiation plates were then washed in dH_2O and stained with 1% (w/v) Alizarin Red S, whereas the fat differentiation plates were washed with PBS and stained with 0.3% (w/v) Oil-Red-O (both BDH Laboratory, Poole, UK).

2.3.2 Colony forming ability

MSC colony forming assays were performed according to the methods described by the Tulane Centre for Gene Therapy. One hundred MSCs were plated on a 10cm diameter culture dish and cultured for 14 days. After this time period, the cells were washed with PBS and stained with 3% (w/v) Crystal Violet in 100% methanol for 10 minutes. The number of colonies 2mm or larger in diameter were counted and expressed as a percentage of the original 100 cells plated to give the percentage colony forming unit.

2.4 Side population cells

Hoechst 33342 is a nuclear binding dye that stains all cells. The side population (SP) defines a subgroup of cells with the ability to efflux this dye with a multi-drug transporter.

2.4.1 Side population identification and sorting

To identify the side population, previously described protocols were followed

(Goodell et al., 1996). H357, MDAMB231, and A549 cells were harvested at full confluence, resuspended at $1x10^6$ cells/ml in medium, and incubated at 37°C for 10 minutes. Cells were then labelled with 2.5, 5, or 7.5μg/ml Hoechst 33342 for 45, 60, or 90 minutes at 37°C to determine the required incubation time. The labelling was also repeated in the presence of the multi-drug transporter inhibitor reserpine at concentrations of 5μM and 50μM. The cells were counterstained with 2.5μg/ml propidium iodide (PI) to label dead cells, which were excluded from the analysis, and then placed on ice. They were analysed by flow cytometry on either a FACSCalibur or LR2 machine (both Becton Dickenson). Hoechst red and blue fluorescence was detected using the UV excitation laser with the 620 long pass and 440/40 bandpass filters respectively. PI was detected with excitation by the blue (488nm) laser and 610/20 nm filter. For SP analysis, at least $1 x10^5$ total events were collected, and all subsequent analysis was performed using FlowJo software (Tree Star Inc., OR, US). The SP was a small subgroup of cells that stained poorly with Hoechst and appeared to locate off the side of the main population of cells. This population was lost with the use of reserpine. The optimal staining conditions were 5μg/ml Hoechst 33342 for 45 minutes and 7.5μg/ml Hoechst 33342 for 60 minutes for the H357 and A549 cells respectively. Fluorescence-activated cell sorting (FACS) of the SP and non-SP cells was performed using a MoFlo High-Performance Cell Sorter (Dako, Glostrup, Denmark).

2.4.2 Colony-forming assays

Two hundred SP or non-SP H357 cells were seeded per 6-well plate and cultured for 14 days. Colonies were washed, fixed using 3% (w/v) paraformaldehyde (PFA), and stained with Rhodanile Blue overnight. Colonies were counted using an Olympus CK2 inverted phase-contrast light microscope (Olympus, Essex, UK). A large colony was defined as greater than 32 cells per colony, and abortive colonies were defined as colonies that contained fewer than 32 cells according to the previously described system (Jones & Watt, 1993). In mitoxantrone dihydrochloride dose–response assays, 200 H357 cells were plated per well of a 6-well plate and cultured in the presence of 0, 1, or 10ng/ml of mitoxantrone for 3 days. The wells were then

washed 3 times with PBS and the normal medium replaced. After a further 14 days, the cultures were fixed, stained, and counted.

2.5 Production of plasmid constructs

2.5.1 Production of TRAIL DNA for plasmid

E. coli bacteria containing the plasmid (PCMVsport6) with full length human TRAIL (clone: IRATp970G0G0955D6) were obtained from RZPD (Berlin, Germany). These bacteria were streaked onto an LB agar selection plate containing 50µg/ml ampicillin, and incubated overnight at 37ºC. A single colony was picked from this freshly streaked selection plate and used to inoculate a 5ml starter culture of LB broth (Fisher Scientific, Loughborough, UK) containing 50µg/ml ampicillin. This was incubated for 6 hours at 37ºC on an orbital shaker at 220 rpm. 2ml of the starter culture were then transferred to 200mls of LB broth containing 50µg/ml ampicillin for overnight incubation on the orbital shaker at the same conditions. The plasmid DNA contained within the bacteria in the LB broth was purified using the Purelink HiPure Plasmid DNA Maxiprep Kit (Invitrogen) as follows. Bacteria were harvested by centrifugation of the LB broth at 4000g for 10 minutes. The pellet was resuspended in 10mls of resuspension buffer (50 mM Tris-HCl pH8, 10mM EDTA) with 20mg/ml RNase A, before mixing with 10mls lysis buffer (0.2M NaOH, 1% (w/v) SDS) to release the plasmid from the bacteria. The cell debris and genomic DNA were then precipitated out of solution with 10mls precipitation buffer (3.1M potassium acetate pH5.5) and centrifugation at 12000g for 10 minutes. The supernatant containing the plasmid was then passed through a pre-packed, equilibrated anion exchange column and the negatively charged phosphates on the DNA backbone interacted with the positive charges on the surface of the resin, allowing the removal of RNA, proteins, carbohydrates and other impurities with the wash buffer (0.1M sodium acetate pH5, 825mM NaCl). The plasmid DNA was eluted from the column under high salt conditions, with the elution buffer (100mM Tris-HCl pH8.5, 1.25M NaCl) and precipitated by centrifuging at 15000g for 30 minutes at 4ºC in 10.5mls isopropanol. The plasmid DNA was then washed with

70% (v/v) ethanol, recentrifuged at 15000g for 5 minutes and resuspended in 200 µl of TE buffer (10mM Tris-HCl pH8, 0.1mM EDTA).

The purified DNA was diluted and quantified by using an Ultrospec 3000 spectrophotometer (GE Healthcare, Amersham, UK) to measure the UV absorbance at 260nm (A_{260}). The yield of DNA (µg/ml) was calculated by A_{260} x 50 x dilution factor, which is based on the assumption that A_{260} = 1 for a 50µg/ml solution.

This DNA was then used as a template for PCR reactions.

2.5.1.1 PCR conditions

PCR conditions were optimised using a range of magnesium concentrations (2.5-4mM) and annealing temperatures (56-60ºC). The optimal conditions for the TRAIL DNA were 20ng of plasmid DNA in a total of 25µl of PCR reaction mix (final concentrations 3mM $MgCl_2$, 0.4µM each of forward and reverse primers, 1 U/ml Taq DNA polymerase, 200µM deoxyribonucleotide triphosphate (dNTP), 1x NH_4SO_4 buffer in distilled and deionised water (ddH20); all reagents from Bioline, London, UK). The PCR microtubes were covered and placed in a pre-programmed tetrad thermocycler (MJ Research, CA, USA). The thermocycling conditions used were an initial denaturing cycle (94°C, 2mins) followed by 30 cycles of denaturing, annealing and extension (94°C, 45 secs; 56°C, 45 secs; 72°C, 1 min) and a final cycle of extension (72°C, 2 mins). The primers were designed to ensure that the DNA sequence encoding the full length TRAIL ((flTRAIL); amino acids 1-281) and the extracellular portion of TRAIL ('soluble TRAIL'; sTRAIL) (amino acids 114-281) were flanked by the restriction enzymes Mlu1 and BstB1 at the 5' and 3' ends respectively (Table 2.1, Figure 2.1).

Primer	Nucleotide sequence
5' flTRAIL	5'-GTACGCGTGCCACCATGGCTATGATGGAGGTCCAGG-3'
3' flTRAIL	5'-GTCGTTCGAATTAGCCAACTAAAAAGGCC-3'
5' sTRAIL	5'-GTACGCGTGCCACCATGGTGAGAGAAAGAGGTCCTCAG-3'
3' sTRAIL	5'-GTCGTTCGAATTAGCCAACTAAAAAGGCC-3'

Table 2.1 Primers used to flank full length (fl) and soluble (s) TRAIL with Mlu1 and BstB1 restriction enzymes.

Gel separation electrophoresis was used to confirm the products were of the expected size (flTRAIL 864 base pairs (bp), sTRAIL 528 bp). The gel was prepared by dissolving 1.5% agarose (w/v) in 100mls 1 x TBE (0.045 M Tris-Borate, 0.001M EDTA, pH8). Ethidium bromide was added to the gel at a final concentration of 0.5µg/ml). The gel, once solidified, was placed in a gel tank filled with 1 x TBE running buffer. 2µl of 5 x loading buffer (5% Orange G (w/v) in glycerol) was mixed with 8µl of each PCR product and run on a lane of the gel. A DNA molecular marker (Marker VIII, 0.25µg/ml, Boehringer, Mannheim, Germany) was also used. The gel was run for 35 minutes at 80 volts. The DNA bands were then visualised using a UV transilluminator (FLA-3000, Fuji, Bedford, UK) and Syngene Gene Genius Bio-imaging system (Synoptics, MD, US).

After confirmation that the products were of the correct size, the DNA from the PCR was purified using the QIAquick PCR Purification Kit (Qiagen, Crawley, UK). The PCR mix was diluted 1:6 into Buffer PBI, which has a high salt content and allows the DNA to absorb to the silica membrane of the spin columns. These were then centrifuged at 16200g for 1 minute, washed with 750 µl of buffer PE and centrifuged twice more for 1 minute to remove the other impurities such as primers and enzymes from the mix. The DNA was then eluted with 10µl ddH20, and the yield reassessed by measuring the absorbance at 260nm as above.

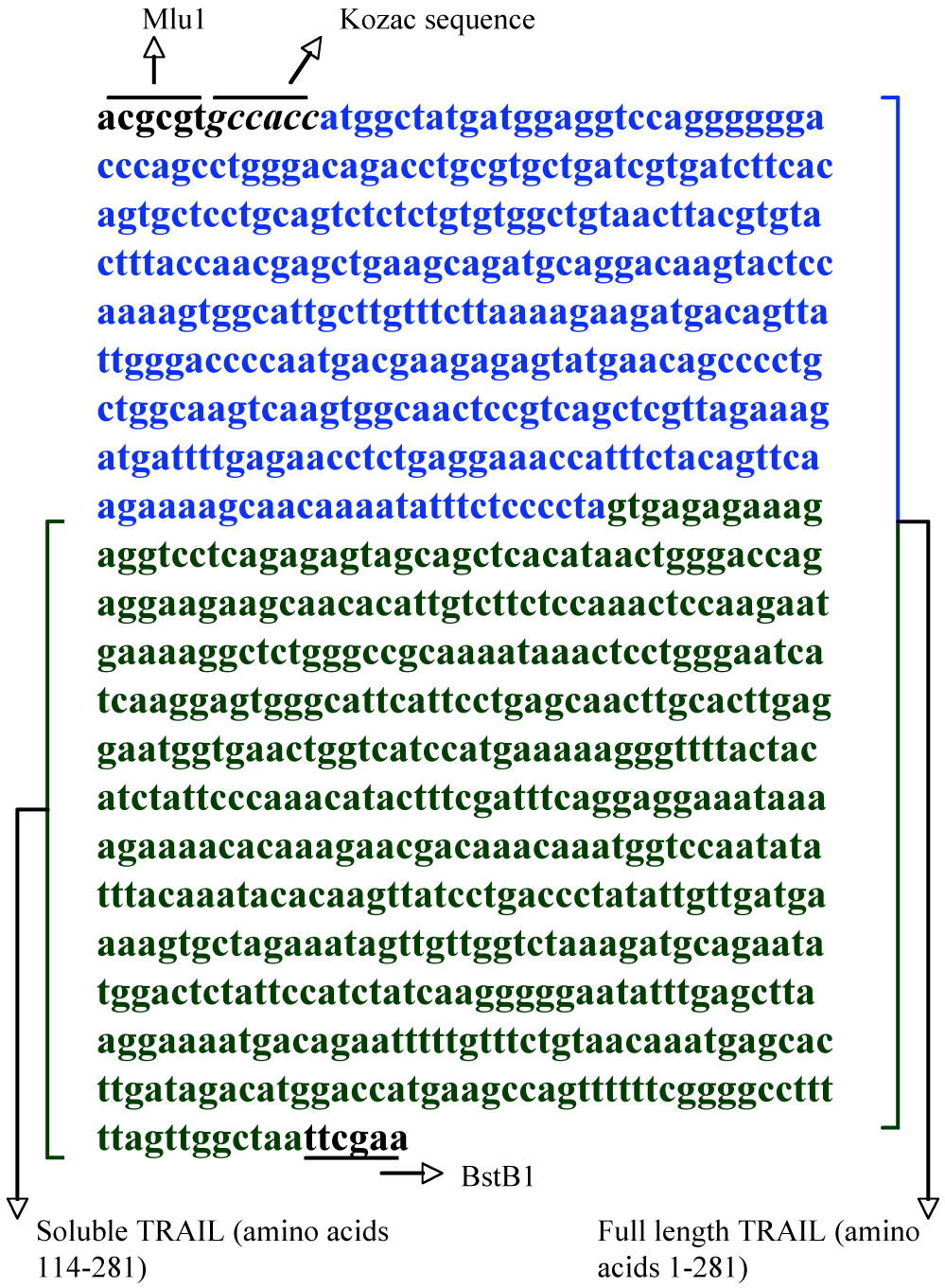

Figure 2.1 The sequence of full length TRAIL containing the restriction enzymes Mlu1 and BstB1

2.5.2 Production of lentiviral backbone for plasmid

The lentiviral plasmid vector carrying the Tetracycline (Tet)-inducible system (Figure 2.2A, a kind gift from A. Thrasher, London, UK) was used as a backbone for the incorporation of TRAIL DNA. This plasmid had been produced from a pRRL-derived self inactivating backbone into which the Tet-on system elements had been introduced, and had shown to have low background activity and high levels of induction over months in vitro and in vivo (Barde et al., 2006).

The TRAIL gene that had been cloned as above could have been directly inserted into this lentiviral backbone. However, Dr. Susana Aguilar had also used this lentiviral plasmid vector for the addition of a different insert, the human dickoff (DKK) gene. With this gene, internal ribosome entry site-green fluorescent protein (IRES-GFP) had also been added to the lentiviral plasmid vector, which would be a useful addition to my plasmid, allowing readout of the TRAIL transgene expression. In order to insert DKK and IRES-GFP into the lentiviral plasmid backbone, the DKK gene had first been cloned into the pENTR1A vector tool containing IRES-GFP (Figure 2.2B). This had been done by flanking the DKK with the restriction enzymes Sal1 (at the 5' end) and BamH1 (at the 3' end) by PCR amplification of DKK, using the primers in Table 2.2.

Primer	Nucleotide sequence
5' DKK	5'-ACGCGTCGACATGATGGCTCTGGGCGCAGC-3'
3' DKK	5'- ACGCGGATCCTTACGTAGAATCGAGACCGA -3'

Table 2.2 Primers used to flank DKK with Sal1 and BamH1 restriction enzymes to allow entry into the pENTR1A plasmid adjacent to IRES-GFP .

The DKK gene was then inserted into the pENTR1A vector adjacent to the IRES-GFP with the Sal1 and BamH1 restriction enzymes. The DKK-IRES-GFP section was then flanked by Mlu1 and EcoRV restriction enzymes by further PCR

amplification, using the primers in Table 2.3, in order to position it into the Tet-inducible lentiviral plasmid

Primer	Nucleotide sequence
5' DKK-IRES-GFP	5'-ACGCACGCGTATGATGGCTCTGGGCGC-3'
3' DKK-IRES-GFP	5'-ACGCGATATCTCGAGTGCGGCCGCTTTA -3'

Table 2.3 Primers used to flank DKK-IRES-GFP with Mlu1 and EcoRV restriction enzymes to allow entry into the Tet-inducible lentiviral plasmid.

This section was then cut out of this vector and positioned into the lentiviral plasmid using the Mlu1 and Eco RV restriction sites, which also removed the alkaline phosphatase section from the original lentiviral plasmid vector (Figure 2.2C). This produced an intermediate plasmid, lentivirus plasmid DKK, which I directly worked with.

Unique restriction enzyme cutting sites (Mlu1, BstB1) that flanked the DKK gene were found on this intermediate plasmid using NEBcutter v2.0 (http://tools.neb.com/NEBcutter2/index.php) allowing the DKK gene to be removed and the TRAIL gene to be inserted whilst retaining the useful IRES-GFP readout construct (Figure 2.2D,E).

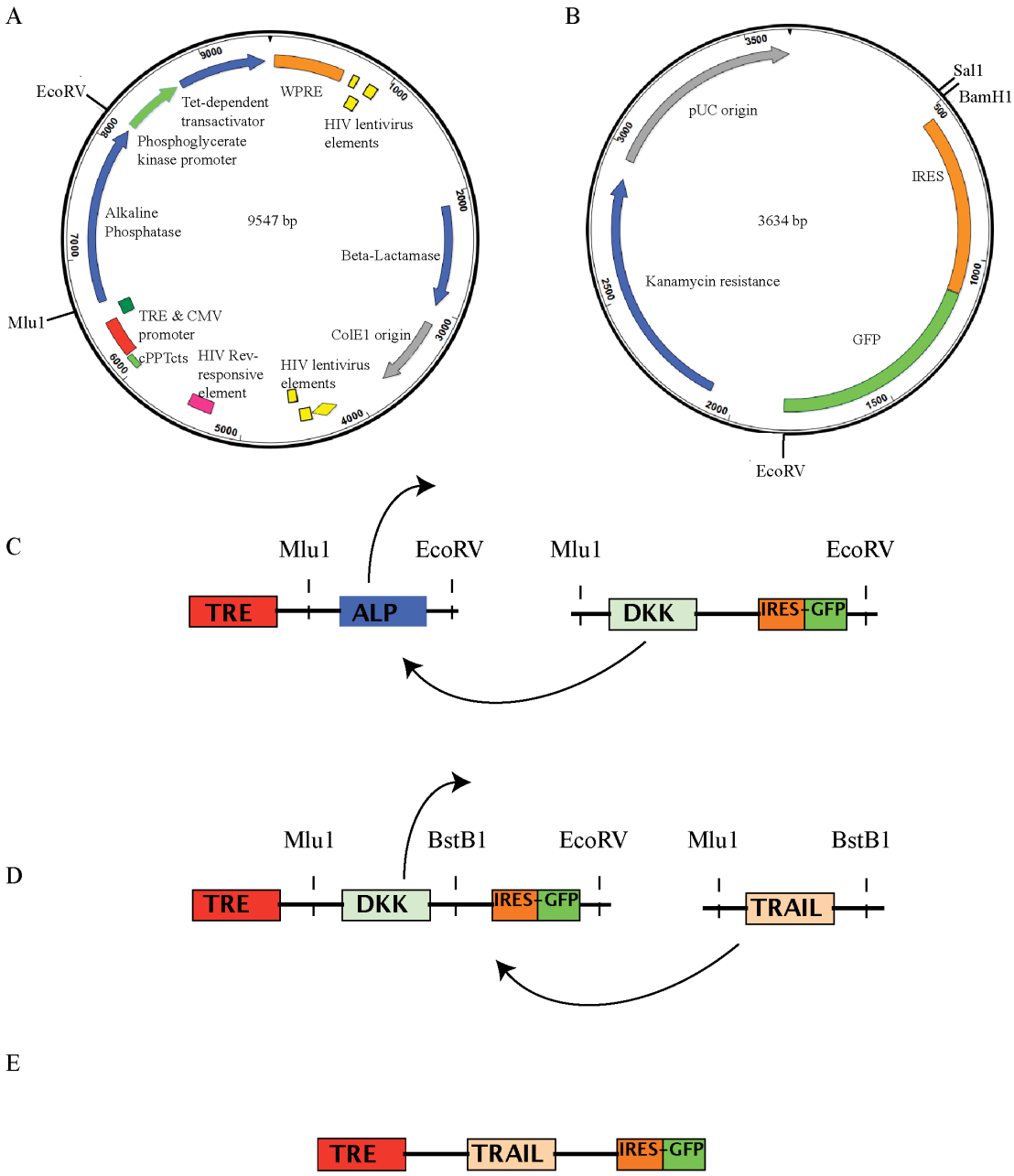

Figure 2.2 Production of plasmid constructs.
A) Original tetracycline (Tet)-inducible lentivirus, B) pENTR1A vector containing IRES-GFP, used for cloning Dickoff (DKK) next to IRES-GFP. C-E) simplified plasmid manipulation, C) alkaline phosphatase (ALP) section cut out of Tet-inducible lentivirus with Mlu1/EcoRV and replaced with DKK-IRES-GFP. D) DKK section cut out of Tet-inducible lentivirus with Mlu1/BstB1 and replaced with TRAIL (soluble or full length). E) Final Tet-inducible TRAIL lentivirus plasmid with GFP readout. WPRE: Woodchuck hepatitis virus responsive element, cPPTcts: central polypurine tract with termination sequence, CMV: cytomegalovirus, IRES: internal ribosome entry site, GFP: green fluorescent protein, HIV: human immunodeficiency virus.

2.5.2.1 Restriction enzyme digestion

All restriction digests were performed with enzymes and buffers supplied by New England Biolabs ((NEB), Hitchin, UK), unless otherwise stated. The purified flTRAIL and sTRAIL DNA flanked by Mlu1 and BstB1 products produced in section 2.2.1.1 were digested sequentially with the restriction enzymes BstB1 (1x Buffer 4, 1000 U/ml BstB1 in 100µl ddH20 for 1 hour at 65ºC) and Mlu1 (1x Buffer 3, 500 U/ml Mlu1 in 100µl ddH20 for 1 hour at 37ºC) with DNA purification between the 2 reactions using the QIAquick PCR Purification Kit as described above.

The intermediate lentivirus plasmid DKK was also digested sequentially with BstB1 and Mlu1. To stop religation of single cut vectors, dephosphorylation of the 5' ends was performed using 260U/ml alkaline phosphatase, calf intestinal (CIP) and 1x buffer 3 (both from NEB) in ddH20 for 90 minutes at 37ºC. The product from the digest and dephosphorylation reactions was then run on a 1% (w/v) agarose gel using the HyperLadder1 molecular weight marker (Bioline). A 1% (instead of 1.5%) agarose gel was used to allow the larger products to run efficiently. An ultraviolet lamp was used to demonstrate the 823bp DKK gene and the separate 9350bp lentiviral plasmid. The lentiviral plasmid was cut out of the gel and a QIAquick Gel Extraction Kit (Qiagen) was used to isolate and purify the DNA for the Tet-on lentiviral plasmid backbone, which was cut at Mlu1 and BstB1 restriction sites. The gel segment containing this lentivirus plasmid backbone was weighed and dissolved in Buffer QG (300µl of added for each 100mg of gel) at 50ºC. Isopropanol (100µl of added for each 100mg of gel) was then added and the solution placed in a spin column, where the DNA adsorbed to the silica membrane. These columns were then centrifuged at 16200g for 1 minute, washed with 500 µl of buffer QG and recentrifuged. 750 µl of buffer PE was then added to the column and centrifuged twice more for 1 minute to ensure removal of the impurities. The DNA was then eluted with 10µl ddH20 and the yield reassessed by measuring the absorbance at 260nm as above. This construct was then used for the incorporation of the TRAIL DNA.

2.5.3 Production of the flTRAIL, sTRAIL, and empty Tet-inducible plasmid.

The soluble and full length TRAIL inserts were separately ligated with the lentiviral plasmid vector at room temperature for 1 hour using 20000U/ml T4 DNA Ligase and 2µl DNA T4 Ligase Reaction Buffer (both from NEB) made up to a reaction volume of 20µl with ddH20. Molar ratios of 0:1, 1:1, 5:1,and 10:1 (insert:vector) were used in separate reactions with 50ng (10µl) of the vector in each reaction. The ligation mixtures were transformed into library efficient *E. coli* DH5α competent cells (Invitrogen) by mixing 50µl of the competent cells with 4µl (10ng plasmid) of the ligation mix. This mixture was incubated on ice for 30 minutes, followed by 42ºC for 45 seconds and ice for 2 minutes. It was then added to 900µl S.O.C. medium (Invitrogen) and incubated at 37ºC, 220rpm for 1 hour in an orbital shaker. The solution was then centrifuged at 800g for 3 minutes and the pelleted bacteria resuspended in 200µl S.O.C. medium before being plated on ampicillin (50µg/ml) impregnated LB agar plates and incubated at 37ºC overnight. Individual colonies were apparent following incubation from all the ligation mixtures apart from the negative control (0:1; insert:vector).

Before using these colonies to produce large quantities of sTRAIL and flTRAIL lentivirus plasmid with a maxiprep procedure as in 2.5.1, several of the individual bacterial colonies were tested for the presence of the TRAIL containing plasmids by colony PCR and a faster miniprep procedure. Colony PCR involved the same PCR conditions as in section 2.5.1.1, with a loop used to transfer a small amount of an individually marked bacterial colony to a total of 25µl of PCR reaction mix (final concentrations 3mM $MgCl_2$, 0.4µM each of forward and reverse primers, 1 U/ml Taq DNA polymerase, 200µM deoxyribonucleotide triphosphate (dNTP), 1x NH_4SO_4 buffer in ddH20). The majority of colonies produced TRAIL products on this PCR suggesting the incorporation of the TRAIL lentiviral plasmid. Selections of these colonies were then used to inoculate 5ml starter cultures of LB broth containing 50µg/ml ampicillin. These were incubated for 6 hours at 37ºC on an orbital shaker at 220 rpm, before 1.5mls were used for a miniprep using the FastPlasmid mini kit (Eppendorf, Cambridge, UK). The 1.5 ml culture was centrifuged at 16200g to pellet the bacteria, which was resuspended in 400µl of an ice cold lysis solution containing a mixture of enzymes and detergents that serves to

resuspend the bacterial pellet and lyse bacteria, denature and solubilise the cellular components, degrade RNA, and trap DNA. The lysate was then added to spin columns and centrifuged at 16200g for 1 minute prior to the addition of 400µl alcohol based-wash buffer and 2 further centrifuges. The DNA was then eluted in 50µl of TE buffer (10mM Tris-HCl pH8.5, 0.1mM EDTA). The purified plasmid DNA was quantified by measuring the UV absorbance at 260nm. A miniprep produces significantly less purified plasmid than the maxiprep, however it is a much quicker procedure and was used to test the accuracy of the plasmid DNA before the maxiprep was performed.

To confirm that the DNA product from the minprep was correct, the plasmid DNA was cut with restriction enzymes, run on a 1% agarose gel and the bands visualised using a UV transilluminator, as previously. In order to distinguish between the planned TRAIL lentivirus plasmid and the original intermediate plasmid with DKK inserted, restriction enzyme cutting sites that cut the lentivirus plasmid TRAIL differently from the original intermediate lentivirus plasmid DKK were found on using NEBcutter v2.0. The restriction enzyme Xba1 (Fermentas, Ontario, Canada) was able to cut the TRAIL lentivirus plasmid twice leaving 2 products of 808 base pairs (bp) and either 9401bp (flTRAIL) or 9288bp (sTRAIL), whereas the enzyme cut the intermediate lentivirus plasmid DKK three times producing 7405bp, 808bp, 1960bp fragments (Figure 2.3A,B). This enzyme (1x Buffer Y^+/Tango/BSA, 75U/ml Xba1) was added to 0.5µg DNA from the miniprep, made up to 20µl in ddH20, and incubated overnight at 37ºC before running on the agarose gel (Figure 2.3C).

The remainder of the 5ml LB starter cultures that had produced the correct flTRAIL and sTRAIL lentiviral plasmid products on miniprep were then used to inoculate 200mls of LB broth containing 50µg/ml ampicillin for overnight incubation on the orbital shaker prior to purification using the Purelink HiPure Plasmid DNA Maxiprep Kit as described earlier (2.5.1). After production, purification and quantification of the sTRAIL and flTRAIL lentivirus plasmids, the validity of the constructs were confirmed by DNA sequence analysis (Cogenics, Essex, UK).

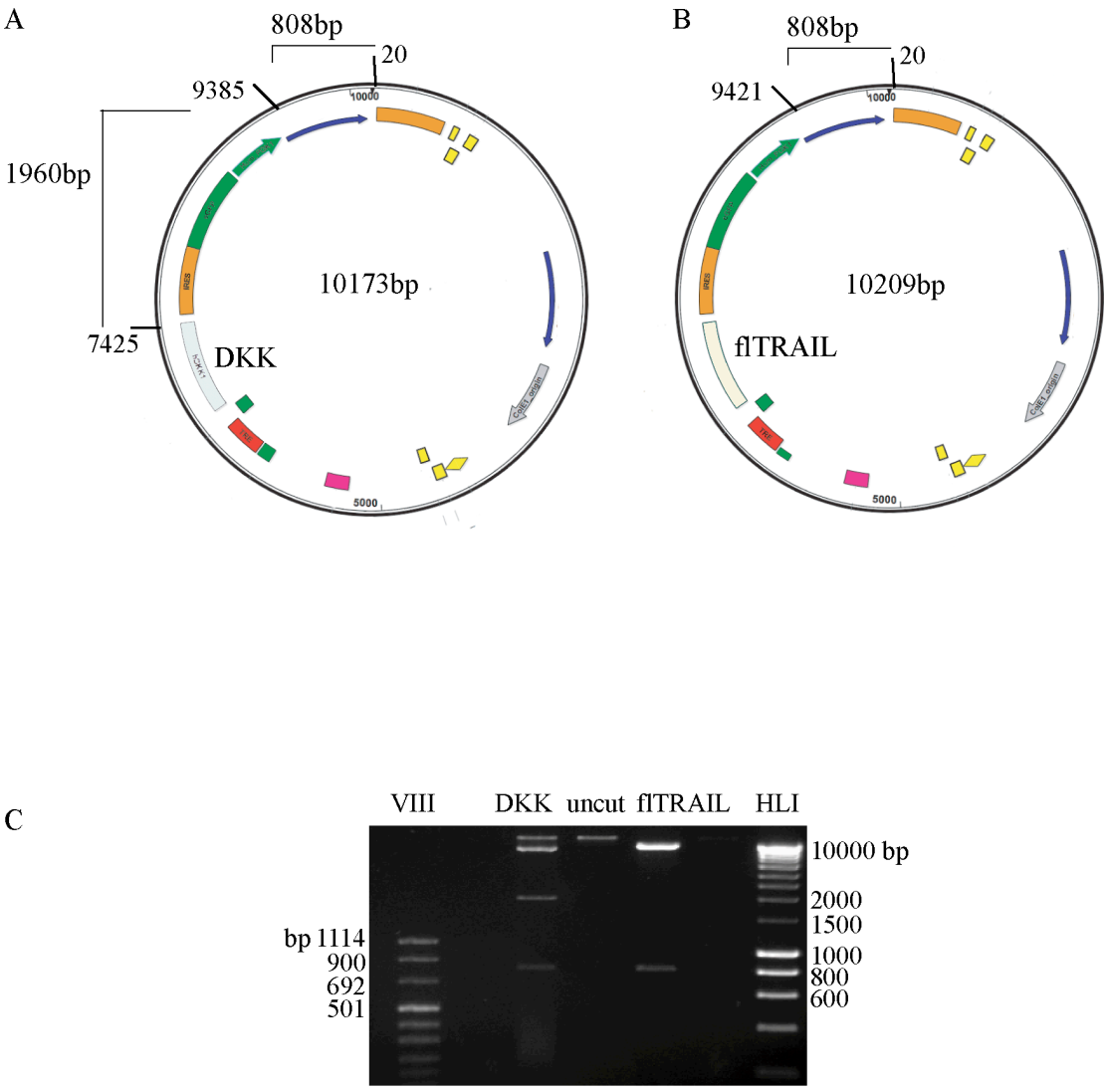

Figure 2.3 Xba1 digestion distinguishes the TRAIL lentivirus plasmid from the intermediate DKK lentivirus plasmid.

A-B) Xba1 restriction enzyme cutting sites on A) Intermediate DKK inducible lentivirus plasmid and B) full length TRAIL (flTRAIL) inducible lentivirus plasmid. C) UV visualisation of Xba1 cut plasmid on a 1% agarose gel. The DKK lentivirus plasmid is cut 3 times with Xba1 and produces 10173bp (uncut), 9365bp, 1960bp, and 808bp segments, whereas the flTRAIL lentivirus plasmid can be distinguished from this by being cut only twice and producing 9401bp and 808 bp segments. The uncut flTRAIL vector (uncut) (10209bp) is also shown as a negative control. DNA molecular weight marker VIII (VIII) and hyperladder I (HLI) molecular weight markers were used.

An empty vector lentivirus plasmid containing IRES-GFP, but neither DKK nor TRAIL had been produced and sequenced by Dr. Susana Aguilar. Briefly, IRES-GFP flanked by the restriction enzymes Mlu1 and EcoRV was produced by PCR of the pENTR1A plasmid, using the primers in Table 2.4. The PCR product was then ligated into the lentiviral plasmid using the Mlu1 and EcoRV restriction sites in the same way as the DKK had been introduced (section 2.5.2).

Primer	**Nucleotide sequence**
5' IRES-GFP	5'-ACGCACGCGTGCCCCTCTCCCTCCC-3'
3' IRES-GFP	5'-ACGCGATATCTCGAGTGCGGCCGCTTTA-3'

Table 2.4 Primers used to flank IRES-GFP with Mlu1 and EcoRV restriction enzymes to allow entry into the Tet-inducible lentiviral plasmid.

In order to amplify the amount of this empty vector lentivirus plasmid, it was transformed into DH5α *E. coli,* streaked onto LB agar plates overnight and the colonies used to inoculate LB broth as a substrate for maxiprep production and purification, as with flTRAIL and sTRAIL lentivirus plasmids. The plasmid product (0.5μg) was then checked by cutting out the IRES-GFP section (1331bp) with EcoRV and Mlu1 restriction enzymes (1x buffer 3, 500 U/ml Mlu1, 1000U/ml EcoRV, 100μg/ml BSA, made up to 20μl in dH_2O and incubated at 37°C for 1 hour) and demonstrating the correct product sizes (1331bp and 7969bp) after running on a 1% agarose gel.

At the end of the maxipreps, between 1.5 and 2mg of validated flTRAIL, sTRAIL, and empty lentivirus plasmid were produced and stored at -20°C for further use.

2.6 Plasmid introduction into cells

2.6.1 Transient transfection

Transient transfection was used to assess the function of the flTRAIL, sTRAIL and empty lentivirus plasmids within cells using a simple and rapid technique. Transfection describes the introduction of nucleic acids into cells by non-viral methods. It typically involves the opening of transient pores in the cell membranes to allow the uptake of the plasmid. The cationic polymer polyethylenimine (PEI), which binds to the negatively charged DNA and is taken up in the cell by endocytosis, and Fugene (Roche Diagnostics Ltd, Burgess Hill, UK), a blend of non-liposomal lipids, were used for transfection

For PEI-based transfection, $1x10^6$ 293T cells were seeded in a 6-well plate. The following day, at 80-90% cell confluence 75μl Optimem plus 3-15μl of 10mM polyethylenimine (PEI) was added to a mixture of 75μl Optimem and 3μg of plasmid. After 20 minutes the solution was added to the 6-well plate and they were incubated at 37°C for 4 hours. The medium was then replaced with normal medium and 10μg/ml doxycycline. The success of the transient transfection procedure was then assessed by the proportion of GFP-positive cells on flow cytometry. Using this assessment, 9μl of PEI in the above reaction was found to be optimal.

For Fugene-based transfection, $3x10^5$ 293T cells were seeded in a 6-well plate. The following day, 2μg of plasmid was added to 150μl Optimem plus 6μl of Fugene and after 20 minutes, the solution was added to the 50-60% confluent 293T cells. The cells were incubated at 37°C for 4 hours and the medium was then replaced with normal medium and 10μg/ml doxycycline. The success of the transient transfection procedure with this technique was similarly assessed by GFP expression. This technique was found to be less successful than the PEI-based transfection, which was therefore used for further experiments and lentivirus production.

2.6.2 Stable transduction

The advantage of transient transfection is the ability to assess the function of the plasmid within cells using a simple and rapid technique. However, the DNA is not inserted into the nuclear genome and is hence lost after cell division. For this project, the stable and long-term expression of the transgene was necessary. The transduction of cells generally describes the introduction of nucleic acids into cells by viral methods and the use of a lentivirus enables incorporation of the DNA into the host cell's genome with stable transgene expression.

2.6.2.1 Production of lentivirus

Lentiviral vectors, pseudotyped with the vesicular stomatitis G protein (VSV-G), were produced by transfecting 293T cells with the plasmids, as follows. Twelve million 293T cells were seeded in a 175 cm^2 flask. The following day, at 80-90% cell confluence, the medium was exchanged for 15mls of Optimem plus 10mls of a solution made by mixing 3.6ml PEI and 56.4ml Optimem, to 600μg TRAIL plasmid, 450μg of the packaging construct pCMV-dR8.74, 150μg of a plasmid producing the VSV-G envelope (pMD.G2) and 60mls Optimem (both pCMV-dR8.74 and pMD.G2 were a kind gift from A. Thrasher, UCL, London, UK).

The cells were incubated at 37ºC for 4 hours and the medium was then exchanged for the normal cellular medium. The following day, the medium was exchanged for 17ml of normal medium into which the lentivirus was secreted. This medium containing the virus was collected and purified by centrifugation at 2500rpm at 4ºC to remove cell debris, and then filtered through a 0.45μm membrane. The virus was subsequently concentrated by ultracentrifugation at 18000 rpm at 4ºC (SW28 rotor, Optima LE80K Ultracentrifuge, Beckman, High Wycombe, UK). The viral pellet was resuspended in 50μl PBS, centrifuged at 4000rpm 4ºC and the supernatant containing the virus stored at -80ºC before use.

2.6.2.2 Titration of lentivirus

The amount of collected virus generated by the above method was quantified by titrating different dilutions of the virus with 293T and Hela cells. Fifty thousand cells were seeded onto each well of a 12-well plate. The following day at 30-40% cell confluency, the medium was exchanged for medium containing virus dilutions of 1/100, 1/1000, 1/10000, and 1/100000 and 4μg/ml of polybrene, which is a cationic polymer enabling efficient cellular uptake of the virus. The following day, the medium was replaced with normal medium and 10μg/ml doxycycline. After a further 48 hours, the cells were trypsinised and the percentage of GFP-positive cells at each viral dilution assessed by flow cytometry. The viral titre was calculated in virus particles/ml as below:

$$\text{Viral titre} = \frac{\%\text{ of GFP cells} \times \text{dilution of virus} \times \text{number of cells infected (i.e. 50000)}}{100}$$

2.6.2.3 Stable transduction of MSCs

Human mesenchymal stem cells were transduced with the lentivirus when 30-40% confluent in a similar manner to the 293T and Hela cells above. The amount of virus used was expressed as the number of virus particles per MSC. This is defined as the multiplicity of infection (MOI). For MSC transduction, an MOI of 10 (in accordance with previous reports (Aguilar et al., 2007; Chan et al., 2005)) and 20 was used. The transduced MSCs were then cultured with 10μg/ml doxycycline and the success of the transduction quantified by the percentage of GFP-positive MSCs on flow cytometry assessment.

2.7 In vitro TRAIL transgene expression

2.7.1 Antibodies

The primary antibodies used for flow cytometry were a rabbit polyclonal antibody to TRAIL (H257, sc-7877, 1μg/ml), and a mouse monoclonal antibody to TRAIL (2E5, sc-51709, 2.5μg/ml), both from Santa Cruz Biotechnology (CA, US).

The primary antibodies used for western blotting were a rabbit polyclonal antibody to TRAIL (H257, sc-7877, 1μg/ml) and a mouse monoclonal antibody to β-actin (sc-130300, 0.2μg/ml), both from Santa Cruz Biotechnology.

2.7.2 Flow cytometry

Flow cytometric analysis was performed on either a FACSCalibur or LR2 machine. Electronic compensation of the recording was performed to minimise overlap of emission spectra. Samples were gated according to forward scatter and side scatter characteristics to exclude cell debris and cell doublets. A minimum of $1x10^5$ gated events was collected for each sample analysed. Sample analysis and quantitation was performed using FlowJo Software.

GFP fluorescence was detected using a blue excitation laser (488nm) and 530/30 nm band pass filter. The secondary antibody AlexaFluor 647 binding was detected using a red excitation laser (635nm) and 660/20 nm band pass filter. Dead cells were detected with 2.5μg/ml PI or 1μg/ml 4',6-diamidino-2-phenylindole (DAPI). PI was detected with the blue laser and 610/20 nm filter, whereas DAPI detection utilised the ultraviolet laser (355nm) for excitation and a band pass filter at 440/40 nm. DiI-labelling (Invitrogen) of cells was detected using the blue excitation laser and 575/26nm band pass filter. TRAIL surface antibody detection was performed by washing cells with PBS followed by mobilisation with 300μl 0.05% trypsin in EDTA. Cells were pelleted by centrifugation (300g, 5 mins) and then resuspended in 100μl of PBS with the primary antibody for 30 minutes at room temperature. The

cells were washed and resuspended in 100µl of PBS with a AlexaFluor 647 goat anti-mouse or goat anti-rabbit secondary antibody for 30 minutes at room temperature, before washing and resuspending in 500µl of PBS.

2.7.3 Western blots

2.7.3.1 Sample collection and preparation

Cells were grown in 12-well plates. Supernatants were collected and centrifuged (300g, 5mins) to remove cells and cell debris and then stored prior to western blotting at -80°C. Cell lysates were obtained by lysing the cells with 100µl RIPA buffer (1% (v/v) Igepal Ca-630, 0.5% (w/v) Sodium deoxycholate, 0.1% (w/v) sodium dodecyl sulphate (SDS)) supplemented with complete protease inhibitor cocktail (Complete-mini; Roche Diagnostics Ltd.) and left to stand for 5 minutes. The cell layer was subsequently scraped with a pipette tip and the lysate centrifuged (16200g, 10 mins, 4°C) to remove insoluble cell debris. The supernatant was collected and the DNA sheered by passing the sample 15 times through a 25G needle. Samples were stored at -80 °C.

2.7.3.2 BCA protein assay

To ensure equivalent amounts of protein were loaded for the different samples, protein concentration of cell lysates or supernatants was assessed using the bicinchoninic acid (BCA) protein assay (Thermo Fisher Scientific, IL, US). 20µl of each sample or standard (bovine serum albumin (BSA)) was added to 200µl of BCA working reagent in a 96-well plate. The plate was agitated on a plate shaker for 30 seconds, and then incubated at 37°C for 30 minutes prior to reading the absorbance at 550nm on a Titertek Multiscan MCC/340 plate reader (Labsystems, Turku, Finland). The absorbance of the samples was compared to the standards (of known protein concentration) to ascertain the sample protein concentration.

2.7.3.3 Western blotting procedures

Samples were diluted in dH_2O to equivalent protein concentrations and mixed with 5x Laemmli Buffer (3.125mM Tris-base pH 6.8, 10% (w/v) SDS, 20% (v/v) glycerol, 50mM Dithiothreitol (DTT), in dH_2O with bromophenol blue). The samples were then incubated on a heat block for 10 min at 110°C and placed on ice prior to loading on the western blot gel. A 10% SDS-polyacrylamide resolving gel (10% (v/v) acryamide mix (0.27% bis-acrylamide)) (Geneflow Ltd., Fradley, UK), 0.04% (v/v) tetramethylethylenediamine (TEMED), 0.1% (w/v) ammonium persulphate (APS), 0.1% (w/v) SDS, 0.3M Tris-base (pH8.8), in dH_2O) with a 2.5% stacking gel (2.5% acrylamide mix, 0.05% TEMED, 0.05% APS, 0.05% SDS, 0.06M Tris (pH6.8), in dH_2O) was prepared and 25µl samples added to the wells. 5µl of SeeBlue® Plus 2 protein ladder (Invitrogen) was also loaded. The gel was run at 100V in Tris/Glycine/SDS running buffer (0.25M Tris-base, 1.92M Glycine, 1% SDS, in dH_2O).

Following separation, the gel was removed from the cassette and proteins were transferred onto a Hybond-ECL nitrocellulose membrane (GE Healthcare), using a horizontal semi-dry transfer method (NovaBlot; Pharmacia LKB, Uppsala, Sweden) with transfer buffer (25mM Tris-base, 0.2M glycine, 1% (w/v) SDS, 20% (v/v) methanol in dH_2O) at a current of 0.8mA per cm^2 of gel, for 1 hour. The quality of protein transfer was assessed by briefly staining the membrane with 0.1% (w/v) PonceauS solution and then the blot was placed in Tris-buffered saline (TBS)(20mM Tris-base, 150mM NaCl, pH7.4) containing 0.1% (v/v) Tween20 (TBST).

Blots were incubated with blocking buffer containing 5% (w/v) non-fat dry milk in TBST for 1 hour. Blots were then incubated with primary antibodies in 5% (w/v) BSA in TBST overnight at 4°C. All blots were then washed 3 x 5 mins in TBST and incubated for 1 hour at room temperature with HRP-conjugated secondary antibody. After further washing in TBST, 2ml of ECL reagent (GE Healthcare) was applied to the membrane and incubated for 1 minute. Excess reagent was drained off and immunoreactive bands were visualized by exposing the membrane to autoradiography film (Hyperfilm, GE Healthcare), for between 30 seconds and 5 minutes.

2.7.4 ELISA assay

ELISAs were performed using the human TRAIL Quantikine ELISA kit (R&D systems, Abingdon, UK). Cell supernatants were prepared by removing particulates by centrifugation (300g, 5 mins). Cell lysates were prepared by suspending cells in the supplied cell lysis buffer at 37 °C for 30 minutes at 1 x 10^7 cells/ml, followed by centrifugation (500g, 15 mins). Samples (50µl) containing equal amounts of protein (assessed by the BCA assay) were added to 100µl of assay diluent RD1S and incubated at room temperature onto preprepared ELISA plates for two hours on a horizontal orbital microplate shaker set at 500rpm. The plates were washed 4 times with wash buffer and 200µl TRAIL conjugate added to the wells for 2 hours at room temperature on the orbital shaker. The plates were then rewashed 4 times and 400µl of a colour substrate solution added before they were incubated in the dark. The reaction was stopped after 30 minutes with the addition of 50µl stop solution. The absorbance at 450nm was determined on a Titertek Multiscan MCC/340 plate reader and compared to known concentrations of recombinant TRAIL (R&D systems), which were used to produce a standard curve, to ascertain the TRAIL protein concentration in the samples. The readings at 540nm were subtracted from the 450nm values to correct for optical imperfections in the plate.

2.8 In vitro TRAIL transgene functional assessment

2.8.1 Agonists and antibodies

For experiments assessing the pharmacological modulation of coculture experiments, the following compounds were used; the pan-caspase inhibitor zVADfmk at 1µg/ml, a soluble recombinant TRAIL at 200ng/ml and a neutralising TRAIL antibody at 250ng/ml (the latter two from R & D Systems).

2.8.2 Coculture experiments

Human MSCs transduced with the full length TRAIL plasmid (MSCFLT) were plated at different ratios with cancer cells. A total of 1x10^5 cells were plated

together in 2ml of the normal MSC medium in each 6-well plate. The following day, 10μg/ml doxycycline, or other active agents, were added to the cocultures and left for 48 hours.

In order to differentiate between cancer cells and MSCFLT, cancer cells were stained with DiI before coculture. The cells to be stained were collected at a concentration of $1x10^6$/ml in medium without serum and 5μl/ml of DiI was added and incubated for 20 minutes at 37ºC. Following this the cells were washed twice in PBS before use. For the coculture of SP cancer cells and MSCFLTs, the cancer cells were stained with DiI as above and then sorted into SP and non-SP populations by FACS as previously described. The freshly sorted SP and non-SP cells were then immediately cocultured with the MSCFLT cells.

2.8.2.1 Apoptosis assessment

The apoptosis and death of the cells in coculture were assessed by Annexin V-based flow cytometry. Media, including floating cells, was collected from each well. Adherent cells were washed with PBS and mobilised with 300μl 0.05% trypsin in EDTA. All cells were collected into centrifuge tubes containing the previously removed media and were pelleted by centrifugation (300g, 5 mins). Cells were washed in medium, centrifuged (300g, 5 mins) and then resuspended in 500μl of Annexin V binding buffer with 5μl of Annexin V-647 antibody (Invitrogen) for 40 minutes on ice. 2μg/ml DAPI or 5μg/ml PI was then added to each sample before flow cytometry analysis. Annexin V is a 35–36 kDa calcium-dependent phospholipid binding protein that has a high affinity for phosphatidlserine. Phosphatidlserine is located on the cytoplasmic side of the cell membrane, inaccessible to cell surface binding proteins, in normal viable cells. In apoptotic cells, it is translocated to the outer plasma membrane, thus exposing it to the external cellular environment and allowing binding of Annexin V. The Annexin V is also able to pass through the membrane of dead cells that have lost their membrane integrity and bind to phosphatidlserine in the interior of the cell. These dead cells however will also stain with the cell impermeant dead cell stains PI or DAPI. Consequently, Annexin $V^-/DAPI^-$ (or PI^-) cells were judged to be viable, Annexin

$V^+/DAPI^-$ cells were considered to be undergoing apoptosis, and Annexin $V^+/DAPI^+$ cells were considered late apoptotic or necrotic, and recorded as dead.

2.8.2.2 Production of dominant negative FADD cancer cells

The mechanism of TRAIL induced apoptosis is via the extrinsic apoptotic pathway. On binding the ligand, activation of the TRAIL receptor leads to recruitment of FADD and caspase 8; the start of the caspase cascade. In order to demonstrate the apoptosis and death caused by the MSCFLT cells was similarly by this mechanism, defective FADD constructs were transduced into Hela cancer cells to disrupt the first part of the extrinsic apoptosis pathway.

AM12s transduced with dominant negative FADD/GFP (dnFADD) or GFP (empty vector) constructs were obtained as a kind gift from Dr. Sam Janes in the host laboratory. In brief, the AM12s were produced as follows. Phoenix packaging cells were transduced with a retroviral vector containing dnFADD/GFP or GFP alone, and 5μg/ml of polybrene. The confluent Phoenix cells released virus into the culture medium. 2.5ml of this medium was collected, filtered through a 0.45μm membrane, and added to AM12 cells with 5μg/ml of polybrene. The AM12 cells had been plated at a density of $2x10^5$ cells per $100mm^2$ dish the previous day. After culture for 12 hours, the medium was replaced with normal medium and the transduced AM12 cells were selected in 2.5μg/ml puromycin.

The dnFADD and empty AM12s were grown to 80% confluence. The medium containing the virus was then collected, filtered through a 0.45μm membrane, and added to Hela cells (30% confluence) with 5μg/ml polybrene. After 24 hours, the medium was changed to normal Hela medium, the cells were then selected with 1μg/ml puromycin, and the expression of GFP checked with an inverted-fluorescent Axiovert S100 microscope (Carl Zeiss Ltd., Herts., UK).

2.8.3 Colony forming ability in coculture

Two hundred freshly FACS-sorted SP or non-SP H357 cells were seeded per six-well plate. MSCFLT cells were separately cultured and their continued proliferation prevented by the addition of 4μg/ml mitomycin C for 2 hours before being washed with PBS. Mitomycin C is an inhibitor of DNA synthesis and nuclear division and is commonly used to metabolically inactivate feeder cells in the culturing of specific cells. The day after the SP and non-SP cells had been seeded, $5x10^4$ mitomycin C-treated MSCFLT cells were added, with or without 10μg/ml of doxycycline. The use of mitomycin C would prevent the continued growth of the MSCFLT and permit SP and non-SP colony formation. After 14 days of coculture, colonies were washed, fixed using 3% PFA, and stained with Rhodanile Blue overnight. Colonies were counted as previously described.

2.9 In vitro assessment of MSC homing to tumours

2.9.1 Antagonists

The neutralising antibodies used for the cell migration assays were a rabbit IgG antiserum fraction against IL-6 (Sigma, 1- 100 μg/ml), and a goat affinity isolated antibody against IL-8 (Sigma, 0.1-10 μg/ml).

2.9.2 Cell migration assay

Migration of MSCs across a transwell was performed to assess in vitro migration, as described previously (Nakamizo et al., 2005; Schmidt et al., 2006; Xin et al., 2007). $1.5x10^5$ cancer cells or 293T cells were plated in 800μl of normal medium containing either 0% or 10% FBS on the bottom well of a transwell plate (8μm pore membrane; Becton Dickenson, Oxford, UK). After 24 hours, neutralising antibodies were added to the bottom well and $4x10^4$ MSCs in 300μl of the same medium (without antibodies) were added to the upper well. The MSCs were allowed to migrate across the membrane for 6-24 hours at 37°C. The cells attached to the upper

side of the membrane were then wiped away with a cotton bud, before the cells that had migrated to the lower side of the membrane were fixed and stained using a Rapid Romanowsky staining kit (Raymond Lamb, Eastbourne, UK). The membranes were removed from the transwells and mounted on slides. The number of cells that had migrated to the lower side of the membrane was counted by taking an average of five fields of view at x10 magnification (Olympus BX40).

2.9.3 Human cytokine array kit

A human cytokine array kit (R&D Systems) was used to assess multiple chemokines and cytokines produced by cancer cells in parallel. The nitrocellulose array membranes contained selected capture antibodies spotted in duplicate.

Cells were grown in 12-well plates. Supernatants were collected and centrifuged (300g, 5mins) to remove cells and cell debris and then stored at -80°C. 1ml of each sample was added to 0.5mls of array buffer and 15µl of detection antibody cocktail and incubated at room temperature for 1 hour. The membranes were blocked prior to use with 2mls array buffer for one hour on a rocking platform at room temperature and following this, the sample mixture was added and the membranes incubated overnight at 4°C. The following day, the membranes were washed 3 times in wash buffer, prior to the addition of 1.5ml Streptavidin-HRP for 30 minutes at room temperature. The membranes were rewashed 3 times and protein binding was detected using the ECL-chemiluminescense detection system (GE Healthcare). Positive signals were detected by exposing the membrane to autoradiography film (GE Healthcare) for 1-10 minutes. This kit was also used to investigate the cytokines and chemokines produced in vivo. For this, whole lungs, individual lobes, or subcutaneous tumours were removed from the mouse and immediately snap frozen in liquid nitrogen. This tissue was then pulverised into a fine powder under liquid nitrogen and stored at -80°C before use. The tissue powder was weighed and standardised before homogenisation in 600µl PBS containing 1% (v/v) Triton X-100 and supplemented with complete protease inhibitor cocktail (Complete-mini; Roche Diagnostics Ltd.). This sample was then centrifuged at 16200g for 5 minutes before the supernatant was used in the array as above.

Semi-quantitative analysis of the cytokine array was performed using densitometery. Films were transformed into digital format by transmissive greyscale scanning at 300dpi on a standard flat bed scanner (Epson, Herts., UK). The scanned images were transferred to the public domain NIH Image J program (developed at the US National Institutes of Health and available at http://rsbinfo.nih.gov/nih-image/) and the optical density of each signal was calculated with reference to a calibration curve (specifically generated by scanning a Kodak photographic step tablet (Kodak, Herts., UK) with known optical density gradient using the same settings as described above). The optical density of the target was then normalised against the optical density of the positive controls, thus allowing correction for protein loading and enabling a meaningful comparison between samples.

2.10 In vivo models

2.10.1 Animals

Six-week old nude and NOD/SCID mice (Harlan, Bicester, UK) were kept in filter cages at the central biological services facility, University College London. The animals were kept on a 12 hour light/dark cycle at 25°C and were provided with filtered air, and autoclaved food and water *ad libitum*. All animal studies were performed in accordance with British Home Office procedural and ethical guidelines

2.10.2 Models

2.10.2.1 Subcutaneous model

Subcutaneous tumours were obtained by the injection of $2x10^6$ MDAMB231, A549, or H357 cells subcutaneously into the left flank with a 29G needle. The cells were prepared and then suspended in 200μl PBS and kept on ice before injection. Tumours were measured every 3-5 days with callipers, and the volume calculated as $4/3\pi r^3$, where r denoted the measured radius.

2.10.2.2 Lung cancer model

A direct injection, lung cancer model was developed with reference to previously described methodology (Doki et al., 1999; Yamaura et al., 1999; Yamaura et al., 2000). A549 cells were prepared and resuspended in a 20μl mixture of PBS and 1mg/ml Matrigel (Becton Dickenson) at a concentration of $1x10^6$/ml. Matrigel is a soluble basement membrane preparation and was used to prevent the cells from leaking out of the lung. Animals were anaesthetised with Halothane (3%) in 2 l/min Oxygen. The left thoracic wall was shaved and cleaned with alcohol. A 5mm incision was made approximately 5mm distal to the angle of the scapula and tissue, fat and muscles were separated by blunt dissection. The left lung motion was observed through the pleura and a 29G needle was then used to inject the cells into the lung at a depth of approximately 3mm. The incisions were sutured using 4.0 prolene and the mice were returned to their cages following recovery. Mice were sacrificed and the lungs harvested at 10-day intervals to ascertain the progression and natural history of this model.

2.10.2.3 Metastatic model

Two million MDAMB231 or A549 cells were prepared and suspended in 200μl PBS and kept on ice before intravenous injection into the lateral tail vein. Mice were sacrificed and the lungs harvested at 10-day intervals to ascertain the progression and natural history of this model.

2.10.3 Use of TRAIL-transduced MSCs

The MSCFLT cells were labelled with CM-DiI using the same protocol described earlier for DiI staining. In the subcutaneous models, MSCFLT cells were either delivered coincidentally with the cancer cells; $2x10^6$ MDAMB231 were mixed with $0.75x10^6$ MSCFLT cells in 200μl PBS and kept on ice before subcutaneous injection, or after tumours had become established; $1x10^6$ MSCFLTs in 50μl PBS were injected into established subcutaneous tumours.

In the metastatic models, 0.5 $x10^6$ - $0.75x10^6$ MSCFLT cells were suspended in 200µl PBS and kept on ice before intravenous injection into the lateral tail vein. The MSCFLTs were injected at timepoints varying between 2 and 34 days after the cancer models had been set up and the exact timings and doses are described in the individual experiments in the results section.

To activate the TRAIL constructs in the MSCFLT cells, mice were fed water containing 2mg/ml doxycycline and 3% (w/v) sucrose.

2.11 Tissue preparation

2.11.1 Histological processing

Mice were sacrificed by CO_2 asphyxiation, followed by laparotomy and exsanguination. Lungs were harvested as follows; the thoracic cavity was opened and the trachea exposed and intubated with a 22G venflon. The lungs were then insufflated with 4% (w/v) PFA at a pressure of 20cm H_2O before the trachea was ligated. The heart and lungs were then removed *en block,* weighed, and placed in 4% PFA at 4°C. After 4 hours, samples were transferred to 15% (w/v) sucrose in PBS and stored overnight at 4°C. Samples were then washed in 30% (v/v) ethanol and transferred to 70% (v/v) ethanol. Lung specimens were divided into separate lobes and along with the heart were processed in paraffin wax. 3µm sections were cut from paraffin embedded specimens and mounted on polylysine slides (VWR, Leicestershire, UK) for staining. Subcutaneous tumours were excised, weighed, and processed in a similar fashion.

2.11.2 Preparation of ex-vivo tumour cells

The tumours were excised and placed in ice cold PBS. They were then finely chopped, incubated with 0.1% (w/v) collagenase A (Roche Diagnostics Ltd.) in PBS and passed successively through a 70µm filter and a 40µm filter (Becton Dickenson) to remove tissue debris. The resulting cell suspension was centrifuged (300g, 5 mins),

and the cell pellet re-suspended in normal cell culture medium. The cells were transferred to 75cm^2 tissue culture flasks and incubated at 37°C in a humidified, 5% CO_2 atmosphere for continued cell growth.

2.11.3 Tissue homogenisation

For real time RTPCR, and the measurement of the production of cytokines and chemokines, whole lungs, individual lobes, or subcutaneous tumours were removed and immediately snap frozen in liquid nitrogen. This tissue was then pulverised into a fine powder under liquid nitrogen and stored at -80°C before use.

2.12 Immunohistochemistry

2.12.1 Antibodies

The primary antibodies used for immunohistochemical localization studies were a rabbit polyclonal antibody to GFP (A6455, 1/1000) from Invitrogen, a rabbit monoclonal antibody to Ki67 (SP6, VP-RMO4, 1/200) from Vector Laboratories (Peterborough, UK), and goat polyclonal antibodies to TRAIL (K-18, sc-6079, 4μg/ml), and vimentin (C-20, sc-7557, 1μg/ml), both from Santa Cruz Biotechnology.

2.12.2 Immunoperoxidase technique

For immunohistochemical staining, 3μm sections were dewaxed and rehydrated by immersion in xylene followed by decreasing concentrations of ethanol through to water. They were then washed twice in PBS. To unmask antigenic epitopes, sections were pre-treated by immersion in 0.01M sodium citrate and microwave heating at high power for two consecutive periods of ten minutes. Pre-treated sections were then washed twice in PBS. Endogenous peroxidise was blocked by immersing sections in 3% (v/v) H_2O_2 for 30 minutes at room temperature. Sections

were then washed twice in PBS and treated with a 1 in 6 solution of serum (matching that in which the secondary antibody was raised e.g. goat serum for a goat anti-rabbit secondary antibody) in PBS containing 4 drops/ml of Avidin block (Vector Laboratories) for 20 minutes at room temperature. Samples were then drained before addition of primary antibody in 1% (w/v) BSA in PBS with 4 drops/ml of Biotin block (Vector Laboratories) for 1-2 hours at room temperature. Appropriate isotype controls were used for each experiment. Samples were washed twice in PBS then treated with a 1:200 dilution of biotinylated secondary antibody (Dako) in PBS 1% (w/v) BSA for 1 hour at room temperature. Samples were rewashed in PBS before the addition of 1:200 Streptavadin HRP (Dako) in PBS for 30 minutes at room temperature. Sections were washed in PBS again, before 3,3-Diaminobenzidine (DAB) peroxidise substrate (Vector Laboratories) was added for 10 minutes at room temperature. Samples were drained, rinsed in dH_2O, counterstained with Gill's Haematoxylin, dehydrated in Xylene and mounted on a coveraid system (Sakura Firetek, CA, US). Microscopy was performed with an Olympus BX 40 light microscope.

The optimal pre-treatment regimen and primary antibody concentration was determined by performing a titration with each antibody with suitable positive and negative controls. This consisted of a range of antibody concentrations, including the recommended dilution, and different antibody unmasking pre-treatments including no pre-treatment, 10µg/ml Proteinase K, or microwave heating in citrate buffer. These sections were then immunohistochemically stained and the optimal conditions selected. The microwave heating in citrate buffer was used for pre-treatment for all the primary antibodies, unless otherwise stated.

2.12.3 Immunofluorescence

For immunohistochemical staining, 3µm sections were dewaxed and washed 3 times in PBS. The CM-DiI retained fluorescence, despite the fixation and dewaxing procedures. The slides were then counterstained with 1µg/ml DAPI and washed twice in distilled water before mounting with Immu-mount (Thermo Electron Corp., PA, US)

For staining of ex-vivo cells, the cells were cultured onto tissue culture plastic microscope slides (Nunc). They were fixed with 4% (w/v) PFA for 20 minutes at room temperature, washed 3 times in PBS, and permeabilised with 0.2% (v/v) Triton X-100 in PBS for 5 minutes. The cells were then blocked with PBS containing 5% (v/v) goat serum, before application of the primary antibody diluted in the blocking solution for 1 hour. After 3 washes, the fluorescent secondary antibody (Alexa 488, 2μg/ml) was applied for a further hour. The cells were then rewashed and 1μg/ml DAPI applied and mounted with Immu-mount. Microscopy was performed with a Carl Zeiss Axioskop 2 fluorescent microscope or with Dr. Liwen Lu on a Bio-Rad MRC 1024 confocal microscope (both Carl Zeiss Ltd.).

2.12.4 TUNEL staining

Apoptosis was detected on histological sections with TUNEL (TdT-mediated dUTP-X nick **e**nd labelling) staining. This relies on the enzymatic labelling of the double-stranded and single-stranded DNA breaks that result from caspase-induced DNA cleavage. The enzyme, terminal deoxynucleotidyl transferase (TdT), catalyzes the template-independent polymerization of deoxyribonucleotides to the 3'-end of single- and double-stranded DNA (Walker & Quirke, 2001).

An in situ cell death detection kit (Roche Diagnostics Ltd.) was used for TUNEL staining. 3μm sections were dewaxed, and washed 3 times in PBS. The tissues were then permeabilised with 10μg/ml Proteinase K for 10 minutes, washed in PBS, and incubated with 50μl of the TUNEL reaction mix at 37 °C, in the dark for 1 hour. The slides were then rinsed in PBS 3 times and analysed with a fluorescent microscope.

2.13 Real-time RT-PCR analysis

In order to minimise degradation of RNA, all reagents were made with molecular biology grade DEPC-treated deionised water (Ambion, TX, USA). All equipment

was cleaned thoroughly using RNaseZap and nuclease free pipette tips (Continental Lab Products, CA, US) were used for all procedures involving RNA.

2.13.1 RNA extraction

RNA was isolated using TRIzol reagent. TRIzol is a solution containing phenol and guanidine isothiocyanate. This dissolves the cell components, while maintaining RNA integrity. 1ml of TRIzol was added to either each well of a 6-well plate, or to a micro-centrifuge tube containing homogenized, snap frozen, ex vivo tissue. The cells in the 6-well plate were scraped with a pipette tip, while the ex vivo tissue was pipetted and vortexed to ensure lysis. The solution was then transferred to a micro-centrifuge tube, and 200µl chloroform added. The tubes were then vortexed and left at room temperature for 5 minutes, before centrifugation at 16200g (15 minutes at 4°C) to separate the mixture into upper aqueous and lower organic phases. The upper aqueous phase containing the RNA was removed to a fresh micro-centrifuge tube and the RNA precipitated with the addition of 0.5ml isopropanol followed by incubation at room temperature for 10 minutes and centrifugation (16200g, 15 minutes, 4°C). The supernatants were discarded and the RNA pellets washed with 500µl ice-cold 75% (v/v) ethanol followed by centrifugation (16200g, 15 minutes, 4°C). The washed pellets were then air dried, before resuspension in 17µl nuclease-free water.

Total RNA was DNase-treated to remove contaminating genomic DNA using an Ambion DNA-free kit. This kit uses DNase I to nonspecifically cleave genomic DNA into 5' phosphorylated oligonucleotides. The 17µl isolated total RNA was added to 2µl DNase buffer, and 1µl DNase I reagent, vortexed, and incubated for 20 minutes at 37°C. The reaction mixtures were placed on ice, and 2µl inactivation resin, which binds DNase I, was then added. The tubes were vortexed and incubated at room temperature for 1 minute, before centrifugation at 2300g for 2.5 minutes at 4°C to pellet the inactivation resin. The supernatant containing the RNA was removed to fresh tubes without disturbing the DNase inactivation resin, which was then discarded.

The quantity of RNA was assessed using the Ultrospec 3000 spectrophotometer by measuring the A_{260}, as described previously with DNA quantification. The yield of RNA (µg/ml) was calculated by A_{260} x 40 x dilution factor, which is based on the assumption that A_{260} = 1 for a 40µg/ml solution. The quality of the RNA was then assessed by running samples on an agarose gel. Samples were prepared as 1µl total RNA dissolved in 11µl DEPC-treated water, with 3µl loading buffer (48% (v/v) deionoised formamide (Invitrogen), 6% (v/v) formaldehyde (BDH), 5% (v/v) glycerol, 0.1% (v/v) ethidium bromide 20 mM MOPS, 5 mM sodium acetate and 1 mM EDTA pH 8.0 made up in DEPC-treated water and dyed with bromophenol blue). Each RNA sample was heated to 65°C for 5 minutes and placed on ice prior to loading. The RNA was separated through a 1.5% agarose-formaldehyde gel (6% (v/v) formaldehyde, 1.5% (w/v) agarose, 20mM MOPS, 5mM sodium acetate, 1mM EDTA, pH 8.0, made using DEPC–treated water) at 80mV for 45 minutes. RNA images were then visualised using a UV transilluminator as with the DNA previously. A ratio of approximately 2:1 of the intensities of the 28S rRNA to the 18S rRNA bands was taken as confirmation that the RNA was not significantly degraded.

2.13.2 cDNA synthesis

Complementary DNA (cDNA) was prepared by reverse transcription using an RT-PCR kit from Applied Biosystems (Warrington, UK). 1µg total RNA of each sample was added to a reaction mix of 5mM $MgCl_2$, 1x reverse transcriptase buffer, 2.5mM dNTP mix, 2.5µM random hexamers, 1U/µl RNase inhibitor, 2.5U/µl MuLv reverse transcriptase, in a 20µl reaction volume. The mix was incubated at room temperature for 10 minutes, 42°C for 15 minutes, 99°C for 5 minutes, and then 5°C for 5 minutes, using a pre-programmed tetrad thermocycler.

2.13.3 Primer design

Primers were designed using internet based software. The ENSEMBL database (http://www.ensembl.org/index.html) was used to find accession numbers for genomic RNA and DNA. These were then inserted into Spidey

(http://www.ncbi.nlm.nih.gov/spidey/), to align genomic and RNA sequences, and locate intron/exon boundaries. Primers were designed to be intron-spanning, to minimize the risk of genomic DNA amplification. The primer-design software, Primer 3 (http://fokker.wi.mit.edu/primer3/input.htm), was used to design primer sequences according to the parameters: product size 85-130bp, primer size 18-22bp, primer melting temperature 58-62°C, with an optimum of 60°C and a maximum temperature difference of 0.5°C, primer GC% 40-60%, and maximum poly-X set at 3.

Primers were then selected from the list, and run *in silico*, using FastPCR software (http://www.biocenter.helsinki.fi/bi/Programs/fastpcr.htm), and checked for the formation of primer dimers. The products were then searched through BLAST (http://blast.ncbi.nlm.nih.gov/Blast.cgi?CMD=Web&PAGE_TYPE=BlastHome) nucleotide to check the specificity of each primer for the intended sequence. Primers were synthesized by Invitrogen, and reconstituted in ultrapure nuclease-free water.

Primer	Nucleotide sequence
5' TRAIL	5'-TTCACAGTGCTCCTGCAGTC-3'
3' TRAIL	5'-AAGCAATGCCACTTTTGGAG-3'
5' 18S	5'-TTGACGGAAGGGCACCACCAG-3'
3' 18S	5'-GCACCACCACCCACGGAATCG-3'

Table 2.5 Primers used for real time RTPCR of TRAIL and the housekeeping gene 18S.

2.13.4 Real time RTPCR

Real time RTPCR was performed on a Roche LightCycler 1.5 Real-time Detection System and analysed using LightCycler Real-time PCR Detection System Software version 3.5 (Roche Diagnostics Ltd.). Real time PCR using Lightcycler technology relies on the incorporation of a fluorescent dye into double stranded DNA. As copies

of DNA increase with each PCR cycle so does fluorescence and this can be detected and measured by the Lightcycler thus allowing quantification of copy number. cDNA (1µl) was added to 19µl of a mastermix containing Precision Mastermix (SYBR Green) (PrimerDesign, Hampshire, UK), forward and reverse primers (final concentration 500nM), and $MgCl_2$ in nuclease-free water, and placed in a glass LightCycler capillary. Each capillary was centrifuged for 2 minutes at 2000rpm at 4°C, placed in the LightCycler carousel, and run under the following cycling conditions: one cycle of 50 °C for two minutes, and then 95 °C for two minutes followed by forty-five cycles of 95 °C for five seconds, 55 °C for five seconds and then 72 °C for fifteen seconds.

For each primer pair, the optimum magnesium concentration was determined, by running a reaction mix of template cDNA known to express the gene of interest, with varying magnesium concentrations. The magnesium concentration giving the steepest exponential section of the amplification curve, which usually also gave the lowest cycle number at which amplification was detectable, was selected.

The efficiency of each primer pair was also verified. This was necessary because the $2^{-\Delta\Delta CT}$ analysis method assumes a primer efficiency of 2, so that the product will increase exponentially during amplification. In order to determine the primer efficiency, half-logarithmic dilutions of template cDNA were used in a reaction mix with the optimum magnesium concentration. Crossing threshold (Ct) values were defined as the earliest point of the linear region of the exponential section of the amplification curve to reach a minimum threshold of detection. The log concentrations of the template cDNA were then plotted against the Ct value and the slope of the resultant line determined. Efficiency was then calculated as: efficiency = $10^{(-1/slope)}$. Primers were only used if the reaction efficiency was greater than 95%.

To quantify differences in mRNA target gene expression in each sample, Ct values were determined from the linear region of the logarithmic amplification plot. Each sample was also tested for expression of the housekeeping gene 18S and the Ct values were analysed by normalizing the target gene Ct to the housekeeping gene Ct. Fold change was calculated using the standard $2^{-\Delta\Delta Ct}$ method (Livak & Schmittgen, 2001). Statistical analysis was performed on ΔΔCt values. The melting curve of each

product was analysed to verify that a single product had been obtained for each primer pair, indicated by a single melting curve.

2.14 Metastases Quantification

The number and size of tumour nodules were assessed in haematoxylin and eosin (H&E) sections using similar methodology to that previously described (Zhang et al., 2008). Photomicrographs of representative sections of the entire lung were taken at x2 magnification. This created a complete picture of all lobes of the lungs of the mice. Image analysis software (SimplePCI High Performance Imaging Software, Hamamatsu Photonics, Herrsching, Germany) was used to trace around the metastatic deposits and the lung sections and then calculate lung and metastasis area and number of metastases.

2.15 Statistics

Statistical analysis was performed using GraphPad Prism v4 (GraphPad Software, CA, USA). Multiple groups were analysed by Anova with Tukey (one-way) or Bonferroni (two-way) post-hoc tests. Single group data was assessed using Students t-test. Results were considered to be statistically significant for $p \leq 0.05$. All in vitro experiments were performed in triplicate, unless otherwise specified.

CHAPTER 3. RESULTS I - MSCs engineered to express inducible TRAIL

The first aim of this project was to be able to transduce MSCs to express TRAIL, under the control of doxycycline. This chapter discusses this aim with the production of TRAIL-transduced MSCs and investigates the function and ability of these cells to destroy cancer cells in vitro.

3.1 Mesenchymal stem cell properties

Stem cells need to be able to self-renew indefinitely and divide asymmetrically producing a replicate cell and a more differentiated daughter. Mesenchymal stem cells should be able to differentiate into stromal cells including bone, fat, and cartilage. Fully characterised MSCs were purchased from Tulane University and rechecked and shown to have successful colony forming ability, producing a mean of 48 ± 2.8 colonies from 100 cells, demonstrating their self renewal properties, and were also stimulated to produce bone and fat cells, demonstrating their multipotency (Figure 3.1).

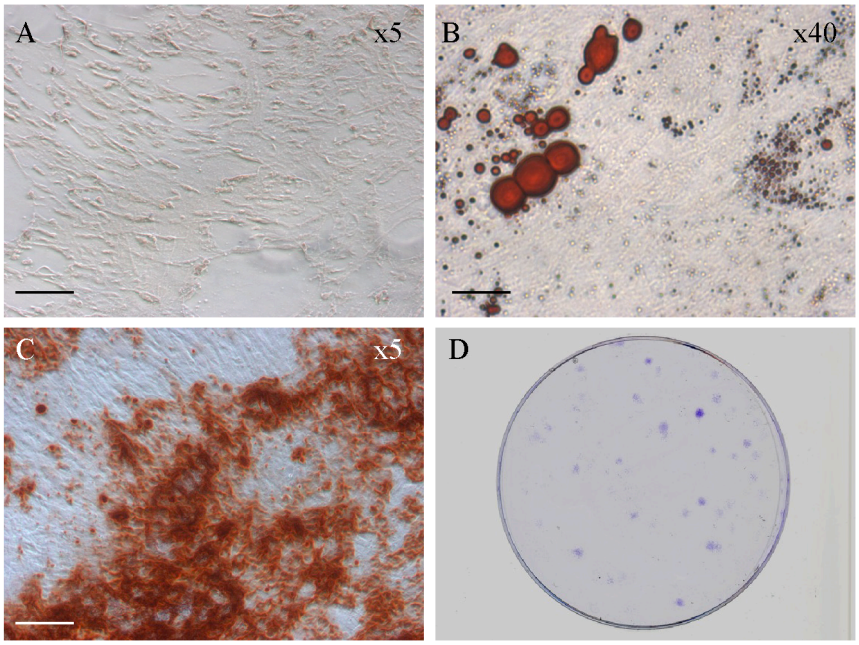

Figure 3.1 Characterisation of MSCs.
A) MSCs cultured on a 6-well plate. B) Differentiation to adipocytes, Oil-Red-O staining. C) Differentiation to osteoblasts, Alizarin Red S staining. D) Colony forming ability demonstrated by the growth of 50 colonies from 100 cells. Scale bars represent 40 μm at x 5 magnification and 5 μm at x 40 magnification.

3.2 Expression of TRAIL in transduced cells

3.2.1 Transient transfection

Human embryonic 293T kidney cells were transiently transfected with the full length TRAIL (flTRAIL), soluble TRAIL (sTRAIL), and empty vector (ev) constructs all containing IRES-GFP. To optimise transient transfection conditions, Fugene and PEI transfection agents were used at different concentrations. GFP expression was used as a marker of successful expression of the construct and assessed by flow cytometry. There was very little GFP expression with Fugene as a transfection agent. PEI, used at between 1 and 5μl per μg of plasmid DNA, gave the optimal GFP expression with the three constructs at 3μl per μg of plasmid DNA. Under these conditions, up to 60% of 293T cells transiently transfected with either the empty vector or the sTRAIL vector had GFP expression when exposed to doxycycline for 2 days. This percentage was lower for the flTRAIL construct (37%). The Tet-on system was also very leaky with similar percentages of GFP-positive cells without doxycycline, however the intensity of GFP expression was lower in these cells (Figure 3.2).

In addition to flow cytometry for GFP expression, the cells were stained with an anti-TRAIL antibody to assess for surface expression of TRAIL. There was some evidence of TRAIL expression on the cells transfected with the full length TRAIL and exposed to doxycycline (2.3%; Figure 3.2F). As with GFP expression, a lower level of TRAIL expression was also evident without the use of doxycycline (0.7%; Figure 3.2E). As expected, there was no evidence of surface expression of TRAIL on the cells transfected with either the empty vector or the extracellular portion of TRAIL (≤0.1%; Figure 3.2B,D).

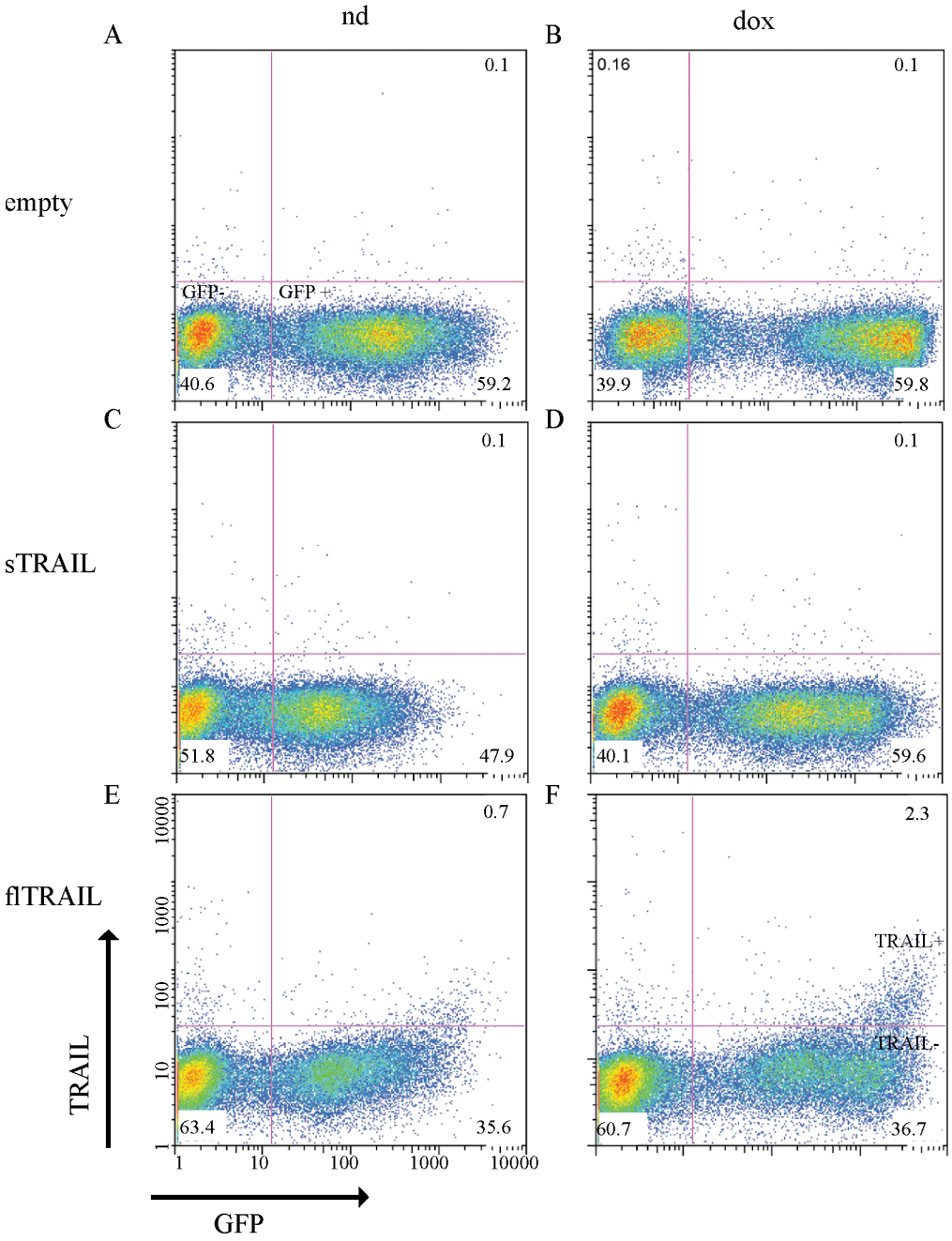

Figure 3.2 Transient transfection of 293T cells
Flow cytometry plots (marked with cell percentage) assessing the success of transient transfection of 293T cells with empty (A,B), soluble TRAIL (sTRAIL, C,D), and full length TRAIL (flTRAIL, E,F) constructs. The tetracycline-on system appears leaky with the transient transfection, as GFP is expressed in a similar percentage of cells without doxycycline (nd) (A,C,E). There is however an increased intensity of GFP fluorescence in the cells activated with doxycycline (dox) (B,D,F). There is only a small amount of TRAIL protein expressed on the surface of the cells transfected with flTRAIL and activated with doxycycline (F).

In view of the relatively low expression of TRAIL, as assessed by flow cytometry, western blots of the cell lysates and supernatants were performed. This confirmed the production of the 32kDa TRAIL protein in the cells transfected with flTRAIL. There was also evidence of the production of the extracellular portion of TRAIL (21kDa) in the cell lysates of those cells transfected with sTRAIL. There was no TRAIL in either control cells or cells transfected with the empty vector (Figure 3.3). There was no TRAIL protein in the supernatant with any of the transfected or control cells.

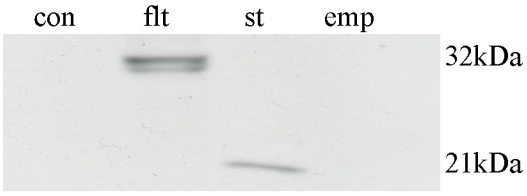

Figure 3.3 Transiently transduced 293T cells produce TRAIL.
Western blot of 293T cells transiently transduced with full length TRAIL (flt), soluble TRAIL (st), empty vector (emp), or nothing (con). Flt and st proteins should be 32kDa and 21 kDa respectively.

3.2.2 Stable transduction

With transient transfection, DNA is not usually inserted into the nuclear genome and hence is lost after cell division. Stable viral transduction involves incorporation of foreign DNA into the genome allowing it to be passed to all progeny. Lentivirus containing flTRAIL and sTRAIL was produced and used to transduce human embryonic 293T kidney cells at different concentrations. As with the transient transfection, flow cytometry analysis of GFP expressing cells was used as a surrogate for successful plasmid incorporation, and used to calculate the number of viral particles per ml.

3.2.2.1 Full length, membrane-bound TRAIL

Full length TRAIL (flTRAIL) virus ratios of 1/100, 1/1000, 1/10000, and 1/100000 were added to the 293T cells and achieved 69.6, 37.4, 3.8, 0.4 % of GFP positive cells respectively. The lower viral ratios usually give more accurate results, as there is less likely to be multiple plasmids per cell. With this in mind, and using the calculation below, there were around $2x10^7$ virus particles/ml of virus solution.

$$\text{Viral titre} = \frac{\%\text{ of GFP cells x dilution of virus x number of cells infected (i.e. 50000)}}{100}$$

The Tet-on system was not leaky with the stable transduction and GFP was only expressed by the cells exposed to doxycycline (69.6% compared to 3.3% GFP +ve cells at 1/100 lentivirus dilution; Figure 3.4).

Most lentivirus titrations are actually performed with Hela cells. As these cells are cervical cancer cells, there was concern that these cells would be killed by the TRAIL activation, and hence unsuitable for use in determining the virus concentration. Propidium iodide, a nuclear binding dye that fluorescently stains dead cells, was used to ascertain the number of cells killed by transduction and activation of the TRAIL transgene. With 293T cell titration, the number of dead cells did not significantly increase with the use of doxycycline and activation of the transgene (1/1000 virus; 3.1% dead cells with doxycycline, 5.7% without; Figure 3.5B), suggesting that these cells were resistant to TRAIL-induced apoptosis, as expected. Conversely, when Hela cancer cells were utilised for the virus titration, a large amount of cell death occurred with doxycycline activation (1/1000 virus 25.4% dead cells with doxycycline, 3.6% without doxycycline; Figure 3.5A). This experiment justified the original decision to use 293T cells for the virus titration, but also suggested the functionality of the TRAIL transgene at specifically killing cancer cells.

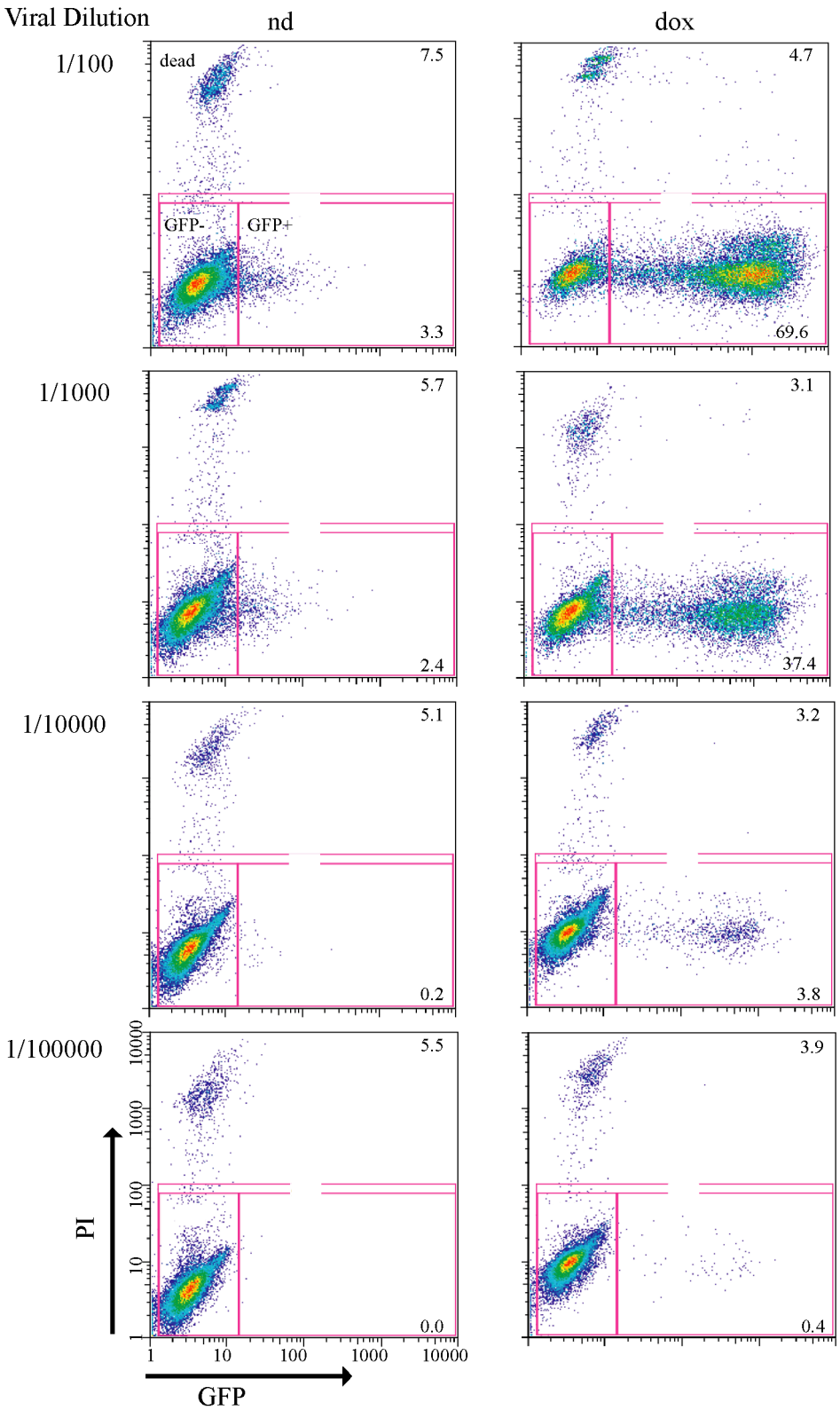

Figure 3.4 Full length TRAIL lentivirus titrated with 293T cells.
flTRAIL lentivirus was added to 5x10^4 293T cells at viral dilutions ranging from 1/100 to 1/100000. Flow cytometry was used to assess the percentage of cells expressing GFP to ascertain the number of viral particle/ml. This stable transduction of 293T cells demonstrated transgene activation (GFP expression) only on activation with doxycycline (dox) and not in the cells without doxycycline (nd). Propidium iodide (PI) was used to assess the number of dead cells.

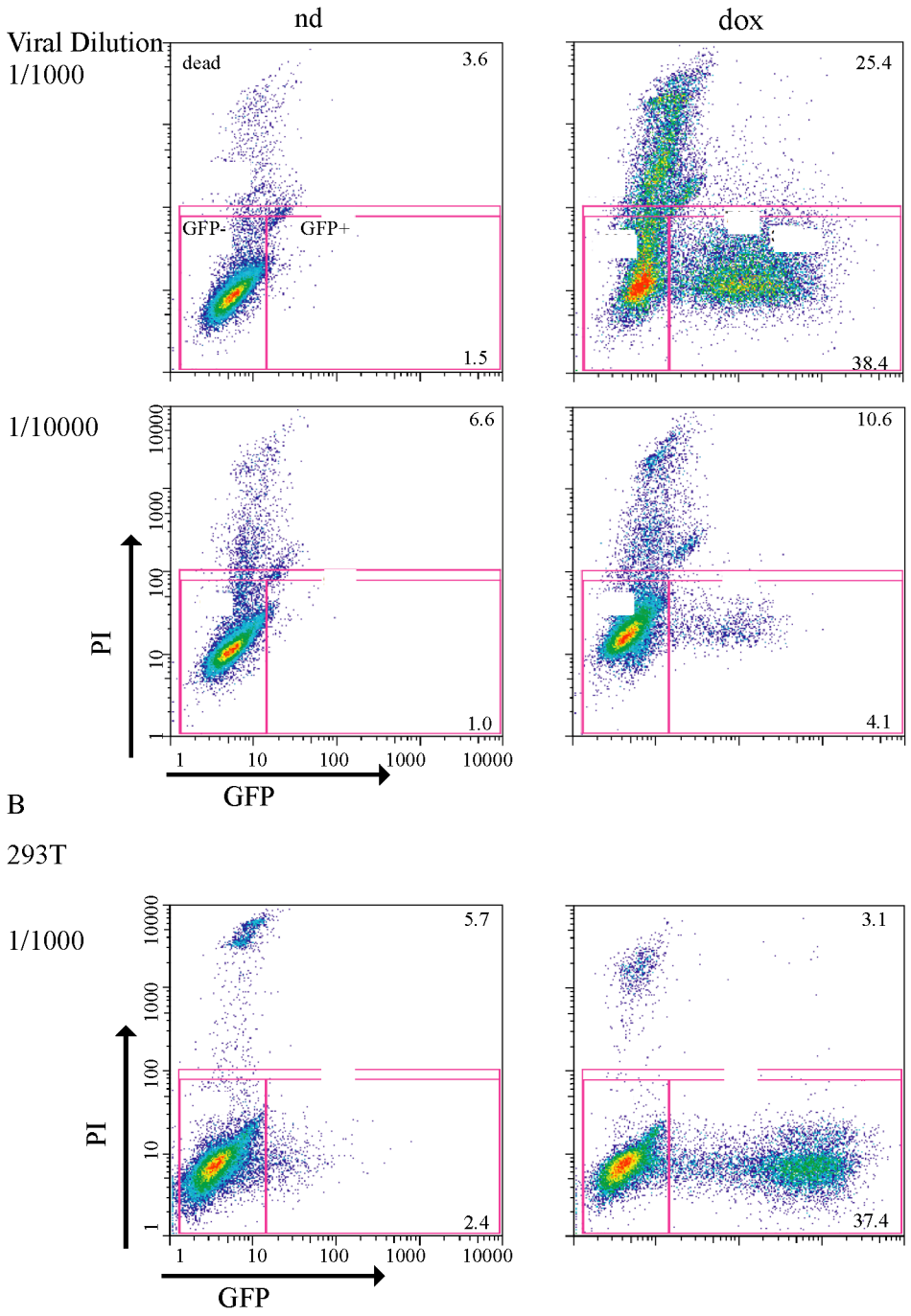

Figure 3.5 Hela cells are killed by transduction with the full length TRAIL lentivirus and activation with doxycycline.

A) flTRAIL lentivirus was added to 5x10^4 Hela cells at different viral dilutions. Flow cytometry assessed the percentage of cells expressing GFP, as a marker of successful transduction, and the percentage of dead cells with propidium iodide (PI). GFP was only expressed when the cells were activated with doxycycline (dox), and was associated with a large increase in cell death. B) The dox-induced cell death was not seen with transduction of the 293T cells. Neither GFP expression nor death was seen in Hela cells without dox-induced transgene activation (nd).

Mesenchymal stem cells were next stably transduced with flTRAIL at different multiplicities of infection (MOI). The MOI is the number of virus particles per MSC and can easily be defined with the knowledge of the number of cultured MSCs and the viral titre as above. An MOI of 10 was chosen for future experiments producing 82.1 ± 0.4% successful transduction (GFP expression) at day seven, while limiting the number of dead cells to 4.8 ± 1.8% (Figure 3.6C). As with the 293T cells, and again as expected, the low MSC death rate suggests these cells are resistant to TRAIL-induced apoptosis.

An ELISA for TRAIL protein expression was used to show that the stable TRAIL-transduced MSCs (MSCFLT) were able to produce TRAIL protein. TRAIL was only produced when the transgene was activated by doxycycline and there was more TRAIL production after 4 days of doxycycline compared to after 1 day exposure (15.0 ± 0.3 vs. 9.8 ± 1.4 pg TRAIL/μg total protein; $p<0.05$, Anova) (Figure 3.6D). In addition to the cell lysates, there was 502.9 ± 235.1 pg/ml TRAIL evident in the doxycycline-stimulated MSCFLT cell supernatants, compared to 12.3 ± 20.9 pg/ml in the supernatants of MSCFLT cells without doxycycline ($p=0.02$, t-test). The MSCFLT cells retained their MSC characteristics after the transduction process, including the capacity to differentiate into fat and bone stromal tissues.

3.2.2.2 Soluble TRAIL

A soluble TRAIL (sTRAIL) lentivirus containing the extracellular portion (amino acids 114-281) of TRAIL was also produced and virus ratios of 1/100, 1/1000, 1/10000, and 1/100000 were added to the 293T cells and achieved 63.3, 16.7, 1.3, 0.1 % of GFP positive cells respectively. Using the same rationale and calculation as with flTRAIL, this produced an sTRAIL viral yield of $7x10^6$ viral particles/ml. As with the flTRAIL system, the Tet-on system was specific with stable transduction and GFP was only expressed by the cells exposed to doxycycline (63.3% compared to 0.6% GFP +ve cells at 1/100 lentivirus dilution; Figure 3.7A).

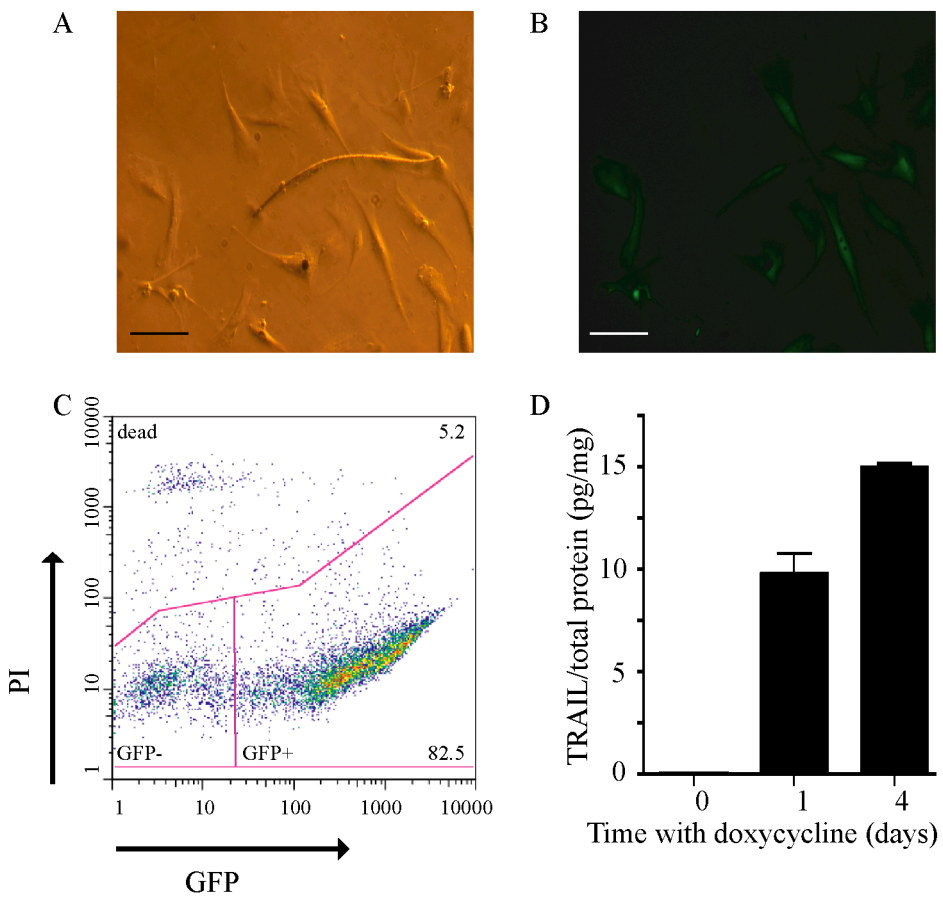

Figure 3.6 MSCs transduced with full length TRAIL lentivirus express GFP and TRAIL under doxycycline control.
*MSCs are transduced with flTRAIL and activation of the transgene with doxycycline leads to GFP expression. A) light and (B) fluorescent microscopy. Scale bars represent 20μm. C) Flow cytometry demonstrates >80% GFP+ve cells. D) ELISA demonstrates that TRAIL protein is also produced by the doxycycline-activated, MSCFLT lysates. PI: propidium iodide. **p<0.01, *p<0.05.*

Unlike with the flTRAIL, the use of Hela cells for the sTRAIL virus titration did not produce an increase in cell death. At 1/1000 virus, there were 6.5% and 7.7% dead Hela cells in the doxycycline and no doxycycline groups respectively. This result suggested a lack of activity of the sTRAIL, despite activation of the transgene (as judged by GFP expression; Figure 3.7B). MSCs were transduced with sTRAIL at an MOI of 10 (42.0 ± 25.5% GFP expression). No TRAIL protein was detectable by ELISA with either cell lysate or supernatant.

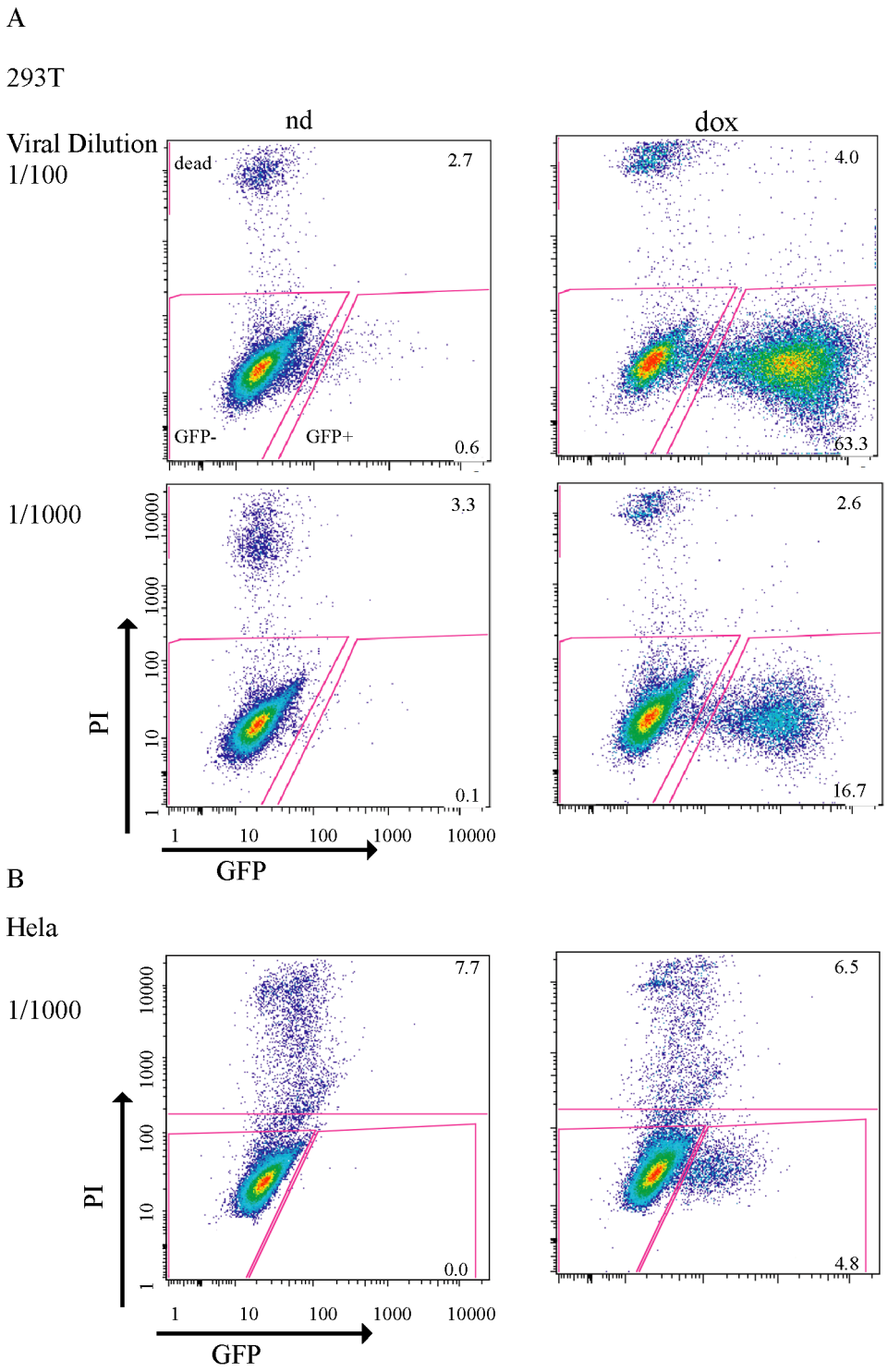

Figure 3.7 293T and Hela cells transduced with soluble TRAIL lentivirus express GFP but are not killed.

A-B) sTRAIL lentivirus was added to 5x10^4 293T (A) or Hela (B) cells at different viral dilutions. Flow cytometry demonstrated GFP expression only when the cells were activated with doxycycline (dox). B) Unlike with full length TRAIL transduction, there was no increase in death in the Hela cells when the sTRAIL transgene was activated with dox. nd: no doxycycline.

The lack of sTRAIL expression on permanently transduced cells, coupled with the apparent lack of apoptotic functional effect on the Hela cell virus titration, focused the remainder of the project on flTRAIL. The initial idea behind the use of sTRAIL was a possible paracrine apoptotic effect (Kim et al., 2006). However, there is also evidence to suggest that membrane-bound TRAIL is superior in activating the receptor DR5, and that some cells which are not sensitive to soluble TRAIL apoptose when the TRAIL is tethered to a cell membrane (Carlo-Stella et al., 2006; Muhlenbeck et al., 2000; Wajant et al., 2001). In addition, the demonstration of TRAIL protein in the supernatant of the MSCFLT cells, suggested that these cells would also be able to have a paracrine effect.

3.2.3 Control of TRAIL expression with doxycycline

The above experiments demonstrated that, in the stable transduction model, the Tet-on system was very specific; only cells exposed to doxycycline expressed the transgene. The sensitivity of the system and its speed of response to addition or subtraction of doxycycline were then investigated. Flow cytometry showed <0.5% GFP expression before activation with doxycycline. This increased to 66.5 ± 2.9% after one day of doxycycline exposure, with near maximal activation by day 2 (74.7 ± 2.5%). On removal of the doxycycline stimulus, after the cells had been exposed for 5 days, the percentage of GFP positive cells remained high for 5-7 days, however the intensity of GFP dropped significantly by day 3 (Figure 3.8A,B). On day 7 there was only 12.2 ± 1.0%) of weakly positive GFP cells.

In addition to GFP expression, the timescale of the transgene activation with doxycycline was also investigated by measuring TRAIL protein expression. Western blots demonstrated TRAIL protein expression in MSCFLT lysates was maximal after 2 days of doxycycline stimulus, but very little protein remained 1 day after its removal (Figure 3.8C). The apparent disparity in the speed at which the GFP and TRAIL proteins return to baseline levels following doxycycline removal could be explained either by differences in degradation of the two proteins, or by the increased sensitivity of flow cytometry in comparison to western blotting.

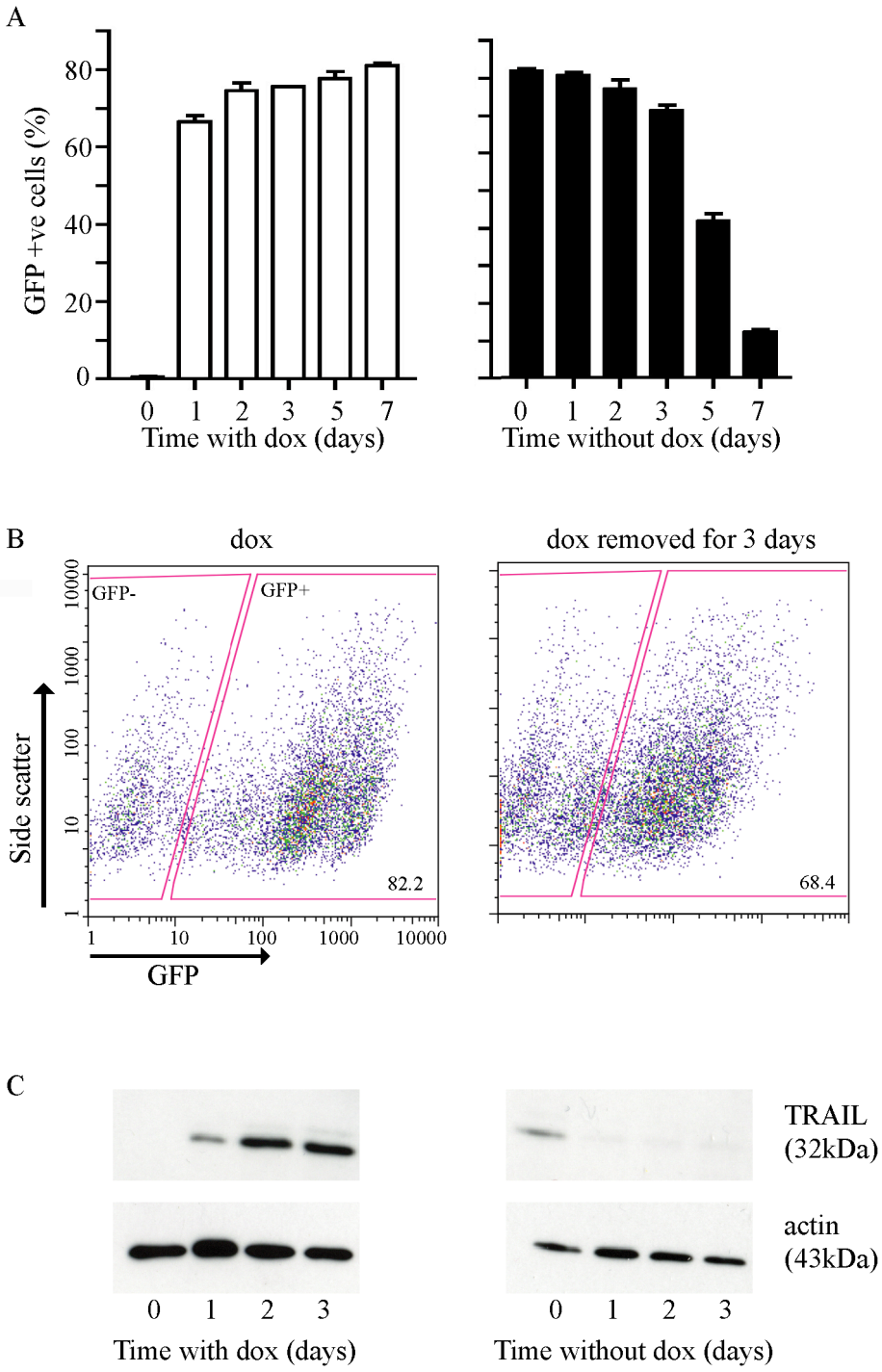

Figure 3.8 Timescale of full length TRAIL transgene activation with doxycycline.
A) Bar chart displaying results from triplicate flow cytometry experiments. GFP is expressed by full length TRAIL-transduced MSCs (MSCFLT) within 1 day of doxycycline (dox) exposure and remains for 3 days after dox removal. B) Representative flow cytometry plots demonstrating a reduction in intensity of GFP expression 3 days after dox removal despite similar numbers of GFP +ve cells. C) Western blots of MSCFLT lysates showing maximum expression of TRAIL after two days of doxycycline treatment (10µg protein loaded) and loss of expression one day after doxycycline removal (5µg protein loaded), with actin loading controls.

3.3 Function of TRAIL in transduced cells

Having demonstrated the successful transduction of MSCs and their ability to express TRAIL in a tetracycline-induced system, it was necessary to assess the function of the expressed TRAIL. Apoptotic function had been suggested in the viral titration with Hela cells. As described in section 3.2.2.1, there was an increase in cell death, which was proportional to the amount of cells successfully transduced (Figure 3.5A). This result was expected, as Hela cells are a cervical cancer cell line sensitive to TRAIL-mediated apoptosis, whereas the 293T cells (and MSCs) are not cancer cells and hence are expected to be resistant to the effects of TRAIL.

3.3.1 Coculture experiments

To demonstrate the ability of TRAIL-expressing MSCs to kill tumour cells, the two cell types were cocultured and death assessed with phase microscopy (Figure 3.9A) and Annexin V flow cytometry (Figure 3.9B). Annexin V binds phosphatidylserine, which is translocated from the inner membrane to the cell surface soon after the induction of apoptosis. PI and DAPI are nuclear binding dyes that are excluded from live, viable cells, but fluorescently stain the nucleus of dead cells. Annexin V^- /$DAPI^-$ cells were judged to be live. Annexin V^+/$DAPI^-$ cells were considered to be undergoing apoptosis. Annexin V^+/$DAPI^+$ cells were recorded as being dead.

In preliminary coculture experiments both $1x10^5$ and $4x10^5$ total cells per 6-well plate were used and the following cell combinations were cocultured 1) cancer cells alone, 2) cancer cells with normal, non-transduced MSCs and doxycycline (to control for the addition of doxycycline), 3) cancer cells with MSCFLT without doxycycline (to control for the MSCFLT), and 4) cancer cells with MSCFLT with doxycycline (to assess the effect of TRAIL expression). The higher density cocultures led to a large background death rate due to overconfluency and hence the lower density ($1x10^5$) cells were used for further experiments. There was no increased death and apoptosis with either the addition of normal, non-transduced MSCs and doxycycline, or MSCFLT without doxycycline (Figure 3.9B).

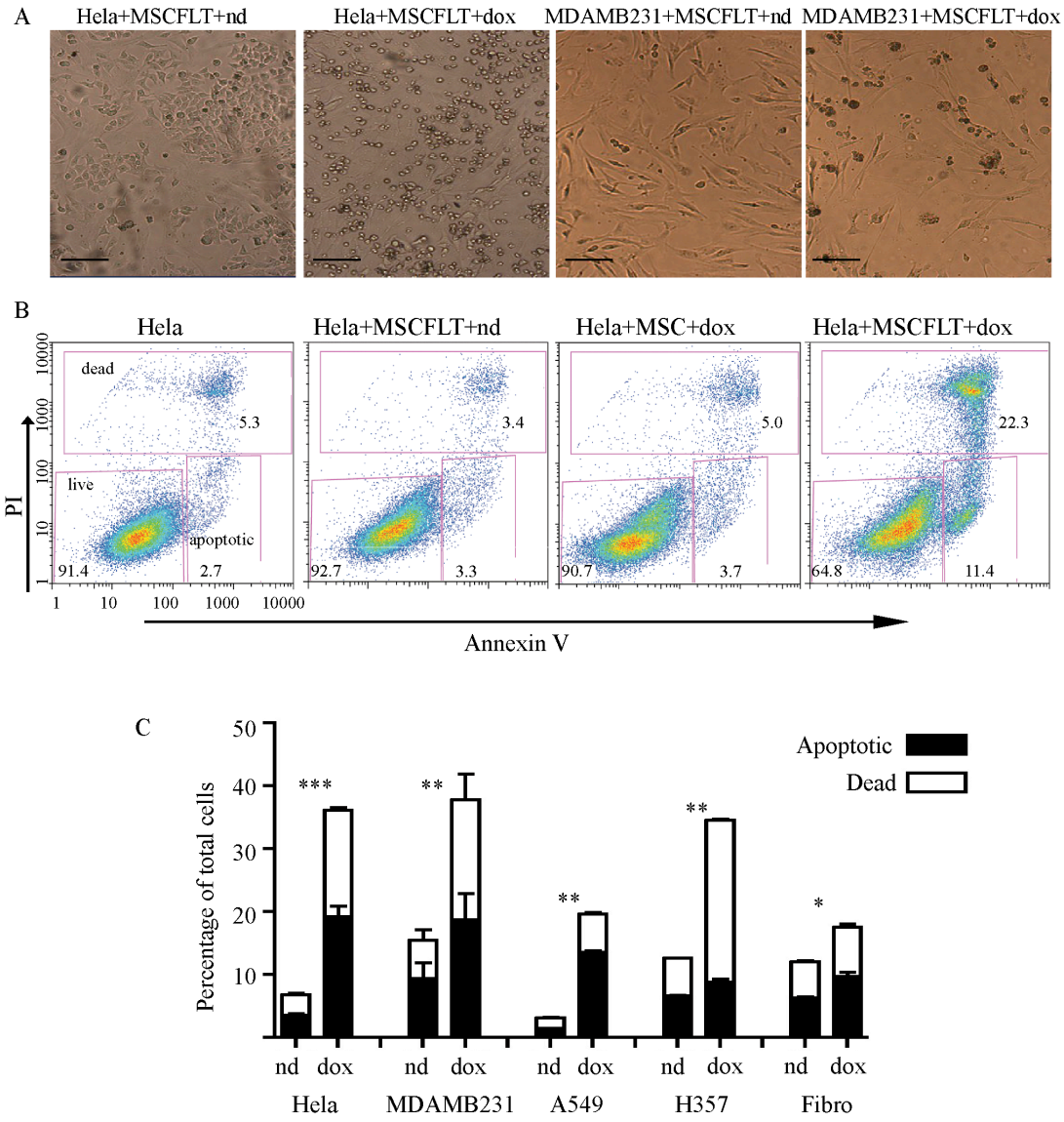

Figure 3.9 TRAIL-expressing MSCs cause cancer cell apoptosis in vitro.
*A) Phase microscopy demonstrating an increase in cell death (rounded and floating cells) when MSCFLT cells were activated by doxycycline (dox) in co-culture with Hela and MDAMB231 cells. Scale bars represent 40μm. B) Representative flow cytometry plots demonstrating an increase in death and apoptosis when Hela cells were co-cultured with dox treated MSCFLTs compared to no dox (nd), untreated controls or dox-treated normal MSCs. (C) Flow cytometry results from triplicate apoptosis assays showing an increase in death and apoptosis of total cells in cancer cell and MSCFLT co-cultures after dox treatment. ***p<0.001, **p<0.01, *p<0.05.*

Both apoptosis (Annexin V+/PI-) and death (Annexin V+/PI+) increased significantly when doxycycline was added to the cancer and MSCFLT cocultured cells. This effect was observed with lung cancer (A549; apoptotic and dead cells increased from 3.1 ± 0.1% to 19.6 ± 0.8%; p=0.001, t test; with the addition of doxycycline), breast cancer (MDAMB231; 15.4 ± 1.7% to 37.7 ± 6.5%; p=0.001, t-test), squamous cell cancer (H357; 12.5 ± 0.3% to 36.1 ± 3.5%; p=0.001, t-test) and cervical cancer (Hela; (6.7 ± 1.0% to 36.1 ± 3.5%; p=0.0001, t-test) cells. There was a minimal increase in death and apoptosis of fibroblasts in coculture with MSCFLT cells (12.0 ± 0.5% to 17.5 ± 2.1%; p=0.01, t-test)(Figure 3.9C).

The supernatant from doxycycline-activated MSCFLT cells contained TRAIL protein on an ELISA, as described in 3.2.2.1. When added to Hela cancer cells this supernatant caused 38.8 ± 1.2% death and apoptosis compared to the 13.0 ± 1.3% death and apoptosis with the use of the non-TRAIL containing supernatant from MSCFLT without doxycycline (p<0.0001, t-test; Figure 3.10).

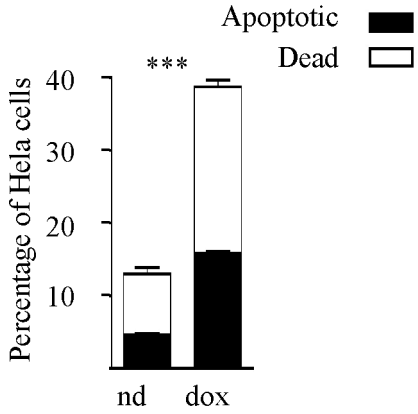

Figure 3.10 The supernatant of TRAIL-expressing MSCs contains functional TRAIL.
*Bar chart from triplicate flow cytometry experiments demonstrating a significant increase in apoptosis and death of Hela cells when they were cultured with the supernatant from MSCFLT cells with doxycycline (dox) compared to without doxycycline (nd). ***p<0.0001.*

3.3.2 Specific death of cancer cells

The above experiments demonstrated an increase in cell death and apoptosis of the combination of cells in the coculture. The apoptotic cells were likely to be the cancer cells from the single cell viral transduction data (section 3.2.2.1). It was not possible to separate the cell types by size on flow cytometry so the experiments were repeated with prior labelling of the cancer cell populations with a fluorescent dye (DiI). The apoptosed and dead cells were shown to come specifically from the cancer cell population. The addition of doxycycline increased the dead and apoptotic Hela cells from 6.1 ± 0.7% to 50.7 ± 2.7% ($p<0.0001$, Anova), whereas there was no significant increase in apoptosis and death in the GFP-positive MSCFLT cells with doxycycline (14.5 ± 6.1% to 8.3 ± 4.6%)(Figure 3.11).

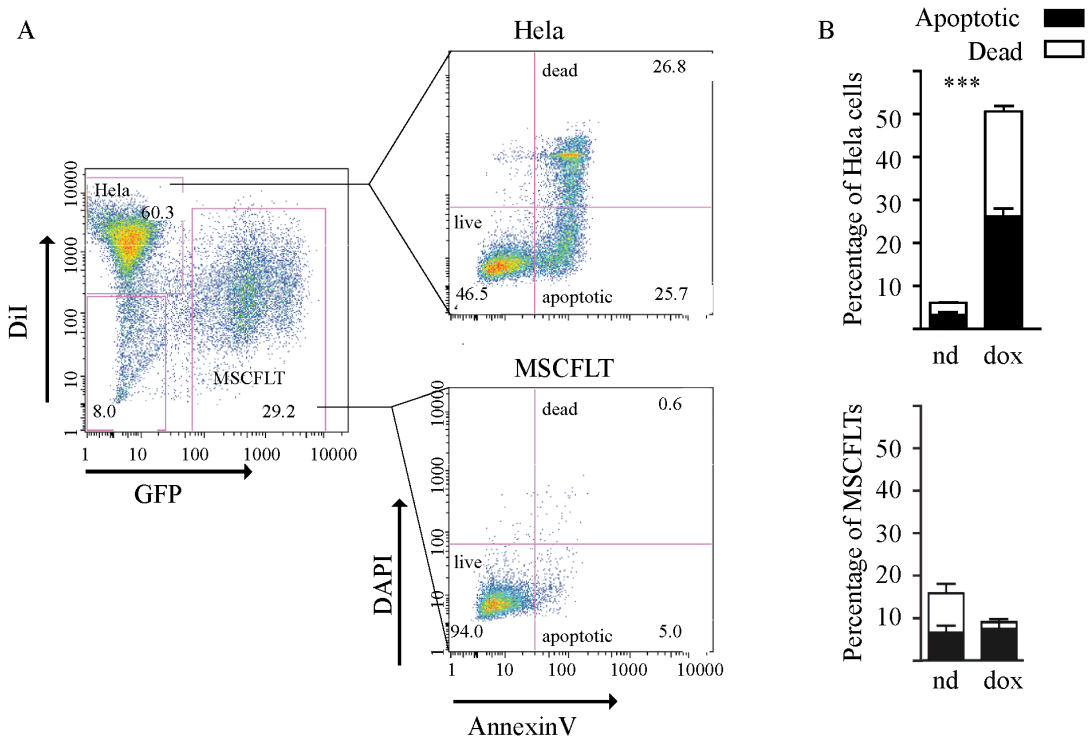

Figure 3.11 The cancer cells are specifically killed in coculture with TRAIL-expressing MSCs.
*A) Hela cancer cells were stained with DiI before coculture with MSCFLT and doxycycline (dox). By gating on the separate cell populations, the flow cytometry plots demonstrate that >50% of the Hela cells undergo apoptosis or die, whereas the MSCFLTs remain viable. B) Bar chart representing triplicate flow cytometry experiments demonstrating the increase in apoptosis and death of the Hela cells in coculture with the addition of dox compared to without dox (nd), in contrast to theMSCFLT cells. ***p<0.001.*

3.3.3 Dose dependent effect

For clinical applications, it would be unlikely to attain a 1:1 ratio of MSCFLT and cancer cells, so it is important to be able to demonstrate a killing effect at much lower concentrations of MSCFLT cells. Coculture experiments were repeated with lower numbers of MSCFLT cells. A significant increase in apoptosis and death of the cancer cells was achieved at all concentrations of MSCFLT used; $p<0.001$ at ratio MSCFLT:Hela cell of 1:16. There was a cell ratio-dependent effect; the greater the number of MSCFLT cells, the greater the death and apoptosis of Hela cells (Figure 3.12A). The coculture experiments were performed by plating the cancer and MSCFLT cells for 24 hours before the addition of doxycycline and there was a further time period before TRAIL was expressed on the MSCFLT cell surface. Consequently, this experiment underestimated the true killing capacity of MSCFLT cells, as the seeding ratios did not account for the increased proliferation of the cancer cells in comparison with the MSCFLTs before the expression of TRAIL.

3.3.4 Mechanism of MSCFLT-induced cancer cell death

The previous experiments have demonstrated that the combination of doxycycline and MSCFLT cells can cause apoptosis and death of a range of cancer cells, but that either agent alone does not reproduce this. MSCFLT cells had also been shown to express TRAIL protein when induced with doxycycline. The next set of experiments set out to demonstrate that MSCFLT cells kill cancer cells by induction of the extrinsic apoptotic pathway by TRAIL.

3.3.4.1 Death of cancer cells by TRAIL expression

A TRAIL antibody with some ability to neutralise the bioactivity of TRAIL was added to the MSCFLT and Hela cell cocultures. The antibody was used at a dose to give maximal neutralising effect (250ng/ml)(Matthews & Neale, 1987). The amount of MSCFLT-induced death and apoptosis was significantly reduced with this antibody (38.0 ± 0.5% compared to 50.7 ± 3.8%; $p<0.001$, Anova), however not back to baseline (11.5 ± 1.5%) (Figure 3.12B).

The doxycycline-induced MSCFLTs were potent inducers of death and apoptosis of Hela cells, producing a larger proportion of apoptotic and dead cells in comparison to high doses (200ng/ml, designed to give maximal effect) of a commercially available recombinant soluble TRAIL (50.7% ± 3.8% compared to 27.5 ± 0.7%; $p<0.001$, Anova) (Figure 3.12B).

3.3.4.2 Death of cancer cells by extrinsic apoptosis pathway

The caspases are a family of closely related enzymes crucial to apoptosis (see section 1.2). zVADfmk is a cell permeable, pan-caspase inhibitor that inhibits apoptosis. Application of this compound to the 1:1 cocultured MSCFLTs and Hela cells caused a 51.6% reduction in death and apoptosis compared to a DMSO treated control of (26.5 ± 0.7% compared to 54.8 ± 3.0%; $p=0.003$, t-test) confirming the importance of caspases, and the apoptotic pathway in the cell death (Figure 3.12C).

Upon receptor binding of the TRAIL ligand, the death domain in the cytoplasmic region of the TRAIL receptor recruits FADD and caspase 8, leading to apoptosis by the extrinsic pathway. To confirm the mechanism of MSCFLT-induced cancer cell death is via the extrinsic pathway, Hela cancer cells were retrovirally transduced with a dominant negative FADD (dnFADD) construct or an empty vector (Janes & Watt, 2004). The dnFADD consists of the death domain that binds to the TRAIL receptor, but not the domain responsible for caspase 8 recruitment. Overexpression of dnFADD in these cancer cells should inhibit the recruitment of caspase 8 and the subsequent formation of the death inducing signal complex, a prerequisite for extrinsic apoptosis. There was a significant reduction (16.4 ± 1.4% compared to 42.9 ± 4.9%; $p<0.018$, t-test) in death and apoptosis of Hela cells transduced with dnFADD after coculture with doxycycline-activated MSCFLT cells (Figure 3.12C). This data provides strong evidence that MSCFLT cells induce apoptosis via the extrinsic pathway.

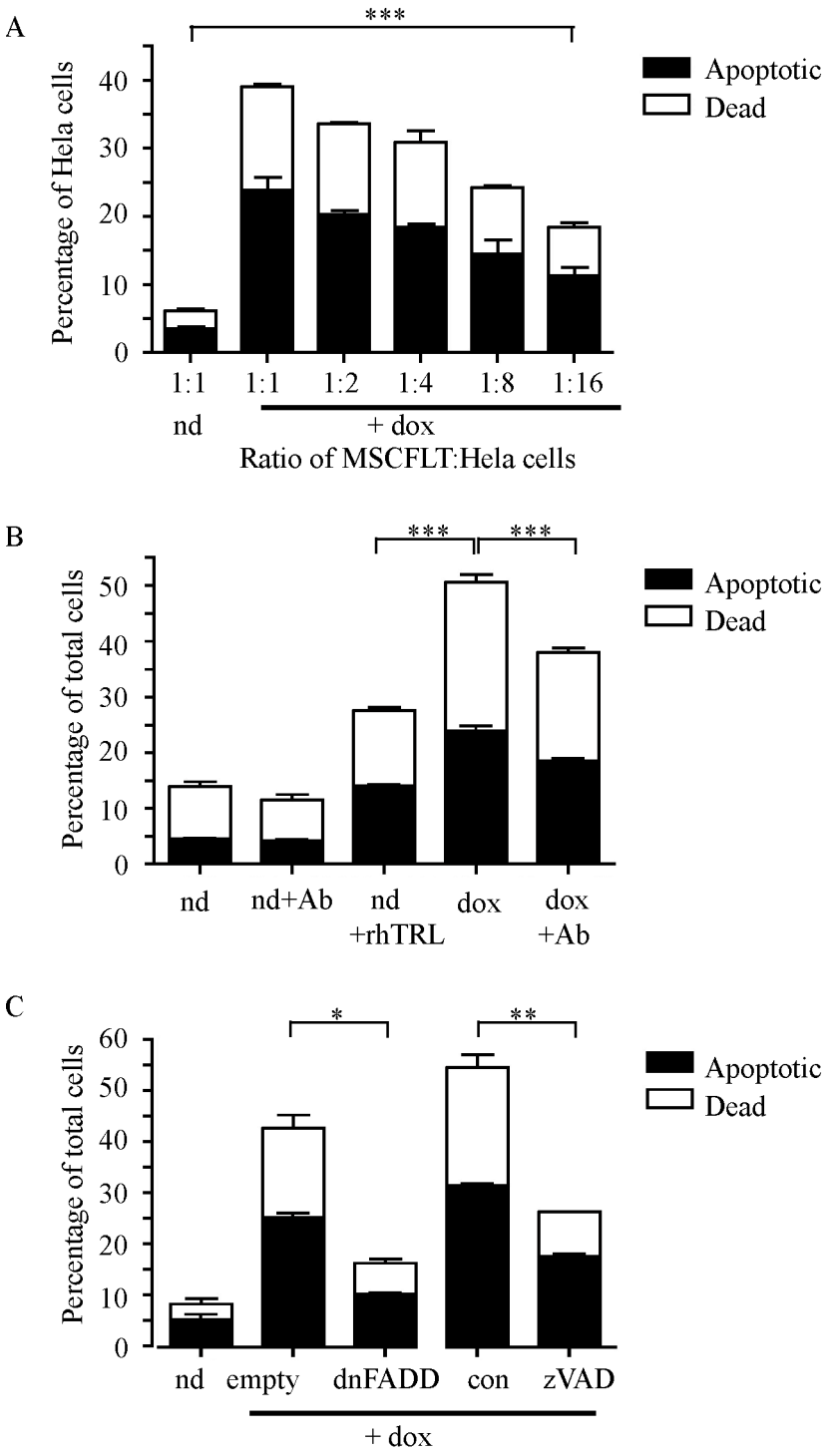

Figure 3.12 TRAIL-expressing MSCs induce cancer cell apoptosis at low MSC to cancer cell ratios via the extrinsic apoptotic pathway.

*A-C) Bar charts representing triplicate flow cytometry apoptosis assays. A) The death and apoptosis of Hela cells is increased in coculture with doxycycline (dox)-activated MSCFLT cells even at low 1:16 ratios, compared to no dox controls (nd). (B) Induced cell death and apoptosis is higher using the dox-activated MSCFLTs than with recombinant TRAIL (rhTRL), and can be partially blocked with blocking antibody (Ab). (C) Cell death and apoptosis is reduced in Hela cells expressing dominant negative Fas-associated death domain (dnFADD) in comparison with those transduced with an empty vector (empty) in addition to when zVADfmk (zVAD), a pan-caspase inhibitor, is used compared to the control (con). ***$p<0.001$, **$p<0.01$, *$p<0.05$.*

3.4 Summary

This chapter has demonstrated

- MSCs can be permanently transduced with lentivirus constructs.
- MSCs can express full length TRAIL in a doxycycline-inducible manner.
- The doxycycline induced TRAIL expression is specific and sensitive.
- TRAIL-expressing MSCs are able to specifically cause cancer cell apoptosis and death in vitro.
- The MSCFLT-induced cancer cell apoptosis and death is retained even at low MSCFLT : cancer cell ratios
- The MSCFLT-induced cancer cell apoptosis and death is via the extrinsic apoptotic pathway.

CHAPTER 4. RESULTS II – Homing of MSCs to cancer

Having produced MSCFLT cells, armed with the ability to express TRAIL and kill cancer cells in vitro, the next step was to ensure that they could migrate to tumours both in vitro and in vivo. This chapter addresses the second aim of the project; the specific migrating ability of the MSCs, and develops murine cancer models to demonstrate tumour homing in vivo. As much of this chapter describes work done in vivo, it begins with a description of the development of the tumour models.

4.1 Cancer Models

For this project, with the future aim of translational applicability, human cancer xenograft models, human MSCs, and human TRAIL constructs were used.

For xenograft tumour models, immunocompromised mice were needed, so that the human cancer cells would not be rejected by the murine immune system. Three different tumour models were developed; a subcutaneous tumour model to allow tumour visualisation during the experiments, a direct lung injection model for lung cancer, and a metastatic lung cancer model produced by intravenous cancer cell delivery. Both A549 and MDAMB231 breast cells were used for the xenograft models.

4.1.1 Nude mice

Nude mice were initially used for the xenograft models. These mice have a deletion in the FOXN1 gene on chromosome 11 and the defect is autosomal recessive (Segre et al., 1995). These mice have a rudimentary, dysfunctional thymus and are T-cell deficient. They do however have normally functioning B-cells and NK cells. Subcutaneous injection of A549 cells produced tumours in 6/8 nude mice after 8 weeks, but the size of the tumour was small and inconsistent. MDAMB231 cells produced 0/6 tumours after 12 weeks. Direct lung injection of A549 cells produced small areas of lung tumours in 10/12 mice, however again the model was not uniform or reproducible with some parenchymal, mediastinal, and pleural tumours. Intravenous injection of MDAMB231 cells produced small areas of tumours in the lung as early as eight days following injection.

Due to the unsuccessful growth, long latency, and lack of reproducibility with some of the tumour models, NOD/SCID mice were then used for the xenograft models.

4.1.2 NOD/SCID mice

In these mice, the SCID (Severe Combined Immunodeficiency) mutation has been transferred onto the diabetes-susceptible NOD (Non-Obese Diabetic) background. Mice homozygous for this mutation have a block in lymphocyte development and have a lack of functioning B-cells and T-cells. There are also abnormalities of the innate immunity with defective NK and macrophage function (Shultz et al., 1995). The increase in immunodeficiency in comparison to the nude mice should encourage faster and more reproducible tumour growth with the different models.

Subcutaneously injected MDAMB231 cells developed into reproducible subcutaneous tumours in 13/15 mice within 3 weeks, and this subcutaneous model was used for further experimentation (Figure 4.1A,B). A549 cells were directly injected into the lungs of NOD/SCID mice. Tumours were produced in 5/5 mice. In two of these mice, a single lobe tumour was formed. The remaining three mice had a predominantly pleural tumour pattern (Figure 4.1J-L). In view of the lack of consistent lung tumours in this model, it was not used for further experimentation For the metastatic model, either MDAMB231 or A549 cells were intravenously injected into NOD/SCID mice and the lungs were evaluated at 10, 20 and 30 days (n=3 per time point). Metastatic tumours were found in the lungs at all time points in all of the mice. This model was very reproducible (Figure 4.1C-I) and used for further experimentation.

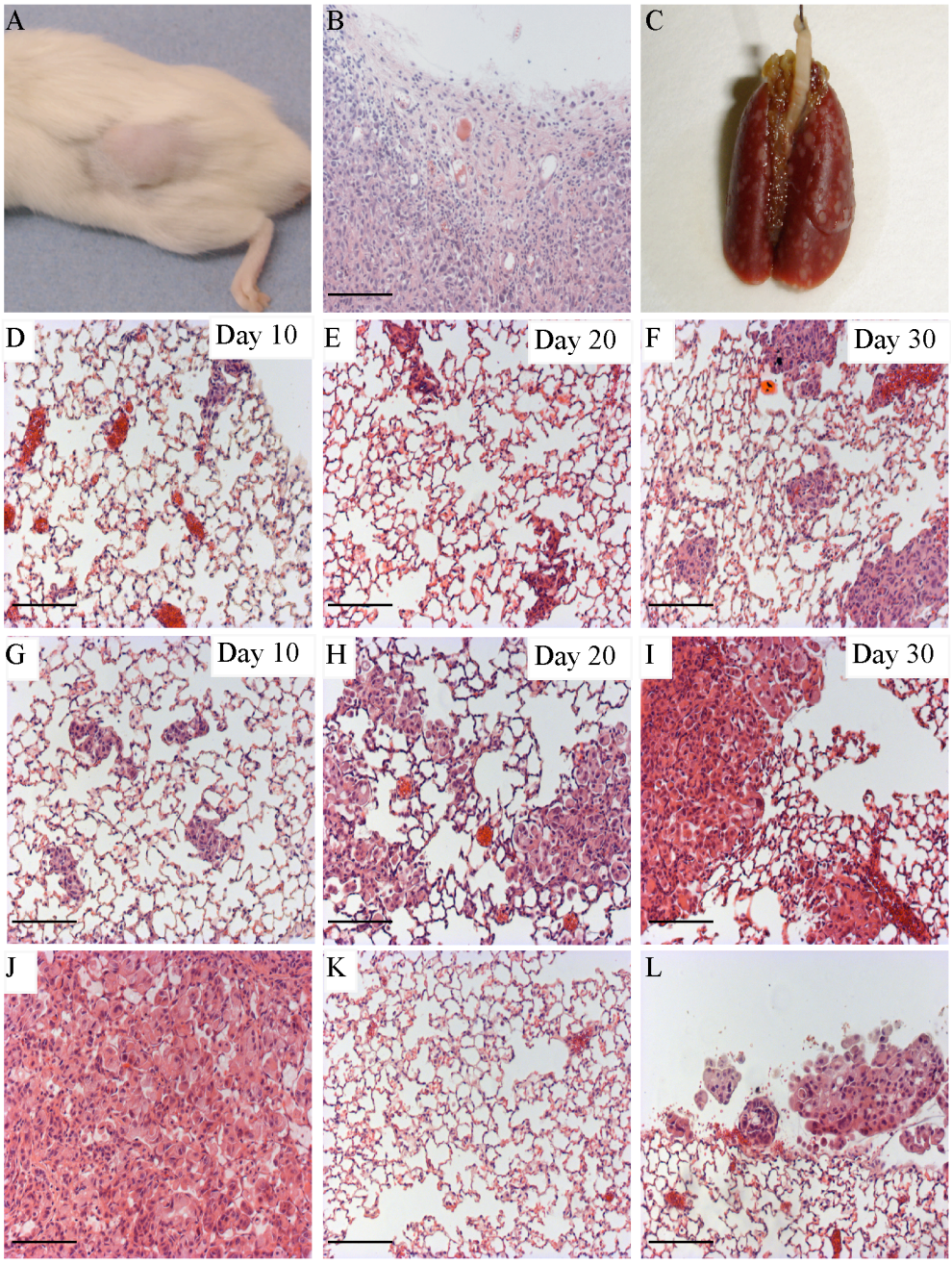

Figure 4.1 Tumour models.
A) subcutaneous (s/c) tumour model: $2x10^6$ MDAMB231 s/c; B) H&E histology. C-I) metastatic model $2x10^6$ MDAMB231 (C-F) or A549 (G-I) cells iv. C) Macroscopic appearance of lungs, D-I) H&E histology of lungs day 10-30. J-L) H&E histology of direct lung cancer model: $1x10^6$ A549 cells injected directly into the lung with matrigel. Results were inconsistent with both single lobe lung tumour produced (J) (normal lobe in same mouse (K)), and pleural-based tumours in other mice (L) with the same technique. Scale bars represent 20μm.

4.2 MSC migration to tumours

4.2.1 In vitro

Transwell experiments were used to demonstrate the ability of MSCs to home towards tumours. MSCs were placed in the top chamber and allowed to migrate through a membrane with 8μm pores towards different cell cultures or media in the bottom chamber. The number of MSCs migrating through the membrane towards the cells was used as a measure of the ability of MSCs to home to a particular cell type (Figure 4.2A). A549, MDAMB231, and Hela cancer cell cultures were used to attract the MSCs, with 293T cells and medium alone used as controls. The results demonstrated a significantly increased migration to the MDAMB231 cells, with 250.4 ± 0.8 cells per microscope field migrating across the membrane in 24 hours compared to 293T cells (98.6 ± 9.3) and medium (57.6 ± 7.6) ($p<0.001$, Anova). There was not a significantly increased migration towards the A549 and Hela cells in comparison with the 293T cells (Figure 4.2B). In setting up these transwell migration studies, several variables were altered. The time of migration was trialled at 6 and 24 hours and although the cell medium of both the upper and lower sections of the transwells was always the same for each experiment, the serum content was varied to contain either 10% or 0%, as there was a lack of consistency in the literature (Nakamizo et al., 2005; Schmidt et al., 2006; Xin et al., 2007). With no serum in the upper and lower transwell sections, migration of the serum-starved MSCs was poor and inconsistent. Furthermore, migration to chemotactic gradients in vivo will also occur on the background of basal growth factors in serum. Consequently, for these experiments, 10% serum in both the upper and lower wells was used and migration occurred for 24 hours.

There was no difference in the in vitro migrating ability towards cancer cells of transduced MSCFLTs (92.3 ± 0.5 cells/field), or MSCFLTs activated with doxycycline (82.2 ± 2.1) in comparison to normal non-transduced MSCs (98.4 ± 10.8) (Figure 4.2C). This suggests that both the transduction and the expression of TRAIL do not influence the tumour homing capabilities of the cell.

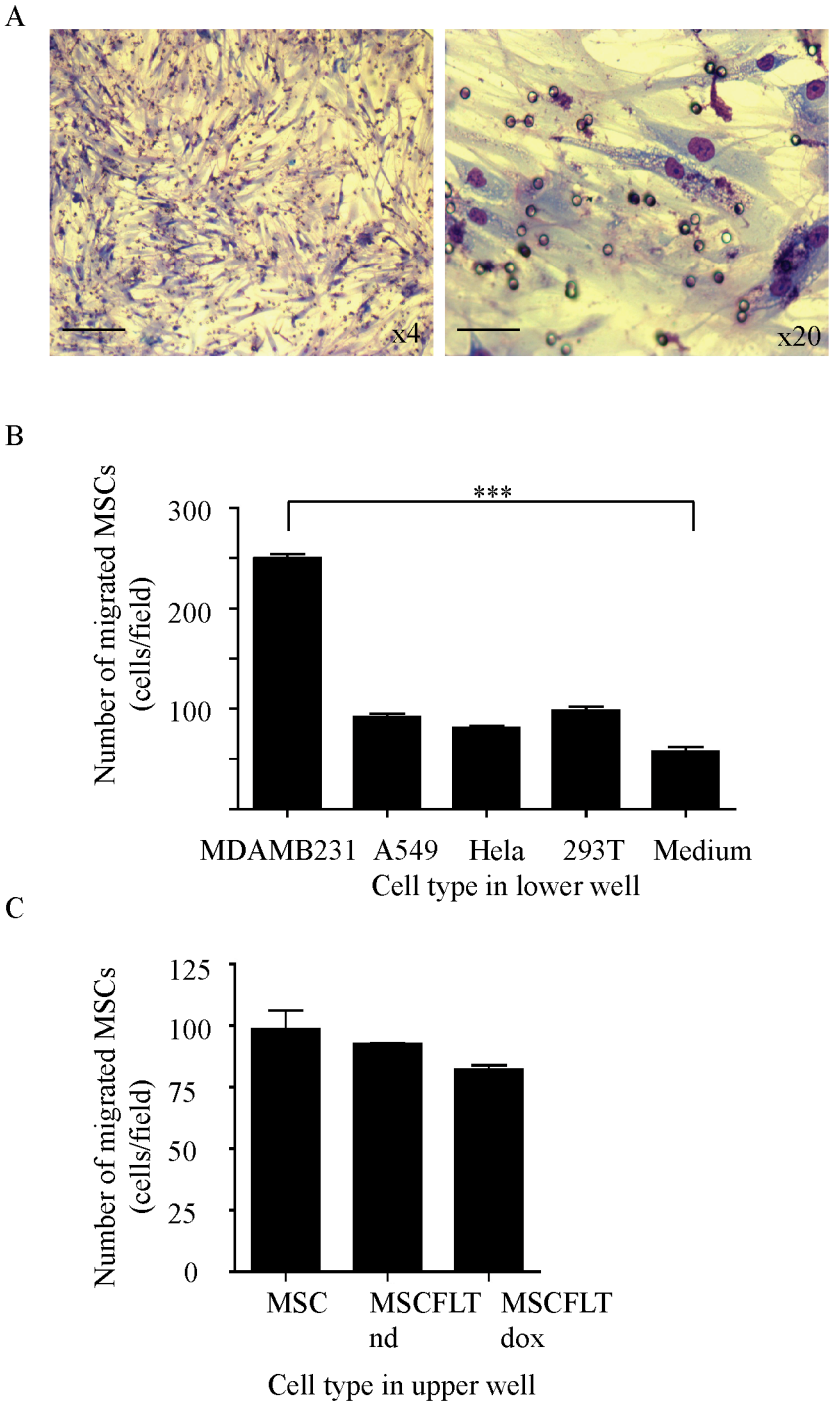

Figure 4.2 MSCs migrate to some cancer cells in vitro and transduction does not affect this migration

*A) Transwell migration studies with staining of MSCs that have migrated to the underside of the transwell. x4 mag scale bar represents 50μm, x20 mag represents 10μm. B) Increased number (per microscopic field) of MSCs migrating through the transwell membrane toward MDAMB231 cells, but not towards other (A549, Hela) cancer cell types compared to control 293T cells or medium alone (***p<0.001). C) No difference in migration towards MDAMB231 cells between MSCs and MSCFLT, with (dox) or without (nd) doxycycline.*

4.2.2 In vivo

4.2.2.1 Coinjection

MSCs and MSCFLT cells were DiI-labelled and coinjected subcutaneously with tumour cells appeared to be able to incorporate throughout the tumour (Figure 4.3A,B). The pattern of incorporation was different when the MSCs were injected into established subcutaneous tumours at day 45. In this model, MSC incorporation was found predominantly in the stroma surrounding the tumours (Figure 4.3C,D).

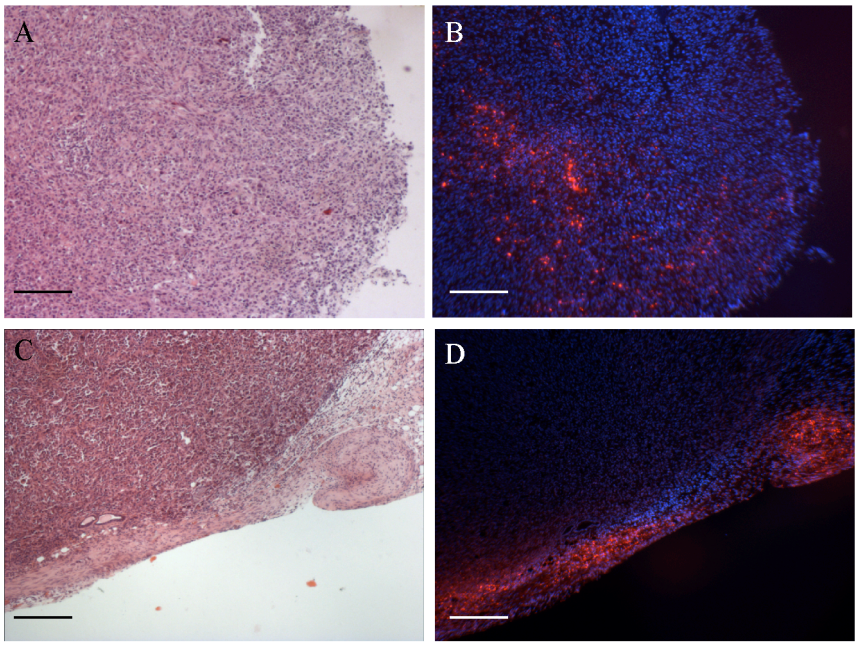

Figure 4.3 Incorporation of MSCs into subcutaneous tumours when directly injected.
A-B) $0.75x10^6$ DiI-labelled MSCs (red) were coinjected subcutaneously with $2x10^6$ MDAMB231 cells. A) H&E staining of tumours harvested at day 42. B) Fluorescent microscopy of a contiguous section with DAPI nuclear counterstain, demonstrating incorporation of MSCs throughout the tumour. C-D) MSCs incorporate predominantly in the tumour stroma when injected at day 45 into established subcutaneous tumours. C) H&E staining D) fluorescent microscopy. Scale bars represent 50μm.

4.2.2.2 Systemic introduction

MSCs or MSCFLT cells labelled with DiI, were injected intravenously at day 10 into the A549 and MDAMB231 metastatic models. At day 30, the mice were harvested and immunofluorescence showed the incorporation of DiI-labelled cells into the lung metastases in both tumour models, but the incorporation appeared more tumour-targeted in the case of the MDAMB231 cells (Figure 4.4). This was consistent with the in vitro transwell migration data suggesting an increased homing to MDAMB231 cells. On the basis of these results, the MDAMB231 cells were used for the metastatic cancer model. There was a negligible amount of DiI labelling seen in the lungs of MSC treated mice without lung metastases. Similarly, DiI-stained fibroblasts were not detected in the tumours or indeed the lungs 10 days after injection. This histological data shows MSCs preferentially engraft and are maintained in the in vivo tumour environment compared to surrounding lung parenchyma while fibroblasts are not.

There was also evidence of homing of intravenously delivered MSCFLT cells to subcutaneous tumours. MSCFLT cells were delivered at day 10, 20, and 30 following subcutaneous breast cancer implantation, and shown to be present in the subcutaneous tumours when the mice were harvested at day 38 (Figure 4.5A,B).

In addition to the lungs and subcutaneous tumours, the liver, spleen, kidneys, and heart were also harvested. Only very small amounts of DiI-labelled cells were seen in the liver and spleen, and there was no incorporation into any of the other organs (figure 4.5C-F).

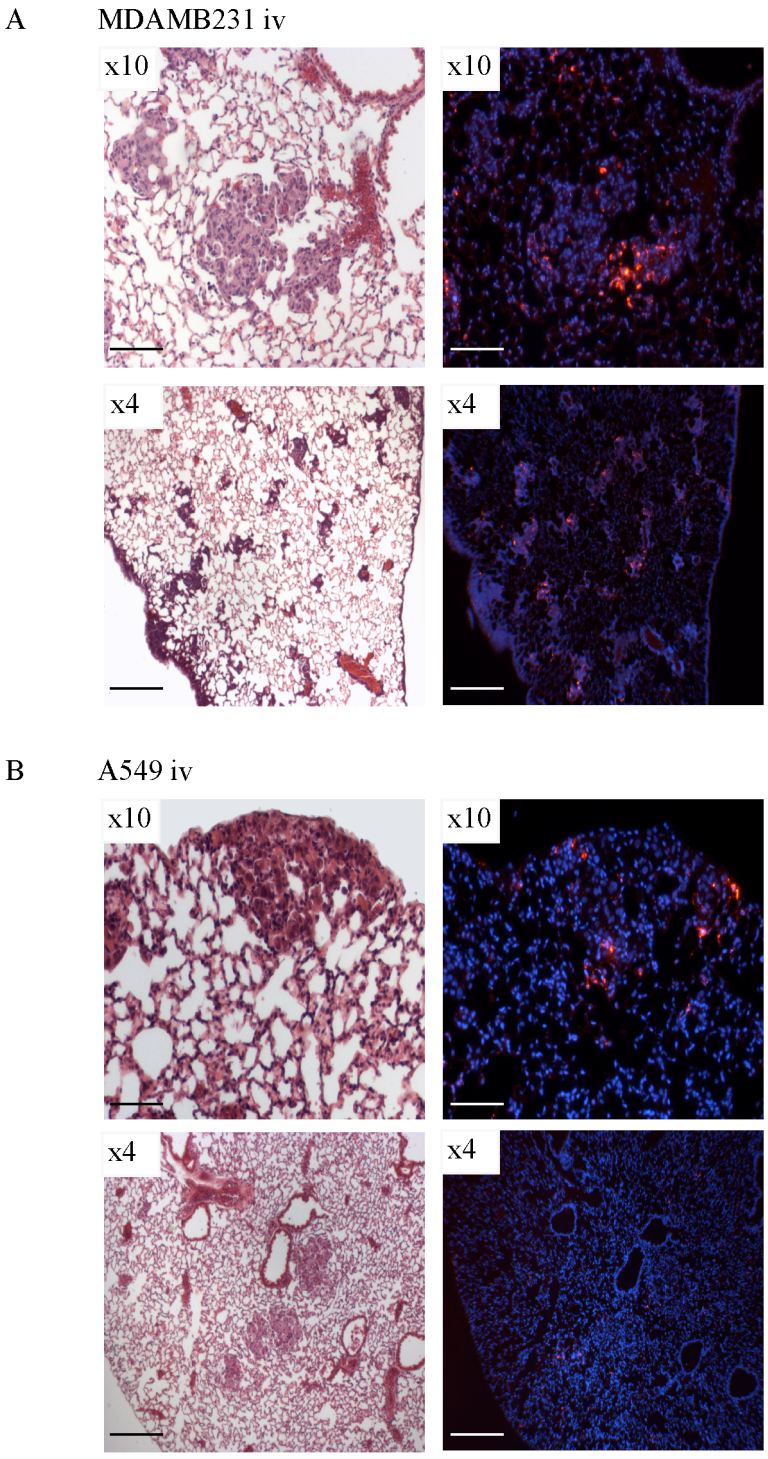

Figure 4.4 MSCs migrate to metastases in vivo.
DiI-labelled (red) MSCs or MSCFLTs injected intravenously at day 10 and shown to localise to MDAMB231 (A) and A549 (B) lung metastases on fluorescent microscopy with DAPI nuclear counterstain, and H&E contiguous sections from day 30 harvested lungs. The MSCFLT cells appear to target more specifically to the MDAMB231 metastases. x10 mag scale bar represents 20μm and x4 mag scale bar represents 50μm.

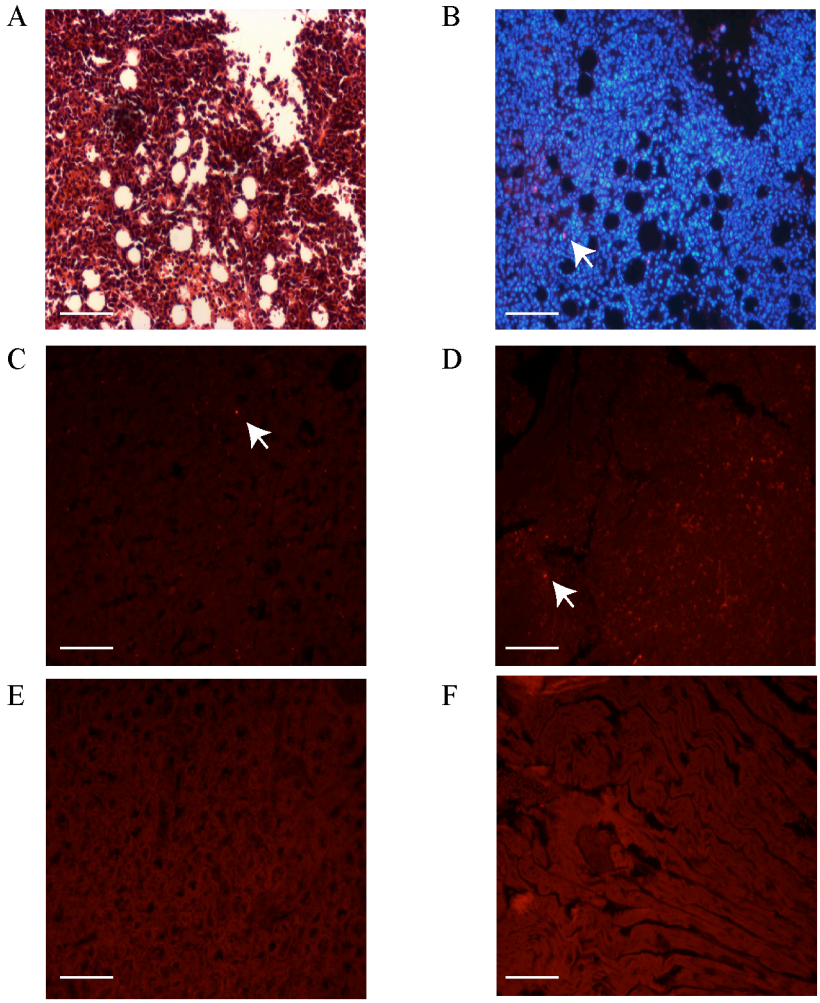

Figure 4.5 MSCs migrate to subcutaneous tumours, and have negligible incorporation into normal organs

DiI-labelled (red) MSCFLT cells were injected intravenously at day 10, 20, 30 and shown to incorporate into MDAMB231 subcutaneous tumours. A) H&E staining of sections from day 38 harvested tumours and B) fluorescent microscopy of contiguous sections showing DiI incorporation (marked by arrow), with DAPI nuclear counterstain. C-F) There is minimal DiI-labelled cells in the liver (C) and spleen (D)(marked by arrows) and none in the kidney (E) and heart (F). Scale bars represent 20μm.

4.2.3 Tumour cell lines produce multiple cytokines and chemokines

Unlike leukocyte and haematopoietic stem cell migration, the specific chemokines, cytokines and growth factors that are instrumental in MSC migration have not yet been determined. It is likely that multiple cytokines operate in combination, and that there is some redundancy. In view of this, a cytokine array panel, with duplicate capture antibodies spotted on a nitrocellulose membrane, was used to simultaneously profile the relative levels of multiple cytokines in a single sample, in order to highlight possible important candidates (Figure 4.6A). In view of the strong in vitro migration of MSCs towards specifically MDAMB231 cancer cells, the chemokine production of this cell line was profiled in comparison to the other cancer cell lines and controls. Consequently, the supernatant of confluent MDAMB231, 293T, A549, and Hela cells (without serum) were used as samples for the cytokine array. Densitometry analysis with NIH Image J program software was performed to convert the dot plots into values, and large differences (at least double) between the samples were plotted on a bar chart (Figure 4.6B). The results demonstrated a large increase in the factors C5a, granulocyte macrophage colony stimulating factor (GMCSF), IL-6 and IL-8 in the MDAMB231 supernatant compared to the other cell supernatants. Other interesting results included the large concentration of serpin E1 in all the cancer cell supernatants, the large amount of CXCL1 and CCL5 chemokines in the A549 and Hela cells respectively, and the lack of significant CXCL12, a chemokine important in haemopoietic stem cell migration and a candidate for MSC migration, in any of the supernatants.

4.2.4 Ex-vivo tumours produce multiple cytokines and chemokines

The rationale of using MSCs to express TRAIL was for them to home to tumours for targeted therapy. The in vitro data suggested that the MDAMB231 cell line had the greatest ability to attract the MSCs in a transwell experiment and analysis of the chemokines in the supernatant has suggested possible candidates for this increased migration. In vitro, the A549 and Hela cell line caused the same MSC migration as the controls. However, it is important to appreciate that the in vitro experiment is a poor recreation of the in vivo situation and should only be used as a guide. The

tumour stroma is extremely important, both for its affects on tumour behaviour, but also its contribution to bone marrow cell recruitment. Publications have suggested that the tumour stroma is critical for the recruitment of bone marrow-derived stem cells (Sangai et al., 2005). In vitro cell cultures are just collections of tumour cells without the supporting stroma and map of blood vessels necessary to recreate proper cell recruitment.

In view of this, ex vivo lungs with multiple MDAMB231 metastases were homogenized and the chemokine array profile compared to normal mouse lungs. The chemokine profile of an ex vivo, homogenized, subcutaneous MDAMB231 tumour was also investigated. The aim of this experiment was to ascertain whether any of the chemokines suggested in the in vitro experiments were specifically produced by tumours in vivo, to give some clinical validity to the in vitro work. As previously, densitometry analysis was performed to convert the dot plots into values, and large differences (at least double) between the lung and lung with breast cancer metastases were plotted on a bar chart (Figure 4.6C). This showed an increased expression in the lung containing metastases of soluble intercellular adhesion molecule-1 (sICAM- 1), IL-6, IL-8, macrophage migration inhibitory factor (MIF), CCL4, and serpin E1, with CXCL12 and IL-10 increasing by just under double compared to the lung without metastases. The homogenized subcutaneous breast tumour contained very high levels of IL-6, IL-8, MIF, and serpin E1.

On the basis of these global chemokine arrays, IL-6 and IL-8 became attractive candidates as important tumour-derived signals leading to MSC migration. They were both increased predominantly in the MDAMB231 cell line, to which the MSC migrated most effectively in the in vitro transwell experiments. They were also increased in ex vivo lung homogenates containing breast metastases in comparison to normal lung homogenates, and finally, they were present at high levels in ex vivo subcutaneous breast tumour homogenates, to which MSCs also homed. Previous data had also suggested a potential role of these factors in MSC migration. The IL-8 receptors, CXCR1 and CXCR2, are critical in leukocyte migration (Luster et al., 2005; Spaeth et al., 2008), and have been shown to be responsible for some in vitro MSC migration in one study (Ringe et al., 2007). Similarly, functional IL-6 receptors have been demonstrated on MSCs (Schmidt et al., 2006). Furthermore,

both primary breast cancers and breast cancer cell lines produce IL-6 and IL-8 (Dwyer et al., 2007; Gutova et al., 2008), and these cytokines have been implicated in the increased migration of MSCs seen after intensive exercise (Schmidt et al., 2009).

4.2.5 In vitro cytokine neutralisation

The transwell migration of MSCs to MDAMB231 cells (section 4.2.1) was repeated with the use of neutralising antibodies to IL-6 and IL-8, at concentrations suggested by previous studies (Bastian et al., 1998; Okamoto et al., 2000). Although at the lowest dose of IL-8 (0.1μg/ml) there was a statistically significant reduction in MSC migration ($p<0.05$, Anova) this was not repeated at higher doses and there was generally no reduction in MSC migration with the use of either inhibitor (Figure 4.7A). To ensure this result was not secondary to the insensitivity of the neutralising antibodies in the presence of serum, the experiment was repeated with serum-free medium in the upper and lower compartments of the transwell. With these experimental conditions, as previously discussed, migration of the serum-starved MSCs was poor and inconsistent, however there was no significant reduction in MSC migration toward the cancer cells with the addition of either IL-6 or IL-8 neutralising antibodies (Figure 4.7B). These results may suggest that IL-6 and IL-8 are not important in MSC homing towards tumours; however they may also reflect the likely considerable redundancy in the system with multiple chemokines producing similar effects.

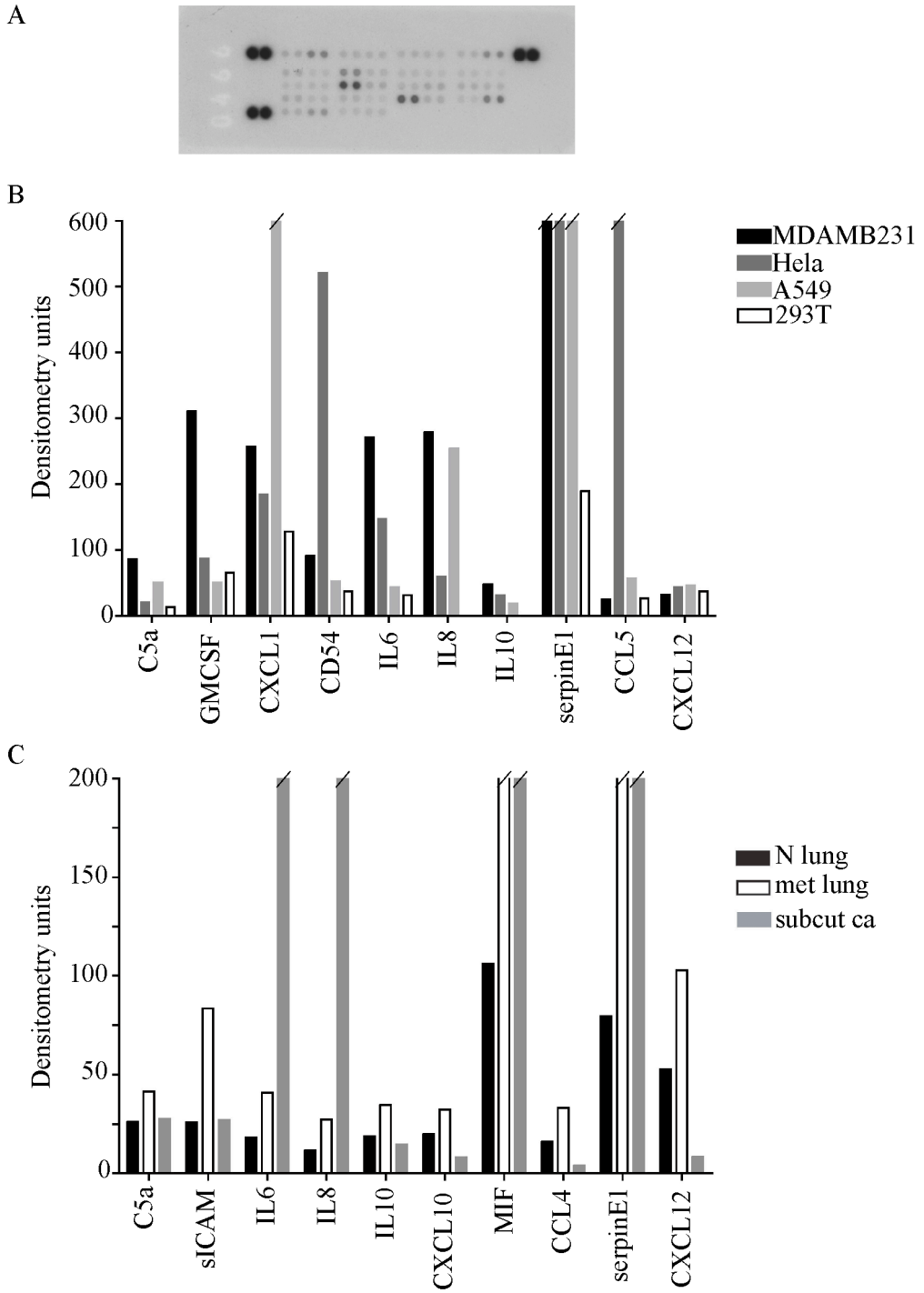

Figure 4.6 Cancer cells produce multiple cytokines and chemokines in vitro and in vivo. *Human cytokine array panels (A) were used to determine possible candidates for the increased MSC migration demonstrated in certain conditions. B) MDAMB231 cells in vitro produce increased C5a, GMCSF, IL-6,8,10 compared to the other cancer and control cell lines. C) Homogenized, ex vivo lung with multiple MDAMB231 metastases (met lung) produced more C5a, sICAM, IL-6,8,10, CXCL10, MIF, CCL4, serpinE1 and CXCL12 than normal control lungs (N lung). Of these, homogenized, ex vivo, subcutaneous MDAMB231 tumours (subcut ca) produced large amounts of IL6,8, MIF, and serpinE1. Diagonal lines represent values in excess of the axes.*

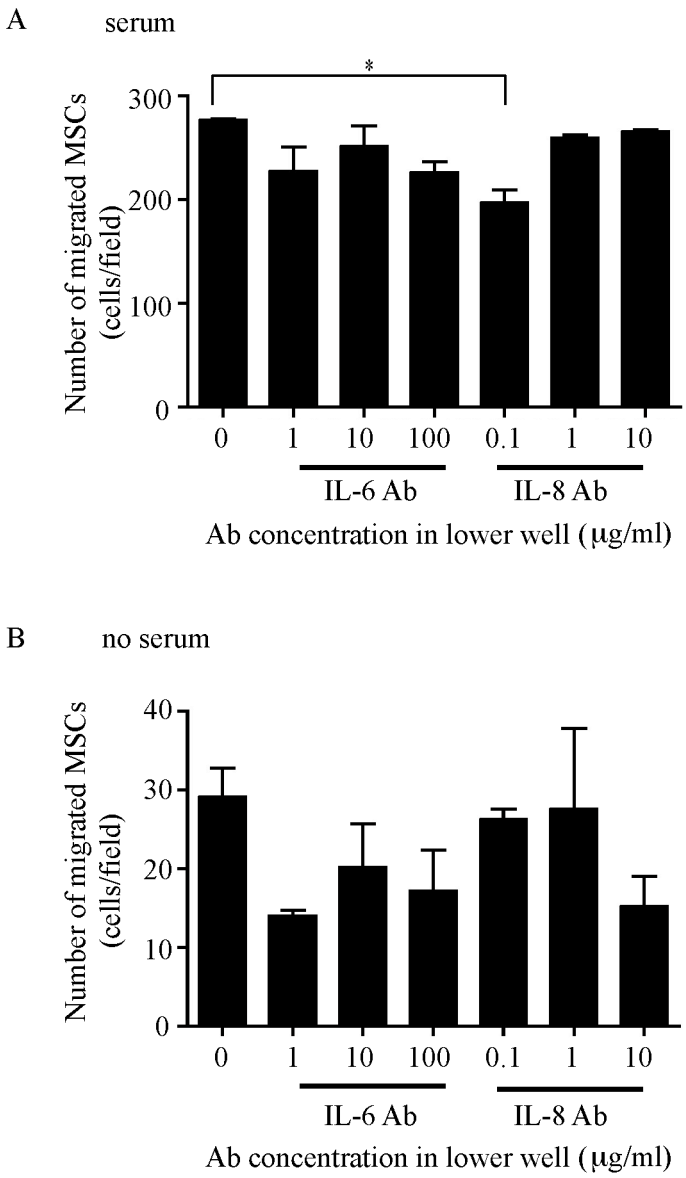

Figure 4.7 MSC migration to cancer cells is not reduced by IL-6 or IL-8 inhibitors.
*A) With 10% serum in the upper and lower wells, transwell migration studies demonstrated a reduction in MSC migration to MDAMB231 cells at the lowest dose of IL-8 neutralising antibody (Ab)(0.1μg/ml), however this was not repeated at higher doses and there was generally no reduction in MSC migration with the use of either inhibitor, or when the experiment was repeated in serum free conditions (B), *$p<0.05$.*

4.2.6 Future migration work

Much of this work focusing on the identification of chemokines and cytokines important in the MSC migration towards tumour tissue is preliminary and is a proposed future project in the Janes' laboratory. Although no effect in blocking IL-6 and IL-8 has been established in this thesis, future work may focus further on these possible candidates. Experiments will need to establish the presence of IL-6 and IL-8 receptors on the MSC, and then use a combination of ligand and neutralising antibody experiments to demonstrate a specific functional effect, both in establishing and then blocking MSC migration in vitro and in vivo. The use of receptor blockers, or silencing RNA to prevent the expression of receptors on the surface of MSCs may also be useful, however there is a lack of receptor specificity, the IL-8 receptors CXCR1 and 2 are also bound by CXCL6 and CXCL1 and 7 respectively. The contribution of other cytokines and chemokines to the homing of MSCs to tumours should also be assessed in further work. Serpin E1 is also highlighted in the cytokine profile arrays as a molecule produced in high concentrations by tumour tissue (Figure 4.6B,C). This is a serine protease inhibitor, which functions predominantly as an inhibitor of fibrinolysis, but is also associated with tumour invasiveness (Chazaud et al., 2002). It may also augment MSC tumour-tropism (Gutova et al., 2008), making it an attractive candidate for further research.

4.3 Summary

This chapter has demonstrated

- The development of a subcutaneous and lung metastatic cancer model which are reproducible

- MSCs are able to migrate to cancer cells in vitro, particularly to MDAMB231 breast cancer cells.

- MSCs are able to specifically migrate to lung metastases and subcutaneous tumours in vivo.

- The mechanism of MSC homing to tumours is likely to be due to chemokine gradients. IL-6 and IL-8 are produced by MDAMB231 cells in vitro, and as lung metastases and subcutaneous tumours in vivo, and are promising candidates for further study.

- Preliminary experiments neutralising IL-6 and IL-8 did not alter MSC migration in vitro.

CHAPTER 5. RESULTS III – In vivo tumour effects of TRAIL-expressing MSCs

Cancer cells have been shown to be susceptible to the MSCFLT cells in vitro, with an increase in death and apoptosis on coculture. This chapter focuses on combining the cancer cell killing and homing abilities of these engineered MSCs by using them as a cellular therapy in a variety of cancer models. The aim was to demonstrate an effect in vivo and to determine whether the use of TRAIL-expressing MSCs could alter the clinical course of tumour growth.

5.1 Subcutaneous tumour model

The advantage of the subcutaneous tumour model is that the cancer can be visualised throughout the experiment. Longitudinal growth measurements can be taken during the course of the study, providing further information on the effects and timings of therapy. Two million MDAMB231 cells were used to create the subcutaneous tumours as the experiments described above had suggested a superior MSC migration to this cell type. The doxycycline-induced, MSCFLT cells were used as therapies, with the same cells without doxycycline used as controls for the effects of TRAIL. Treatment of the subcutaneous tumours was either by coinjection of the cancer and MSCFLT cells, direct intratumoural injection of the MSCFLT cells or intravenous MSCFLT delivery. The coinjection and intratumoural injection experiments were performed to investigate whether the TRAIL-expressing MSCs were able to cause cancer cell apoptosis and death in vivo, and whether this would alter the cancer growth. The systemic MSCFLT treatment would take this a step further, also relying on the specific homing abilities.

5.1.1 Coinjection

As a proof of principle, $2x10^6$ MDAMB231 cancer cells were coinjected with $0.75x10^6$ MSCFLT cells subcutaneously into NOD/SCID mice. The mice were equally split into three groups (n=3 per group), with the first group of mice receiving doxycycline (thus switching the construct on to produce TRAIL) in the drinking water from day 0. The second group of mice received doxycycline at day 25, after the tumour had become established ($0.25 \pm 0.1cm^3$), and the final group of mice received no doxycycline (Figure 5.1). The results showed an early divergence in tumour growth between group 1 and the other two groups. The group exposed to doxycycline from day 0 had significantly reduced tumour growth in comparison to the other groups. This remained throughout the experiment and was strongly significant at day 42 ($0.03 \pm 0.01cm^3$ compared to $0.59 \pm 0.18cm^3$ in the mice that received no doxycycline) ($p<0.001$, 2-way Anova). In the group where doxycycline was used at day 25, there was reduced tumour growth; however this did not reach

statistical significance (Figure 5.1C). The same patterns were observed in comparing the tumour weights at the end of the experiment, with a significantly reduced tumour weight in the mice treated with MSCFLTs and doxycycline from day 0 compared to mice that received no doxycycline (0.07 ± 0.02g vs. 0.60 ± 0.07g) ($p<0.01$, Anova) (Figure 5.1D).

This proof of principle experiment was repeated with much larger numbers. Activation of the TRAIL transgene at day 0 (n=10) again resulted in a significantly reduced tumour size compared to the mice that received no doxycyline (n=7) (0.12 ± 0.12cm^3 vs. 0.66 ± 0.49cm^3)($p<0.001$, 2-way Anova), however there was no change in the tumour growth when TRAIL was activated after the tumour had already become established at day 25 (n=7) (Figure 5.2A-B).

Histological analysis of the sections demonstrated large areas of necrosis in the tumours of the mice exposed to doxycycline. There was also evidence of DiI staining in these areas of necrosis, suggesting the involvement of the MSCFLT cells in the necrosis (Figure 5.2D). Furthermore, TUNEL staining of excised tumours demonstrated areas of apoptosis co-localised with DiI-labelled MSCFLT cells (Figure 5.2E).

The subcutaneous tumours were excised and digested to a single cell suspension. Confocal microscopy of the ex vivo DiI-labelled cells included cells of MSC type morphology that stained with an anti-vimentin antibody (Figure 5.2F). This suggested that the DiI staining seen in histological section was representative of the injected MSCFLT cells, and that they had kept, at least in part, their phenotype.

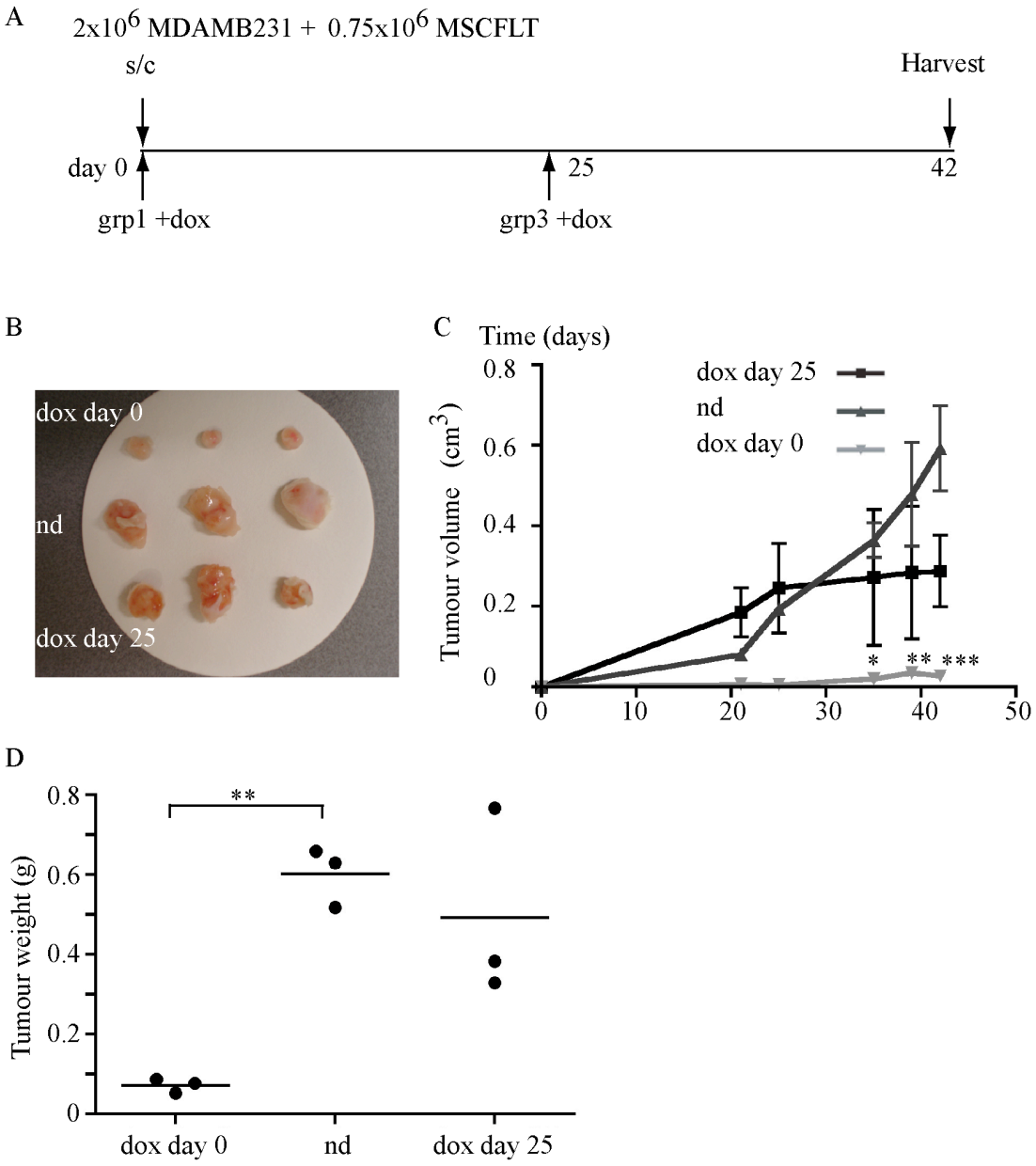

Figure 5.1 TRAIL-expressing MSCs reduce the growth of subcutaneous tumours.
*A) Subcutaneous tumours were produced by the coinjection of 2x10^6 MDAMB231 cells and 0.75x10^6 MSCFLT cells, and the mice were treated with doxycycline (dox) at day 0 (grp1) or day 25 (grp3) or with no dox (nd). B) Macroscopic appearance of the tumours. C-D) Dox treatment from day 0 led to a reduced tumour size (C) and weight (D) compared to the nd group (grp2). Although there was a trend to reduced tumour growth if TRAIL was activated at day 25, this was not significant. *p<0.05, **p<0.01, ***p<0.001.*

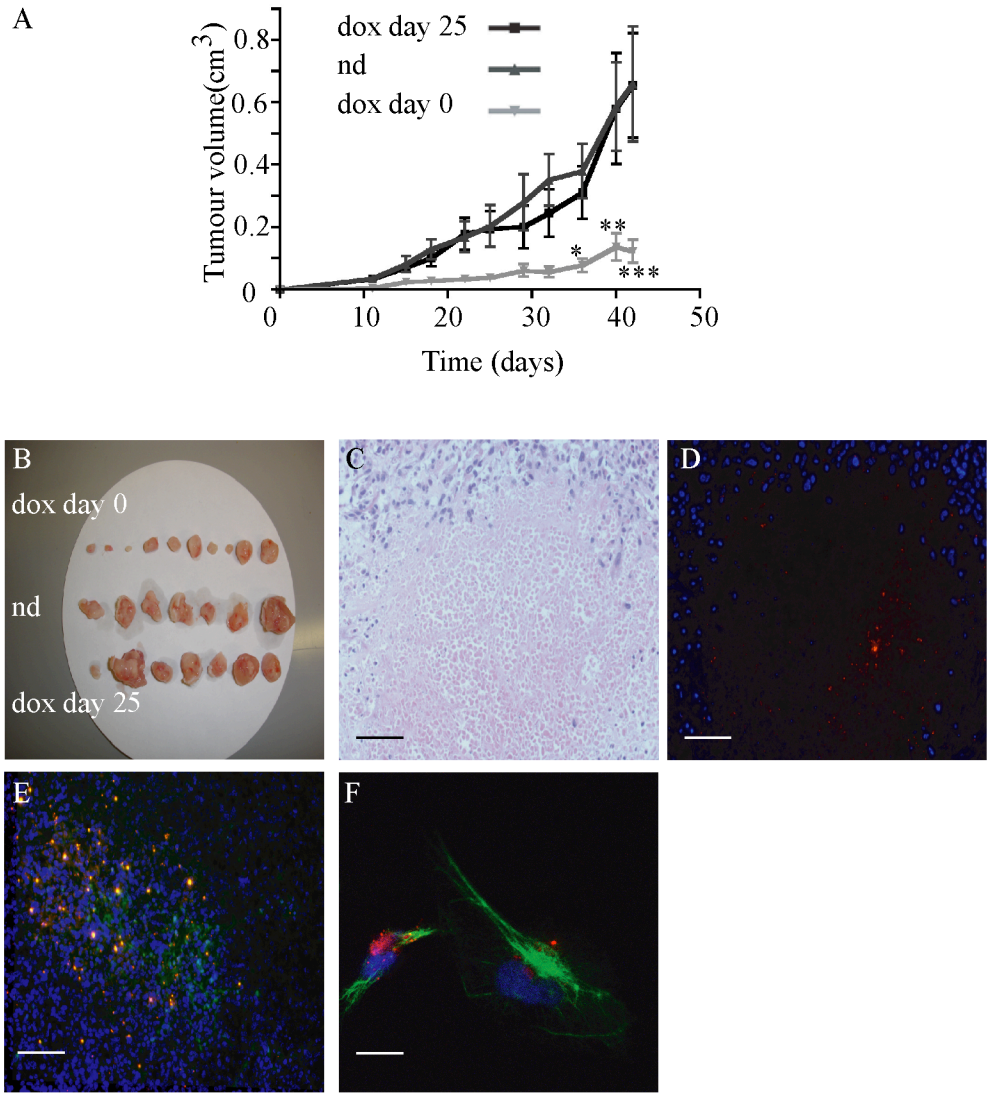

Figure 5.2 TRAIL-expressing MSCs reduce the growth of subcutaneous tumours.
*Subcutaneous tumours were produced by the coinjection of $2x10^6$ MDAMB231 cells and $0.75x10^6$ MSCFLT cells, and the mice were treated with doxycycline (dox) at day 0 or day 25 or with no dox (nd). A) Dox treatment from day 0 led to a reduced tumour size compared to the nd group. There was no reduction in tumour growth if TRAIL was activated at day 25. B) Macroscopic appearance of the tumours. C) H&E immunohistochemistry showing large areas of necrosis within the tumours in mice treated with dox from day 0. D) Contiguous fluorescent microscopy sections showing MSCFLTs (DiI - red) in these necrotic areas (DAPI nuclear counterstain - blue). Scale bar represents 20µm. E) TUNEL staining (green) demonstrated areas of tumour apoptosis localised with areas of MSCFLTs (DiI - red) within the tumours in mice treated with dox from day 0 (DAPI - blue). Scale bar represents 20µm. F) Ex vivo single cell digestion and culture showed DiI-positive (red) cells with MSC morphology that co-stained with vimentin (green) (DAPI - blue). Scale bar represents 2µm. *p<0.05, **p<0.01, ***p<0.001.*

5.1.2 Intratumour Delivery

TRAIL-expressing MSCs are therefore able to incorporate into early tumours and affect cancer growth. A further experiment was performed to see if they could incorporate into and affect the clinical course of established tumours.

Two million MDAMB231 cells were injected subcutaneously into NOD/SCID mice. Subcutaneous tumours were allowed to grow until day 45 with an average size of $0.28 \pm 0.11 cm^3$. The mice were then split into three groups; the tumours of group one were injected with $0.75x10^6$ MSCFLT cells and exposed to doxycycline (n=4), group two were also injected with MSCFLT cells, but these mice were not exposed to doxycycline (n=4), and group three were injected with PBS intratumourly (n=5), and exposed to doxycycline (Figure 5.3A). The tumours of all three groups continued to grow following this treatment and there was no difference in subsequent growth over the next 12 days, or the final weight at day 57 (Figure 5.3B-D).

5.1.3 Systemic Delivery

The coinjection model had demonstrated an ability of the TRAIL-expressing MSCs to modulate tumour growth in vivo. Intratumoural injection of MSCFLT cells would be a valid delivery route clinically for visualised tumours, however it would not be applicable in many clinical situations such as therapy for lung cancer metastases. Furthermore, intratumoural delivery does not utilise the homing property of the cells, one of the main reasons for their use. For this, MSCFLT cells were intravenously injected into mice to treat subcutaneous tumours (Figure 5.4). Two million MDAMB231 cells were injected subcutaneously into NOD/SCID mice and the mice were treated at days 10, 20, and 30 with intravenous delivery of $0.5x10^6$ MSCFLT cells with doxycycline (n=10), or MSCFLT without doxycycline (n=11), or PBS with doxycycline (n=9) (Figure 5.4A). The mice were harvested at day 35, and despite the presence of DiI-labelled MSCs within the tumour mass (Figure 5.4B), there was no effect of the therapy on subcutaneous tumour growth or final weight (Figure 5.4C,D).

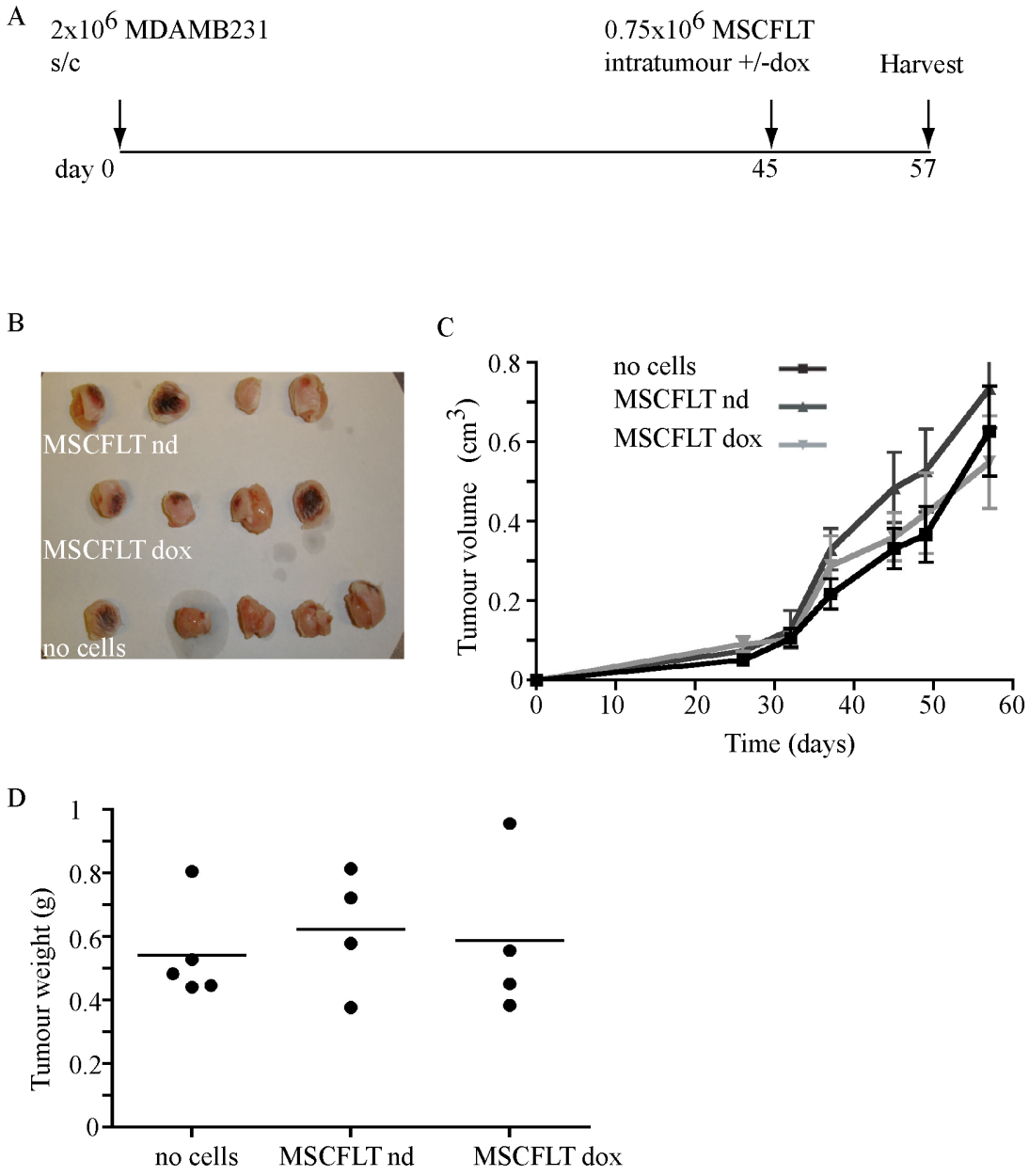

Figure 5.3 Intratumour delivery of TRAIL-expressing MSCs does not reduce the growth of established subcutaneous tumours.
A) MDAMB231 subcutaneous tumours were treated at day 45 with intratumour delivery of TRAIL-transduced MSCs (MSCFLT) or phosphate-buffered saline control (no cells). B) Macroscopic appearance of the tumours. C-D) There was no effect on tumour growth (C) or weight (D) with the use of MSCFLT, with either doxycycline induced TRAIL activation (dox) or no doxycycline (nd).

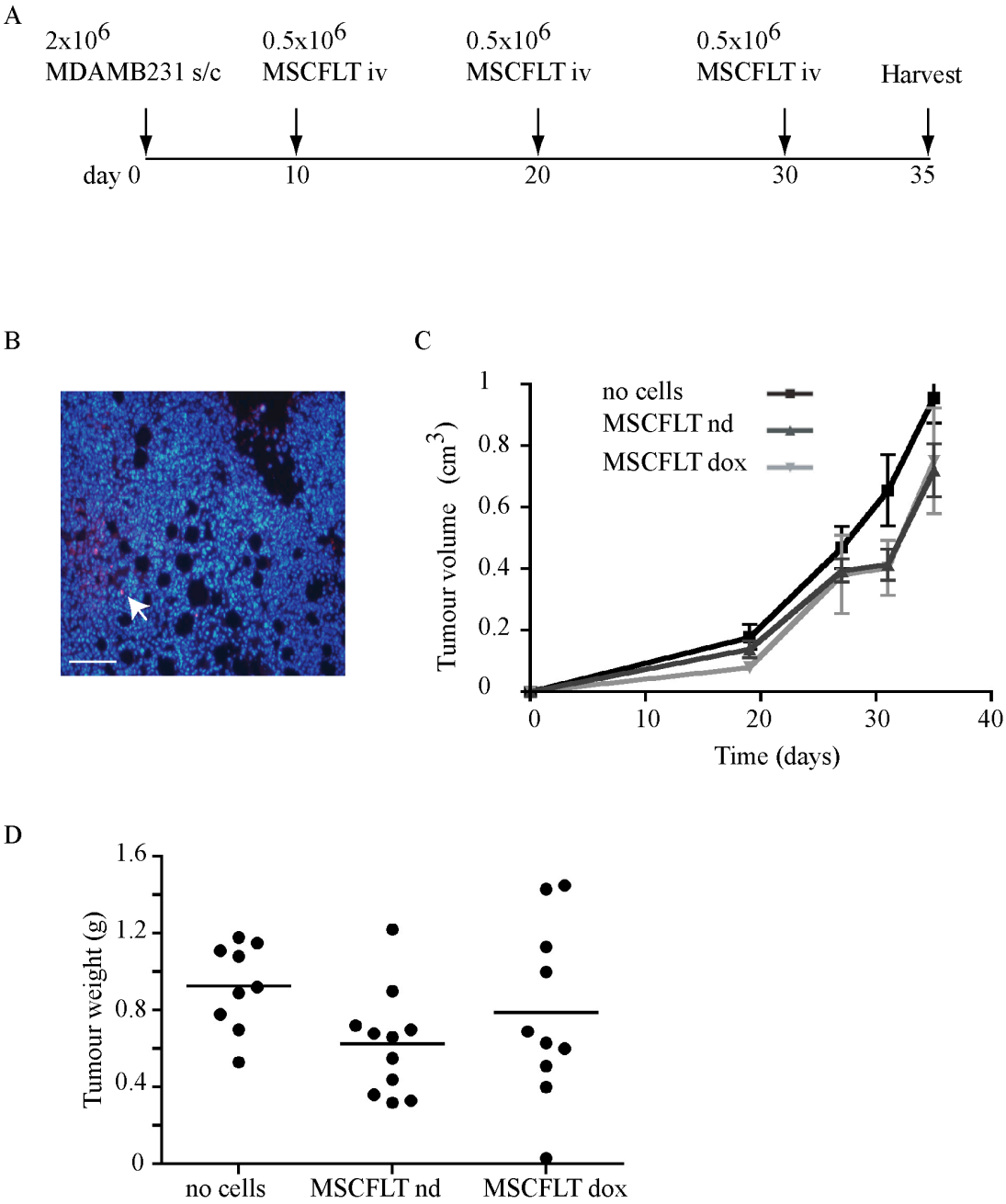

Figure 5.4 Systemic delivery of TRAIL-expressing MSCs does not reduce the growth of subcutaneous tumours.
A) MDAMB231 subcutaneous tumours were treated at days 10, 20, 30 with intravenous delivery of MSCFLT cells or phosphate-buffered saline control (no cells). B) Fluorescent microscopy demonstrating the DiI-labelled MSCFLTs (red) migrated to the subcutaneous tumour. DAPI nuclear counterstain - blue. Scale bar represents 20μm. C-D) There was no effect on tumour growth (C) or weight (D) with the use of MSCFLT with either doxycycline induced TRAIL activation (dox) or no doxycycline (nd).

5.2 Metastatic tumour model

The subcutaneous models demonstrated the ability of a high concentration of MSCFLTs to affect the growth of primary tumours when at an early stage of tumour growth, with no effect on established tumours. The advantage of the metastasis model would be to also utilise the specific tumour homing of the MSCFLT cells. The metastatic deposits would also be more similar to the early tumours, and whereas primary tumours can often be treated with surgery, it is the secondary cancer metastasis that leads to the majority of cancer death, therefore providing a very worthwhile target for the MSCFLT treatment.

5.2.1 Systemic Delivery

Two million intravenously injected MDAMB231 cells were used to produce lung metastases in NOD/SCID mice. MSCFLT cells were then delivered intravenously at days 7, 14, 21 and 28 (Figure 5.5A). The mice received MSCFLT and doxycycline, MSCFLTs alone, or PBS and doxycycline (n=8 per group). They were harvested at day 35 and each lobe of every mouse was analysed histologically to determine the area and number of metastases. Tumour metastases were found in all mice (8/8) without MSCFLT and all mice with MSCFLT without the use of doxycycline (8/8). In the MSCFLT plus doxycycline arm, three out of eight mice were tumour free ($p=0.032$, Chi^2) (Figure 5.5B). In addition to the elimination of metastases with MSCFLT plus doxycycline, the lung weight, which serves as a correlate for metastatic load, was also significantly reduced in the MSCFLT plus doxycycline group compared to the PBS-treated mice (0.22 ± 0.03g vs. 0.29 ± 0.06g)($p<0.01$, Anova). Similar results were achieved when metastases numbers per lung area (0.04 ± 0.05 vs. 0.27 ± 0.04)($p<0.001$, Anova), or the total metastasis area per lung area (2.40 ± 2.66 vs. 14.29 ± 3.46)($p<0.001$, Anova), were used as an endpoint (Figure 5.5C-E). Three mice had to be excluded from these latter analyses, as the lungs did not inflate during the fixation procedure.

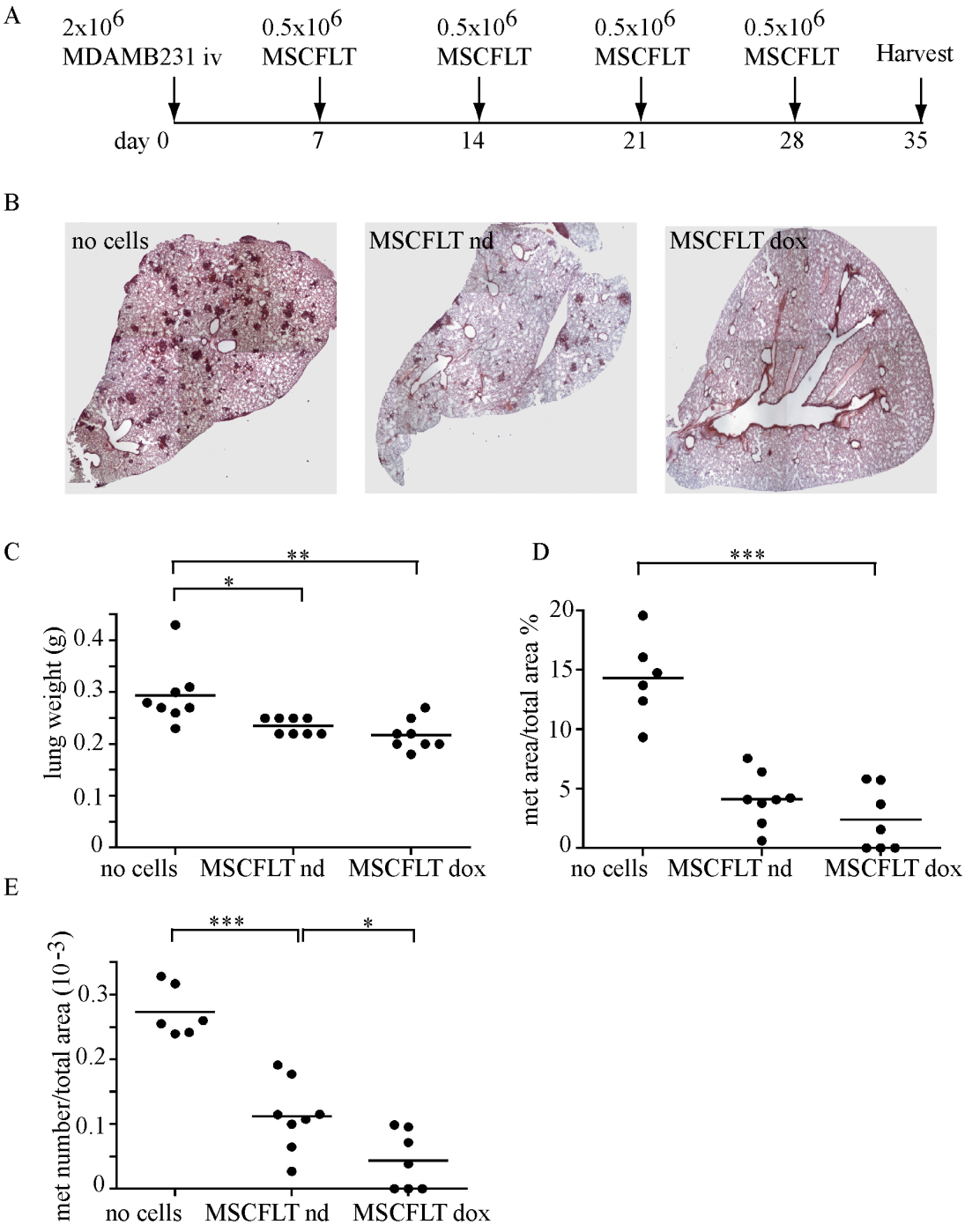

Figure 5.5 TRAIL-expressing MSCs reduce the growth of lung metastases.
*A) 2 million MDAMB231 cells were injected intravenously at day 0 followed by intravenous treatment with phosphate-buffered saline (no cells) or MSCFLT cells at days 7, 14, 21 and 28 with (dox) or without (nd) doxycycline. B) Representative histology of lung lobes in the three experimental groups. Metastases remained, but were reduced, after injection of MSCFLT without dox, while dox-induced TRAIL activation of MSCFLTs eliminated metastases in 3 of 8 mice (p=0.03). C-E) Reduction in lung weight (C) and metastases area (D) and number (E) per lung area with the use of MSCFLTs both with and without doxycycline treatment. There was a further significant reduction between dox-activated and nd MSCFLT. ***p<0.001, **p<0.01, *p<0.05.*

MSCFLT cells delivered to control mice without doxycycline were unable to clear the metastases in any mice, but did have less metastases per area ($p<0.001$, Anova), a lower total metastasis area per lung area ($p<0.001$, Anova), and a reduced lung weight ($p<0.05$, Anova) than the untreated mice. MSCFLT plus doxycycline treatment however produced a further significant reduction in metastases number ($p<0.05$, Anova) (Figure 5.5E).

In a subsequent experiment, TRAIL and GFP were both shown to be expressed in vivo by the MSCFLT cells with immunohistochemistry when mice were harvested two days after treatment with MSCFLT and doxycycline (Figure 5.6A,B). TRAIL mRNA derived from the lungs of these mice was also increased (Figure 5.6C).

5.2.2 Early, prophylactic delivery

The ability of TRAIL-expressing MSCs to reduce, and in some cases eliminate, the development of lung metastases is very exciting. On the basis of these results and the results from the subcutaneous experiments suggesting a greater tumour modulating effect at early tumour timepoints, the next experiment attempted to prevent the development of metastases in a greater percentage of mice by administering the cellular therapy at earlier timepoints. Two million MDAMB231 cells were intravenously injected into NOD/SCID mice. The mice received $0.5x10^6$ MSCFLT and doxycycline (n=8), $0.5x10^6$ MSCFLT alone (n=9), or PBS and doxycycline (n=10) intravenously at days 0, 1, and 5. Mice were harvested at day 35 and analysed as above. All mice developed lung metastases, with no differences in final lung weight, or metastasis number and area per lung area (Figure 5.7).

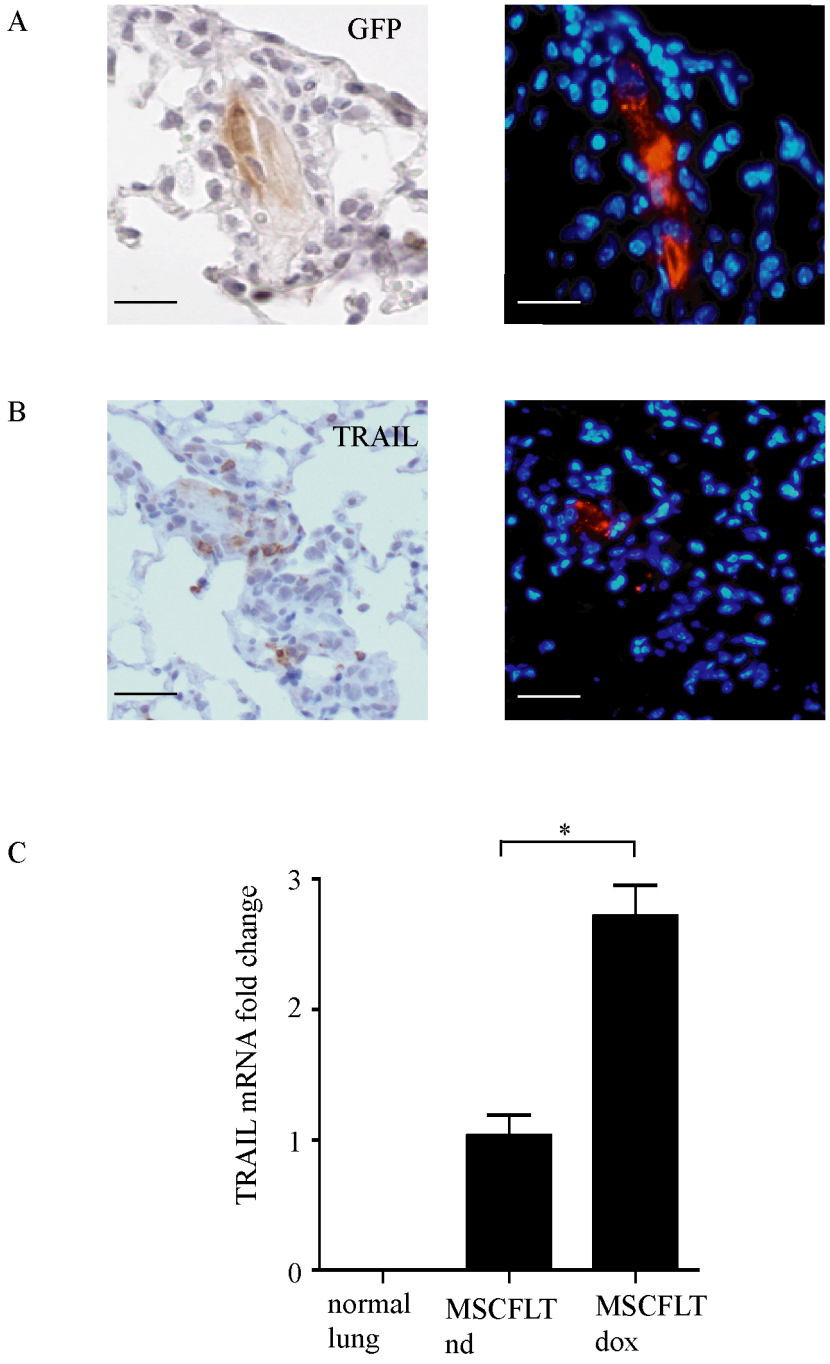

Figure 5.6 TRAIL and GFP can be detected in the lung metastases following intravenous delivery of TRAIL-expressing MSCs.
*Mice with MDAMB231 lung metastases were harvested 2 days after delivery of 0.5x10^6 DiI-labelled, MSCFLT cells. A) Immunohistochemistry demonstrating cells expressing GFP (scale bar represents 5μm) and B) TRAIL (scale bar represents 10μm) and contiguous immunofluorescence sections showing these cells also express DiI (red). DAPI nuclear counterstain – blue. B) There was an increase in TRAIL mRNA from lung digests from mice treated with MSCFLT and doxycycline (dox) compared to mice treated with MSCFLT without dox (nd). *p<0.05.*

5.3 Physiological metastatic tumour model

Similar metastasis models created by the intravenous injection of cancer cells in immunocompromised mice have been used in several previous studies (Studeny et al., 2002; Studeny et al., 2004; Xin et al., 2007). A more physiological metastasis model, whereby cancer cells detach from a primary tumour and migrate and seed metastases was also developed for this project by allowing MDAMB231 subcutaneous tumours to grow and produce lung metastases. Two million MDAMB231 cells were injected subcutaneously into NOD/SCID mice and the mice were treated with $0.5x10^6$ MSCFLT and doxycycline (n=10), $0.5x10^6$ MSCFLT alone (n=11), or PBS and doxycycline (n=9) intravenously at days 10, 20, and 30. Although there was no effect on the primary tumour growth (see 5.1.3), there was a reduction in the metastatic load with the MSCFLT therapy, consistent with the other metastatic model. Tumour metastases were found in all mice (9/9) without MSCFLT cells and 10/11 mice with MSCFLT cells without the use of doxycycline. In the MSCFLT plus doxycycline group, 3/10 mice were tumour free ($p=0.138$, Chi^2) (Figure 5.8B). There was a significant reduction in metastases number per lung area (0.01 ± 0.01 vs. 0.03 ± 0.02) and total metastasis area per lung area (0.82 ± 0.95 vs. 3.82 ± 1.38) (both $p<0.05$, Anova) in the MSCFLT and doxycycline group compared to the PBS-treated mice (Figure 5.8C,D).

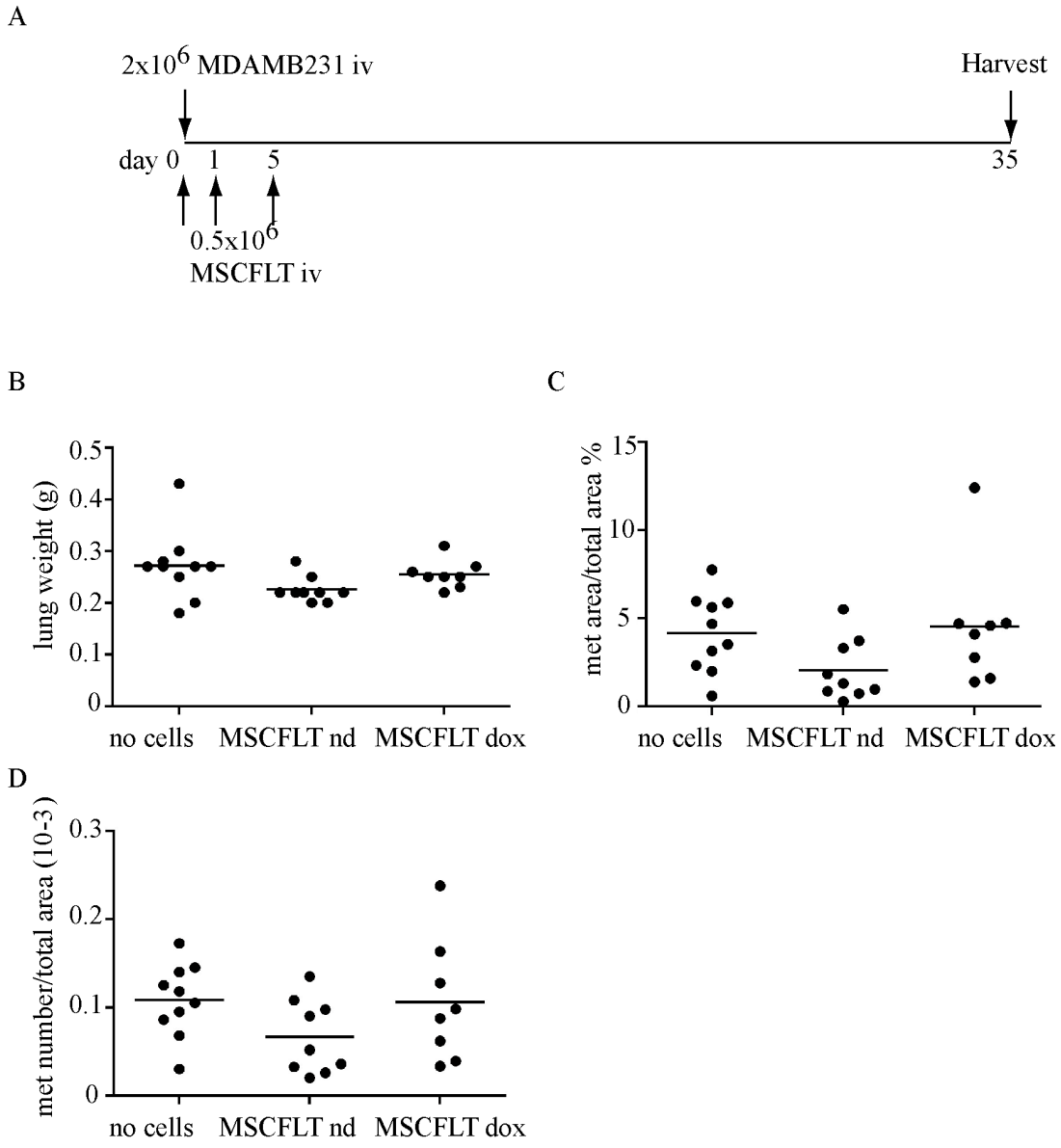

Figure 5.7 Early systemic delivery of TRAIL-expressing MSCs does not prevent the development of metastases.
A) 2 million MDAMB231 cells were injected intravenously at day 0 followed by intravenous treatment with phosphate-buffered saline (no cells) or MSCFLT cells at days 0, 1, and 5 with (dox) or without (nd) doxycycline. B-D) No reduction in lung weight (B) and metastases area (C) and number (D) per lung area with the use of MSCFLTs both with and without doxycycline treatment.

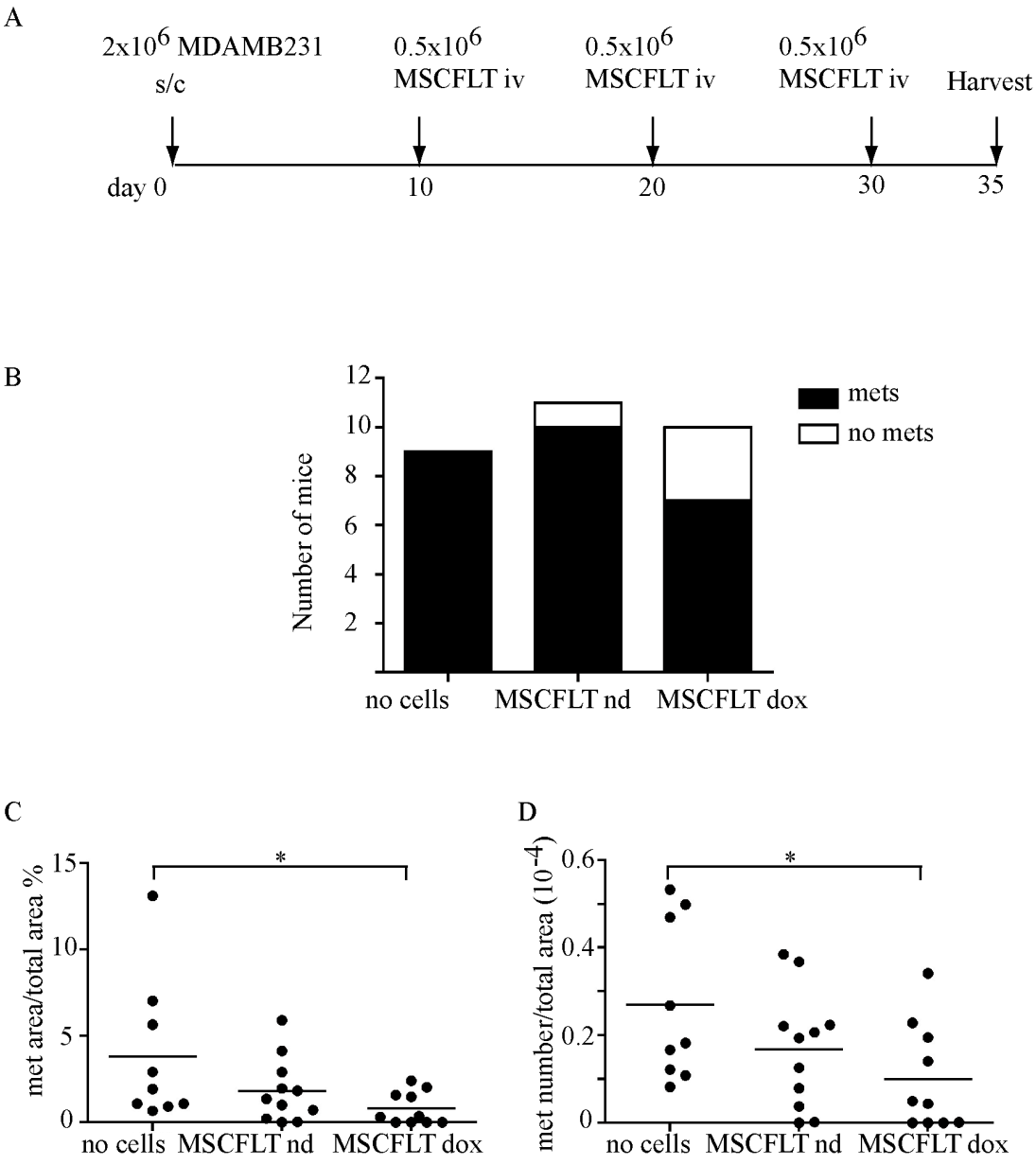

Figure 5.8 TRAIL-expressing MSCs reduce the growth of physiological lung metastases. *A) 2 million MDAMB231 cells were injected subcutaneously at day 0 and treated intravenously with phosphate-buffered saline (no cells) or MSCFLT cells at days 10, 20, and 30 with (dox) or without (nd) doxycycline. B) Dox-induced TRAIL activation of MSCFLTs eliminated metastases in 3 of 10 mice (p=0.14). C-D) Reduction in metastases area (D) and number (E) per lung area with the use of dox-activated MSCFLT cells compared to the no cell-treated mice. *p<0.05.*

5.4 Summary

This chapter has demonstrated

- MSCFLT cells significantly reduce the growth of early subcutaneous tumours when coinjected.

- MSCFLT cells do not alter the growth of established subcutaneous tumours when delivered by coinjection, intratumour injection, or intravenously.

- MSCFLT cells home to and reduce the development of lung metastases in 2 different models, eliminating metastases in some subjects.

- MSCFLT cells cannot prevent metastases before they have developed.

CHAPTER 6. RESULTS IV – Cancer stem cells and the side population

6.1 Introduction

6.1.1 Cancer Stem Cells

Cancers are composed of a heterogeneous mix of cells with varying differentiation, proliferation and tumorigenic properties (Heppner, 1984). Indeed, in vivo studies have demonstrated that within a cancer population, only a small percentage of cells are able to initiate tumour development (Al-Hajj et al., 2003; Lapidot et al., 1994). Many believe that the heterogeneous groups of cells includes a small population of cancer cells with stem cell properties, so called 'cancer stem cells', with the capacity to self-renew and differentiate asymmetrically (Visvader & Lindeman, 2008). Conventional cancer treatments may eradicate the tumour bulk but spare populations of cancer stem cells, which are able to restore tumour tissue and lead to recurrence. This may explain why an initial tumour regression does not necessarily translate to an improved patient survival in many clinical trials for advanced cancers (Wicha et al., 2006). Possible mechanisms for the resistance of cancer stem cells to treatments include their increased ability to repair damaged DNA (Bao et al., 2006), the activation of survival pathways (Hambardzumyan et al., 2008), and the increased expression of ATP binding cassette protein (ABC) transporters (Dean et al., 2005). The identification and destruction of these cells may therefore improve cancer treatment responses.

6.1.2 Side Population

Cell surface markers have been used in some cancers to produce a population of cells enriched with stem cell properties, for example CD133 in the identification of human

glioma (Singh et al., 2004) and colon cancer (Ricci-Vitiani et al., 2007) stem cells. However these markers appear specific to particular tumours, and no marker has identified cancer stem cells across tumour types. Normal stem cell characteristics are often utilised to identify this population. This includes the ability to efflux nuclear dyes such as Hoechst 33342, which binds to DNA. The efflux of Hoechst is due to ABC transporters, in particular ABCG2/BCRP1 (Zhou et al., 2001). These Hoechst-effluxing cells were originally described in the bone marrow and termed 'side population' due to their appearance on flow cytometry plots (Goodell et al., 1996). They have since been shown in a variety of normal tissues, where they possess stem-like properties (Wu & Alman, 2008). These Hoechst-effluxing cells have also been identified in many cancers, including lung (Ho et al., 2007; Sung et al., 2008), breast (Engelmann et al., 2008), oesophageal (Huang et al., 2009), hepatocellular (Kamohara et al., 2008), glioma (Harris et al., 2008), and renal (Addla et al., 2008) cancer cell lines, in addition to primary cancer cells (Barrett et al., 1995; Hirschmann-Jax et al., 2004; Szotek et al., 2006; Wu et al., 2007).

The side population cells within cancers have many stem-like properties, including the ability to repopulate both the SP and non-SP cell compartments (Ho et al., 2007; Kondo et al., 2004; Zhang et al., 2009), an increased ability to form colonies (Zhang et al., 2009) and generate complex spheroids in 3D culture (Addla et al., 2008), a high telomerase activity (Ho et al., 2007), and increased quiescence (Ho et al., 2007). They have also been shown to express a number of stem-like genes (including OCT-4, SOX-2, and BMI-1) (Huang et al., 2009; Zhang et al., 2009), ABC transporter genes (including ABCG2) (Huang et al., 2009; Zhang et al., 2009), and genes involved in the Wnt (Addla et al., 2008; Haraguchi et al., 2006; Huang et al., 2009), Notch (Addla et al., 2008; Huang et al., 2009), PI3K/Akt pathways, and cell cycle regulation (Zhou et al., 2007). Side population cells derived from both primary tumours (Wu et al., 2007) and cancer cell lines (Chiba et al., 2006; Ho et al., 2007) also have an increased ability to initiate tumours compared to the majority of the tumour cells, when xenografted into immunodeficient mice. These features have led to suggestions that these cells may fill the role of the putative cancer stem cell (Giangreco et al., 2007; Hadnagy et al., 2006), although other groups have not demonstrated such stem cell-like behaviour of the SP cells in certain cancers (Burkert et al., 2008; Lichtenauer et al., 2008).

In addition to the ability of these cells to repopulate tumours, they are also able to escape death by many chemotherapeutic agents, due in part to their increased ABC transporter expression (Chiba et al., 2006) which, in addition to effluxing Hoechst, is also able to efflux lipophilic chemotherapy agents such as doxorubicin (Doyle & Ross, 2003), and methotrexate (Chen et al., 2003). Furthermore, chemotherapy and radiation treatments preferentially target rapidly proliferating cells in comparison to what may be the relatively quiescent cancer stem cells. This combination of resistance and tumour initiation makes it likely that these side population cells are central to tumour growth and recurrence, and stresses the importance that future cancer therapeutics are able to target these cells. I hypothesise that TRAIL therapy would target SP and non-SP cells equally.

6.2 Results

6.2.1 Squamous and lung cancer cell lines contain an ABC transporter side population

Many cancer cell lines and primary cells contain a side population. In order to determine whether squamous cell, lung and breast carcinomas might also contain a similar subpopulation of drug-resistant SP cells, confluent H357 (squamous), A549 (lung) and MDAMB231 (breast) cancer cell lines were incubated with Hoechst 33342 dye and analysed by flow cytometry. A characteristic SP fraction was detected in the H357 and A549 cell lines, but not the MDAMB231 cells, which is consistent with a previous report (Engelmann et al., 2008). The squamous and lung SPs were both reserpine sensitive, indicating their dependence on ABC-type transporter activity (Figure 6.1).

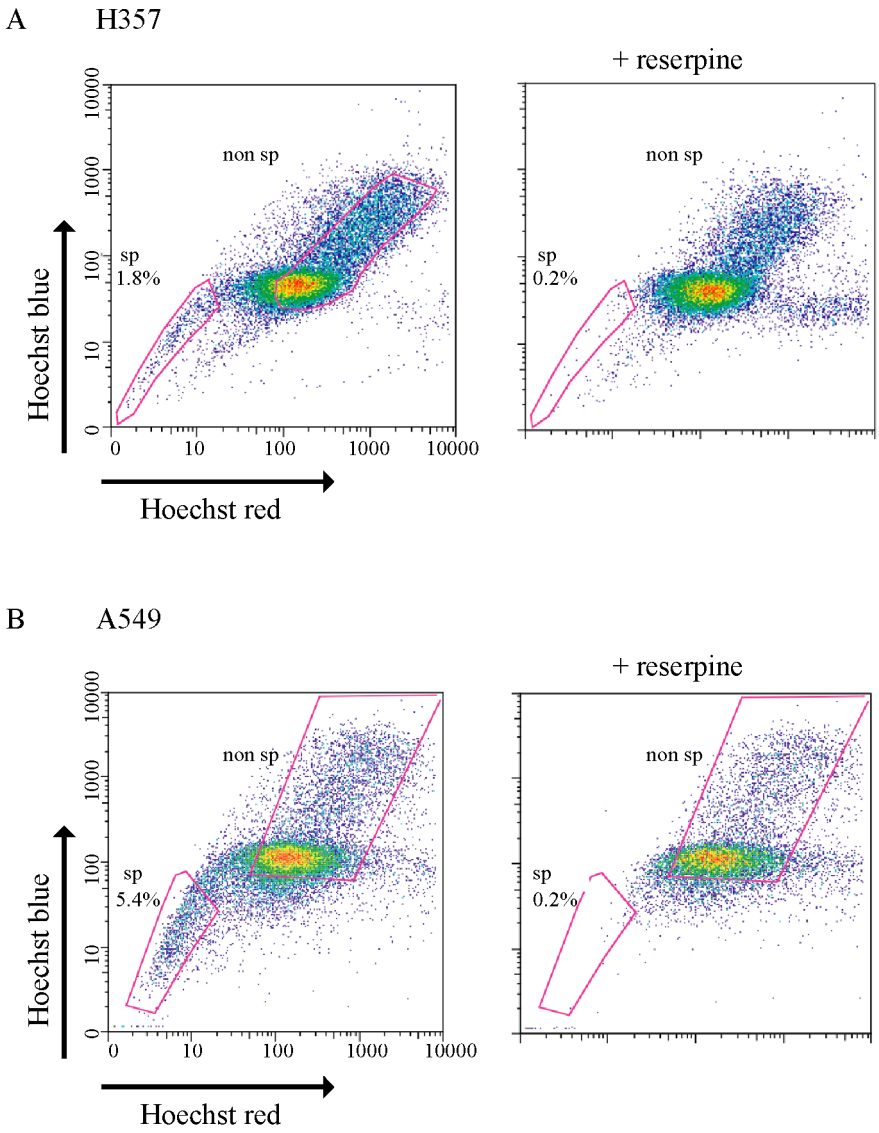

Figure 6.1 Squamous cancer and lung cancer cell lines contain a side population.
A-B) Representative flow cytometry plots demonstrating the H357 (A) and A549 (B) cancer cell lines contain a side population (SP) of cells that stain poorly with Hoechst. This population disappears with the ABC transporter inhibitor, reserpine. The gates show the cells defined as SP and non-SP for the experiments.

6.2.2 The SP cells exhibit stem-like characteristics in vitro

The ability to form expanding colonies of cells is a typical stem cell characteristic. The ability of both SP and non-SP H357 cells to form colonies was investigated and taken as an indicator of their individual proliferative capacity. SP cells were shown to have an increased clonogenic potential compared to non-SP cells when 200 cells of both types were separately plated in 6-well plates. This experiment was performed by Laura Pritchard, a student in the laboratory (Appendix B, Figure 4). Similar results were suggested by my own experiments (section 6.2.5).

6.2.3 The SP cells exhibit stem-like characteristics in vivo

To test for in vivo tumorigenic potential, which is the feature most often taken to signify the presence of cancer stem cells, the tumour formation capacity of H357 SP and non-SP cells were compared. Two million SP cells (n=6) or 2 million non-SP H357 cells (n=6) were subcutaneously injected into the flank of NOD/SCID mice and allowed to grow for 49 days. In accordance with previous attempts to grow H357 cells in an in vivo model (Janes & Watt, 2004; Jones et al., 1996), none of the non-SP cell grafts produced tumours (Figure 6.2A,B). Interestingly, three of six SP sorted and engrafted cell populations did produce subcutaneous tumours with an average volume of $0.038cm^3$ (Figure 6.2A,B). Human H357 squamous cell carcinomas were confirmed by H&E, and active cell proliferation was demonstrated by staining for Ki67, a cell cycle protein expressed from G1 through to the end of the M phase of the cell cycle (Figure 6.2C,D). To my knowledge, this is the first demonstration of an H357 cell population's ability to produce tumours in vivo strongly suggesting that the SP contains a unique population of cancer stem-like cells.

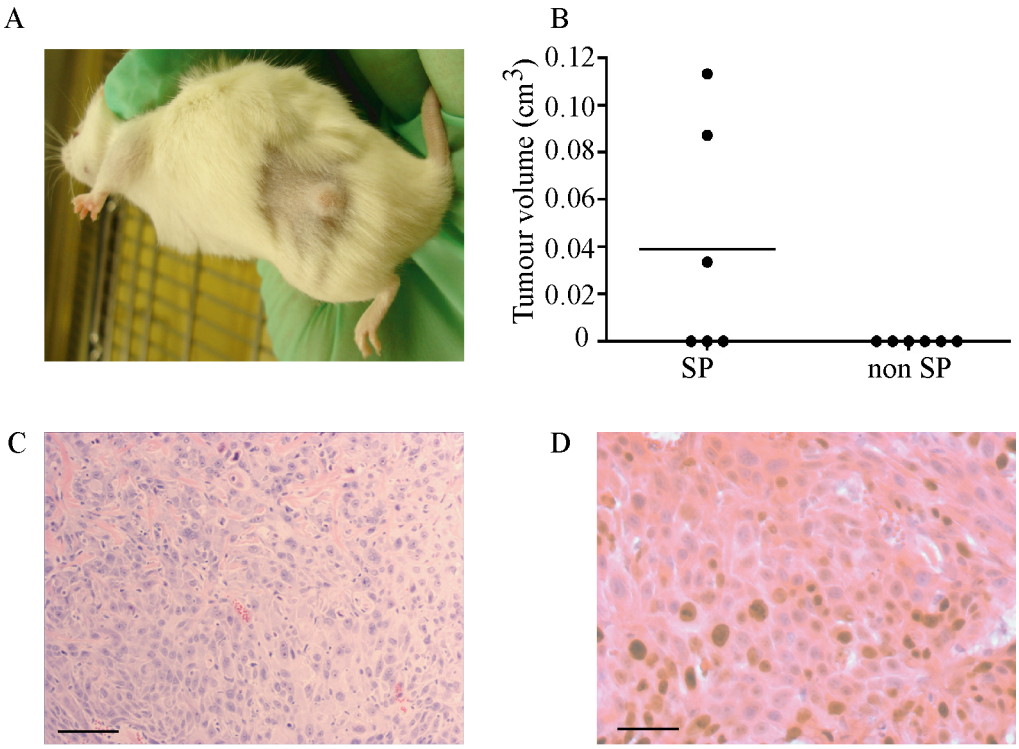

Figure 6.2 The SP cells are tumorigenic in vivo.
A,B) Subcutaneous injection of 2x10^6 H357 side population (SP) cells led to tumours in 3/6 NOD/SCID mice, compared to 0/6 tumours when 2x10^6 non-SP cells were used. C) H&E staining confirmed a squamous cell carcinoma (scale bar represents 20μm) with D) high proliferation shown by Ki67 staining (scale bar represents 10μm).

6.2.4 The SP cells are chemoresistant

The observation that H357-SP cells exhibited elevated Hoechst 33342 efflux, indicated that these cells may possess resistance to cytotoxic chemotherapeutic drugs, including mitoxantrone. Colony forming assays were performed to assess SP and non-SP H357 cells for mitoxantrone sensitivity. Two hundred cells were cultured in the presence of 0, 1 and 10ng/ml mitoxantrone for 3 days followed by 14 days culture in mitoxantrone-free media and the numbers of large colonies were compared. The SP subgroup of H357 cells was capable of maintaining significantly more large colonies than the non-SP cells in mitoxantrone (Figure 6.3A) (10ng/ml; 38.3 ± 4.5 large colonies with the SP compared to 3.0 ± 1.0 with the non-SP cells; $p<0.05$, 2-way Anova). This raw data (Figure 6.3) was from the experiments of Laura Pritchard. (see also Appendix B, Figure 6), and I have adapted it for this project. In addition, similar experiments to this have been repeated by myself (6.2.6).

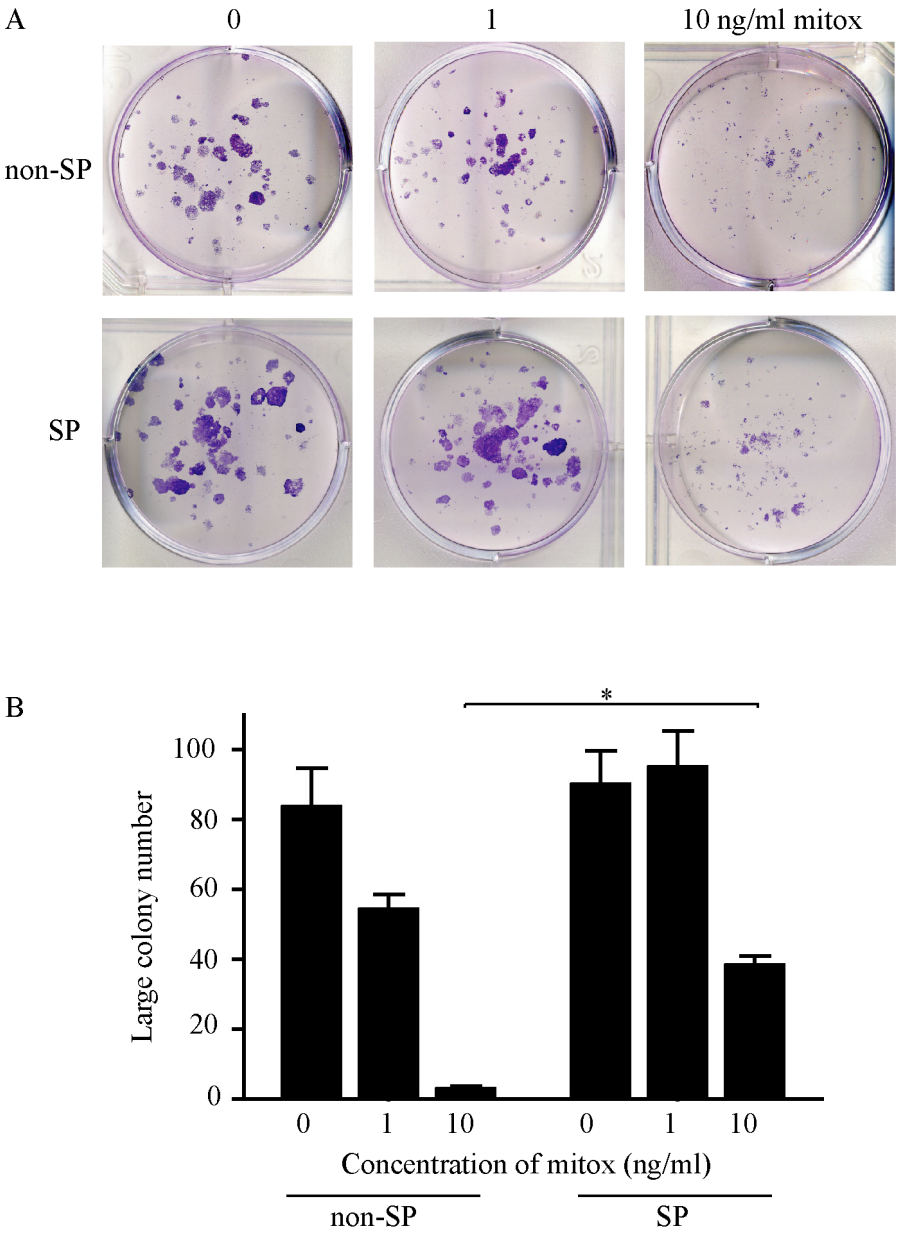

Figure 6.3 The SP cells have an increased resistance to mitoxantrone.
*A) 200 side population (SP) or non-SP H357 cells were plated for colony forming assays before the addition of 0, 1, or 10ng/ml of mitoxantrone (mitox). The plates were stained with rhodanile blue. B) Quantification of large colony numbers from (A) demonstrates an increased ability of SP cells to form large colonies in 10ng/ml mitoxantrone. * $p<0.05$.*

6.2.5 The SP cells can be killed by TRAIL-expressing MSCs

In the previous chapters, TRAIL-expressing MSCs have been shown to have the ability to cause cancer cell death and a decrease in tumour and metastasis development in vivo. The cancer stem cell hypothesis suggests that the destruction of the cancer stem cell candidates is also crucial for a cancer therapy. Having isolated a population enriched for possible cancer stem cells (SP) in both squamous and lung cancer cell lines, their susceptibility to the TRAIL-expressing MSC therapy was tested in coculture experiments. SP and non-SP cells were freshly flow-sorted from DiI-stained H357 and A549 cells (Figure 6.1) and immediately cocultured with the MSCFLT cells. The death and apoptosis of the cancer cells in coculture was assessed by Annexin V flow cytometry as previously described. There was a significant increase in death and apoptosis of both the SP and non-SP subgroups of H357 cells with the use of doxycycline and activation of the TRAIL transgene (SP: 13.4 ± 1.4% increased to 68.1 ± 5.5%, non-SP: 16.1 ± 1.4% increased to 60.9 ± 2.5%) (Figure 6.4) and A549 (SP: 2.7 ± 0.5% increased to 27.7 ± 1.9%, non-SP: 4.4 ± 1.5% increased to 30.4 ± 1.6%) (Figure 6.5) (both $p<0.001$, Anova). There was no difference between the SP and non-SP subgroups in their response to the TRAIL-expressing MSCs in both cancer cell lines (Figure 6.4, 6.5).

The susceptibility of the cancer cell subpopulations to TRAIL-expressing MSCs was further assessed with colony forming assays. Two hundred freshly sorted, DiI-stained SP or non-SP H357 cells were added to a 6-well plate. The following day, $5x10^4$ MSCFLT cells (treated with mitomycin C to prevent their further growth) were added to the plates and the TRAIL transgene either activated or not with doxycycline. As had previously been shown (see 6.2.2), colony formation was greater in the SP subgroup compared to the non-SP cells (60.0 ± 1.7 large colonies in the SP cells compared to 34.0 ± 7.8 large colonies in the non-SP cells)($p<0.001$, 2-way Anova). Colony formation was significantly inhibited in both cell subgroups with the doxycycline-induced activation of the TRAIL transgene of the MSCs (SP: 60 ± 1.7 large colonies reduced to 14.7 ± 4.2 large colonies with TRAIL expression, non-SP: 34.0 ± 7.8 large colonies reduced to 8.0 ±1.7 large colonies with TRAIL expression) (both $p<0.001$, 2-way Anova) (Figure 6.6).

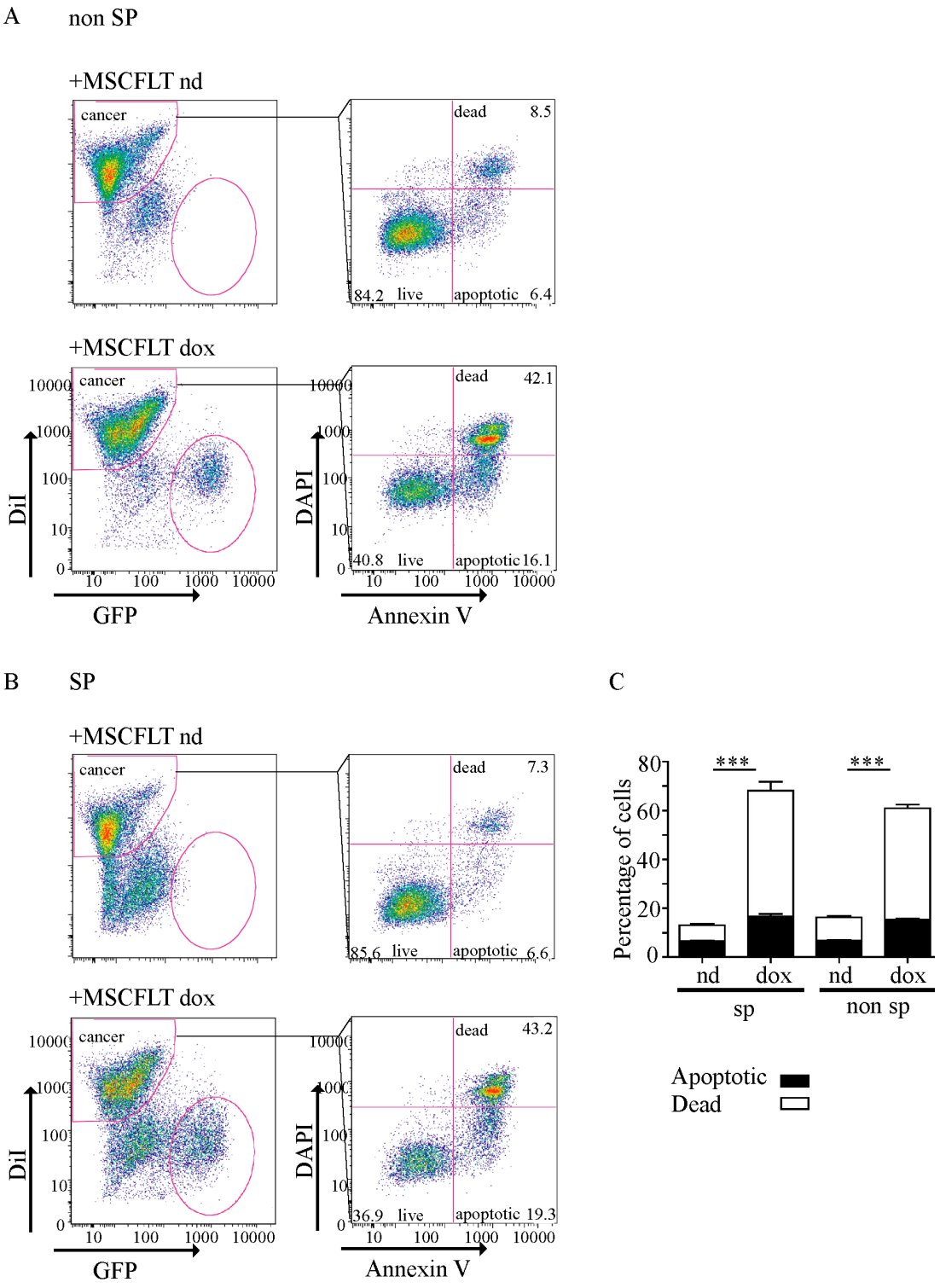

Figure 6.4 TRAIL-expressing MSCs lead to death and apoptosis of H357 SP and non-SP cells.

*Freshly sorted DiI-labelled H357 side population (SP) and non-SP cells were cocultured with MSCFLT cells with (dox) or without (nd) doxycycline. A-B) Representative flow cytometry plots demonstrating the percentage of apoptotic and dead non-SP (A) and SP (B) H357 cells. C) Bar chart representing triplicate experiments demonstrating the increase in death and apoptosis with doxycycline–induced TRAIL expression in both the SP and non-SP subgroups. *** $p<0.001$.*

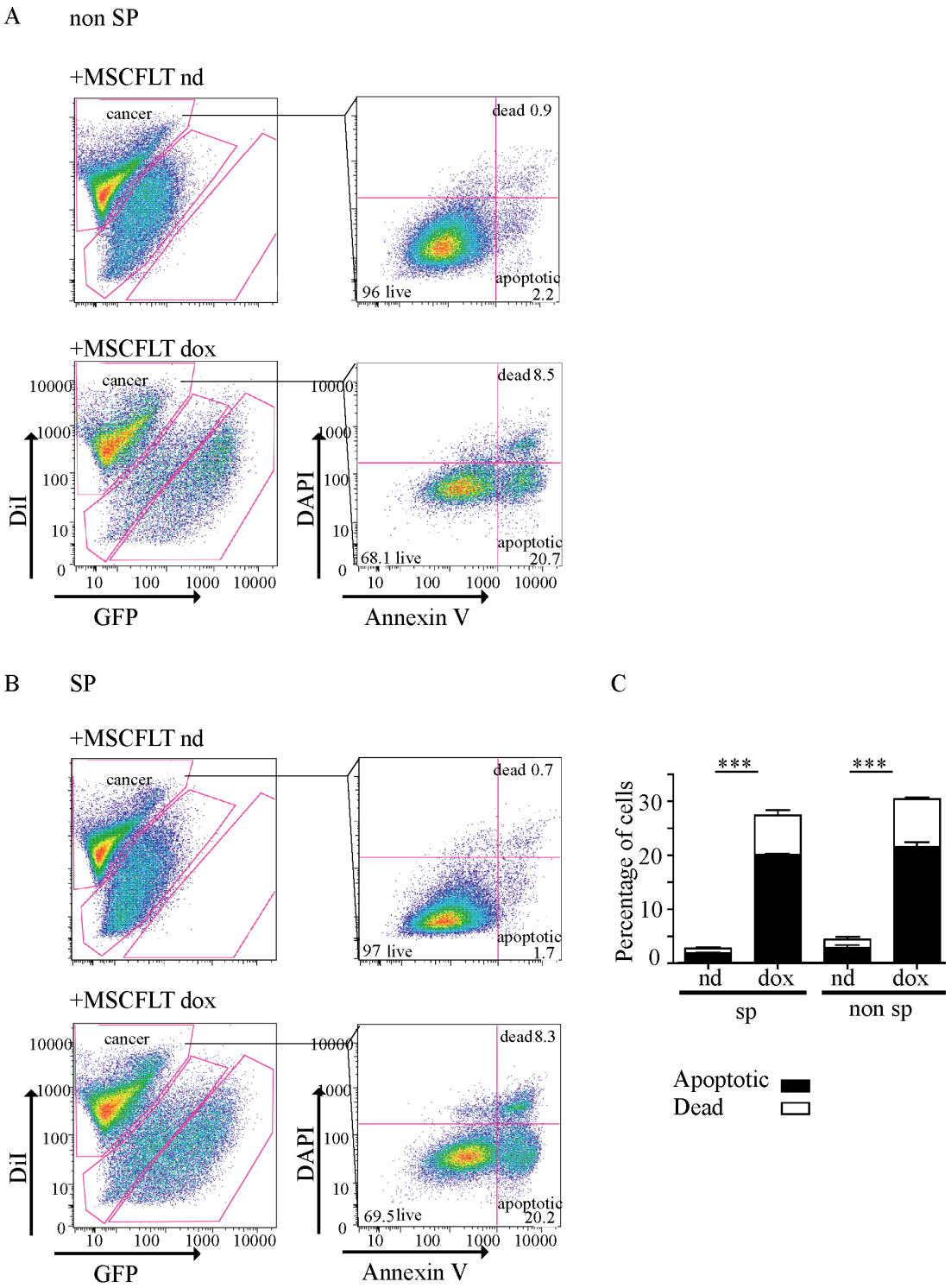

Figure 6.5 TRAIL-expressing MSCs lead to death and apoptosis of A549 SP and non-SP cells.

*Freshly sorted DiI-labelled A549 side population (SP) and non-SP cells were cocultured with MSCFLT cells with (dox) or without (nd) doxycycline. A-B) Representative flow cytometry plots demonstrating the percentage of apoptotic and dead non-SP (A) and SP (B) A549 cells. C) Bar chart representing triplicate experiments demonstrating the increase in death and apoptosis with doxycycline–induced TRAIL expression in both the SP and non-SP subgroups. *** $p<0.001$.*

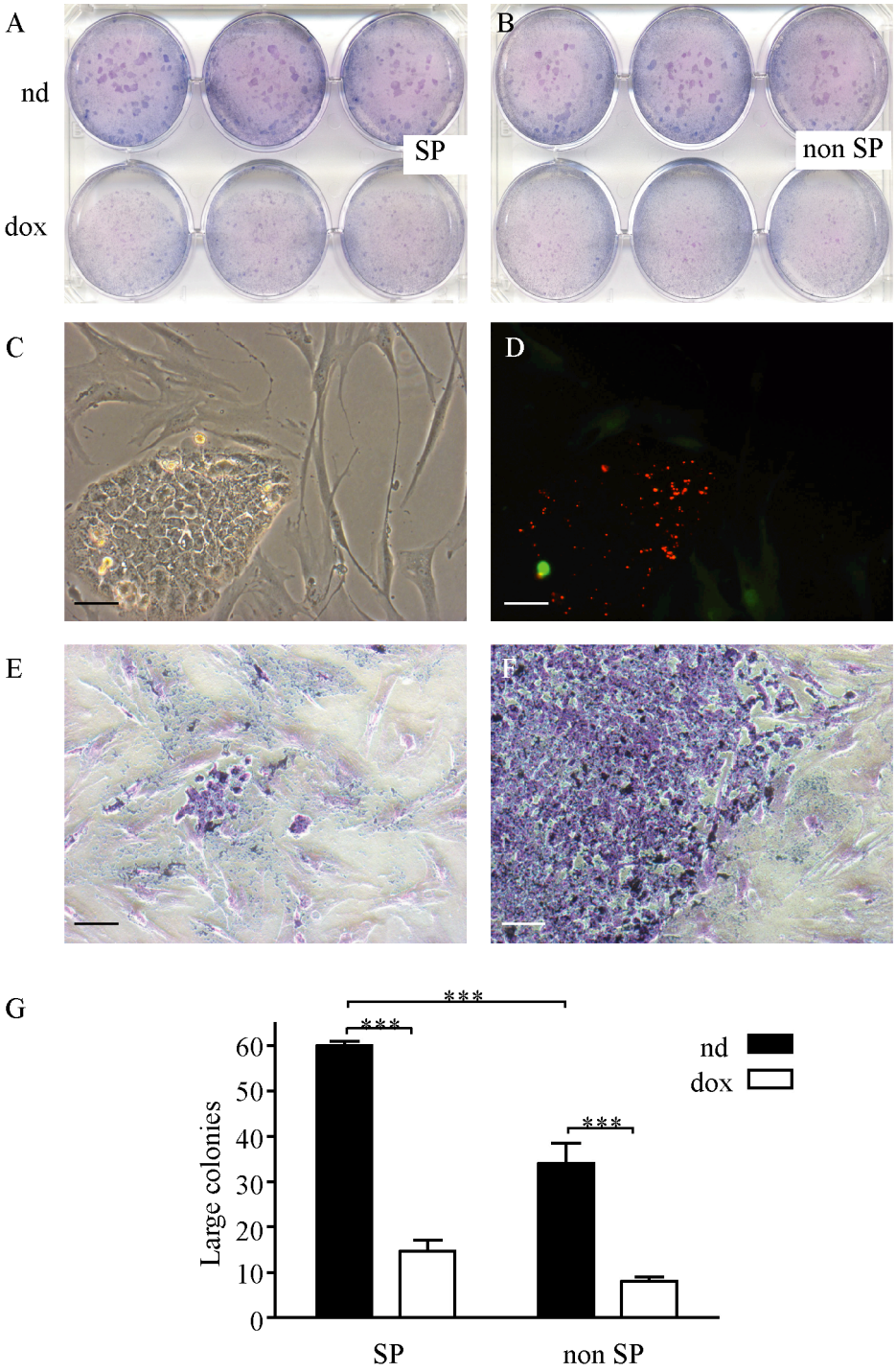

Figure 6.6 TRAIL-expressing MSCs reduce the clonigenic potential of H357 SP and non-SP cells.

*A-B) Two hundred DiI-labelled, side population (SP)(A) or non-SP (B) H357 cells were plated for colony forming assays before the addition of $5x10^4$ MSCFLT cells. C) Phase and D) fluorescent microscopy demonstrate the GFP from the doxycycline (dox)-activated MSCFLTs surrounding the DiI-labelled H357 colonies. E) A small (<32 cell) abortive colony and F) a large colony stained with rhodanile blue. G) Quantification of large colony numbers from (A,B) demonstrates a reduction in large colonies with dox–induced TRAIL expression in both SP and non-SP cells compared to the cocultures without dox (nd). Furthermore, SP cells produced more colonies than non-SP cells. Scale bars represent 25μm. *** $p<0.001$.*

6.2.6 The addition of TRAIL-expressing MSCs to mitoxantrone treatment causes additional cancer cell killing

DiI-labelled, side population H357 cells were treated with 10ng/ml mitoxantrone for 3 days followed by coculture with MSCFLT cells. The Annexin V flow cytometry assay was used to determine the apoptotic and dead SP cancer cells. There was a significant increase in dead and apoptotic cells with the addition of doxycycline and activation of the TRAIL transgene (56.3 ± 10.0% with doxycycline, compared to 33.9 ± 2.4% without doxycyline)($p<0.01$, Anova) (Figure 6.7). This suggests a further cancer killing effect of the TRAIL-expressing MSCs above and beyond the mitoxantrone chemotherapy agent. Indeed, when TRAIL was not expressed with doxycycline, the use of mitoxantrone alone did not significantly increase the dead and apoptotic cancer cells, consistent with a degree of mitoxantrone chemoresistance of the SP cells as discussed above (33.9 ± 2.4% with mitoxantrone compared to 24.56 ± 4.2% without mitoxantrone)($p>0.05$, Anova) (Figure 6.7).

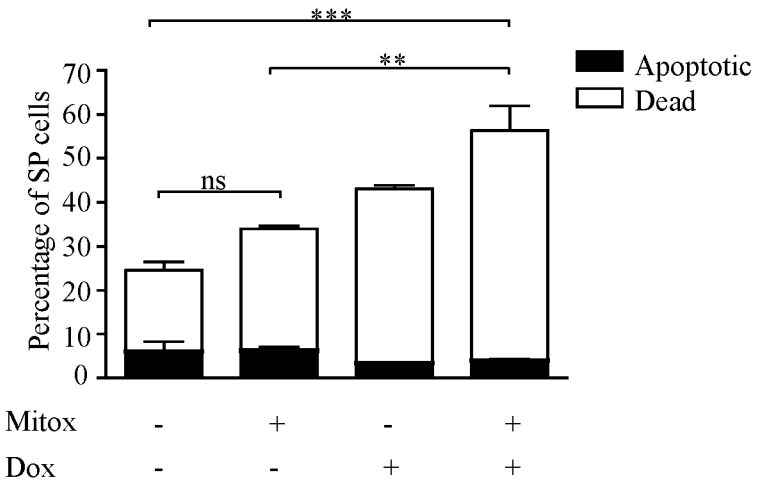

Figure 6.7 TRAIL-expressing MSCs produce additional SP cancer cell killing to mitoxantrone treatment.
*Side population (SP) H357 cells were exposed to mitoxantrone (Mitox) and then cocultured with MSCFLT cells. Bar chart represents triplicate flow cytometry experiments and demonstrates a further increase in death and apoptosis of the SP cells with the addition of doxycycline (Dox) and activation of MSCFLT TRAIL expression. *** $p<0.001$, ** $p<0.01$, ns non-significant.*

6.3 Discussion

There are some limitations with the present evidence suggesting the presence of cancer stem cells in solid tumours. The hypothesis is primarily supported by the significantly increased ability of selected 'stem-like' cancer cells to produce transplanted tumours. Furthermore, in vivo radiation experiments have demonstrated that only a fraction of cancer cells may need to be killed to cure the tumour (Hendry et al., 1994). However, the transplantation model may not best define the population of cancer cells that have the ability to regrow cancers in their original niche. The transplants do not include the other stromal and non-malignant cells of the original tumour and hence provide a different environment in which to test tumour growth. In addition it is possible that the 'stemness' of a cancer cell may be a dynamic process, with a population of cells with variable stem cell properties constantly changing over time (Hill, 2006).

There are also issues with the identification of the putative cancer stem cell. Surface markers are non-specific to the cancer cells and may also be modified by the methods used to disaggregate cells from the tumour for selection. Selection of cells by the Hoechst assay is toxic to cells and hence a comparison between the biological characteristics of the SP and non-SP cells is difficult. Secondly, the dye efflux is a dynamic process and hence defining the side population is critically dependent on variables including the concentration of Hoechst and length of staining. The SP cells are also unlikely to be a pure population of cancer stem cells. Despite this, the technique is well recognised at producing an enriched source of stem-like cells and unlike cell surface markers, has the ability to sort these cells from different populations.

One feature of the side population, or subgroup of cells enriched for stem cells, is their resistance to common oncological treatments. These studies have demonstrated that this subpopulation has some resistance to chemotherapy agents such as mitoxantrone. This subgroup of cells has also been shown to be more capable of tumour initiation in a subcutaneous model. The combination of increased treatment resistance and ability to repopulate tumours suggest new treatments should be able to

target these cells effectively. The in vitro coculture experiments with MSCFLT cells demonstrate that these TRAIL-expressing cells are able to kill SP and non-SP cells in both squamous and lung cell lines with equal efficacy. This suggests that TRAIL-expressing MSCs would be a useful potential agent for cancer treatment either alone, or potentially in combination with other radiotherapy and chemotherapy regimes. The benefits of a combination approach were also demonstrated in these studies, with an improved SP killing using a combination of mitoxantrone and TRAIL-expressing MSCs. As has been mentioned previously, cancer recurrence is common post surgical removal (with curative intent) of the primary tumour. This may be due to a few malignant cells, which remain dormant at distant sites until relapse. These cells are usually quiescent but have the ability to repopulate tumours, features making them candidates to be cancer stem cells. As the TRAIL-expressing MSCs seem also able to destroy these cells, this may provide a further rationale for their use post primary tumour removal.

6.4 Summary

This chapter has demonstrated

- Several cancer cell lines contain a side population, which have stem cell characteristics.

- The cancer cell side population have enhanced colony forming ability and in vivo tumorigenic potential.

- The cancer cell side population have some chemoresistance.

- The cancer cell side population can be killed by the MSCFLT cells.

CHAPTER 7. DISCUSSION

7.1 Overview

Cancer treatment has traditionally relied upon chemotherapy and radiotherapy, in addition to surgery. Despite improvements in management, cancer is still one of the leading causes of death in the world. Many cancers have developed resistance to present therapies. In addition, chemotherapy and radiotherapy are generally poorly selective and cause damage and death of normal cells as well as the cancer cells, leading to treatment side effects including, in some cases, death.

An improved cancer therapy would be able to specifically target cancer cells and have little effect on the normal tissues. This thesis has developed this idea and moved away from traditional treatment approaches by combining two disparate areas of research. The first is based on the observations that MSCs appear to home to, or at least engraft preferentially within, tumours. This provides a perfect delivery vehicle for a new cancer therapy, directing treatment specifically to the tumours. The second area of research focuses on the discovery of a new member of TNF family; TRAIL. This transmembrane protein is able to cause tumour cell apoptosis and death without affecting normal cells, providing a specific therapy with minimal side effects. The combination of these two approaches, to produce a TRAIL-expressing MSC is consequently particularly attractive.

In this project, mesenchymal stem cells have been engineered to express TRAIL under the sensitive control of the Tetracycline-on inducible system. These cells were able to kill cancer cell lines in vitro via the extrinsic death pathway to a higher degree than recombinant protein. In vivo, the TRAIL-expressing MSCs reduced the growth of early subcutaneous tumours, while in a systemically delivered metastasis model these cells reduced metastases but most significantly eliminated metastases in some mice.

7.2 Mesenchymal Stem Cells

Mesenchymal stem cells are isolated based on their combination of surface markers, adherence to plastic in culture, and differentiating ability. The lack of a definitive marker to characterise an MSC has resulted in a lack of uniformity, with many published studies using different definitions and characterisations of this cell type (Weiss et al., 2008). Furthermore, although the majority of MSCs are isolated from the bone marrow, other sources including umbilical cord blood, placenta, and adipose tissue have also been identified and used (Lee et al., 2004; Li et al., 2007; Puissant et al., 2005). The MSCs from these different sources have been shown to have varying gene expressions and lineage tendencies (Kern et al., 2006). Culture conditions, expansion, and the MSC microenvironment have all been shown to alter the characteristics and behaviour of MSCs (Rombouts & Ploemacher, 2003; Stolzing & Scutt, 2006), and there is also the possibility of different subgroups of cells within the MSC compartment (Phinney, 2007). This variability of cell type has made comparisons between studies difficult. The lack of consensus has led to the recent development of a set of criteria to define an MSC, published by the International Society for Cellular Therapy (Dominici et al., 2006). In view of these issues in the MSC field, the MSCs used in this project were obtained from the repository at Tulane University. These cells had been extensively characterised according to the necessary criteria, and importantly had been validated and used for many of the published studies (Spaeth et al., 2009; Stoff-Khalili et al., 2007). These MSCs were further tested on receipt, demonstrating colony forming ability, and the ability to differentiate into multiple stromal lineages. They had been extracted from the bone marrow of a single human female donor and were expanded for all the applications in this project. All experiments were performed with as low a passage number as possible, typically between 4 and 8.

In addition to the tumour-homing properties, MSCs are readily expandable, with up to 50 population doublings in 10 weeks (Giordano et al., 2007). They are also easily transduced with integrating vectors due to their high levels of amphotrophic receptors (Marx et al., 1999). Studies with both retroviral and lentiviral vector transfer have demonstrated long-term in vitro and in vivo expression of a range of

transgenes including human IL-3 over 17 passages (6 months) (Lee et al., 2001), Factor VIII (FVIII) over many months (Van Damme et al., 2006), and GFP over 20 passages (Chan et al., 2005). Transduced MSCs retained their stem cell properties and were able to differentiate into osteogenic, adipogenic, and chondrogenic lineages while expressing the transgene. In addition, differentiated MSCs also maintained transgene expression after differentiation (Lee et al., 2001). Viral transduction does not therefore appear to alter the characteristics and behaviour of the MSCs, and this was similarly found in this project. The transduced MSCs retained their differentiation profile, and migrated to cancer cells in vitro and in vivo with the same efficiency as the non-transduced MSCs.

Mesenchymal stem cells are also widely acknowledged to be immunoprivileged and non-allogenic and xenograft MSCs can be used without the use of prior immunomodulation. In our models this was not important, as the mice were already immunocompromised, however this has great clinical implications, where engineered MSCs could be used in patients as a cell therapy, without the considerations and complications surrounding immunomodulation prior to their use. This property could theoretically allow the development of an MSC bank, where cells could be stored and used 'off the shelf' for patients. Such standardised preparations of MSCs are being used in many clinical trials including cardiac disease, GvHD, and Crohn's disease, and the low immunogenicity has obviated the need for human leukocyte antigen (HLA) matching (Weiss et al., 2008). In experimental xenograft transplantation models, rat MSCs have been shown to survive in a mouse model, however they have not been able to produce bone (Wang et al., 2007). It is important to consider therefore, particularly with xenotransplantation, that the lack of immune recognition does not necessarily translate into a fully functional MSC.

7.3 Viral transduction

For the cell engineering, lentivirus constructs were produced for the transduction. Lentiviruses were used in view of potential significant advantages over other vector systems. Adenoviral vector expression is transient as the vector does not integrate

into the host genome. Adenoviral vectors also often produce a significant host immune response to the adenovirus. Retroviral vectors have the advantage of incorporating into the host DNA, providing long term gene expression, however they produce the possibility of incorporation errors such as host gene transactivation secondary to the potent viral enhancer element. This is thought to be one of the factors leading to the development of leukaemia in immunocompromised patients treated with this gene therapy (Hacein-Bey-Abina et al., 2003). Lentiviral vectors are less likely to cause transactivation of host genes at vector integration. The promoter region in viral long terminal repeat (LTR) sequences can be modified extensively, inactivating it in the integrated vector genome. Furthermore, lentiviral vectors have the ability to stably transduce both dividing and quiescent cells (Kyriakou et al., 2006), which is another significant advantage when using stem cells that are often quiescent or slow growing. The use of lentiviral vectors has demonstrated more efficient MSC transduction and in vivo engraftement than the retroviral vectors with GFP and FVIII transgene expression (Van Damme et al., 2006). Lentiviral vectors also provide more long lasting transgene expression, with one study demonstrating maintenance over 14 weeks in culture, with a concurrent decrease in transgene expression in the retroviral-transduced cells (Chan et al., 2005). In addition to the problems with longevity of transgene expression, our transient transduction experiments showed additional problems with a leaky and unspecific tetracycline control of the transgene.

Cell types were transduced successfully with the transgene, as documented by the GFP expression. A multiplicity of infection of 10 was used to transduce the MSCs with the lentivirus, in accordance to previous reports (Aguilar et al., 2007; Chan et al., 2005). At this MOI, the transduction efficiency of MSCs was greater than 80%. It was noted that this percentage of GFP-positive cells remained through several passages, in accordance with the existing long-term transgene data (Chan et al., 2005; Lee et al., 2001; Van Damme et al., 2006). In addition, transgene expression remained even with repeated activation and deactivation with doxycycline. The stable transgene expression over many passages suggested that the MSCFLT cells had neither a survival advantage nor disadvantage when the TRAIL was expressed or silent, or in comparison to the non-transduced MSCs, again consistent with the existing literature (Chan et al., 2005; Lee et al., 2001; Van Damme et al., 2006). An

improved transduction efficiency of greater than 90% could be achieved by an MOI of 20, without any excess death of the MSCs. For the purposes of this project however, a stable transduction efficiency of 80% was sufficient and allowed lower production amounts of the lentivirus. With this in mind an MOI of 10 was used in further experiments.

7.4 TRAIL transgene

The successful transduction of cells and GFP expression also translated to TRAIL expression as demonstrated by the western blots and ELISA data. The flow cytometry data was less convincing in demonstrating significant cell surface protein expression. However this has also been found in other studies (Wenger et al., 2006), and may be due to lack of antibody sensitivity. TRAIL is a type 2 transmembrane protein, however it may also be proteolytically cleaved to produce a soluble molecule. Previous studies using viral transduction of cells with full length TRAIL have demonstrated that the apoptosis-inducing effect in these studies is cell-based and not transferred to the medium. The authors have inferred from this that soluble TRAIL is not released into the supernatant by the transduced cells (Kagawa et al., 2001; Ucur et al., 2003). Soluble proteins generally have better access to targets than non-secreted proteins and an improved anti-tumour effect has been demonstrated in some in vitro and in vivo studies (Kim et al., 2006). In view of this potentially increased anti-tumour effect, a soluble TRAIL plasmid for lentiviral transduction was also produced. This contained just the extracellular portion of the TRAIL molecule (amino acids 114-281). In the transiently transduced 293T cells, both full length TRAIL protein (32kDa) and soluble TRAIL protein (21kDa) were demonstrated in the 293T cell lysates by western blot and ELISA. However, no sTRAIL was demonstrated in the cell supernatant, suggesting that the soluble portion of TRAIL is produced but not released into the supernatant in these transiently transduced cells. This is in agreement with studies suggesting that a secretion signal peptide is necessary to produce excretion of this molecule (Kim et al., 2006; Kim et al., 2004; Wu et al., 2001; Wu & Hui, 2004). In contrast, there are two publications suggesting that simple transduction of cells with the extracellular component of

TRAIL is enough to produce a functional, soluble TRAIL (Ma et al., 2005; Shi et al., 2005). The stable transduction of MSCs with the soluble TRAIL transgene was similarly only partially successful, with GFP expression but no evidence of corresponding TRAIL protein expression. Conversely, TRAIL protein expression was evident in both the cell lysates and the cell supernatants of MSCs transduced with the full length TRAIL transgene. The production of TRAIL protein in the supernatant by the full length TRAIL-transduced MSCs is in contrast to most (Kagawa et al., 2001; Ucur et al., 2003), but not all (Wei et al., 2001) of the literature demonstrating no anti-cancer effect of the supernatant of full length TRAIL-transduced cells. In addition to the literature suggesting an increased anti-tumour effect of soluble TRAIL, studies have also suggested the relative benefits of the membrane-bound version. Whereas DR4 is activated by soluble or membrane-bound TRAIL, DR5 appears to require membrane-bound or cross-linked TRAIL for activation. Furthermore, some cells which are not sensitive to soluble TRAIL apoptose when the TRAIL is tethered to a cell membrane (Carlo-Stella et al., 2006; Muhlenbeck et al., 2000; Wajant et al., 2001). In view of the potential advantages of membrane-bound TRAIL, the production of TRAIL protein in the supernatant by the full length TRAIL-transduced cells, and the lack of sTRAIL expression in the stably transduced MSCs, this project focused on the use of the full length TRAIL transgene.

7.4.1 Tetracycline inducible

The ability to turn on and off the transgene is especially useful in this model as it allows for tight controls in experiments, in addition to the ability to switch on TRAIL at different stages of tumour growth, including both pre-tumourous states and after tumour establishment. Far from being just a useful research tool, it can be envisaged that such a system could have clinical applications. Possible imaging techniques may be used with labeled MSCs to allow in vivo tracking of these cells and TRAIL activated only when the cells are located in the tumour vicinity. Treatment can be turned on specifically to be coincident to chemotherapy or radiotherapy regimes, with the expression turned off between these courses. Furthermore, all the treatments can be turned off when no longer needed but have the potential to be reinstated simply with an antibiotic, in the case of relapse. The in

vitro studies have shown the TRAIL protein to be expressed within one day of doxycycline use, and to lose expression one to two days after the doxycycline stimulus is removed. The timescale of the GFP expression was slightly different with a similar activation in one day but a gradual loss of GFP over five to seven days following doxycycline removal. The differences may be secondary to the differences in protein degradation or the relative sensitivities of the western and flow cytometry analyses.

7.5 In vitro cell death

The functionality of the MSCFLT cells was demonstrated by coculture experiments. By labelling the cancer cells, it was evident that the MSCs remained alive and killed the surrounding cancer cells. Four different tumour cell lines, representing different organ cancers, showed sensitivity to the TRAIL expressed by MSCs. In addition, cancer cells resistant to mitoxantrone chemotherapy were also sensitive to this approach. In contrast, non-cancer cells appeared relatively unharmed. There was no increase in death or apoptosis of 293T cells or the MSCs themselves with TRAIL, and although more fibroblasts appeared to die, the increase was minimal.

For the coculture experiments, the cells were at near confluence overnight and then doxycycline was added for two days. The cells were cocultured at confluence to allow maximal close apposition of cell types to enable greatest ligand receptor interaction. Two days were found to be sufficient to allow for TRAIL expression and the apoptosis of cells. If the cells were left together for longer periods (five or seven days), there was increased cancer cell death, however there was also increased death in the control cells due to overconfluence. In vivo these problems of overconfluence do not occur. Consequently, the MSCFLT cells will be apposed to the cancer cells for longer and may lead to a greater proportion of cancer cell death than suggested by the in vitro data. The supernatant of full length TRAIL-transduced MSCs was also able to cause the apoptosis and death of cancer cells, suggesting that the MSCFLT cells would be able to cause death of a greater number of cancer cells than those immediately apposed.

The cancer cell death was dependent on the expression of TRAIL by the MSCs. Neither coculture of cancer cells with normal MSCs and doxycycline, nor MSCFLT cells without doxycycline led to increased death and apoptosis. Other studies have shown different effects, with one demonstrating an increase in apoptosis of cancer cells in coculture with MSCs (Lu et al., 2008). However, as described in the introduction, there is presently little consensus on the effects of MSCs themselves on cancer cells.

Much of the in vitro work in this project used MSCFLT and cancer cells cocultured at a ratio of 1:1. For clinical applications, there would not be a 1:1 ratio of MSCFLT and cancer cells, so it is important to be able to demonstrate an effect at much lower concentrations of MSCFLT cells. The data showed that unsurprisingly there was a dose dependent effect; however even at initial cocultures of 1:16 (MSCFLT:cancer cell) the effect was strongly significant. Cancer cells proliferated at a much faster rate than the MSCFLT cells. When cocultured at a ratio of 1:1 without doxycycline, the ratio had reduced to 1:3.6 by the end of the coculturing experiment (2.5 days). Consequently, even though the original coculturing occurred at the stated ratios, this overestimated the proportion of MSCFLT cells by the time the TRAIL was active. Up to 40 % of the myofibroblasts of the tumour stroma have been found to be bone marrow-derived in some studies (Ishii et al., 2003) and consequently there is potential for these in vivo findings to be translated into in vivo models.

The use of zVADfmk and the dominant negative FADD construct illustrated the extrinsic apoptosis pathway as the mechanism of death in the in vitro studies. The use of the dnFADD construct does not reduce the death completely to the level of the no-doxycycline state, which is most likely to be as a result of incomplete expression and efficiency of the dnFADD construct.

7.6 Migration

MSCs have the ability to preferentially migrate to cancers. This project demonstrated this in vivo with the use of the lipid dye CM-DiI. DiI labelling is technically very easy, causing a diffuse cytoplasmic staining which does not affect the behaviour and culture of the cells. It has been validated as a technique for labelling and tracking human cells transplanted into mice in a study whereby DiI-stained cells were further characterised as human origin with the use of an in situ hybridisation technique, which clearly differentiated between human and mouse nuclei (Schormann et al., 2008). The majority of DiI-labelled cells were found to be of human transplanted origin, with a small number of labelled cells containing murine DNA, presumably having been taken up by the host cells from degenerated donor cells. In this project, vimentin staining of ex vivo DiI cells was also used to demonstrate a mesenchymal morphology and staining pattern, as would be expected from the labelled donor MSCs.

The precise mechanism behind the specific homing of MSCs to the multiple tumours in this project is difficult to pinpoint. The most likely cause of preferential migration is the release of chemotactic gradients from the tumours. MSCs have a large variety of chemokine and cytokine receptors on their cell surface, and respond functionally to the ligands in vitro. Furthermore, manipulation of these receptors and ligands has been shown to alter the migration patterns in vivo. Tumours are also known to produce a large array of chemokines and cytokines, which could serve as ligands for the MSC receptors (Dwyer et al., 2007). Nevertheless, although migration mechanisms have been well characterized for haemopoietic stem cells, with the importance of the ligand CXCL12 and its receptor CXCR4 highlighted, the contributions of individual chemokines and cytokines in MSC migration have not been determined. Previous studies that have attempted to determine the mechanism of MSC migration have focused on investigating the chemokine receptors present on the cell surface of MSCs and their functional importance in vitro. Such an approach however has led to a lack of consensus between studies, with different receptors postulated (Honczarenko et al., 2006; Ponte et al., 2007; Ringe et al., 2007; Sordi et al., 2005; Von Luttichau et al., 2005). The differences are likely to be due to

experimental conditions, with variations in the MSCs and their microenvironments, altering receptor expression and activation. In this project, the problem was approached by investigating the chemokines produced by the tumours both in vitro and in vivo. In vitro, the MSCs migrated preferentially to MDAMB231 cells and array panels were used to suggest the chemokines particularly produced by this cell line. To improve the model, the chemokines produced by this cell line in vivo were then investigated by using the same array panels with homogenized, ex vivo tumours as the substrate. Although this does add some validity to the in vivo work, it is important to realise that the detected differences may also be due in part to the presence of human cells within a mouse model, as opposed to a specific feature of the tumour. With these limitations in mind, on the basis of these results, IL-6 and IL-8 were highlighted as possible candidates. It is likely however that there is significant redundancy in the chemokine driven migration of MSCs and further work will be required to characterise the process in more detail.

In addition to the chemotactic gradient produced by cancers, other possible explanations exist for the observation that the MSCs appeared to migrate to and localize within the lung metastases. Metastases themselves preferentially home to particular sites within the body, and this explains the clinical observations of certain tumours producing distinct metastasis patterns; for example breast cancer typically produces lung, bone, liver, and lymph node metastases, whereas the lymph nodes and bones are the most frequent sites for secondary spread of colon cancer. The importance of a chemokine mediated metastasis model was first suggested on the basis that CXCR4 and CCR7 were heavily expressed on breast tumours but not normal breast tissue and that the ligands, CXCL12 and CCL21, exhibited peak levels of expression in the lung, bone marrow, liver, and lymph nodes, the frequent sites of metastasis. CXCL12, CCR7, and organ protein extracts promoted migration and invasion of the cancer cells in vitro and this could be reduced with the use of CXCR4 neutralising antibodies, which also reduced breast cancer metastases in vivo (Muller et al., 2001). This model has now been extended to the metastasis of a range of human cancers and expression of CXCR4 is correlated inversely with survival of several cancers including breast (Chu et al., 2008), lung (Reckamp et al., 2009), osteosarcoma (Laverdiere et al., 2005), and melanoma (Scala et al., 2005). It is possible therefore that instead of responding to a chemotactic gradient produced by

the tumours, the MSCs are instead attracted down the same migratory paths as the metastatic cancer cells, towards the chemokines released by the sites of metastasis such as the lung. The DiI-labelled MSCs were however largely seen within the tumours. There is also the possibility that the systemically delivered MSCs lodge and embolise in the lung vasculature (Khakoo et al., 2006; Weiss et al., 2008), producing the picture of apparent homing to the metastases.

Against both of these possibilities, this project has demonstrated that intravenously delivered MSCs are able to migrate to subcutaneous tumours, as well as the lung metastases. This, in addition to the in vitro data showing migration to cancer cells, would suggest that there is a specific homing to cancers and that this is likely to be driven by their production of cytokines and chemokines.

7.7 In vivo models

The in vivo tumour models in this project demonstrated that the TRAIL-expressing MSCs were able to kill cancer cells in vivo and have effects on cancer growth, progression, and metastasis.

MSCFLT cells significantly reduced the growth of subcutaneous tumours, when coinjected with MDAMB231 cells and activated with doxycycline. If the doxycycline activation and TRAIL expression was delayed until the tumour had become established at day 25, there was no effect on reducing its size. In this experiment however the proportion of MSCFLT cells at day 25 would be low, as the MDAMB231 cells would have proliferated at a far greater rate than the MSCFLT cells. With this in mind, more clinically relevant models were produced, with MSCFLT cells delivered either intratumourly or intravenously in mice with established subcutaneous MDAMB231 tumours. There was however also no effect on tumour size and growth with the doxycycline-activated MSCFLT in either of these models. This suggested a role of MSCFLT in early cancer treatment, but did not rule out a potential use of these cells in established primary tumours, where,

although not affecting primary tumours growth, they may influence survival or metastatic spread.

A metastatic lung cancer model was developed by the intravenous delivery of MDAMB231 cells. This was a very reproducible model and produced multiple lung metastases in all of the NOD/SCID mice (around 100) during the project. Treatment of these mice with intravenous doxycycline-activated MSCFLT cells led to a significant reduction in metastasis number and size. Furthermore, in a significant proportion of mice, no metastases developed at all. There was a significant effect of metastasis reduction with the use of MSCFLT cells without doxycycline, suggesting that the MSCs themselves had some anti-cancer effect. The expression of TRAIL by these cells however led to a significant additional effect and the elimination of metastases in some mice. The antitumour effects of the MSCs alone have been described previously in a variety of cancer models with different mechanisms postulated to explain the effect including the stimulation of cancer cell cycle arrest (Lu et al., 2008), an increase in apoptosis (Sun et al., 2009), and the downregulation of several pro-survival and proliferating signaling pathways (Khakoo et al., 2006; Qiao et al., 2008a; Qiao et al., 2008b). In contrast, other studies have demonstrated a protumorigenic effect of MSCs, with an increase in tumour size and metastasis, which have also been ascribed to multiple mechanisms including immunosuppressive effect (Djouad et al., 2003) and the production of trophic factors (Karnoub et al., 2007; Kyriakou et al., 2006; Sasser et al., 2007).

Although the intravenous delivery of MDAMB231 cells produced a very reproducible lung metastases model, this does not accurately recreate the development of metastases, whereby cells detach from the primary tumour and migrate and seed tumour development in other organs. A more physiological metastatic model was therefore developed, whereby subcutaneous tumours were allowed to grow and the mice developed lung metastases directly from these primary tumours. These mice were treated with intravenous MSCFLT cells and similar effects of the reduction in metastases were observed. This suggested that MSCFLT cells may have little or no effect on reducing the growth of established primary tumours outside the lung, but may still have a role in the prevention of metastases.

A final experiment looked at the possibility of preventing metastases with very early MSCFLT treatment. This intravenous therapy was delivered at days 0, 1, and 5 after intravenous MDAMB231 cells, before metastases would have developed. There was no effect of this treatment and all mice developed lung metastases. This may suggest that small tumours or metastases, or tumour vasculature are necessary in order to produce sufficient chemokines and cytokines to attract the MSCFLT cells, which are unable to efficiently target multiple individual cells, as suggested by other authors (Djouad et al., 2003).

Summarising the in vivo experiments, this thesis has demonstrated the ability of the MSCFLT cells to influence early tumour development and metastatic spread, which is in line with the proposed predominant physiological role of TRAIL; the immune surveillance against cancer cells.

With the aim of future translational therapeutics, human cancer xenograft models, human MSCs and human TRAIL constructs were used in this project. The use of human cancer cells necessitated immunocompromised mice to avoid rejection of the foreign cells. NOD/SCID mice have greater levels of immunocompromise than nude mice, with additional B cell and NK cell deficiencies, and these mice provided more consistent and faster growing tumours than the nude mice. It is important to note that no animal models are ideal representations of human disease. Human TRAIL has 65% homology to murine TRAIL (Wiley et al., 1995), and there are also differences in the receptors in mice and humans. In the mouse only one death-inducing receptor with homology to DR5 has been discovered, in addition to two decoy receptors (mDcTrailr1, msDcTrailr2) (Lawrence et al., 2001). The use of human TRAIL is more relevant to the death and apoptosis of human cancer cells, but the effects of human TRAIL on the normal murine cells may be different to the response of normal human cells, particularly with the known lack of a receptor with homology to DR4 in mice. This may underestimate the adverse effects of the TRAIL therapy, however reassuringly these have been negligible both with the use of murine TRAIL in mice (Song et al., 2006) and in early human trials (Ashkenazi, 2008; Greco et al., 2008; Hotte et al., 2008; Johnstone et al., 2008). It is also important to note that the immunocompromised mice used in this project will have very little of their own host immune response to the tumours. This could possibly be

seen as a limitation of the model in accurately reflecting the clinical situation, however many patients with cancers will also have degrees of immunocompromise secondary to traditional therapies.

7.8 Translation

The ultimate goal of this research is for the development of a cellular therapy for humans. The directed anticancer treatment described in this thesis has significant potential for translation to clinical medicine.

This thesis has demonstrated a role of MSCFLT cells in early cancer treatment and the elimination of metastases. This effect on metastases is extremely important, as secondary spread is the main cause of mortality and morbidity in cancer patients. Many patients with solid organ tumours remain at significant risk of future metastatic disease despite primary tumour resection and chemo- and radiotherapy. The recurrence rate following surgery of curative intent, despite tumour negative lymph nodes, is up to 40% in non-small cell lung cancer, 30% in colon cancer, 25% in breast cancer and 15-50% in prostate cancer (Riethdorf et al., 2008). Identifying these patients at significant risk of future metastatic disease is now becoming a reality with the use of highly sensitive and specific molecular and cytological techniques, which allow the detection of very small numbers of circulating tumour cells in the blood and bone marrow (Lang et al., 2007; Riethdorf et al., 2008). The detection of these cells, presumably resistant to the hosts endogenous immune-surveillance, are related to metastatic recurrence and poorer prognosis, and could be amenable to MSC directed TRAIL therapy. Further work would be necessary to define the optimal timing of therapy, as this project showed an inability of the MSCFLT cells to prevent the development of metastases when delivered too early, before the metastases had developed.

The most likely position for MSCFLT therapy in cancer treatment would be in combination with present radiotherapy and chemotherapy agents. The combination of TRAIL with these agents has shown significantly increased efficacy in vitro and

in vivo, and this is being utilised in clinical trials. The MSC component of the therapy developed in this project may also benefit from combination treatment. The homing of these cells to tumours has been shown to significantly increase with the use of radiation. This has been demonstrated with irradiated glioma, breast and colon cancer xenograft models in addition to a syngeneic, murine, breast carcinoma model (Klopp et al., 2007; Zielske et al., 2008). The latter study showed increased MSC migration to cancer cells in vitro and in vivo with the increased tropism thought to be secondary to the increased inflammation and expression of cytokines from the irradiated tissue, in addition to the upregulation of chemokine receptors on the MSCs exposed to the irradiated tumour cells (Klopp et al., 2007).

TRAIL-expressing MSC therapy is applicable to most cancers. Many cancers are directly sensitive to the delivery of TRAIL, and resistant cells can be sensitised to TRAIL by combination with traditional cancer therapies or other agents. Interestingly, cancer cells resistant to TRAIL as part of a primary skin tumour became sensitive on detachment in the initial stages of metastasis, by the downregulation of the ERK signalling pathway (Grosse-Wilde et al., 2008). Similar results have also been reported with breast (Goldberg et al., 2001) and ovarian (Lane et al., 2008) carcinoma cells, again highlighting the metastasis suppressor role of TRAIL.

TRAIL causes cancer apoptosis and death by a different pathway to chemotherapy and radiotherapy and can also be used in treatment failure with resistant tumours. Importantly, this therapy appears able to kill potential cancer stem cells, which are often relatively quiescent and have other stem-like characteristics allowing survival and cancer relapse in the face of traditional anticancer treatments. TRAIL-expressing MSCs appear to have very little host toxicity and are specifically directed to cancers throughout the body.

One of the major hurdles in translating basic research into clinical treatments is the issue of safety. It is promising that all the components used in producing the TRAIL-expressing MSC have already entered human clinical trials, with good initial safety and tolerability data. TRAIL therapy, in the form of recombinant protein and monoclonal antibodies to DR4 or DR5, has been used in Phase 2 clinical trials

(Ashkenazi, 2008; Greco et al., 2008; Hotte et al., 2008; Johnstone et al., 2008). Exogenous MSCs have been delivered in clinical trials covering a variety of different applications including the promotion of haematopoietic recovery (Koc et al., 2000), GvHD (Le Blanc et al., 2008), osteogenesis imperfecta (Horwitz et al., 2002), ischaemic cardiac disease (Hare & Chaparro, 2008), Crohn's disease (Weiss et al., 2008), and COPD (Iyer et al., 2009) and so far neither acute nor long term adverse effects have been reported following their infusion. The lentivirus used in this project also has good initial safety data following a trial in HIV (Levine et al., 2006), and present studies utilising it in adrenal leukodystrophy and sickle cell anaemia are ongoing.

CHAPTER 8. SUMMARY AND FUTURE DIRECTIONS

This thesis has demonstrated that mesenchymal stem cells can be engineered to express TRAIL under the sensitive control of the Tetracycline-on inducible system. These cells were able to kill cancer cell lines in vitro via the extrinsic death pathway to a higher degree than recombinant protein. In vivo, the TRAIL-expressing MSCs reduced the growth of early subcutaneous tumours, while in a systemically-delivered metastasis model they reduced metastases, but most significantly eliminated metastases in a proportion of mice. The success of the project has produced excitement that this therapy may have clinical application, and as such in depth, preclinical human safety studies are a natural progression.

However, there are still many unanswered basic science questions that future laboratory work would hopefully address. The optimal timing of delivery and number of cells needed is unknown. Early delivery of a greater number of MSCs improved the numbers of MSCs and the outcome of a cerebral ischaemia model (Chen et al., 2001; Omori et al., 2008). A cell number plateau was reached in a rat model of brain injury, with no difference between the delivery of 1 or 3 million MSCs (Wu et al., 2008). In each of these models however the lesion has a well-defined initiation, which is not apparent with cancer development. Future experiments should address these issues to give some appreciation of when MSCFLT cells should be delivered for the treatment of both primary tumours and their metastases. It is also unclear whether repeated smaller treatments or solitary injections of large numbers of cells would produce the best response.

In addition to optimising the delivery protocol, further experiments would focus on the mechanisms involved in MSC homing towards tumours. The work performed in this thesis suggests the importance of chemokine and cytokine gradients produced by tumours, and the possible roles of IL-6 and IL-8. Further experimentation would

involve the identification of chemokine receptors present on the surface of the MSCs, and how these change with alterations to the MSC microenvironment, or culture conditions. Specifically, the proximity of MSCs to cancer cells, the culture confluence and passage number would be addressed. The use of receptor blockers or silencing RNA to prevent the expression of receptors on the surface of MSCs may also be useful for in vitro and in vivo studies. There is likely to be significant redundancy in the system and hence it is likely that combinations of ligands and antagonists will be required. It would also be interesting to try and augment the migration process. This has been suggested by low dose irradiation of primary tumours (Klopp et al., 2007; Zielske et al., 2008), however this approach would be less suited to multiple metastatic deposits. Further transduction of MSCFLT cells to overexpress chemokine and cytokine receptors may increase tumour specific migration and improve the anticancer effects. Future work could also assess the efficacy of MSC homing towards tumours in different locations and at different stages of development. Homing towards lung metastases may be more efficient than metastases in other locations such as the liver, as systemically delivered MSCs reach the lung vasculature at first pass. The effects of the MSCFLT cells should therefore also be investigated in other metastatic models such as liver metastasis, and with different tumour sizes. The chemokine gradient theory would suggest that the most efficient homing would occur with larger more established tumours producing increased concentrations of chemokines. This may explain the lack of effect on preventing metastases when MSCFLT cells were delivered very early, before metastases had developed. This model could be repeated with the cancer cells and MSCFLT cells transduced to overexpress specific chemokine ligands and receptors respectively, to ascertain whether an increased attractive signal could improve the effects.

A development that would help with the further investigations into optimising delivery and the migration of the MSCFLT cells is the ability to track the MSCs in vivo in real time, without sacrificing the mouse. This would also have significant clinical applications, as the proximity of the MSCFLT cells to the tumours could be assessed before activating the TRAIL protein expression. Other groups have used luciferase bioluminescence in mouse models for this function (Sasportas et al., 2009). However, this has both temporal and spatial detection limitations. Novel imaging

contrast agents have emerged that open up the possibility of visualizing stem cell transplants in vivo using magnetic resonance imaging (MRI) (Bulte & Kraitchman, 2004). In pilot work, carried out as part of this project, bio-compatible magnetic iron oxide (Fe_3O_4) superparamagnetic nanoparticles iron oxide nanoparticles have been introduced into MSCs to enable localized cellular-level sensing, while retaining full viability. Future work would build on these initial observations to track the delivery of MSCFLT cells.

The side population has been highlighted in this thesis as a candidate for a cancer stem cell. These cells have been shown to have some chemoresistance and in vivo tumour initiating properties. Future work would use these side population cells in further in vivo tumour models and look at the effects of chemotherapy, radiotherapy and MSCFLT individually, and in combination, to try and recreate the clinical scenario of tumours with some resistance to traditional therapies.

CHAPTER 9. REFERENCES

Abe, R., Donnelly, S.C., Peng, T., Bucala, R. & Metz, C.N. (2001). Peripheral blood fibrocytes: differentiation pathway and migration to wound sites. *J Immunol*, **166,** 7556-62.

Addla, S.K., Brown, M.D., Hart, C.A., Ramani, V.A. & Clarke, N.W. (2008). Characterization of the Hoechst 33342 side population from normal and malignant human renal epithelial cells. *Am J Physiol Renal Physiol*, **295,** F680-7.

Aguilar, S., Nye, E., Chan, J., Loebinger, M., Spencer-Dene, B., Fisk, N., Stamp, G., Bonnet, D. & Janes, S.M. (2007). Murine but not human mesenchymal stem cells generate osteosarcoma-like lesions in the lung. *Stem Cells*, **25,** 1586-94.

Al-Hajj, M., Wicha, M.S., Benito-Hernandez, A., Morrison, S.J. & Clarke, M.F. (2003). Prospective identification of tumorigenic breast cancer cells. *Proc Natl Acad Sci U S A*, **100,** 3983-8.

Anderson, S.A., Glod, J., Arbab, A.S., Noel, M., Ashari, P., Fine, H.A. & Frank, J.A. (2005). Noninvasive MR imaging of magnetically labeled stem cells to directly identify neovasculature in a glioma model. *Blood*, **105,** 420-5.

Anjos-Afonso, F., Siapati, E.K. & Bonnet, D. (2004). In vivo contribution of murine mesenchymal stem cells into multiple cell-types under minimal damage conditions. *J Cell Sci*, **117,** 5655-64.

Annabi, B., Lee, Y.T., Turcotte, S., Naud, E., Desrosiers, R.R., Champagne, M., Eliopoulos, N., Galipeau, J. & Beliveau, R. (2003). Hypoxia promotes murine bone-marrow-derived stromal cell migration and tube formation. *Stem Cells*, **21,** 337-47.

Ashkenazi, A. (2008). Directing cancer cells to self-destruct with pro-apoptotic receptor agonists. *Nat Rev Drug Discov*, **7,** 1001-12.

Ashkenazi, A. & Dixit, V.M. (1998). Death receptors: signaling and modulation. *Science*, **281,** 1305-8.

Ashkenazi, A., Pai, R.C., Fong, S., Leung, S., Lawrence, D.A., Marsters, S.A., Blackie, C., Chang, L., McMurtrey, A.E., Hebert, A., DeForge, L., Koumenis, I.L., Lewis, D., Harris, L., Bussiere, J., Koeppen, H., Shahrokh, Z. & Schwall, R.H. (1999). Safety and antitumor activity of recombinant soluble Apo2 ligand. *J Clin Invest*, **104,** 155-62.

Assmus, B., Honold, J., Schachinger, V., Britten, M.B., Fischer-Rasokat, U., Lehmann, R., Teupe, C., Pistorius, K., Martin, H., Abolmaali, N.D., Tonn, T., Dimmeler, S. & Zeiher, A.M. (2006). Transcoronary transplantation of progenitor cells after myocardial infarction. *N Engl J Med*, **355,** 1222-32.

Augello, A., Tasso, R., Negrini, S.M., Cancedda, R. & Pennesi, G. (2007). Cell therapy using allogeneic bone marrow mesenchymal stem cells prevents tissue damage in collagen-induced arthritis. *Arthritis Rheum*, **56,** 1175-86.

Bao, S., Wu, Q., McLendon, R.E., Hao, Y., Shi, Q., Hjelmeland, A.B., Dewhirst, M.W., Bigner, D.D. & Rich, J.N. (2006). Glioma stem cells promote radioresistance by preferential activation of the DNA damage response. *Nature*, **444,** 756-60.

Barbash, I.M., Chouraqui, P., Baron, J., Feinberg, M.S., Etzion, S., Tessone, A., Miller, L., Guetta, E., Zipori, D., Kedes, L.H., Kloner, R.A. & Leor, J. (2003). Systemic delivery of bone marrow-derived mesenchymal stem cells to the infarcted myocardium: feasibility, cell migration, and body distribution. *Circulation*, **108,** 863-8.

Barde, I., Zanta-Boussif, M.A., Paisant, S., Leboeuf, M., Rameau, P., Delenda, C. & Danos, O. (2006). Efficient control of gene expression in the hematopoietic system using a single Tet-on inducible lentiviral vector. *Mol Ther*, **13,** 382-90.

Barrett, P., Hobbs, R.C., Coates, P.J., Risdon, R.A., Wright, N.A. & Hall, P.A. (1995). Endocrine cells of the human gastrointestinal tract have no proliferative capacity. *Histochem J*, **27,** 482-6.

Barth, P.J., Ebrahimsade, S., Hellinger, A., Moll, R. & Ramaswamy, A. (2002a). CD34+ fibrocytes in neoplastic and inflammatory pancreatic lesions. *Virchows Arch*, **440,** 128-33.

Barth, P.J., Ebrahimsade, S., Ramaswamy, A. & Moll, R. (2002b). CD34+ fibrocytes in invasive ductal carcinoma, ductal carcinoma in situ, and benign breast lesions. *Virchows Arch*, **440,** 298-303.

Barth, P.J., Ramaswamy, A. & Moll, R. (2002c). CD34(+) fibrocytes in normal cervical stroma, cervical intraepithelial neoplasia III, and invasive squamous cell carcinoma of the cervix uteri. *Virchows Arch*, **441,** 564-8.

Bastian, S., Paquet, J.L., Robert, C., Cremers, B., Loillier, B., Larrivee, J.F., Bachvarov, D.R., Marceau, F. & Pruneau, D. (1998). Interleukin 8 (IL-8) induces the expression of kinin B1 receptor in human lung fibroblasts. *Biochem Biophys Res Commun*, **253,** 750-5.

Belyanskaya, L.L., Marti, T.M., Hopkins-Donaldson, S., Kurtz, S., Felley-Bosco, E. & Stahel, R.A. (2007). Human agonistic TRAIL receptor antibodies Mapatumumab and Lexatumumab induce apoptosis in malignant mesothelioma and act synergistically with cisplatin. *Mol Cancer*, **6,** 66.

Bernardo, M.E., Zaffaroni, N., Novara, F., Cometa, A.M., Avanzini, M.A., Moretta, A., Montagna, D., Maccario, R., Villa, R., Daidone, M.G., Zuffardi, O. & Locatelli, F. (2007). Human bone marrow derived mesenchymal stem cells do not undergo transformation after long-term in vitro culture and do not exhibit telomere maintenance mechanisms. *Cancer Res*, **67,** 9142-9.

Bhowmick, N.A., Neilson, E.G. & Moses, H.L. (2004). Stromal fibroblasts in cancer initiation and progression. *Nature*, **432,** 332-7.

Bolden, J.E., Peart, M.J. & Johnstone, R.W. (2006). Anticancer activities of histone deacetylase inhibitors. *Nat Rev Drug Discov*, **5,** 769-84.

Bonnet, D. (2003). Biology of human bone marrow stem cells. *Clin Exp Med*, **3,** 140-9.

Broaddus, V.C., Dansen, T.B., Abayasiriwardana, K.S., Wilson, S.M., Finch, A.J., Swigart, L.B., Hunt, A.E. & Evan, G.I. (2005). Bid mediates apoptotic synergy between tumor necrosis factor-related apoptosis-inducing ligand (TRAIL) and DNA damage. *J Biol Chem*, **280,** 12486-93.

Bucala, R., Spiegel, L.A., Chesney, J., Hogan, M. & Cerami, A. (1994). Circulating fibrocytes define a new leukocyte subpopulation that mediates tissue repair. *Mol Med*, **1,** 71-81.

Bulte, J.W. & Kraitchman, D.L. (2004). Iron oxide MR contrast agents for molecular and cellular imaging. *NMR Biomed*, **17,** 484-499.

Burkert, J., Otto, W.R. & Wright, N.A. (2008). Side populations of gastrointestinal cancers are not enriched in stem cells. *J Pathol*, **214,** 564-73.

Burns, T.F., Bernhard, E.J. & El-Deiry, W.S. (2001). Tissue specific expression of p53 target genes suggests a key role for KILLER/DR5 in p53-dependent apoptosis in vivo. *Oncogene*, **20,** 4601-12.

Cardone, A., Tolino, A., Zarcone, R., Borruto Caracciolo, G. & Tartaglia, E. (1997). Prognostic value of desmoplastic reaction and lymphocytic infiltration in the management of breast cancer. *Panminerva Med*, **39,** 174-7.

Carlo-Stella, C., Lavazza, C., Di Nicola, M., Cleris, L., Longoni, P., Milanesi, M., Magni, M., Morelli, D., Gloghini, A., Carbone, A. & Gianni, A.M. (2006). Antitumor activity of human CD34+ cells expressing membrane-bound tumor necrosis factor-related apoptosis-inducing ligand. *Hum Gene Ther*, **17,** 1225-40.

Cassatella, M.A. (2006). On the production of TNF-related apoptosis-inducing ligand (TRAIL/Apo-2L) by human neutrophils. *J Leukoc Biol*, **79,** 1140-9.

Chamberlain, G., Fox, J., Ashton, B. & Middleton, J. (2007). Concise review: mesenchymal stem cells: their phenotype, differentiation capacity, immunological features, and potential for homing. *Stem Cells*, **25,** 2739-49.

Chan, J., O'Donoghue, K., de la Fuente, J., Roberts, I.A., Kumar, S., Morgan, J.E. & Fisk, N.M. (2005). Human fetal mesenchymal stem cells as vehicles for gene delivery. *Stem Cells*, **23,** 93-102.

Chazaud, B., Ricoux, R., Christov, C., Plonquet, A., Gherardi, R.K. & Barlovatz-Meimon, G. (2002). Promigratory effect of plasminogen activator inhibitor-1 on invasive breast cancer cell populations. *Am J Pathol*, **160,** 237-46.

Chen, J., Li, Y., Wang, L., Zhang, Z., Lu, D., Lu, M. & Chopp, M. (2001). Therapeutic benefit of intravenous administration of bone marrow stromal cells after cerebral ischemia in rats. *Stroke*, **32,** 1005-11.

Chen, X., Lin, X., Zhao, J., Shi, W., Zhang, H., Wang, Y., Kan, B., Du, L., Wang, B., Wei, Y., Liu, Y. & Zhao, X. (2008). A tumor-selective biotherapy with prolonged impact on established metastases based on cytokine gene-engineered MSCs. *Mol Ther*, **16,** 749-56.

Chen, X.C., Wang, R., Zhao, X., Wei, Y.Q., Hu, M., Wang, Y.S., Zhang, X.W., Zhang, R., Zhang, L., Yao, B., Wang, L., Jia, Y.Q., Zeng, T.T., Yang, J.L., Tian, L., Kan, B., Lin, X.J., Lei, S., Deng, H.X., Wen, Y.J., Mao, Y.Q. & Li, J. (2006). Prophylaxis against carcinogenesis in three kinds of unestablished tumor models via IL12-gene-engineered MSCs. *Carcinogenesis*, **27,** 2434-41.

Chen, Z.S., Robey, R.W., Belinsky, M.G., Shchaveleva, I., Ren, X.Q., Sugimoto, Y., Ross, D.D., Bates, S.E. & Kruh, G.D. (2003). Transport of methotrexate, methotrexate polyglutamates, and 17beta-estradiol 17-(beta-D-glucuronide) by ABCG2: effects of acquired mutations at R482 on methotrexate transport. *Cancer Res*, **63,** 4048-54.

Cheng, Z., Ou, L., Zhou, X., Li, F., Jia, X., Zhang, Y., Liu, X., Li, Y., Ward, C.A., Melo, L.G. & Kong, D. (2008). Targeted migration of mesenchymal stem cells modified with CXCR4 gene to infarcted myocardium improves cardiac performance. *Mol Ther*, **16,** 571-9.

Chiba, T., Kita, K., Zheng, Y.W., Yokosuka, O., Saisho, H., Iwama, A., Nakauchi, H. & Taniguchi, H. (2006). Side population purified from hepatocellular carcinoma cells harbors cancer stem cell-like properties. *Hepatology*, **44,** 240-51.

Choi, J.J., Yoo, S.A., Park, S.J., Kang, Y.J., Kim, W.U., Oh, I.H. & Cho, C.S. (2008). Mesenchymal stem cells overexpressing interleukin-10 attenuate collagen-induced arthritis in mice. *Clin Exp Immunol*, **153,** 269-76.

Chu, Q.D., Panu, L., Holm, N.T., Li, B.D., Johnson, L.W. & Zhang, S. (2008). High Chemokine Receptor CXCR4 Level in Triple Negative Breast Cancer Specimens Predicts Poor Clinical Outcome. *J Surg Res*.

Chuntharapai, A., Dodge, K., Grimmer, K., Schroeder, K., Marsters, S.A., Koeppen, H., Ashkenazi, A. & Kim, K.J. (2001). Isotype-dependent inhibition of tumor growth in vivo by monoclonal antibodies to death receptor 4. *J Immunol*, **166,** 4891-8.

Chute, J.P. (2006). Stem cell homing. *Curr Opin Hematol*, **13,** 399-406.

Cogle, C.R., Theise, N.D., Fu, D., Ucar, D., Lee, S., Guthrie, S.M., Lonergan, J., Rybka, W., Krause, D.S. & Scott, E.W. (2007). Bone marrow contributes to epithelial cancers in mice and humans as developmental mimicry. *Stem Cells*, **25,** 1881-7.

Corcione, A., Benvenuto, F., Ferretti, E., Giunti, D., Cappiello, V., Cazzanti, F., Risso, M., Gualandi, F., Mancardi, G.L., Pistoia, V. & Uccelli, A. (2006). Human mesenchymal stem cells modulate B-cell functions. *Blood*, **107,** 367-72.

Cretney, E., Takeda, K., Yagita, H., Glaccum, M., Peschon, J.J. & Smyth, M.J. (2002). Increased susceptibility to tumor initiation and metastasis in TNF-related apoptosis-inducing ligand-deficient mice. *J Immunol*, **168,** 1356-61.

Cretney, E., Uldrich, A.P., Berzins, S.P., Strasser, A., Godfrey, D.I. & Smyth, M.J. (2003). Normal thymocyte negative selection in TRAIL-deficient mice. *J Exp Med*, **198,** 491-6.

De Becker, A., Van Hummelen, P., Bakkus, M., Vande Broek, I., De Wever, J., De Waele, M. & Van Riet, I. (2007). Migration of culture-expanded human mesenchymal stem cells through bone marrow endothelium is regulated by matrix metalloproteinase-2 and tissue inhibitor of metalloproteinase-3. *Haematologica*, **92,** 440-9.

De Wever, O. & Mareel, M. (2003). Role of tissue stroma in cancer cell invasion. *J Pathol*, **200,** 429-47.

Dean, M., Fojo, T. & Bates, S. (2005). Tumour stem cells and drug resistance. *Nat Rev Cancer*, **5,** 275-84.

Degli-Esposti, M.A., Dougall, W.C., Smolak, P.J., Waugh, J.Y., Smith, C.A. & Goodwin, R.G. (1997a). The novel receptor TRAIL-R4 induces NF-kappaB and protects against TRAIL-mediated apoptosis, yet retains an incomplete death domain. *Immunity*, **7,** 813-20.

Degli-Esposti, M.A., Smolak, P.J., Walczak, H., Waugh, J., Huang, C.P., DuBose, R.F., Goodwin, R.G. & Smith, C.A. (1997b). Cloning and characterization of TRAIL-R3, a novel member of the emerging TRAIL receptor family. *J Exp Med*, **186,** 1165-70.

Desmouliere, A., Guyot, C. & Gabbiani, G. (2004). The stroma reaction myofibroblast: a key player in the control of tumor cell behavior. *Int J Dev Biol*, **48,** 509-17.

Direkze, N.C. & Alison, M.R. (2006). Bone marrow and tumour stroma: an intimate relationship. *Hematol Oncol*, **24,** 189-95.

Direkze, N.C., Forbes, S.J., Brittan, M., Hunt, T., Jeffery, R., Preston, S.L., Poulsom, R., Hodivala-Dilke, K., Alison, M.R. & Wright, N.A. (2003). Multiple organ engraftment by bone-marrow-derived myofibroblasts and fibroblasts in bone-marrow-transplanted mice. *Stem Cells*, **21,** 514-20.

Direkze, N.C., Hodivala-Dilke, K., Jeffery, R., Hunt, T., Poulsom, R., Oukrif, D., Alison, M.R. & Wright, N.A. (2004). Bone marrow contribution to tumor-associated myofibroblasts and fibroblasts. *Cancer Res*, **64,** 8492-5.

Direkze, N.C., Jeffery, R., Hodivala-Dilke, K., Hunt, T., Playford, R.J., Elia, G., Poulsom, R., Wright, N.A. & Alison, M.R. (2006). Bone marrow-derived stromal cells express lineage-related messenger RNA species. *Cancer Res*, **66,** 1265-9.

Djouad, F., Bony, C., Apparailly, F., Louis-Plence, P., Jorgensen, C. & Noel, D. (2006). Earlier onset of syngeneic tumors in the presence of mesenchymal stem cells. *Transplantation*, **82,** 1060-6.

Djouad, F., Plence, P., Bony, C., Tropel, P., Apparailly, F., Sany, J., Noel, D. & Jorgensen, C. (2003). Immunosuppressive effect of mesenchymal stem cells favors tumor growth in allogeneic animals. *Blood*, **102,** 3837-44.

Doki, Y., Murakami, K., Yamaura, T., Sugiyama, S., Misaki, T. & Saiki, I. (1999). Mediastinal lymph node metastasis model by orthotopic intrapulmonary implantation of Lewis lung carcinoma cells in mice. *Br J Cancer*, **79,** 1121-6.

Dominici, M., Le Blanc, K., Mueller, I., Slaper-Cortenbach, I., Marini, F., Krause, D., Deans, R., Keating, A., Prockop, D. & Horwitz, E. (2006). Minimal criteria for defining multipotent mesenchymal stromal cells. The International Society for Cellular Therapy position statement. *Cytotherapy*, **8,** 315-7.

Doyle, L.A. & Ross, D.D. (2003). Multidrug resistance mediated by the breast cancer resistance protein BCRP (ABCG2). *Oncogene*, **22,** 7340-58.

Dumitru, C.A., Carpinteiro, A., Trarbach, T., Hengge, U.R. & Gulbins, E. (2007). Doxorubicin enhances TRAIL-induced cell death via ceramide-enriched membrane platforms. *Apoptosis*, **12,** 1533-41.

Dvorak, H.F. (1986). Tumors: wounds that do not heal. Similarities between tumor stroma generation and wound healing. *N Engl J Med*, **315,** 1650-9.

Dwenger, A., Rosenthal, F., Machein, M., Waller, C. & Spyridonidis, A. (2004). Transplanted bone marrow cells preferentially home to the vessels of in situ generated murine tumors rather than of normal organs. *Stem Cells*, **22,** 86-92.

Dwyer, R.M., Potter-Beirne, S.M., Harrington, K.A., Lowery, A.J., Hennessy, E., Murphy, J.M., Barry, F.P., O'Brien, T. & Kerin, M.J. (2007). Monocyte

chemotactic protein-1 secreted by primary breast tumors stimulates migration of mesenchymal stem cells. *Clin Cancer Res*, **13,** 5020-7.

Ehrhardt, H., Fulda, S., Schmid, I., Hiscott, J., Debatin, K.M. & Jeremias, I. (2003). TRAIL induced survival and proliferation in cancer cells resistant towards TRAIL-induced apoptosis mediated by NF-kappaB. *Oncogene*, **22,** 3842-52.

El-Zawahry, A., McKillop, J. & Voelkel-Johnson, C. (2005). Doxorubicin increases the effectiveness of Apo2L/TRAIL for tumor growth inhibition of prostate cancer xenografts. *BMC Cancer*, **5,** 2.

Engelmann, K., Shen, H. & Finn, O.J. (2008). MCF7 side population cells with characteristics of cancer stem/progenitor cells express the tumor antigen MUC1. *Cancer Res*, **68,** 2419-26.

Epperly, M.W., Guo, H., Gretton, J.E. & Greenberger, J.S. (2003). Bone marrow origin of myofibroblasts in irradiation pulmonary fibrosis. *Am J Respir Cell Mol Biol*, **29,** 213-24.

Falschlehner, C., Emmerich, C.H., Gerlach, B. & Walczak, H. (2007). TRAIL signalling: decisions between life and death. *Int J Biochem Cell Biol*, **39,** 1462-75.

Ferrari, N., Glod, J., Lee, J., Kobiler, D. & Fine, H.A. (2003). Bone marrow-derived, endothelial progenitor-like cells as angiogenesis-selective gene-targeting vectors. *Gene Ther*, **10,** 647-56.

Frese, S., Pirnia, F., Miescher, D., Krajewski, S., Borner, M.M., Reed, J.C. & Schmid, R.A. (2003). PG490-mediated sensitization of lung cancer cells to Apo2L/TRAIL-induced apoptosis requires activation of ERK2. *Oncogene*, **22,** 5427-35.

Frew, A.J., Lindemann, R.K., Martin, B.P., Clarke, C.J., Sharkey, J., Anthony, D.A., Banks, K.M., Haynes, N.M., Gangatirkar, P., Stanley, K., Bolden, J.E., Takeda, K., Yagita, H., Secrist, J.P., Smyth, M.J. & Johnstone, R.W. (2008). Combination therapy of established cancer using a histone deacetylase inhibitor and a TRAIL receptor agonist. *Proc Natl Acad Sci U S A*, **105,** 11317-22.

Ganten, T.M., Koschny, R., Sykora, J., Schulze-Bergkamen, H., Buchler, P., Haas, T.L., Schader, M.B., Untergasser, A., Stremmel, W. & Walczak, H. (2006). Preclinical differentiation between apparently safe and potentially

hepatotoxic applications of TRAIL either alone or in combination with chemotherapeutic drugs. *Clin Cancer Res*, **12,** 2640-6.

Giangreco, A., Groot, K.R. & Janes, S.M. (2007). Lung cancer and lung stem cells: strange bedfellows? *Am J Respir Crit Care Med*, **175,** 547-53.

Giordano, A., Galderisi, U. & Marino, I.R. (2007). From the laboratory bench to the patient's bedside: an update on clinical trials with mesenchymal stem cells. *J Cell Physiol*, **211,** 27-35.

Glennie, S., Soeiro, I., Dyson, P.J., Lam, E.W. & Dazzi, F. (2005). Bone marrow mesenchymal stem cells induce division arrest anergy of activated T cells. *Blood*, **105,** 2821-7.

Goldberg, G.S., Jin, Z., Ichikawa, H., Naito, A., Ohki, M., El-Deiry, W.S. & Tsuda, H. (2001). Global effects of anchorage on gene expression during mammary carcinoma cell growth reveal role of tumor necrosis factor-related apoptosis-inducing ligand in anoikis. *Cancer Res*, **61,** 1334-7.

Goodell, M.A., Brose, K., Paradis, G., Conner, A.S. & Mulligan, R.C. (1996). Isolation and functional properties of murine hematopoietic stem cells that are replicating in vivo. *J Exp Med*, **183,** 1797-806.

Greco, F.A., Bonomi, P., Crawford, J., Kelly, K., Oh, Y., Halpern, W., Lo, L., Gallant, G. & Klein, J. (2008). Phase 2 study of mapatumumab, a fully human agonistic monoclonal antibody which targets and activates the TRAIL receptor-1, in patients with advanced non-small cell lung cancer. *Lung Cancer*, **61,** 82-90.

Griffith, T.S. & Broghammer, E.L. (2001). Suppression of tumor growth following intralesional therapy with TRAIL recombinant adenovirus. *Mol Ther*, **4,** 257-66.

Griffith, T.S., Rauch, C.T., Smolak, P.J., Waugh, J.Y., Boiani, N., Lynch, D.H., Smith, C.A., Goodwin, R.G. & Kubin, M.Z. (1999). Functional analysis of TRAIL receptors using monoclonal antibodies. *J Immunol*, **162,** 2597-605.

Grosse-Wilde, A., Voloshanenko, O., Bailey, S.L., Longton, G.M., Schaefer, U., Csernok, A.I., Schutz, G., Greiner, E.F., Kemp, C.J. & Walczak, H. (2008). TRAIL-R deficiency in mice enhances lymph node metastasis without affecting primary tumor development. *J Clin Invest*, **118,** 100-10.

Gupta, N., Su, X., Popov, B., Lee, J.W., Serikov, V. & Matthay, M.A. (2007). Intrapulmonary delivery of bone marrow-derived mesenchymal stem cells

improves survival and attenuates endotoxin-induced acute lung injury in mice. *J Immunol*, **179,** 1855-63.

Gutova, M., Najbauer, J., Frank, R.T., Kendall, S.E., Gevorgyan, A., Metz, M.Z., Guevorkian, M., Edmiston, M., Zhao, D., Glackin, C.A., Kim, S.U. & Aboody, K.S. (2008). Urokinase plasminogen activator and urokinase plasminogen activator receptor mediate human stem cell tropism to malignant solid tumors. *Stem Cells*, **26,** 1406-13.

Hacein-Bey-Abina, S., Von Kalle, C., Schmidt, M., McCormack, M.P., Wulffraat, N., Leboulch, P., Lim, A., Osborne, C.S., Pawliuk, R., Morillon, E., Sorensen, R., Forster, A., Fraser, P., Cohen, J.I., de Saint Basile, G., Alexander, I., Wintergerst, U., Frebourg, T., Aurias, A., Stoppa-Lyonnet, D., Romana, S., Radford-Weiss, I., Gross, F., Valensi, F., Delabesse, E., Macintyre, E., Sigaux, F., Soulier, J., Leiva, L.E., Wissler, M., Prinz, C., Rabbitts, T.H., Le Deist, F., Fischer, A. & Cavazzana-Calvo, M. (2003). LMO2-associated clonal T cell proliferation in two patients after gene therapy for SCID-X1. *Science*, **302,** 415-9.

Hadnagy, A., Gaboury, L., Beaulieu, R. & Balicki, D. (2006). SP analysis may be used to identify cancer stem cell populations. *Exp Cell Res*, **312,** 3701-10.

Hakkarainen, T., Sarkioja, M., Lehenkari, P., Miettinen, S., Ylikomi, T., Suuronen, R., Desmond, R.A., Kanerva, A. & Hemminki, A. (2007). Human mesenchymal stem cells lack tumor tropism but enhance the antitumor activity of oncolytic adenoviruses in orthotopic lung and breast tumors. *Hum Gene Ther*, **18,** 627-41.

Hambardzumyan, D., Becher, O.J., Rosenblum, M.K., Pandolfi, P.P., Manova-Todorova, K. & Holland, E.C. (2008). PI3K pathway regulates survival of cancer stem cells residing in the perivascular niche following radiation in medulloblastoma in vivo. *Genes Dev*, **22,** 436-48.

Hanahan, D. & Weinberg, R.A. (2000). The hallmarks of cancer. *Cell*, **100,** 57-70.

Haraguchi, N., Utsunomiya, T., Inoue, H., Tanaka, F., Mimori, K., Barnard, G.F. & Mori, M. (2006). Characterization of a side population of cancer cells from human gastrointestinal system. *Stem Cells*, **24,** 506-13.

Hare, J.M. & Chaparro, S.V. (2008). Cardiac regeneration and stem cell therapy. *Curr Opin Organ Transplant*, **13,** 536-42.

Harris, M.A., Yang, H., Low, B.E., Mukherje, J., Guha, A., Bronson, R.T., Shultz, L.D., Israel, M.A. & Yun, K. (2008). Cancer stem cells are enriched in the side population cells in a mouse model of glioma. *Cancer Res*, **68,** 10051-9.

Hasebe, T., Sasaki, S., Imoto, S. & Ochiai, A. (2000). Proliferative activity of intratumoral fibroblasts is closely correlated with lymph node and distant organ metastases of invasive ductal carcinoma of the breast. *Am J Pathol*, **156,** 1701-10.

Hashimoto, N., Jin, H., Liu, T., Chensue, S.W. & Phan, S.H. (2004). Bone marrow-derived progenitor cells in pulmonary fibrosis. *J Clin Invest*, **113,** 243-52.

Hendry, J.H., West, C.M., Moore, J.V. & Potten, C.S. (1994). Tumour stem cells: the relevance of predictive assays for tumour control after radiotherapy. *Radiother Oncol*, **30,** 11-6.

Heppner, G.H. (1984). Tumor heterogeneity. *Cancer Res*, **44,** 2259-65.

Hill, R.P. (2006). Identifying cancer stem cells in solid tumors: case not proven. *Cancer Res*, **66,** 1891-5; discussion 1890.

Hirschmann-Jax, C., Foster, A.E., Wulf, G.G., Nuchtern, J.G., Jax, T.W., Gobel, U., Goodell, M.A. & Brenner, M.K. (2004). A distinct "side population" of cells with high drug efflux capacity in human tumor cells. *Proc Natl Acad Sci U S A*, **101,** 14228-33.

Ho, M.M., Ng, A.V., Lam, S. & Hung, J.Y. (2007). Side population in human lung cancer cell lines and tumors is enriched with stem-like cancer cells. *Cancer Res*, **67,** 4827-33.

Holen, I. & Shipman, C.M. (2006). Role of osteoprotegerin (OPG) in cancer. *Clin Sci (Lond)*, **110,** 279-91.

Honczarenko, M., Le, Y., Swierkowski, M., Ghiran, I., Glodek, A.M. & Silberstein, L.E. (2006). Human bone marrow stromal cells express a distinct set of biologically functional chemokine receptors. *Stem Cells*, **24,** 1030-41.

Horwitz, E.M., Gordon, P.L., Koo, W.K., Marx, J.C., Neel, M.D., McNall, R.Y., Muul, L. & Hofmann, T. (2002). Isolated allogeneic bone marrow-derived mesenchymal cells engraft and stimulate growth in children with osteogenesis imperfecta: Implications for cell therapy of bone. *Proc Natl Acad Sci U S A*, **99,** 8932-7.

Horwitz, E.M., Prockop, D.J., Fitzpatrick, L.A., Koo, W.W., Gordon, P.L., Neel, M., Sussman, M., Orchard, P., Marx, J.C., Pyeritz, R.E. & Brenner, M.K. (1999).

Transplantability and therapeutic effects of bone marrow-derived mesenchymal cells in children with osteogenesis imperfecta. *Nat Med*, **5,** 309-13.

Horwitz, E.M., Prockop, D.J., Gordon, P.L., Koo, W.W., Fitzpatrick, L.A., Neel, M.D., McCarville, M.E., Orchard, P.J., Pyeritz, R.E. & Brenner, M.K. (2001). Clinical responses to bone marrow transplantation in children with severe osteogenesis imperfecta. *Blood*, **97,** 1227-31.

Hotte, S.J., Hirte, H.W., Chen, E.X., Siu, L.L., Le, L.H., Corey, A., Iacobucci, A., MacLean, M., Lo, L., Fox, N.L. & Oza, A.M. (2008). A phase 1 study of mapatumumab (fully human monoclonal antibody to TRAIL-R1) in patients with advanced solid malignancies. *Clin Cancer Res*, **14,** 3450-5.

Houghton, J., Stoicov, C., Nomura, S., Rogers, A.B., Carlson, J., Li, H., Cai, X., Fox, J.G., Goldenring, J.R. & Wang, T.C. (2004). Gastric cancer originating from bone marrow-derived cells. *Science*, **306,** 1568-71.

Huang, D., Gao, Q., Guo, L., Zhang, C., Jiang, W., Li, H., Wang, J., Han, X., Shi, Y. & Lu, S.H. (2009). Isolation and identification of cancer stem-like cells in esophageal carcinoma cell lines. *Stem Cells Dev*, **18,** 465-73.

Hylander, B.L., Pitoniak, R., Penetrante, R.B., Gibbs, J.F., Oktay, D., Cheng, J. & Repasky, E.A. (2005). The anti-tumor effect of Apo2L/TRAIL on patient pancreatic adenocarcinomas grown as xenografts in SCID mice. *J Transl Med*, **3,** 22.

Ip, J.E., Wu, Y., Huang, J., Zhang, L., Pratt, R.E. & Dzau, V.J. (2007). Mesenchymal stem cells use integrin beta1 not CXC chemokine receptor 4 for myocardial migration and engraftment. *Mol Biol Cell*, **18,** 2873-82.

Ishii, G., Sangai, T., Oda, T., Aoyagi, Y., Hasebe, T., Kanomata, N., Endoh, Y., Okumura, C., Okuhara, Y., Magae, J., Emura, M., Ochiya, T. & Ochiai, A. (2003). Bone-marrow-derived myofibroblasts contribute to the cancer-induced stromal reaction. *Biochem Biophys Res Commun*, **309,** 232-40.

Ishii, G., Sangai, T., Sugiyama, K., Ito, T., Hasebe, T., Endoh, Y., Magae, J. & Ochiai, A. (2005). In vivo characterization of bone marrow-derived fibroblasts recruited into fibrotic lesions. *Stem Cells*, **23,** 699-706.

Ishikawa, E., Nakazawa, M., Yoshinari, M. & Minami, M. (2005). Role of tumor necrosis factor-related apoptosis-inducing ligand in immune response to influenza virus infection in mice. *J Virol*, **79,** 7658-63.

Ishimura, N., Isomoto, H., Bronk, S.F. & Gores, G.J. (2006). Trail induces cell migration and invasion in apoptosis-resistant cholangiocarcinoma cells. *Am J Physiol Gastrointest Liver Physiol*, **290,** G129-36.

Ishizawa, K., Kubo, H., Yamada, M., Kobayashi, S., Numasaki, M., Ueda, S., Suzuki, T. & Sasaki, H. (2004). Bone marrow-derived cells contribute to lung regeneration after elastase-induced pulmonary emphysema. *FEBS Lett*, **556,** 249-52.

Iyer, S.S., Co, C. & Rojas, M. (2009). Mesenchymal stem cells and inflammatory lung diseases. *Panminerva Med*, **51,** 5-16.

Janes, S.M. & Watt, F.M. (2004). Switch from {alpha}v{beta}5 to {alpha}v{beta}6 integrin expression protects squamous cell carcinomas from anoikis. *J Cell Biol*, **166,** 419-431.

Janssen, E.M., Droin, N.M., Lemmens, E.E., Pinkoski, M.J., Bensinger, S.J., Ehst, B.D., Griffith, T.S., Green, D.R. & Schoenberger, S.P. (2005). CD4+ T-cell help controls CD8+ T-cell memory via TRAIL-mediated activation-induced cell death. *Nature*, **434,** 88-93.

Javazon, E.H., Beggs, K.J. & Flake, A.W. (2004). Mesenchymal stem cells: paradoxes of passaging. *Exp Hematol*, **32,** 414-25.

Jemal, A., Siegel, R., Ward, E., Murray, T., Xu, J. & Thun, M.J. (2007). Cancer statistics, 2007. *CA Cancer J Clin*, **57,** 43-66.

Ji, J.F., He, B.P., Dheen, S.T. & Tay, S.S. (2004). Interactions of chemokines and chemokine receptors mediate the migration of mesenchymal stem cells to the impaired site in the brain after hypoglossal nerve injury. *Stem Cells*, **22,** 415-27.

Jin, H., Yang, R., Fong, S., Totpal, K., Lawrence, D., Zheng, Z., Ross, J., Koeppen, H., Schwall, R. & Ashkenazi, A. (2004). Apo2 ligand/tumor necrosis factor-related apoptosis-inducing ligand cooperates with chemotherapy to inhibit orthotopic lung tumor growth and improve survival. *Cancer Res*, **64,** 4900-5.

Jo, M., Kim, T.H., Seol, D.W., Esplen, J.E., Dorko, K., Billiar, T.R. & Strom, S.C. (2000). Apoptosis induced in normal human hepatocytes by tumor necrosis factor-related apoptosis-inducing ligand. *Nat Med*, **6,** 564-7.

Johnstone, R.W., Frew, A.J. & Smyth, M.J. (2008). The TRAIL apoptotic pathway in cancer onset, progression and therapy. *Nat Rev Cancer*, **8,** 782-98.

Jones, J., Sugiyama, M., Speight, P.M. & Watt, F.M. (1996). Restoration of alpha v beta 5 integrin expression in neoplastic keratinocytes results in increased capacity for terminal differentiation and suppression of anchorage-independent growth. *Oncogene*, **12,** 119-26.

Jones, P.H. & Watt, F.M. (1993). Separation of human epidermal stem cells from transit amplifying cells on the basis of differences in integrin function and expression. *Cell*, **73,** 713-24.

Kagawa, S., He, C., Gu, J., Koch, P., Rha, S.J., Roth, J.A., Curley, S.A., Stephens, L.C. & Fang, B. (2001). Antitumor activity and bystander effects of the tumor necrosis factor-related apoptosis-inducing ligand (TRAIL) gene. *Cancer Res*, **61,** 3330-8.

Kamohara, Y., Haraguchi, N., Mimori, K., Tanaka, F., Inoue, H., Mori, M. & Kanematsu, T. (2008). The search for cancer stem cells in hepatocellular carcinoma. *Surgery*, **144,** 119-24.

Kanki-Horimoto, S., Horimoto, H., Mieno, S., Kishida, K., Watanabe, F., Furuya, E. & Katsumata, T. (2006). Implantation of mesenchymal stem cells overexpressing endothelial nitric oxide synthase improves right ventricular impairments caused by pulmonary hypertension. *Circulation*, **114,** I181-5.

Karnoub, A.E., Dash, A.B., Vo, A.P., Sullivan, A., Brooks, M.W., Bell, G.W., Richardson, A.L., Polyak, K., Tubo, R. & Weinberg, R.A. (2007). Mesenchymal stem cells within tumour stroma promote breast cancer metastasis. *Nature*, **449,** 557-63.

Karp, J.M. & Leng Teo, G.S. (2009). Mesenchymal stem cell homing: the devil is in the details. *Cell Stem Cell*, **4,** 206-16.

Kayagaki, N., Yamaguchi, N., Nakayama, M., Eto, H., Okumura, K. & Yagita, H. (1999a). Type I interferons (IFNs) regulate tumor necrosis factor-related apoptosis-inducing ligand (TRAIL) expression on human T cells: A novel mechanism for the antitumor effects of type I IFNs. *J Exp Med*, **189,** 1451-60.

Kayagaki, N., Yamaguchi, N., Nakayama, M., Takeda, K., Akiba, H., Tsutsui, H., Okamura, H., Nakanishi, K., Okumura, K. & Yagita, H. (1999b). Expression and function of TNF-related apoptosis-inducing ligand on murine activated NK cells. *J Immunol*, **163,** 1906-13.

Kelley, R.F., Totpal, K., Lindstrom, S.H., Mathieu, M., Billeci, K., Deforge, L., Pai, R., Hymowitz, S.G. & Ashkenazi, A. (2005). Receptor-selective mutants of

apoptosis-inducing ligand 2/tumor necrosis factor-related apoptosis-inducing ligand reveal a greater contribution of death receptor (DR) 5 than DR4 to apoptosis signaling. *J Biol Chem*, **280,** 2205-12.

Kern, S., Eichler, H., Stoeve, J., Kluter, H. & Bieback, K. (2006). Comparative analysis of mesenchymal stem cells from bone marrow, umbilical cord blood, or adipose tissue. *Stem Cells*, **24,** 1294-301.

Khakoo, A.Y., Pati, S., Anderson, S.A., Reid, W., Elshal, M.F., Rovira, II, Nguyen, A.T., Malide, D., Combs, C.A., Hall, G., Zhang, J., Raffeld, M., Rogers, T.B., Stetler-Stevenson, W., Frank, J.A., Reitz, M. & Finkel, T. (2006). Human mesenchymal stem cells exert potent antitumorigenic effects in a model of Kaposi's sarcoma. *J Exp Med*, **203,** 1235-47.

Khanbolooki, S., Nawrocki, S.T., Arumugam, T., Andtbacka, R., Pino, M.S., Kurzrock, R., Logsdon, C.D., Abbruzzese, J.L. & McConkey, D.J. (2006). Nuclear factor-kappaB maintains TRAIL resistance in human pancreatic cancer cells. *Mol Cancer Ther*, **5,** 2251-60.

Kim, C.Y., Jeong, M., Mushiake, H., Kim, B.M., Kim, W.B., Ko, J.P., Kim, M.H., Kim, M., Kim, T.H., Robbins, P.D., Billiar, T.R. & Seol, D.W. (2006). Cancer gene therapy using a novel secretable trimeric TRAIL. *Gene Ther*, **13,** 330-8.

Kim, M.H., Billiar, T.R. & Seol, D.W. (2004). The secretable form of trimeric TRAIL, a potent inducer of apoptosis. *Biochem Biophys Res Commun*, **321,** 930-5.

Kim, S.M., Lim, J.Y., Park, S.I., Jeong, C.H., Oh, J.H., Jeong, M., Oh, W., Park, S.H., Sung, Y.C. & Jeun, S.S. (2008). Gene therapy using TRAIL-secreting human umbilical cord blood-derived mesenchymal stem cells against intracranial glioma. *Cancer Res*, **68,** 9614-23.

Kimberley, F.C. & Screaton, G.R. (2004). Following a TRAIL: update on a ligand and its five receptors. *Cell Res*, **14,** 359-72.

Kinnaird, T., Stabile, E., Burnett, M.S., Shou, M., Lee, C.W., Barr, S., Fuchs, S. & Epstein, S.E. (2004). Local delivery of marrow-derived stromal cells augments collateral perfusion through paracrine mechanisms. *Circulation*, **109,** 1543-9.

Klopp, A.H., Spaeth, E.L., Dembinski, J.L., Woodward, W.A., Munshi, A., Meyn, R.E., Cox, J.D., Andreeff, M. & Marini, F.C. (2007). Tumor irradiation

increases the recruitment of circulating mesenchymal stem cells into the tumor microenvironment. *Cancer Res*, **67,** 11687-95.

Koc, O.N., Day, J., Nieder, M., Gerson, S.L., Lazarus, H.M. & Krivit, W. (2002). Allogeneic mesenchymal stem cell infusion for treatment of metachromatic leukodystrophy (MLD) and Hurler syndrome (MPS-IH). *Bone Marrow Transplant*, **30,** 215-22.

Koc, O.N., Gerson, S.L., Cooper, B.W., Dyhouse, S.M., Haynesworth, S.E., Caplan, A.I. & Lazarus, H.M. (2000). Rapid hematopoietic recovery after coinfusion of autologous-blood stem cells and culture-expanded marrow mesenchymal stem cells in advanced breast cancer patients receiving high-dose chemotherapy. *J Clin Oncol*, **18,** 307-16.

Kock, N., Kasmieh, R., Weissleder, R. & Shah, K. (2007). Tumor therapy mediated by lentiviral expression of shBcl-2 and S-TRAIL. *Neoplasia*, **9,** 435-42.

Komarova, S., Kawakami, Y., Stoff-Khalili, M.A., Curiel, D.T. & Pereboeva, L. (2006). Mesenchymal progenitor cells as cellular vehicles for delivery of oncolytic adenoviruses. *Mol Cancer Ther*, **5,** 755-66.

Kondo, T., Setoguchi, T. & Taga, T. (2004). Persistence of a small subpopulation of cancer stem-like cells in the C6 glioma cell line. *Proc Natl Acad Sci U S A*, **101,** 781-6.

Kotton, D.N., Ma, B.Y., Cardoso, W.V., Sanderson, E.A., Summer, R.S., Williams, M.C. & Fine, A. (2001). Bone marrow-derived cells as progenitors of lung alveolar epithelium. *Development*, **128,** 5181-8.

Krause, D.S., Theise, N.D., Collector, M.I., Henegariu, O., Hwang, S., Gardner, R., Neutzel, S. & Sharkis, S.J. (2001). Multi-organ, multi-lineage engraftment by a single bone marrow-derived stem cell. *Cell*, **105,** 369-77.

Kucerova, L., Altanerova, V., Matuskova, M., Tyciakova, S. & Altaner, C. (2007). Adipose tissue-derived human mesenchymal stem cells mediated prodrug cancer gene therapy. *Cancer Res*, **67,** 6304-13.

Kucerova, L., Matuskova, M., Pastorakova, A., Tyciakova, S., Jakubikova, J., Bohovic, R., Altanerova, V. & Altaner, C. (2008). Cytosine deaminase expressing human mesenchymal stem cells mediated tumour regression in melanoma bearing mice. *J Gene Med*, **10,** 1071-82.

Kyriakou, C.A., Yong, K.L., Benjamin, R., Pizzey, A., Dogan, A., Singh, N., Davidoff, A.M. & Nathwani, A.C. (2006). Human mesenchymal stem cells

(hMSCs) expressing truncated soluble vascular endothelial growth factor receptor (tsFlk-1) following lentiviral-mediated gene transfer inhibit growth of Burkitt's lymphoma in a murine model. *J Gene Med*, **8,** 253-64.

Lamhamedi-Cherradi, S.E., Zheng, S.J., Maguschak, K.A., Peschon, J. & Chen, Y.H. (2003). Defective thymocyte apoptosis and accelerated autoimmune diseases in TRAIL-/- mice. *Nat Immunol*, **4,** 255-60.

Lane, D., Cartier, A., Rancourt, C. & Piche, A. (2008). Cell detachment modulates TRAIL resistance in ovarian cancer cells by downregulating the phosphatidylinositol 3-kinase/Akt pathway. *Int J Gynecol Cancer*, **18,** 670-6.

Lang, J.E., Hall, C.S., Singh, B. & Lucci, A. (2007). Significance of micrometastasis in bone marrow and blood of operable breast cancer patients: research tool or clinical application? *Expert Rev Anticancer Ther*, **7,** 1463-72.

Lapidot, T., Sirard, C., Vormoor, J., Murdoch, B., Hoang, T., Caceres-Cortes, J., Minden, M., Paterson, B., Caligiuri, M.A. & Dick, J.E. (1994). A cell initiating human acute myeloid leukaemia after transplantation into SCID mice. *Nature*, **367,** 645-8.

Laverdiere, C., Hoang, B.H., Yang, R., Sowers, R., Qin, J., Meyers, P.A., Huvos, A.G., Healey, J.H. & Gorlick, R. (2005). Messenger RNA expression levels of CXCR4 correlate with metastatic behavior and outcome in patients with osteosarcoma. *Clin Cancer Res*, **11,** 2561-7.

Lawrence, D., Shahrokh, Z., Marsters, S., Achilles, K., Shih, D., Mounho, B., Hillan, K., Totpal, K., DeForge, L., Schow, P., Hooley, J., Sherwood, S., Pai, R., Leung, S., Khan, L., Gliniak, B., Bussiere, J., Smith, C.A., Strom, S.S., Kelley, S., Fox, J.A., Thomas, D. & Ashkenazi, A. (2001). Differential hepatocyte toxicity of recombinant Apo2L/TRAIL versions. *Nat Med*, **7,** 383-5.

Le Blanc, K., Frassoni, F., Ball, L., Locatelli, F., Roelofs, H., Lewis, I., Lanino, E., Sundberg, B., Bernardo, M.E., Remberger, M., Dini, G., Egeler, R.M., Bacigalupo, A., Fibbe, W. & Ringden, O. (2008). Mesenchymal stem cells for treatment of steroid-resistant, severe, acute graft-versus-host disease: a phase II study. *Lancet*, **371,** 1579-86.

Lee, J., Hampl, M., Albert, P. & Fine, H.A. (2002). Antitumor activity and prolonged expression from a TRAIL-expressing adenoviral vector. *Neoplasia*, **4,** 312-23.

Lee, K., Majumdar, M.K., Buyaner, D., Hendricks, J.K., Pittenger, M.F. & Mosca, J.D. (2001). Human mesenchymal stem cells maintain transgene expression during expansion and differentiation. *Mol Ther*, **3,** 857-66.

Lee, O.K., Kuo, T.K., Chen, W.M., Lee, K.D., Hsieh, S.L. & Chen, T.H. (2004). Isolation of multipotent mesenchymal stem cells from umbilical cord blood. *Blood*, **103,** 1669-75.

Lee, S.H., Shin, M.S., Kim, H.S., Lee, H.K., Park, W.S., Kim, S.Y., Lee, J.H., Han, S.Y., Park, J.Y., Oh, R.R., Jang, J.J., Han, J.Y., Lee, J.Y. & Yoo, N.J. (1999). Alterations of the DR5/TRAIL receptor 2 gene in non-small cell lung cancers. *Cancer Res*, **59,** 5683-6.

Levine, A.J. (1997). p53, the cellular gatekeeper for growth and division. *Cell*, **88,** 323-31.

Levine, B.L., Humeau, L.M., Boyer, J., MacGregor, R.R., Rebello, T., Lu, X., Binder, G.K., Slepushkin, V., Lemiale, F., Mascola, J.R., Bushman, F.D., Dropulic, B. & June, C.H. (2006). Gene transfer in humans using a conditionally replicating lentiviral vector. *Proc Natl Acad Sci U S A*, **103,** 17372-7.

Li, D., Wang, G.Y., Dong, B.H., Zhang, Y.C., Wang, Y.X. & Sun, B.C. (2007). Biological characteristics of human placental mesenchymal stem cells and their proliferative response to various cytokines. *Cells Tissues Organs*, **186,** 169-79.

Li, L., Thomas, R.M., Suzuki, H., De Brabander, J.K., Wang, X. & Harran, P.G. (2004). A small molecule Smac mimic potentiates TRAIL- and TNFalpha-mediated cell death. *Science*, **305,** 1471-4.

Li, X., Lu, Y., Huang, W., Xu, H., Chen, X., Geng, Q., Fan, H., Tan, Y., Xue, G. & Jiang, X. (2006). In vitro effect of adenovirus-mediated human Gamma Interferon gene transfer into human mesenchymal stem cells for chronic myelogenous leukemia. *Hematol Oncol*, **24,** 151-8.

Li, Y., Chen, J., Chen, X.G., Wang, L., Gautam, S.C., Xu, Y.X., Katakowski, M., Zhang, L.J., Lu, M., Janakiraman, N. & Chopp, M. (2002). Human marrow stromal cell therapy for stroke in rat: neurotrophins and functional recovery. *Neurology*, **59,** 514-23.

Lichtenauer, U.D., Shapiro, I., Geiger, K., Quinkler, M., Fassnacht, M., Nitschke, R., Ruckauer, K.D. & Beuschlein, F. (2008). Side population does not define

stem cell-like cancer cells in the adrenocortical carcinoma cell line NCI h295R. *Endocrinology*, **149,** 1314-22.

Lin, T., Gu, J., Zhang, L., Huang, X., Stephens, L.C., Curley, S.A. & Fang, B. (2002). Targeted expression of green fluorescent protein/tumor necrosis factor-related apoptosis-inducing ligand fusion protein from human telomerase reverse transcriptase promoter elicits antitumor activity without toxic effects on primary human hepatocytes. *Cancer Res*, **62,** 3620-5.

Livak, K.J. & Schmittgen, T.D. (2001). Analysis of relative gene expression data using real-time quantitative PCR and the 2(-Delta Delta C(T)) Method. *Methods*, **25,** 402-8.

Loebinger, M.R., Aguilar, S. & Janes, S.M. (2008). Therapeutic potential of stem cells in lung disease: progress and pitfalls. *Clin Sci (Lond)*, **114,** 99-108.

Loebinger, M.R. & Janes, S.M. (2007). Stem cells for lung disease. *Chest*, **132,** 279-85.

Lu, Y.R., Yuan, Y., Wang, X.J., Wei, L.L., Chen, Y.N., Cong, C., Li, S.F., Long, D., Tan, W.D., Mao, Y.Q., Zhang, J., Li, Y.P. & Cheng, J.Q. (2008). The growth inhibitory effect of mesenchymal stem cells on tumor cells in vitro and in vivo. *Cancer Biol Ther*, **7,** 245-51.

Lu, Z., Hu, X., Zhu, C., Wang, D., Zheng, X. & Liu, Q. (2009). Overexpression of CNTF in Mesenchymal Stem Cells reduces demyelination and induces clinical recovery in experimental autoimmune encephalomyelitis mice. *J Neuroimmunol*, **206,** 58-69.

Luetzkendorf, J., Mueller, L.P., Mueller, T., Caysa, H., Nerger, K. & Schmoll, H.J. (2009). Growth-inhibition of colorectal carcinoma by lentiviral TRAIL-transgenic human mesenchymal stem cells requires their substantial intratumoral presence. *J Cell Mol Med*.

Lunde, K., Solheim, S., Aakhus, S., Arnesen, H., Abdelnoor, M., Egeland, T., Endresen, K., Ilebekk, A., Mangschau, A., Fjeld, J.G., Smith, H.J., Taraldsrud, E., Grogaard, H.K., Bjornerheim, R., Brekke, M., Muller, C., Hopp, E., Ragnarsson, A., Brinchmann, J.E. & Forfang, K. (2006). Intracoronary injection of mononuclear bone marrow cells in acute myocardial infarction. *N Engl J Med*, **355,** 1199-209.

Luster, A.D., Alon, R. & von Andrian, U.H. (2005). Immune cell migration in inflammation: present and future therapeutic targets. *Nat Immunol*, **6,** 1182-90.

Lyden, D., Hattori, K., Dias, S., Costa, C., Blaikie, P., Butros, L., Chadburn, A., Heissig, B., Marks, W., Witte, L., Wu, Y., Hicklin, D., Zhu, Z., Hackett, N.R., Crystal, R.G., Moore, M.A., Hajjar, K.A., Manova, K., Benezra, R. & Rafii, S. (2001). Impaired recruitment of bone-marrow-derived endothelial and hematopoietic precursor cells blocks tumor angiogenesis and growth. *Nat Med*, **7,** 1194-201.

Ma, H., Liu, Y., Liu, S., Kung, H.F., Sun, X., Zheng, D. & Xu, R. (2005). Recombinant adeno-associated virus-mediated TRAIL gene therapy suppresses liver metastatic tumors. *Int J Cancer*, **116,** 314-21.

MacFarlane, M., Inoue, S., Kohlhaas, S.L., Majid, A., Harper, N., Kennedy, D.B., Dyer, M.J. & Cohen, G.M. (2005). Chronic lymphocytic leukemic cells exhibit apoptotic signaling via TRAIL-R1. *Cell Death Differ*, **12,** 773-82.

Maestroni, G.J., Hertens, E. & Galli, P. (1999). Factor(s) from nonmacrophage bone marrow stromal cells inhibit Lewis lung carcinoma and B16 melanoma growth in mice. *Cell Mol Life Sci*, **55,** 663-7.

Martelli, A.M., Tazzari, P.L., Tabellini, G., Bortul, R., Billi, A.M., Manzoli, L., Ruggeri, A., Conte, R. & Cocco, L. (2003). A new selective AKT pharmacological inhibitor reduces resistance to chemotherapeutic drugs, TRAIL, all-trans-retinoic acid, and ionizing radiation of human leukemia cells. *Leukemia*, **17,** 1794-805.

Marx, J.C., Allay, J.A., Persons, D.A., Nooner, S.A., Hargrove, P.W., Kelly, P.F., Vanin, E.F. & Horwitz, E.M. (1999). High-efficiency transduction and long-term gene expression with a murine stem cell retroviral vector encoding the green fluorescent protein in human marrow stromal cells. *Hum Gene Ther*, **10,** 1163-73.

Matthews N, Neale ML. (1987). Cytotoxicity assays for tumour necrosis factor and lymphotoxin. In: Clemens MJ, Morris AG, Gearing AJH, editors. *Lymphokines and interferons, a practical approach.* Oxford: IRL Press. 221.

Matsumoto, R., Omura, T., Yoshiyama, M., Hayashi, T., Inamoto, S., Koh, K.R., Ohta, K., Izumi, Y., Nakamura, Y., Akioka, K., Kitaura, Y., Takeuchi, K. & Yoshikawa, J. (2005). Vascular endothelial growth factor-expressing

mesenchymal stem cell transplantation for the treatment of acute myocardial infarction. *Arterioscler Thromb Vasc Biol*, **25,** 1168-73.

McAnulty, R.J. (2007). Fibroblasts and myofibroblasts: their source, function and role in disease. *Int J Biochem Cell Biol*, **39,** 666-71.

Mei, S.H., McCarter, S.D., Deng, Y., Parker, C.H., Liles, W.C. & Stewart, D.J. (2007). Prevention of LPS-induced acute lung injury in mice by mesenchymal stem cells overexpressing angiopoietin 1. *PLoS Med*, **4,** e269.

Meng, R.D., McDonald, E.R., 3rd, Sheikh, M.S., Fornace, A.J., Jr. & El-Deiry, W.S. (2000). The TRAIL decoy receptor TRUNDD (DcR2, TRAIL-R4) is induced by adenovirus-p53 overexpression and can delay TRAIL-, p53-, and KILLER/DR5-dependent colon cancer apoptosis. *Mol Ther*, **1,** 130-44.

Menon, L.G., Picinich, S., Koneru, R., Gao, H., Lin, S.Y., Koneru, M., Mayer-Kuckuk, P., Glod, J. & Banerjee, D. (2007). Differential gene expression associated with migration of mesenchymal stem cells to conditioned medium from tumor cells or bone marrow cells. *Stem Cells*, **25,** 520-8.

Meurette, O., Fontaine, A., Rebillard, A., Le Moigne, G., Lamy, T., Lagadic-Gossmann, D. & Dimanche-Boitrel, M.T. (2006). Cytotoxicity of TRAIL/anticancer drug combinations in human normal cells. *Ann N Y Acad Sci*, **1090,** 209-16.

Mitsiades, C.S., Treon, S.P., Mitsiades, N., Shima, Y., Richardson, P., Schlossman, R., Hideshima, T. & Anderson, K.C. (2001). TRAIL/Apo2L ligand selectively induces apoptosis and overcomes drug resistance in multiple myeloma: therapeutic applications. *Blood*, **98,** 795-804.

Mohr, A., Henderson, G., Dudus, L., Herr, I., Kuerschner, T., Debatin, K.M., Weiher, H., Fisher, K.J. & Zwacka, R.M. (2004). AAV-encoded expression of TRAIL in experimental human colorectal cancer leads to tumor regression. *Gene Ther*, **11,** 534-43.

Mohr, A., Lyons, M., Deedigan, L., Harte, T., Shaw, G., Howard, L., Barry, F., O'Brien, T. & Zwacka, R. (2008). Mesenchymal stem cells expressing TRAIL lead to tumour growth inhibition in an experimental lung cancer model. *J Cell Mol Med*, **12,** 2628-43.

Motadi, L.R., Misso, N.L., Dlamini, Z. & Bhoola, K.D. (2007). Molecular genetics and mechanisms of apoptosis in carcinomas of the lung and pleura: therapeutic targets. *Int Immunopharmacol*, **7,** 1934-47.

Motoki, K., Mori, E., Matsumoto, A., Thomas, M., Tomura, T., Humphreys, R., Albert, V., Muto, M., Yoshida, H., Aoki, M., Tamada, T., Kuroki, R., Yoshida, H., Ishida, I., Ware, C.F. & Kataoka, S. (2005). Enhanced apoptosis and tumor regression induced by a direct agonist antibody to tumor necrosis factor-related apoptosis-inducing ligand receptor 2. *Clin Cancer Res*, **11,** 3126-35.

Muhlenbeck, F., Schneider, P., Bodmer, J.L., Schwenzer, R., Hauser, A., Schubert, G., Scheurich, P., Moosmayer, D., Tschopp, J. & Wajant, H. (2000). The tumor necrosis factor-related apoptosis-inducing ligand receptors TRAIL-R1 and TRAIL-R2 have distinct cross-linking requirements for initiation of apoptosis and are non-redundant in JNK activation. *J Biol Chem*, **275,** 32208-13.

Muller, A., Homey, B., Soto, H., Ge, N., Catron, D., Buchanan, M.E., McClanahan, T., Murphy, E., Yuan, W., Wagner, S.N., Barrera, J.L., Mohar, A., Verastegui, E. & Zlotnik, A. (2001). Involvement of chemokine receptors in breast cancer metastasis. *Nature*, **410,** 50-6.

Nakamizo, A., Marini, F., Amano, T., Khan, A., Studeny, M., Gumin, J., Chen, J., Hentschel, S., Vecil, G., Dembinski, J., Andreeff, M. & Lang, F.F. (2005). Human bone marrow-derived mesenchymal stem cells in the treatment of gliomas. *Cancer Res*, **65,** 3307-18.

Nakamura, K., Ito, Y., Kawano, Y., Kurozumi, K., Kobune, M., Tsuda, H., Bizen, A., Honmou, O., Niitsu, Y. & Hamada, H. (2004). Antitumor effect of genetically engineered mesenchymal stem cells in a rat glioma model. *Gene Ther*, **11,** 1155-64.

Ng, I.O., Lai, E.C., Ng, M.M. & Fan, S.T. (1992). Tumor encapsulation in hepatocellular carcinoma. A pathologic study of 189 cases. *Cancer*, **70,** 45-9.

Nimmanapalli, R., Perkins, C.L., Orlando, M., O'Bryan, E., Nguyen, D. & Bhalla, K.N. (2001). Pretreatment with paclitaxel enhances apo-2 ligand/tumor necrosis factor-related apoptosis-inducing ligand-induced apoptosis of prostate cancer cells by inducing death receptors 4 and 5 protein levels. *Cancer Res*, **61,** 759-63.

Nitsch, R., Bechmann, I., Deisz, R.A., Haas, D., Lehmann, T.N., Wendling, U. & Zipp, F. (2000). Human brain-cell death induced by tumour-necrosis-factor-related apoptosis-inducing ligand (TRAIL). *Lancet*, **356,** 827-8.

Ogasawara, J., Watanabe-Fukunaga, R., Adachi, M., Matsuzawa, A., Kasugai, T., Kitamura, Y., Itoh, N., Suda, T. & Nagata, S. (1993). Lethal effect of the anti-Fas antibody in mice. *Nature*, **364,** 806-9.

Ohtsuka, T., Buchsbaum, D., Oliver, P., Makhija, S., Kimberly, R. & Zhou, T. (2003). Synergistic induction of tumor cell apoptosis by death receptor antibody and chemotherapy agent through JNK/p38 and mitochondrial death pathway. *Oncogene*, **22,** 2034-44.

Ohuchida, K., Mizumoto, K., Murakami, M., Qian, L.W., Sato, N., Nagai, E., Matsumoto, K., Nakamura, T. & Tanaka, M. (2004). Radiation to stromal fibroblasts increases invasiveness of pancreatic cancer cells through tumor-stromal interactions. *Cancer Res*, **64,** 3215-22.

Okamoto, M., Hiura, K., Ohe, G., Ohba, Y., Terai, K., Oshikawa, T., Furuichi, S., Nishikawa, H., Moriyama, K., Yoshida, H. & Sato, M. (2000). Mechanism for bone invasion of oral cancer cells mediated by interleukin-6 in vitro and in vivo. *Cancer*, **89,** 1966-75.

Omori, Y., Honmou, O., Harada, K., Suzuki, J., Houkin, K. & Kocsis, J.D. (2008). Optimization of a therapeutic protocol for intravenous injection of human mesenchymal stem cells after cerebral ischemia in adult rats. *Brain Res*, **1236,** 30-8.

Orimo, A., Gupta, P.B., Sgroi, D.C., Arenzana-Seisdedos, F., Delaunay, T., Naeem, R., Carey, V.J., Richardson, A.L. & Weinberg, R.A. (2005). Stromal fibroblasts present in invasive human breast carcinomas promote tumor growth and angiogenesis through elevated SDF-1/CXCL12 secretion. *Cell*, **121,** 335-48.

Orkin, S.H. & Morrison, S.J. (2002). Stem-cell competition. *Nature*, **418,** 25-7.

Ortiz, L.A., Gambelli, F., McBride, C., Gaupp, D., Baddoo, M., Kaminski, N. & Phinney, D.G. (2003). Mesenchymal stem cell engraftment in lung is enhanced in response to bleomycin exposure and ameliorates its fibrotic effects. *Proc Natl Acad Sci U S A*, **100,** 8407-11.

Ozaki, Y., Nishimura, M., Sekiya, K., Suehiro, F., Kanawa, M., Nikawa, H., Hamada, T. & Kato, Y. (2007). Comprehensive analysis of chemotactic factors for bone marrow mesenchymal stem cells. *Stem Cells Dev*, **16,** 119-29.

Ozoren, N. & El-Deiry, W.S. (2002). Defining characteristics of Types I and II apoptotic cells in response to TRAIL. *Neoplasia*, **4,** 551-7.

Parekkadan, B., van Poll, D., Suganuma, K., Carter, E.A., Berthiaume, F., Tilles, A.W. & Yarmush, M.L. (2007). Mesenchymal stem cell-derived molecules reverse fulminant hepatic failure. *PLoS One*, **2,** e941.

Peled, A., Petit, I., Kollet, O., Magid, M., Ponomaryov, T., Byk, T., Nagler, A., Ben-Hur, H., Many, A., Shultz, L., Lider, O., Alon, R., Zipori, D. & Lapidot, T. (1999). Dependence of human stem cell engraftment and repopulation of NOD/SCID mice on CXCR4. *Science*, **283,** 845-8.

Peters, B.A., Diaz, L.A., Polyak, K., Meszler, L., Romans, K., Guinan, E.C., Antin, J.H., Myerson, D., Hamilton, S.R., Vogelstein, B., Kinzler, K.W. & Lengauer, C. (2005). Contribution of bone marrow-derived endothelial cells to human tumor vasculature. *Nat Med*, **11,** 261-2.

Phillips, R.J., Burdick, M.D., Hong, K., Lutz, M.A., Murray, L.A., Xue, Y.Y., Belperio, J.A., Keane, M.P. & Strieter, R.M. (2004). Circulating fibrocytes traffic to the lungs in response to CXCL12 and mediate fibrosis. *J Clin Invest*, **114,** 438-46.

Phinney, D.G. (2007). Biochemical heterogeneity of mesenchymal stem cell populations: clues to their therapeutic efficacy. *Cell Cycle*, **6,** 2884-9.

Pittenger, M.F., Mackay, A.M., Beck, S.C., Jaiswal, R.K., Douglas, R., Mosca, J.D., Moorman, M.A., Simonetti, D.W., Craig, S. & Marshak, D.R. (1999). Multilineage potential of adult human mesenchymal stem cells. *Science*, **284,** 143-7.

Pitti, R.M., Marsters, S.A., Ruppert, S., Donahue, C.J., Moore, A. & Ashkenazi, A. (1996). Induction of apoptosis by Apo-2 ligand, a new member of the tumor necrosis factor cytokine family. *J Biol Chem*, **271,** 12687-90.

Pollack, I.F., Erff, M. & Ashkenazi, A. (2001). Direct stimulation of apoptotic signaling by soluble Apo2l/tumor necrosis factor-related apoptosis-inducing ligand leads to selective killing of glioma cells. *Clin Cancer Res*, **7,** 1362-9.

Ponte, A.L., Marais, E., Gallay, N., Langonne, A., Delorme, B., Herault, O., Charbord, P. & Domenech, J. (2007). The in vitro migration capacity of human bone marrow mesenchymal stem cells: comparison of chemokine and growth factor chemotactic activities. *Stem Cells*, **25,** 1737-45.

Puissant, B., Barreau, C., Bourin, P., Clavel, C., Corre, J., Bousquet, C., Taureau, C., Cousin, B., Abbal, M., Laharrague, P., Penicaud, L., Casteilla, L. & Blancher, A. (2005). Immunomodulatory effect of human adipose tissue-derived adult

stem cells: comparison with bone marrow mesenchymal stem cells. *Br J Haematol*, **129,** 118-29.

Pukac, L., Kanakaraj, P., Humphreys, R., Alderson, R., Bloom, M., Sung, C., Riccobene, T., Johnson, R., Fiscella, M., Mahoney, A., Carrell, J., Boyd, E., Yao, X.T., Zhang, L., Zhong, L., von Kerczek, A., Shepard, L., Vaughan, T., Edwards, B., Dobson, C., Salcedo, T. & Albert, V. (2005). HGS-ETR1, a fully human TRAIL-receptor 1 monoclonal antibody, induces cell death in multiple tumour types in vitro and in vivo. *Br J Cancer*, **92,** 1430-41.

Qiao, L., Xu, Z.L., Zhao, T.J., Ye, L.H. & Zhang, X.D. (2008a). Dkk-1 secreted by mesenchymal stem cells inhibits growth of breast cancer cells via depression of Wnt signalling. *Cancer Lett*, **269,** 67-77.

Qiao, L., Zhao, T.J., Wang, F.Z., Shan, C.L., Ye, L.H. & Zhang, X.D. (2008b). NF-kappaB downregulation may be involved the depression of tumor cell proliferation mediated by human mesenchymal stem cells. *Acta Pharmacol Sin*, **29,** 333-40.

Ramasamy, R., Fazekasova, H., Lam, E.W., Soeiro, I., Lombardi, G. & Dazzi, F. (2007a). Mesenchymal stem cells inhibit dendritic cell differentiation and function by preventing entry into the cell cycle. *Transplantation*, **83,** 71-6.

Ramasamy, R., Lam, E.W., Soeiro, I., Tisato, V., Bonnet, D. & Dazzi, F. (2007b). Mesenchymal stem cells inhibit proliferation and apoptosis of tumor cells: impact on in vivo tumor growth. *Leukemia*, **21,** 304-10.

Reckamp, K.L., Figlin, R.A., Burdick, M.D., Dubinett, S.M., Elashoff, R.M. & Strieter, R.M. (2009). CXCR4 expression on circulating pan-cytokeratin positive cells is associated with survival in patients with advanced non-small cell lung cancer. *BMC Cancer*, **9,** 213.

Ren, C., Kumar, S., Chanda, D., Chen, J., Mountz, J.D. & Ponnazhagan, S. (2008a). Therapeutic potential of mesenchymal stem cells producing interferon-alpha in a mouse melanoma lung metastasis model. *Stem Cells*, **26,** 2332-8.

Ren, C., Kumar, S., Chanda, D., Kallman, L., Chen, J., Mountz, J.D. & Ponnazhagan, S. (2008b). Cancer gene therapy using mesenchymal stem cells expressing interferon-beta in a mouse prostate cancer lung metastasis model. *Gene Ther*, **15,** 1446-53.

Renshaw, S.A., Parmar, J.S., Singleton, V., Rowe, S.J., Dockrell, D.H., Dower, S.K., Bingle, C.D., Chilvers, E.R. & Whyte, M.K. (2003). Acceleration of human neutrophil apoptosis by TRAIL. *J Immunol*, **170,** 1027-33.

Ricci-Vitiani, L., Lombardi, D.G., Pilozzi, E., Biffoni, M., Todaro, M., Peschle, C. & De Maria, R. (2007). Identification and expansion of human colon-cancer-initiating cells. *Nature*, **445,** 111-5.

Riethdorf, S., Wikman, H. & Pantel, K. (2008). Review: Biological relevance of disseminated tumor cells in cancer patients. *Int J Cancer*, **123,** 1991-2006.

Ringe, J., Strassburg, S., Neumann, K., Endres, M., Notter, M., Burmester, G.R., Kaps, C. & Sittinger, M. (2007). Towards in situ tissue repair: human mesenchymal stem cells express chemokine receptors CXCR1, CXCR2 and CCR2, and migrate upon stimulation with CXCL8 but not CCL2. *J Cell Biochem*, **101,** 135-46.

Rojas, M., Xu, J., Woods, C.R., Mora, A.L., Spears, W., Roman, J. & Brigham, K.L. (2005). Bone marrow-derived mesenchymal stem cells in repair of the injured lung. *Am J Respir Cell Mol Biol*, **33,** 145-52.

Romagnoli, M., Desplanques, G., Maiga, S., Legouill, S., Dreano, M., Bataille, R. & Barille-Nion, S. (2007). Canonical nuclear factor kappaB pathway inhibition blocks myeloma cell growth and induces apoptosis in strong synergy with TRAIL. *Clin Cancer Res*, **13,** 6010-8.

Rombouts, W.J. & Ploemacher, R.E. (2003). Primary murine MSC show highly efficient homing to the bone marrow but lose homing ability following culture. *Leukemia*, **17,** 160-70.

Rubio, D., Garcia-Castro, J., Martin, M.C., de la Fuente, R., Cigudosa, J.C., Lloyd, A.C. & Bernad, A. (2005). Spontaneous human adult stem cell transformation. *Cancer Res*, **65,** 3035-9.

Ruster, B., Gottig, S., Ludwig, R.J., Bistrian, R., Muller, S., Seifried, E., Gille, J. & Henschler, R. (2006). Mesenchymal stem cells display coordinated rolling and adhesion behavior on endothelial cells. *Blood*, **108,** 3938-44.

Sah, N.K., Munshi, A., Kurland, J.F., McDonnell, T.J., Su, B. & Meyn, R.E. (2003). Translation inhibitors sensitize prostate cancer cells to apoptosis induced by tumor necrosis factor-related apoptosis-inducing ligand (TRAIL) by activating c-Jun N-terminal kinase. *J Biol Chem*, **278,** 20593-602.

Samuels, Y., Diaz, L.A., Jr., Schmidt-Kittler, O., Cummins, J.M., Delong, L., Cheong, I., Rago, C., Huso, D.L., Lengauer, C., Kinzler, K.W., Vogelstein, B. & Velculescu, V.E. (2005). Mutant PIK3CA promotes cell growth and invasion of human cancer cells. *Cancer Cell*, **7,** 561-73.

Sangai, T., Ishii, G., Kodama, K., Miyamoto, S., Aoyagi, Y., Ito, T., Magae, J., Sasaki, H., Nagashima, T., Miyazaki, M. & Ochiai, A. (2005). Effect of differences in cancer cells and tumor growth sites on recruiting bone marrow-derived endothelial cells and myofibroblasts in cancer-induced stroma. *Int J Cancer*, **115,** 885-92.

Sasportas, L.S., Kasmieh, R., Wakimoto, H., Hingtgen, S., van de Water, J.A., Mohapatra, G., Figueiredo, J.L., Martuza, R.L., Weissleder, R. & Shah, K. (2009). Assessment of therapeutic efficacy and fate of engineered human mesenchymal stem cells for cancer therapy. *Proc Natl Acad Sci U S A*, **106,** 4822-7.

Sasser, A.K., Sullivan, N.J., Studebaker, A.W., Hendey, L.F., Axel, A.E. & Hall, B.M. (2007). Interleukin-6 is a potent growth factor for ER-alpha-positive human breast cancer. *Faseb J*, **21,** 3763-70.

Sato, K., Ozaki, K., Oh, I., Meguro, A., Hatanaka, K., Nagai, T., Muroi, K. & Ozawa, K. (2007). Nitric oxide plays a critical role in suppression of T-cell proliferation by mesenchymal stem cells. *Blood*, **109,** 228-34.

Sato, T., Sakai, T., Noguchi, Y., Takita, M., Hirakawa, S. & Ito, A. (2004). Tumor-stromal cell contact promotes invasion of human uterine cervical carcinoma cells by augmenting the expression and activation of stromal matrix metalloproteinases. *Gynecol Oncol*, **92,** 47-56.

Scaffidi, C., Fulda, S., Srinivasan, A., Friesen, C., Li, F., Tomaselli, K.J., Debatin, K.M., Krammer, P.H. & Peter, M.E. (1998). Two CD95 (APO-1/Fas) signaling pathways. *Embo J*, **17,** 1675-87.

Scala, S., Ottaiano, A., Ascierto, P.A., Cavalli, M., Simeone, E., Giuliano, P., Napolitano, M., Franco, R., Botti, G. & Castello, G. (2005). Expression of CXCR4 predicts poor prognosis in patients with malignant melanoma. *Clin Cancer Res*, **11,** 1835-41.

Schachinger, V., Erbs, S., Elsasser, A., Haberbosch, W., Hambrecht, R., Holschermann, H., Yu, J., Corti, R., Mathey, D.G., Hamm, C.W., Suselbeck, T., Assmus, B., Tonn, T., Dimmeler, S. & Zeiher, A.M. (2006). Intracoronary

bone marrow-derived progenitor cells in acute myocardial infarction. *N Engl J Med*, **355,** 1210-21.

Schmaltz, C., Alpdogan, O., Kappel, B.J., Muriglan, S.J., Rotolo, J.A., Ongchin, J., Willis, L.M., Greenberg, A.S., Eng, J.M., Crawford, J.M., Murphy, G.F., Yagita, H., Walczak, H., Peschon, J.J. & van den Brink, M.R. (2002). T cells require TRAIL for optimal graft-versus-tumor activity. *Nat Med*, **8,** 1433-7.

Schmidt, A., Bierwirth, S., Weber, S., Platen, P., Schinkothe, T. & Bloch, W. (2009). Short intensive exercise increases the migratory activity of mesenchymal stem cells. *Br J Sports Med*, **43,** 195-8.

Schmidt, A., Ladage, D., Schinkothe, T., Klausmann, U., Ulrichs, C., Klinz, F.J., Brixius, K., Arnhold, S., Desai, B., Mehlhorn, U., Schwinger, R.H., Staib, P., Addicks, K. & Bloch, W. (2006). Basic fibroblast growth factor controls migration in human mesenchymal stem cells. *Stem Cells*, **24,** 1750-8.

Schmidt, M., Sun, G., Stacey, M.A., Mori, L. & Mattoli, S. (2003). Identification of circulating fibrocytes as precursors of bronchial myofibroblasts in asthma. *J Immunol*, **171,** 380-9.

Schormann, W., Hammersen, F.J., Brulport, M., Hermes, M., Bauer, A., Rudolph, C., Schug, M., Lehmann, T., Nussler, A., Ungefroren, H., Hutchinson, J., Fandrich, F., Petersen, J., Wursthorn, K., Burda, M.R., Brustle, O., Krishnamurthi, K., von Mach, M. & Hengstler, J.G. (2008). Tracking of human cells in mice. *Histochem Cell Biol*, **130,** 329-38.

Secchiero, P. & Zauli, G. (2008). Tumor-necrosis-factor-related apoptosis-inducing ligand and the regulation of hematopoiesis. *Curr Opin Hematol*, **15,** 42-8.

Sedger, L.M., Glaccum, M.B., Schuh, J.C., Kanaly, S.T., Williamson, E., Kayagaki, N., Yun, T., Smolak, P., Le, T., Goodwin, R. & Gliniak, B. (2002). Characterization of the in vivo function of TNF-alpha-related apoptosis-inducing ligand, TRAIL/Apo2L, using TRAIL/Apo2L gene-deficient mice. *Eur J Immunol*, **32,** 2246-54.

Sedger, L.M., Shows, D.M., Blanton, R.A., Peschon, J.J., Goodwin, R.G., Cosman, D. & Wiley, S.R. (1999). IFN-gamma mediates a novel antiviral activity through dynamic modulation of TRAIL and TRAIL receptor expression. *J Immunol*, **163,** 920-6.

Segre, J.A., Nemhauser, J.L., Taylor, B.A., Nadeau, J.H. & Lander, E.S. (1995). Positional cloning of the nude locus: genetic, physical, and transcription maps of the region and mutations in the mouse and rat. *Genomics*, **28,** 549-59.

Sekido, N., Mukaida, N., Harada, A., Nakanishi, I., Watanabe, Y. & Matsushima, K. (1993). Prevention of lung reperfusion injury in rabbits by a monoclonal antibody against interleukin-8. *Nature*, **365,** 654-7.

Shankar, S., Chen, X. & Srivastava, R.K. (2005). Effects of sequential treatments with chemotherapeutic drugs followed by TRAIL on prostate cancer in vitro and in vivo. *Prostate*, **62,** 165-86.

Shankar, S., Singh, T.R. & Srivastava, R.K. (2004). Ionizing radiation enhances the therapeutic potential of TRAIL in prostate cancer in vitro and in vivo: Intracellular mechanisms. *Prostate*, **61,** 35-49.

Shi, J., Zheng, D., Liu, Y., Sham, M.H., Tam, P., Farzaneh, F. & Xu, R. (2005). Overexpression of soluble TRAIL induces apoptosis in human lung adenocarcinoma and inhibits growth of tumor xenografts in nude mice. *Cancer Res*, **65,** 1687-92.

Shin, M.S., Kim, H.S., Lee, S.H., Park, W.S., Kim, S.Y., Park, J.Y., Lee, J.H., Lee, S.K., Lee, S.N., Jung, S.S., Han, J.Y., Kim, H., Lee, J.Y. & Yoo, N.J. (2001). Mutations of tumor necrosis factor-related apoptosis-inducing ligand receptor 1 (TRAIL-R1) and receptor 2 (TRAIL-R2) genes in metastatic breast cancers. *Cancer Res*, **61,** 4942-6.

Shultz, L.D., Schweitzer, P.A., Christianson, S.W., Gott, B., Schweitzer, I.B., Tennent, B., McKenna, S., Mobraaten, L., Rajan, T.V., Greiner, D.L. & et al. (1995). Multiple defects in innate and adaptive immunologic function in NOD/LtSz-scid mice. *J Immunol*, **154,** 180-91.

Simon, A.K., Williams, O., Mongkolsapaya, J., Jin, B., Xu, X.N., Walczak, H. & Screaton, G.R. (2001). Tumor necrosis factor-related apoptosis-inducing ligand in T cell development: sensitivity of human thymocytes. *Proc Natl Acad Sci U S A*, **98,** 5158-63.

Singh, S.K., Hawkins, C., Clarke, I.D., Squire, J.A., Bayani, J., Hide, T., Henkelman, R.M., Cusimano, M.D. & Dirks, P.B. (2004). Identification of human brain tumour initiating cells. *Nature*, **432,** 396-401.

Song, J.H., Tse, M.C., Bellail, A., Phuphanich, S., Khuri, F., Kneteman, N.M. & Hao, C. (2007). Lipid rafts and nonrafts mediate tumor necrosis factor related

apoptosis-inducing ligand induced apoptotic and nonapoptotic signals in non small cell lung carcinoma cells. *Cancer Res*, **67,** 6946-55.

Song, K., Benhaga, N., Anderson, R.L. & Khosravi-Far, R. (2006). Transduction of tumor necrosis factor-related apoptosis-inducing ligand into hematopoietic cells leads to inhibition of syngeneic tumor growth in vivo. *Cancer Res*, **66,** 6304-11.

Sordi, V., Malosio, M.L., Marchesi, F., Mercalli, A., Melzi, R., Giordano, T., Belmonte, N., Ferrari, G., Leone, B.E., Bertuzzi, F., Zerbini, G., Allavena, P., Bonifacio, E. & Piemonti, L. (2005). Bone marrow mesenchymal stem cells express a restricted set of functionally active chemokine receptors capable of promoting migration to pancreatic islets. *Blood*, **106,** 419-27.

Spaeth, E., Klopp, A., Dembinski, J., Andreeff, M. & Marini, F. (2008). Inflammation and tumor microenvironments: defining the migratory itinerary of mesenchymal stem cells. *Gene Ther*, **15,** 730-8.

Spaeth, E.L., Dembinski, J.L., Sasser, A.K., Watson, K., Klopp, A., Hall, B., Andreeff, M. & Marini, F. (2009). Mesenchymal stem cell transition to tumor-associated fibroblasts contributes to fibrovascular network expansion and tumor progression. *PLoS One*, **4,** e4992.

Stoff-Khalili, M.A., Rivera, A.A., Mathis, J.M., Banerjee, N.S., Moon, A.S., Hess, A., Rocconi, R.P., Numnum, T.M., Everts, M., Chow, L.T., Douglas, J.T., Siegal, G.P., Zhu, Z.B., Bender, H.G., Dall, P., Stoff, A., Pereboeva, L. & Curiel, D.T. (2007). Mesenchymal stem cells as a vehicle for targeted delivery of CRAds to lung metastases of breast carcinoma. *Breast Cancer Res Treat*, **105,** 157-67.

Stolzing, A. & Scutt, A. (2006). Effect of reduced culture temperature on antioxidant defences of mesenchymal stem cells. *Free Radic Biol Med*, **41,** 326-38.

Strater, J., Walczak, H., Pukrop, T., Von Muller, L., Hasel, C., Kornmann, M., Mertens, T. & Moller, P. (2002). TRAIL and its receptors in the colonic epithelium: a putative role in the defense of viral infections. *Gastroenterology*, **122,** 659-66.

Studeny, M., Marini, F.C., Champlin, R.E., Zompetta, C., Fidler, I.J. & Andreeff, M. (2002). Bone marrow-derived mesenchymal stem cells as vehicles for interferon-beta delivery into tumors. *Cancer Res*, **62,** 3603-8.

Studeny, M., Marini, F.C., Dembinski, J.L., Zompetta, C., Cabreira-Hansen, M., Bekele, B.N., Champlin, R.E. & Andreeff, M. (2004). Mesenchymal stem cells: potential precursors for tumor stroma and targeted-delivery vehicles for anticancer agents. *J Natl Cancer Inst*, **96,** 1593-603.

Sun, B., Roh, K.H., Park, J.R., Lee, S.R., Park, S.B., Jung, J.W., Kang, S.K., Lee, Y.S. & Kang, K.S. (2009). Therapeutic potential of mesenchymal stromal cells in a mouse breast cancer metastasis model. *Cytotherapy*, **11,** 289-98, 1 p following 298.

Sung, J.M., Cho, H.J., Yi, H., Lee, C.H., Kim, H.S., Kim, D.K., Abd El-Aty, A.M., Kim, J.S., Landowski, C.P., Hediger, M.A. & Shin, H.C. (2008). Characterization of a stem cell population in lung cancer A549 cells. *Biochem Biophys Res Commun*, **371,** 163-7.

Szotek, P.P., Pieretti-Vanmarcke, R., Masiakos, P.T., Dinulescu, D.M., Connolly, D., Foster, R., Dombkowski, D., Preffer, F., Maclaughlin, D.T. & Donahoe, P.K. (2006). Ovarian cancer side population defines cells with stem cell-like characteristics and Mullerian Inhibiting Substance responsiveness. *Proc Natl Acad Sci U S A*, **103,** 11154-9.

Takeda, K., Hayakawa, Y., Smyth, M.J., Kayagaki, N., Yamaguchi, N., Kakuta, S., Iwakura, Y., Yagita, H. & Okumura, K. (2001). Involvement of tumor necrosis factor-related apoptosis-inducing ligand in surveillance of tumor metastasis by liver natural killer cells. *Nat Med*, **7,** 94-100.

Takeda, K., Smyth, M.J., Cretney, E., Hayakawa, Y., Kayagaki, N., Yagita, H. & Okumura, K. (2002). Critical role for tumor necrosis factor-related apoptosis-inducing ligand in immune surveillance against tumor development. *J Exp Med*, **195,** 161-9.

Togel, F., Weiss, K., Yang, Y., Hu, Z., Zhang, P. & Westenfelder, C. (2007). Vasculotropic, paracrine actions of infused mesenchymal stem cells are important to the recovery from acute kidney injury. *Am J Physiol Renal Physiol*, **292,** F1626-35.

Tolar, J., Nauta, A.J., Osborn, M.J., Panoskaltsis Mortari, A., McElmurry, R.T., Bell, S., Xia, L., Zhou, N., Riddle, M., Schroeder, T.M., Westendorf, J.J., McIvor, R.S., Hogendoorn, P.C., Szuhai, K., Oseth, L., Hirsch, B., Yant, S.R., Kay, M.A., Peister, A., Prockop, D.J., Fibbe, W.E. & Blazar, B.R. (2007).

Sarcoma derived from cultured mesenchymal stem cells. *Stem Cells*, **25,** 371-9.

Truneh, A., Sharma, S., Silverman, C., Khandekar, S., Reddy, M.P., Deen, K.C., McLaughlin, M.M., Srinivasula, S.M., Livi, G.P., Marshall, L.A., Alnemri, E.S., Williams, W.V. & Doyle, M.L. (2000). Temperature-sensitive differential affinity of TRAIL for its receptors. DR5 is the highest affinity receptor. *J Biol Chem*, **275,** 23319-25.

Uchibori, R., Okada, T., Ito, T., Urabe, M., Mizukami, H., Kume, A. & Ozawa, K. (2009). Retroviral vector-producing mesenchymal stem cells for targeted suicide cancer gene therapy. *J Gene Med*, **11,** 373-81.

Ucur, E., Mattern, J., Wenger, T., Okouoyo, S., Schroth, A., Debatin, K.M. & Herr, I. (2003). Induction of apoptosis in experimental human B cell lymphomas by conditional TRAIL-expressing T cells. *Br J Cancer*, **89,** 2155-62.

Uno, T., Takeda, K., Kojima, Y., Yoshizawa, H., Akiba, H., Mittler, R.S., Gejyo, F., Okumura, K., Yagita, H. & Smyth, M.J. (2006). Eradication of established tumors in mice by a combination antibody-based therapy. *Nat Med*, **12,** 693-8.

Van Damme, A., Thorrez, L., Ma, L., Vandenburgh, H., Eyckmans, J., Dell'Accio, F., De Bari, C., Luyten, F., Lillicrap, D., Collen, D., VandenDriessche, T. & Chuah, M.K. (2006). Efficient lentiviral transduction and improved engraftment of human bone marrow mesenchymal cells. *Stem Cells*, **24,** 896-907.

Vanoosten, R.L., Moore, J.M., Ludwig, A.T. & Griffith, T.S. (2005). Depsipeptide (FR901228) enhances the cytotoxic activity of TRAIL by redistributing TRAIL receptor to membrane lipid rafts. *Mol Ther*, **11,** 542-52.

Varfolomeev, E., Maecker, H., Sharp, D., Lawrence, D., Renz, M., Vucic, D. & Ashkenazi, A. (2005). Molecular determinants of kinase pathway activation by Apo2 ligand/tumor necrosis factor-related apoptosis-inducing ligand. *J Biol Chem*, **280,** 40599-608.

Visvader, J.E. & Lindeman, G.J. (2008). Cancer stem cells in solid tumours: accumulating evidence and unresolved questions. *Nat Rev Cancer*, **8,** 755-68.

Von Luttichau, I., Notohamiprodjo, M., Wechselberger, A., Peters, C., Henger, A., Seliger, C., Djafarzadeh, R., Huss, R. & Nelson, P.J. (2005). Human adult CD34- progenitor cells functionally express the chemokine receptors CCR1,

CCR4, CCR7, CXCR5, and CCR10 but not CXCR4. *Stem Cells Dev*, **14,** 329-36.

Wagner, K.W., Punnoose, E.A., Januario, T., Lawrence, D.A., Pitti, R.M., Lancaster, K., Lee, D., von Goetz, M., Yee, S.F., Totpal, K., Huw, L., Katta, V., Cavet, G., Hymowitz, S.G., Amler, L. & Ashkenazi, A. (2007). Death-receptor O-glycosylation controls tumor-cell sensitivity to the proapoptotic ligand Apo2L/TRAIL. *Nat Med*, **13,** 1070-7.

Wajant, H., Moosmayer, D., Wuest, T., Bartke, T., Gerlach, E., Schonherr, U., Peters, N., Scheurich, P. & Pfizenmaier, K. (2001). Differential activation of TRAIL-R1 and -2 by soluble and membrane TRAIL allows selective surface antigen-directed activation of TRAIL-R2 by a soluble TRAIL derivative. *Oncogene*, **20,** 4101-6.

Walczak, H., Miller, R.E., Ariail, K., Gliniak, B., Griffith, T.S., Kubin, M., Chin, W., Jones, J., Woodward, A., Le, T., Smith, C., Smolak, P., Goodwin, R.G., Rauch, C.T., Schuh, J.C. & Lynch, D.H. (1999). Tumoricidal activity of tumor necrosis factor-related apoptosis-inducing ligand in vivo. *Nat Med*, **5,** 157-63.

Walker, J.A. & Quirke, P. (2001). Viewing apoptosis through a 'TUNEL'. *J Pathol*, **195,** 275-6.

Wang, Y., Chen, X., Armstrong, M.A. & Li, G. (2007). Survival of bone marrow-derived mesenchymal stem cells in a xenotransplantation model. *J Orthop Res*, **25,** 926-32.

Wang, Y., Huso, D.L., Harrington, J., Kellner, J., Jeong, D.K., Turney, J. & McNiece, I.K. (2005). Outgrowth of a transformed cell population derived from normal human BM mesenchymal stem cell culture. *Cytotherapy*, **7,** 509-19.

Wei, X.C., Wang, X.J., Chen, K., Zhang, L., Liang, Y. & Lin, X.L. (2001). Killing effect of TNF-related apoptosis inducing ligand regulated by tetracycline on gastric cancer cell line NCI-N87. *World J Gastroenterol*, **7,** 559-62.

Weiss, D.J., Kolls, J.K., Ortiz, L.A., Panoskaltsis-Mortari, A. & Prockop, D.J. (2008). Stem cells and cell therapies in lung biology and lung diseases. *Proc Am Thorac Soc*, **5,** 637-67.

Weldon, C.B., Parker, A.P., Patten, D., Elliott, S., Tang, Y., Frigo, D.E., Dugan, C.M., Coakley, E.L., Butler, N.N., Clayton, J.L., Alam, J., Curiel, T.J.,

Beckman, B.S., Jaffe, B.M. & Burow, M.E. (2004). Sensitization of apoptotically-resistant breast carcinoma cells to TNF and TRAIL by inhibition of p38 mitogen-activated protein kinase signaling. *Int J Oncol*, **24,** 1473-80.

Wen, J., Ramadevi, N., Nguyen, D., Perkins, C., Worthington, E. & Bhalla, K. (2000). Antileukemic drugs increase death receptor 5 levels and enhance Apo-2L-induced apoptosis of human acute leukemia cells. *Blood*, **96,** 3900-6.

Wenger, T., Mattern, J., Penzel, R., Gassler, N., Haas, T.L., Sprick, M.R., Walczak, H., Krammer, P.H., Debatin, K.M. & Herr, I. (2006). Specific resistance upon lentiviral TRAIL transfer by intracellular retention of TRAIL receptors. *Cell Death Differ*, **13,** 1740-51.

Wicha, M.S., Liu, S. & Dontu, G. (2006). Cancer stem cells: an old idea--a paradigm shift. *Cancer Res*, **66,** 1883-90; discussion 1895-6.

Wiley, S.R., Schooley, K., Smolak, P.J., Din, W.S., Huang, C.P., Nicholl, J.K., Sutherland, G.R., Smith, T.D., Rauch, C., Smith, C.A. & et al. (1995). Identification and characterization of a new member of the TNF family that induces apoptosis. *Immunity*, **3,** 673-82.

Wolf, D. & Wolf, A.M. (2008). Mesenchymal stem cells as cellular immunosuppressants. *Lancet*, **371,** 1553-4.

Wolf, S., Mertens, D., Pscherer, A., Schroeter, P., Winkler, D., Grone, H.J., Hofele, C., Hemminki, K., Kumar, R., Steineck, G., Dohner, H., Stilgenbauer, S. & Lichter, P. (2006). Ala228 variant of trail receptor 1 affecting the ligand binding site is associated with chronic lymphocytic leukemia, mantle cell lymphoma, prostate cancer, head and neck squamous cell carcinoma and bladder cancer. *Int J Cancer*, **118,** 1831-5.

Wu, C. & Alman, B.A. (2008). Side population cells in human cancers. *Cancer Lett*, **268,** 1-9.

Wu, C., Wei, Q., Utomo, V., Nadesan, P., Whetstone, H., Kandel, R., Wunder, J.S. & Alman, B.A. (2007). Side population cells isolated from mesenchymal neoplasms have tumor initiating potential. *Cancer Res*, **67,** 8216-22.

Wu, G.D., Nolta, J.A., Jin, Y.S., Barr, M.L., Yu, H., Starnes, V.A. & Cramer, D.V. (2003a). Migration of mesenchymal stem cells to heart allografts during chronic rejection. *Transplantation*, **75,** 679-85.

Wu, J., Sun, Z., Sun, H.S., Wu, J., Weisel, R.D., Keating, A., Li, Z.H., Feng, Z.P. & Li, R.K. (2008). Intravenously administered bone marrow cells migrate to damaged brain tissue and improve neural function in ischemic rats. *Cell Transplant*, **16,** 993-1005.

Wu, X., He, Y., Falo, L.D., Jr., Hui, K.M. & Huang, L. (2001). Regression of human mammary adenocarcinoma by systemic administration of a recombinant gene encoding the hFlex-TRAIL fusion protein. *Mol Ther*, **3,** 368-74.

Wu, X. & Hui, K.M. (2004). Induction of potent TRAIL-mediated tumoricidal activity by hFLEX/Furin/TRAIL recombinant DNA construct. *Mol Ther*, **9,** 674-81.

Wu, X.X., Kakehi, Y., Mizutani, Y., Nishiyama, H., Kamoto, T., Megumi, Y., Ito, N. & Ogawa, O. (2003b). Enhancement of TRAIL/Apo2L-mediated apoptosis by adriamycin through inducing DR4 and DR5 in renal cell carcinoma cells. *Int J Cancer*, **104,** 409-17.

Xin, H., Kanehira, M., Mizuguchi, H., Hayakawa, T., Kikuchi, T., Nukiwa, T. & Saijo, Y. (2007). Targeted delivery of CX3CL1 to multiple lung tumors by mesenchymal stem cells. *Stem Cells*, **25,** 1618-26.

Xu, J., Mora, A., Shim, H., Stecenko, A., Brigham, K.L. & Rojas, M. (2007a). Role of the SDF-1/CXCR4 axis in the pathogenesis of lung injury and fibrosis. *Am J Respir Cell Mol Biol*, **37,** 291-9.

Xu, J., Woods, C.R., Mora, A.L., Joodi, R., Brigham, K.L., Iyer, S. & Rojas, M. (2007b). Prevention of endotoxin-induced systemic response by bone marrow-derived mesenchymal stem cells in mice. *Am J Physiol Lung Cell Mol Physiol*, **293,** L131-41.

Yamada, M., Kubo, H., Kobayashi, S., Ishizawa, K., Numasaki, M., Ueda, S., Suzuki, T. & Sasaki, H. (2004). Bone marrow-derived progenitor cells are important for lung repair after lipopolysaccharide-induced lung injury. *J Immunol*, **172,** 1266-72.

Yamaura, T., Doki, Y., Murakami, K. & Saiki, I. (1999). Model for mediastinal lymph node metastasis produced by orthotopic intrapulmonary implantation of lung cancer cells in mice. *Hum Cell*, **12,** 197-204.

Yamaura, T., Murakami, K., Doki, Y., Sugiyama, S., Misaki, T., Yamada, Y. & Saiki, I. (2000). Solitary lung tumors and their spontaneous metastasis in

athymic nude mice orthotopically implanted with human non-small cell lung cancer. *Neoplasia*, **2,** 315-24.

Zappia, E., Casazza, S., Pedemonte, E., Benvenuto, F., Bonanni, I., Gerdoni, E., Giunti, D., Ceravolo, A., Cazzanti, F., Frassoni, F., Mancardi, G. & Uccelli, A. (2005). Mesenchymal stem cells ameliorate experimental autoimmune encephalomyelitis inducing T-cell anergy. *Blood*, **106,** 1755-61.

Zerafa, N., Westwood, J.A., Cretney, E., Mitchell, S., Waring, P., Iezzi, M. & Smyth, M.J. (2005). Cutting edge: TRAIL deficiency accelerates hematological malignancies. *J Immunol*, **175,** 5586-90.

Zhang, P., Zhang, Y., Mao, L., Zhang, Z. & Chen, W. (2009). Side population in oral squamous cell carcinoma possesses tumor stem cell phenotypes. *Cancer Lett*, **277,** 227-34.

Zhang, X., Zhao, P., Kennedy, C., Chen, K., Wiegand, J., Washington, G., Marrero, L. & Cui, Y. (2008). Treatment of pulmonary metastatic tumors in mice using lentiviral vector-engineered stem cells. *Cancer Gene Ther*, **15,** 73-84.

Zhao, Y.D., Courtman, D.W., Deng, Y., Kugathasan, L., Zhang, Q. & Stewart, D.J. (2005). Rescue of monocrotaline-induced pulmonary arterial hypertension using bone marrow-derived endothelial-like progenitor cells: efficacy of combined cell and eNOS gene therapy in established disease. *Circ Res*, **96,** 442-50.

Zhou, J., Wulfkuhle, J., Zhang, H., Gu, P., Yang, Y., Deng, J., Margolick, J.B., Liotta, L.A., Petricoin, E., 3rd & Zhang, Y. (2007). Activation of the PTEN/mTOR/STAT3 pathway in breast cancer stem-like cells is required for viability and maintenance. *Proc Natl Acad Sci U S A*, **104,** 16158-63.

Zhou, S., Schuetz, J.D., Bunting, K.D., Colapietro, A.M., Sampath, J., Morris, J.J., Lagutina, I., Grosveld, G.C., Osawa, M., Nakauchi, H. & Sorrentino, B.P. (2001). The ABC transporter Bcrp1/ABCG2 is expressed in a wide variety of stem cells and is a molecular determinant of the side-population phenotype. *Nat Med*, **7,** 1028-34.

Zhu, W., Xu, W., Jiang, R., Qian, H., Chen, M., Hu, J., Cao, W., Han, C. & Chen, Y. (2006). Mesenchymal stem cells derived from bone marrow favor tumor cell growth in vivo. *Exp Mol Pathol*, **80,** 267-74.

Zielske, S.P., Livant, D.L. & Lawrence, T.S. (2008). Radiation Increases Invasion of Gene-modified Mesenchymal Stem Cells into Tumors. *Int J Radiat Oncol Biol,* Epub ahead of print.

PUBLICATIONS RELATED TO THIS THESIS

SUBMITTED

2009 **Loebinger MR**, Kyrtatos PG, Turmaine M, et al. Magnetic resonance imaging of mesenchymal stem cells homing to pulmonary metastases using biocompatible magnetic nanoparticles. *Cancer Res.* 2009; *manuscript in revision.*

PUBLISHED ORIGINAL PAPERS

2009 **Loebinger MR**, Eddaoudi A, Davies D, et al. Mesenchymal Stem Cell delivery of TRAIL can eliminate Metastatic Cancer. *Cancer Res.* 2009; 69:4134-42.

2008 **Loebinger MR**, Giangreco A, Groot KR, et al. Squamous cell cancers contain a side population of stem-like cells that are made chemosensitive by ABC transporter blockade. *Br. J. Cancer* 2008*;* 98(2):380-87.

2007 Aguilar S, Nye E, Chan J, **Loebinger MR,** et al. Murine but not human mesenchymal stem cells generate osteosarcoma-like lesions in the lung. *Stem cells* 2007; 25(6):1586-94.

PUBLISHED REVIEWS

2008 **Loebinger MR**, Janes SM. Mesenchymal stem cells as vectors for lung disease. *Proc. Am. Thorac. Soc.* 2008; 5:711-16.

Loebinger MR, Aguilar S, Janes SM. Therapeutic potential of stem cells in lung disease: progress and pitfalls. *Clin. Sci.* 2008; 114:99-108.

2007 **Loebinger MR**, Janes SM. Stem cells for lung disease. *Chest* 2007; 132(1):279-85.

AWARDS RELATED TO THIS THESIS

2009 Young Investigator of the Year award, British Association of Lung Research.

Best of American Thoracic Society Scholars award.

International Trainee Fellowship, American Thoracic Society.

Abstract award, Medical Research Society.

Abstract award, American Thoracic Society.

Young Investigator of the Year award, European Respiratory Society.

2008 Young Investigator of the Year award, British Thoracic Society.

APPENDIX. COPIES OF 1ST AUTHOR ORIGINAL PAPERS

A Mesenchymal Stem Cell delivery of TRAIL can eliminate Metastatic Cancer.

B Squamous cell cancers contain a side population of stem-like cells that are made chemosensitive by ABC transporter blockade.

Mesenchymal Stem Cell Delivery of TRAIL Can Eliminate Metastatic Cancer

Michael R. Loebinger,[1] Ayad Eddaoudi,[2] Derek Davies,[3] and Sam M. Janes[1]

[1]Centre for Respiratory Research, Rayne Institute, and [2]Flow Cytometry Facility, Institute of Child Health, University College London; [3]Flow Cytometry Laboratory, Cancer Research UK, London Research Institute, London, England

Abstract

Cancer is a leading cause of mortality throughout the world and new treatments are urgently needed. Recent studies suggest that bone marrow–derived mesenchymal stem cells (MSC) home to and incorporate within tumor tissue. We hypothesized that MSCs engineered to produce and deliver tumor necrosis factor–related apoptosis-inducing ligand (TRAIL), a transmembrane protein that causes selective apoptosis of tumor cells, would home to and kill cancer cells in a lung metastatic cancer model. Human MSCs were transduced with *TRAIL* and the *IRES-eGFP* reporter gene under the control of a tetracycline promoter using a lentiviral vector. Transduced and activated MSCs caused lung (A549), breast (MDAMB231), squamous (H357), and cervical (Hela) cancer cell apoptosis and death in coculture experiments. Subcutaneous xenograft experiments confirmed that directly delivered TRAIL-expressing MSCs were able to significantly reduce tumor growth [0.12 cm^3 (0.04-0.21) versus 0.66 cm^3 (0.21-1.11); $P < 0.001$]. We then found, using a pulmonary metastasis model, systemically delivered MSCs localized to lung metastases and the controlled local delivery of TRAIL completely cleared the metastatic disease in 38% of mice compared with 0% of controls ($P < 0.05$). This is the first study to show a significant reduction in metastatic tumor burden with frequent eradication of metastases using inducible TRAIL-expressing MSCs. This has a wide potential therapeutic role, which includes the treatment of both primary tumors and their metastases, possibly as an adjuvant therapy in clearing micrometastatic disease following primary tumor resection. [Cancer Res 2009;69(10):4134–42]

Introduction

Cancer remains one of the biggest causes of mortality and morbidity throughout the world (1). Present therapy focuses on varying combinations of surgery, chemotherapy, and radiation treatment. Despite healthcare improvements, metastatic disease remains poorly responsive to conventional therapy and a new modality of treatment is urgently needed.

Bone marrow–derived mesenchymal stem cells (MSC) are stromal cells that reside within the adult bone marrow. They are characteristically able to differentiate into bone, cartilage, and fat and have roles in the differentiation of hematopoietic cells. Recent studies have shown an ability of these cells to migrate to and incorporate within the connective tissue stroma of tumors (2–7). This property of MSCs can be used to direct targeting antitumor agents to tumor cells and their micrometastases with improvement in murine tumor models of glioma (4, 8), melanoma (6), and breast (5) and colon (7) cancers.

Tumor necrosis factor–related apoptosis-inducing ligand (TRAIL) is a type 2 transmembrane death ligand that causes apoptosis of target cells through the extrinsic apoptosis pathway. TRAIL is a member of the tumor necrosis factor superfamily, which includes tumor necrosis factor and Fas ligand (9). The expression of tumor necrosis factor and Fas ligand leads to the damage of normal tissues in addition to their proapoptotic effect on transformed cells (10, 11), limiting their clinical applications. Conversely, TRAIL is able to selectively induce apoptosis in transformed cells but not in most normal cells (9, 12, 13), making it a promising candidate for tumor therapy. Intravenous delivery of recombinant TRAIL has, however, met with problems including a short pharmacokinetic half-life (12), necessitating frequent and high doses to produce the desired effect. The use of MSCs as a delivery vector promises to provide both targeted and prolonged delivery of this death ligand.

In this study, we express TRAIL in MSCs using a lentivirus conditionally activated by doxycycline. This system allows a mixed cell and gene therapy approach for metastatic cancers that can be activated and deactivated. We show that MSCs can be infected at high efficiency using the lentivirus system and delivery of TRAIL causes apoptosis of cancer cells through the extrinsic death pathway. *In vivo* models confirm a predilection of engraftment of MSCs within metastatic lung tumors with activation of *TRAIL* resulting in a significant reduction in metastasis number and complete clearance in 38% of mice.

Materials and Methods

Cell culture. Tissue culture reagents were purchased from Invitrogen unless otherwise stated. All cells were obtained from Cancer Research UK, London Research Institute, and cultured in DMEM and 10% fetal bovine serum unless otherwise stated. Human adult MSCs were purchased from Tulane University and cultured in α-MEM with 16% fetal bovine serum. Adipogenic and osteogenic differentiation of MSCs was done as described previously (14, 15).

TRAIL lentivirus construction and transfection of MSCs. A lentiviral plasmid (pRRL-cPPT-hPGK-mcs-WPRE) into which the Tet-On system elements had been introduced (ref. 16; a kind gift from O. Danos, University College London) was used as a backbone for the incorporation of *TRAIL* DNA. The existing reporter gene, *MuSEAP*, was excised using the *Mlu*I and *Eco*RV restriction sites. The *IRES-eGFP* sequence (from pENTR1A) was amplified and restriction sites were introduced by PCR and then inserted into the plasmid in place of *MuSEAP*. Subsequently, human *TRAIL* (amino acids 1-281; RZPD) was similarly amplified and restriction sites were introduced by PCR and then cloned into the lentivirus plasmid, via *Mlu*I

Note: Supplementary data for this article are available at Cancer Research Online (http://cancerres.aacrjournals.org/).

Requests for reprints: Sam M. Janes, Centre for Respiratory Research, Rayne Institute, University College London, Rayne Building, 5 University Street, London WC1E 6JJ, United Kingdom. Phone: 44-20-7679-6926; Fax: 44-20-7679-6973; E-mail: s.janes@ucl.ac.uk.

doi:10.1158/0008-5472.CAN-08-4698

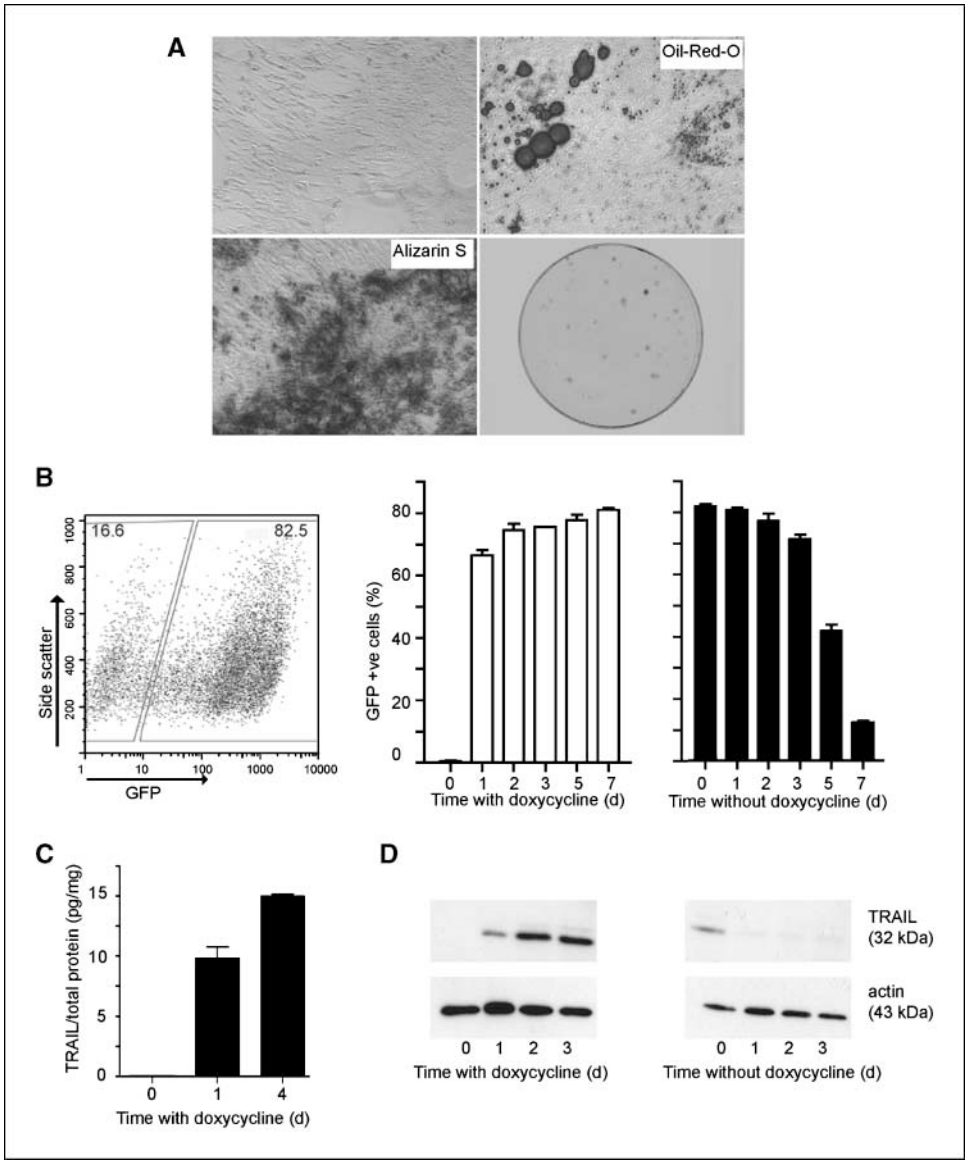

Figure 1. MSC characterization, transduction, and gene expression. *A,* MSCs, differentiation to adipocytes (Oil-Red-O) and osteoblasts (Alizarin Red S; magnification, ×4), and colony-forming ability. *B,* representative flow cytometry for GFP expression in MSCs transduced with the *TRAIL-GFP* lentivirus (MSCFLTs) and activated with doxycycline and timescale of GFP expression with addition or removal of doxycycline. *C,* TRAIL ELISA of MSCFLTs. *D,* Western blots of MSCFLTs showing maximum expression of TRAIL after 2 d of doxycycline treatment (10 μg protein loaded) and loss of expression 1 d after doxycycline removal (5 μg protein loaded) with actin loading controls.

and *Bst*B1 restriction sites, next to the *IRES-eGFP*. The plasmid constructs were confirmed by DNA sequence analysis (Cogenics).

The lentivirus was produced by transfecting 293T cells with 15 mL Opti-Mem plus 10 mL of a solution made by mixing 3.6 mL polyethylenimine (Sigma-Aldrich) and 56.4 mL Opti-Mem to 600 μg *TRAIL* plasmid, 450 μg of the packaging construct pCMV-dR8.74, 150 μg of a plasmid producing the VSV-G envelope, pMD.G2, and 60 mL Opti-Mem (both pCMV-dR8.74 and pMD.G2 were a kind gift from A. Thrasher, University College London). The lentivirus was concentrated by ultracentrifugation at 18,000 rpm (SW28 rotor, Optima LE80K Ultracentrifuge, Beckman) at 4°C and stored at −80°C before use.

Human MSCs were transduced with a multiplicity of infection of 10 virus particles for each cell and 4 μg/mL polybrene (Sigma-Aldrich).

Human TRAIL expression was verified by ELISA (R&D Systems) as per manufacturer's instructions and by Western blot.

Western blots. Supernatants were centrifuged and cells were lysed in radioimmunoprecipitation assay buffer (PBS, 1% Igepal Ca-630, 0.5% sodium deoxycholate, 0.1% SDS; Sigma) supplemented with complete protease inhibitor cocktail (Complete-mini; Roche Diagnostics). Samples were denatured, resolved with a 10% SDS-polyacrylamide gel, and transferred using a semidry transfer method (NovaBlot; Pharmacia LKB).

Blots were then incubated with anti-TRAIL (1 μg/mL H257 rabbit polyclonal antibody; ref. 17; Santa Cruz Biotechnology) or anti-actin (0.24 μg/mL; Sigma) antibodies and detected using enhanced chemiluminescence (GE Healthcare) as per manufacturer's instructions.

Coculture experiments. Human MSCs permanently transduced with the full-length *TRAIL* plasmid (MSCFLT) were plated with target cells. A total of 100,000 cells were plated in each 6-well plate. The following day, doxycycline or other active agents were added to the cocultures and left for 48 h. Staining of target cells was done with the fluorescent dye, DiI, as per manufacturer's instructions (Invitrogen).

Apoptosis and cell death was assessed by flow cytometry (FACSCalibur or LSRII machines; Becton Dickinson). This was done on floating and adherent cells from cocultures using Annexin V-647 antibody (Invitrogen) and 5 μg/mL propidium iodide (PI; Sigma). 4′,6-Diamidino-2-phenylindole (DAPI; 2 μg/mL; Sigma) was used instead of PI when cancer cells were stained with DiI. Annexin V^-/PI^- cells were judged to be nonapoptotic. Annexin V^+/PI^- cells were considered to be apoptotic. Annexin V^+/PI^+ cells were recorded as being dead.

The following compounds were used in coculture experiments: the pan-caspase inhibitor zVADfmk (1 μg/mL; Sigma), a soluble recombinant TRAIL (200 ng/mL; R&D Systems), and a neutralizing TRAIL antibody (250 ng/mL; R&D Systems).

Production of dominant-negative Fas-associated death domain cancer cells. Phoenix packaging cells were transiently transfected with

retroviral vector for the dominant-negative Fas-associated death domain *(dnFADD)/GFP* construct (18) or empty vector and the virus containing supernatant was added to infect AM12 packaging cells as described previously (19). The AM12 cell supernatant was added to Hela cells (30% confluence) with 5 μg/mL polybrene and the cells were selected with 1 μg/mL puromycin (20).

Cell migration assay. An *in vitro* cell migration assay was done to determine the tropism of MSCs for tumor cells according to previously described methods (4, 7, 21). One hundred fifty thousand cancer cells or 293T cells were plated in 800 μL medium on the bottom well of a Transwell plate (8 μm pore membrane; Becton Dickinson) for 24 h before 40,000 MSCs in 300 μL of the same medium were added to the top well. MSCs were allowed to migrate across the membrane for 24 h at 37°C. The cells attached to the top side of the membrane were removed, and the migrated cells on the bottom side were fixed, stained using a Rapid Romanowsky staining kit (Raymond Lamb), and counted (5 fields per well, triplicate wells) at ×10 magnification (Olympus BX40).

Xenograft cancer models. All animal studies were done in accordance with British Home Office procedural and ethical guidelines. Six-week-old NOD/SCID mice (Harlan) were kept in filter cages.

Subcutaneous tumors were obtained by the injection of 2 million MDAMB231 cells in 200 μL PBS subcutaneously into the left flank with a 29 gauge needle. Tumors were measured every 3 to 5 days with calipers, and the volume was calculated as $4/3\pi r^3$, where r is the radius. Metastatic lung tumors were produced by the intravenous delivery of 2 million MDAMB231 in 200 μL PBS into the lateral tail vein.

***In vivo* use of TRAIL-expressing MSCs.** In the subcutaneous models, MSCFLTs labeled with CM-DiI (Invitrogen) as per manufacturer's instructions were either delivered concurrently with the cancer cells; 2 million MDAMB231 with 0.75 million MSCFLT in 200 μL PBS, or after tumors had become established; 1 million MSCFLTs were injected into

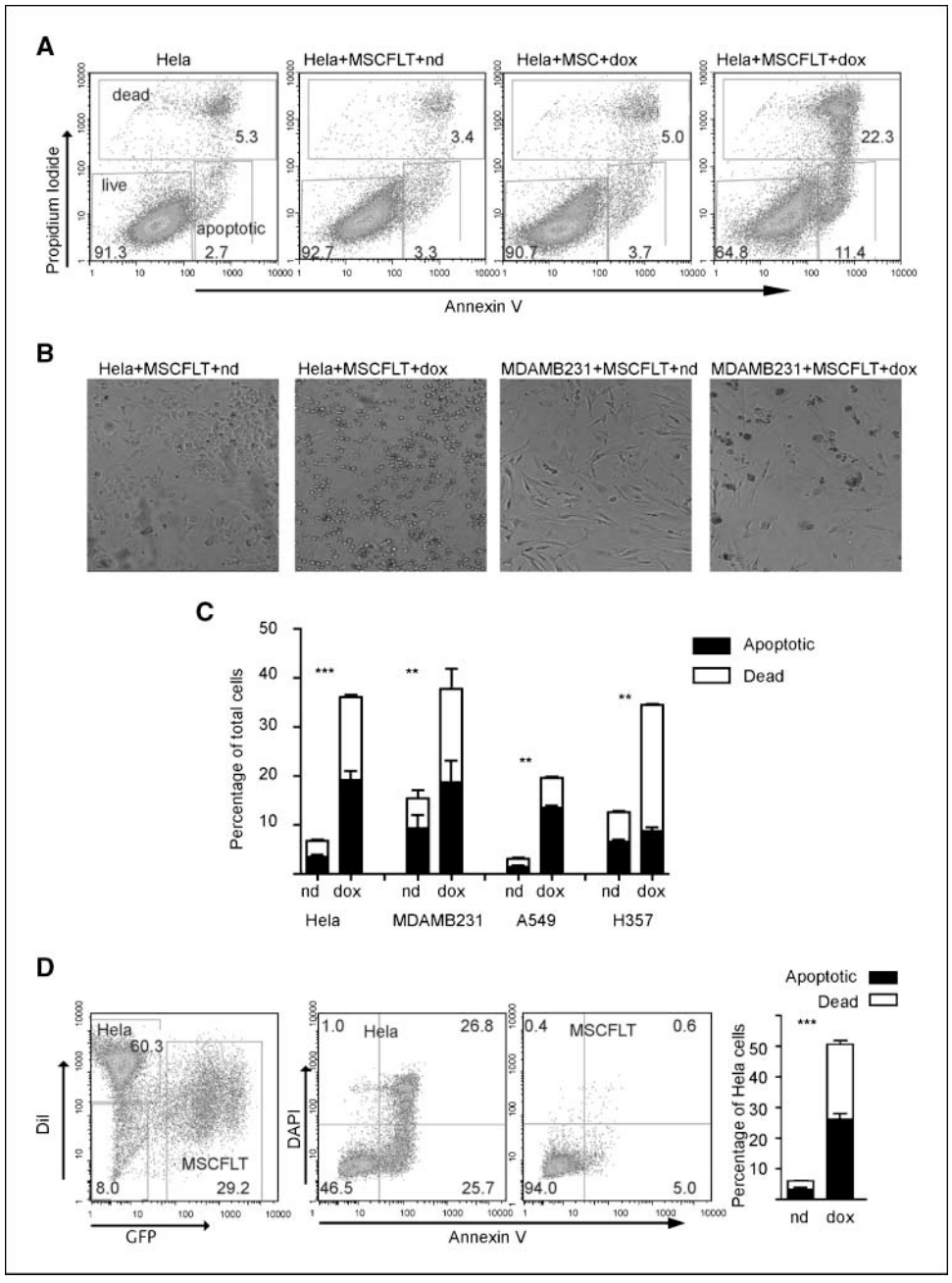

Figure 2. TRAIL-expressing MSCs cause cancer cell apoptosis *in vitro. A,* representative flow cytometry plots showing an increase in death and apoptosis when Hela cells were cocultured with doxycycline (*dox*)-treated MSCFLTs compared with no doxycycline (*nd*), untreated controls, or doxycycline-treated normal MSCs. *B,* phase-contrast microscopy (magnification, ×5) showing an increase in cell death (rounded and floating cells) when MSCFLTs were activated by doxycycline in coculture with Hela and MDAMB231 cells. *C,* flow cytometry results from triplicate apoptosis assays showing an increase in death and apoptosis of total cells in cancer cells and MSCFLT cocultures after doxycycline treatment. *D,* flow cytometry of coculture experiments showed DiI-positive cancer cells were responsible for dead and apoptotic populations. Triplicate experiments. ***, $P < 0.001$; **, $P < 0.01$.

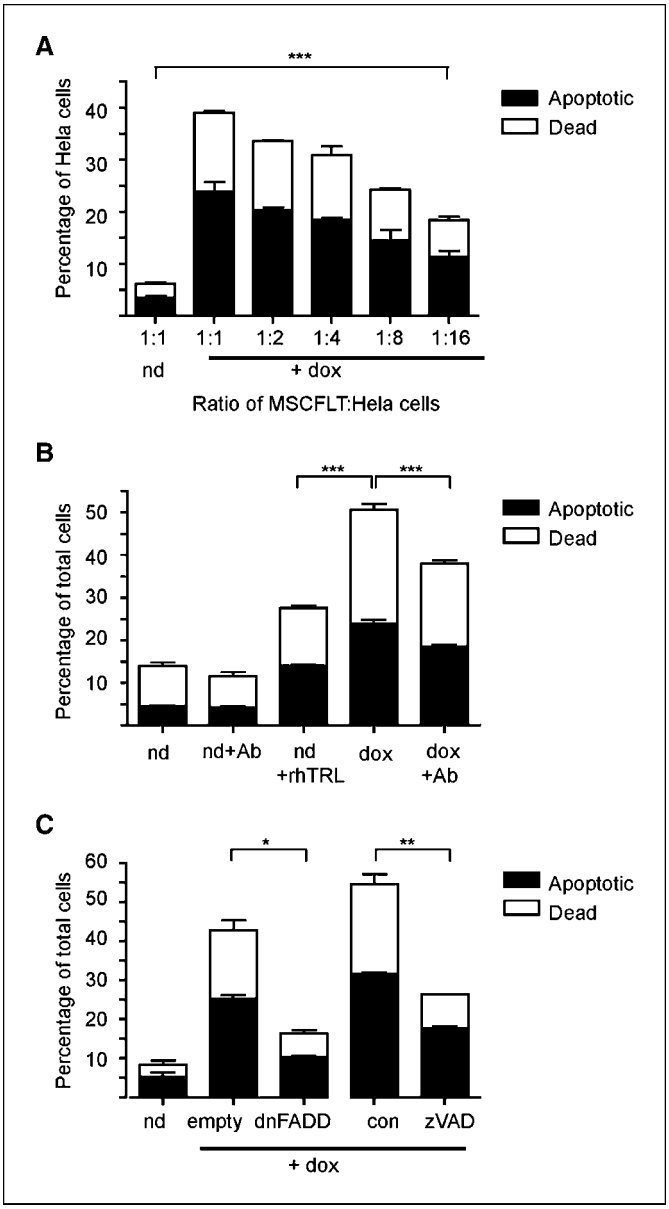

Figure 3. TRAIL-expressing MSC-induced apoptosis occurs at low MSCFLT-to-cancer cell ratios via the extrinsic apoptotic pathway. *A,* flow cytometry apoptosis assays showing an increase in death and apoptosis of Hela cells when MSCFLTs activated with doxycycline were cocultured with Hela cells even at low 1:16 ratios compared with untreated controls. *B,* induced cell death and apoptosis is higher using MSCFLTs than with recombinant TRAIL (*rhTRL*) and can be partially blocked with blocking antibody (*Ab*). *C,* cell death and apoptosis is reduced when using Hela cells expressing dnFADD in comparison with those transduced with an empty vector in addition to when zVADfmk (*zvad*), a pan-caspase inhibitor, is used compared with the control (*con*). ***, $P < 0.001$; **, $P < 0.01$; *, $P < 0.05$.

established subcutaneous tumors. In metastatic models, 0.75 million MSCFLT cells were suspended in 200 μL PBS and injected into the lateral tail vein at 7, 14, 21, and 28 days after the cancer models had been set up (5). To activate the *TRAIL* constructs in the transduced MSCFLTs, mice were fed water containing 2 mg/mL doxycycline and 3% sucrose, with controls fed water with 3% sucrose only.

Mice were sacrificed by CO_2 asphyxiation followed by exsanguination. Subcutaneous tumors were removed and weighed before they were split for digestion with 0.1% collagenase A (Roche Diagnostics) into a single-cell suspension as per manufacturer's protocol or fixed in 4% paraformaldehyde for histology. The lungs were excised and weighed before they were insufflated with a fixed 20 cm pressure of 4% paraformaldehyde and then bathed in 4% paraformaldehyde for histology. In some lungs, the left lobe was removed and snap frozen in liquid nitrogen before insufflation.

Immunohistochemistry. Fixed specimens were embedded in paraffin and cut into 3 μm sections for H&E staining. GFP antibody (rabbit polyclonal; Invitrogen) and TRAIL antibody (rabbit monoclonal; Santa Cruz Biotechnology) were used as primary antibodies and detected with biotinylated secondaries and diaminobenzidine (Vector Laboratories). Fluorescent microscopy was used to detect DiI-positive cells with DAPI counterstain and secondary fluorescent antibodies against primary vimentin antibodies (sc7557; Santa Cruz Biotechnology). TUNEL staining was done according to the manufacturer's instructions (Roche Diagnostics). Microscopy was done using light (Olympus BX40), fluorescent (Carl Zeiss, Axioskop 2), or confocal (Bio-Rad MRC 1024) microscope.

Quantitative real-time reverse transcription-PCR. RNA was extracted from the snap-frozen left lung with Trizol (Invitrogen) and treated with DNase (Ambion). cDNA was synthesized using a reverse transcription-PCR kit according to the manufacturer's instructions (Roche Diagnostics). Real-time PCR amplification was done with Light Thermocycler (Roche Diagnostics) using SYBR Green quantitative PCR kit (Invitrogen) with primers for human *TRAIL* and the control 18S.

Metastases quantification. The number and size of tumor nodules were assessed in H&E sections using similar methodology to that described previously (22). Photomicrographs of representative sections of the entire lung were taken at ×2 magnification. This created a complete picture of all lobes of the lungs of the mice. Image analysis software (SimplePCI High-Performance Imaging Software; Hamamatsu Photonics) was used to trace around the metastatic deposits and the lung sections and then calculate lung and metastasis area and number of metastases.

Statistics. Statistical analysis was done using GraphPad Prism version 4 (GraphPad Software). Multiple groups were analyzed by ANOVA or Kruskal-Wallis tests. Single group data were assessed using Student's *t* test. All *in vitro* experiments were done in triplicate unless specified.

Results

Characterization and *TRAIL* transduction of MSCs. Fully characterized MSCs were purchased from Tulane University and were shown to differentiate into fat and bone in differentiation assays and have the expected colony-forming efficiency ± SD (48 ± 2.83%; Fig. 1*A*). MSCs were stably transduced with our lentivirus expressing TRAIL and GFP under the control of doxycycline at different multiplicities of infection. A multiplicity of infection of 10 was used for further experiments producing 82.13 ± 0.40% successful transduction (GFP expression) at day 7 (Fig. 1*B*) while limiting the number of dead cells 4.8 ± 1.83%.

MSCFLTs were examined for TRAIL and GFP expression using flow cytometry, Western blots, and ELISA. Flow cytometry showed <0.5% GFP expression before activation with doxycycline, whereas, 48 h after doxycycline addition to the medium, this increased to 74.7 ± 2.5% (Fig. 1*B*). Withdrawal of doxycycline, after the cells had been exposed for 5 days, led to a fall in GFP expression with 12.2 ± 1.0% of cells weakly positive at day 7 (Fig. 1*B*; Supplementary Fig. S1).

ELISA and immunoblotting for TRAIL showed that it was only produced when the transgene was activated by doxycycline (Fig. 1*C* and *D*). Western blots showed TRAIL protein expression in MSCFLT lysates was maximal after 2 days of doxycycline stimulus (Fig. 1*D*), but very little TRAIL protein remained after the doxycycline stimulus had been removed for 1 day, following a preceding doxycycline stimulus of 5 days (Fig. 1*D*).

TRAIL-expressing MSCs cause tumor cell death *in vitro*. MSCFLTs were cocultured with tumor cells, and apoptotic and

dead cells increased significantly when doxycycline was added. This effect was observed with lung cancer (A549; apoptotic and dead cells increased from 3.1 ± 0.1% to 19.6 ± 0.8%; $P = 0.001$, t test; with the addition of doxycycline), breast cancer (MDAMB231; 15.4 ± 1.7-37.7 ± 6.5%; $P = 0.001$, t test), squamous cell cancer (H357; 12.5 ± 0.3-34.5 ± 1.0%; $P = 0.001$, t test), and cervical cancer (Hela; 6.7 ± 1.0-36.1 ± 3.5%; $P = 0.0001$, t test) cells (Fig. 2*A-C*). These apoptosed and dead cells were shown to come specifically from the cancer cell population by labeling the cancer cell populations with the fluorescent dye (DiI). Thus, 50.7 ± 2.7% of the Hela cell population were dead or apoptotic compared with only 8.3 ± 4.6% of the MSCFLT population ($P < 0.0001$, t test; Fig. 2*D*).

Coculture experiments were repeated with decreasing numbers of MSCFLTs. A significant increase in apoptosis and death of the cancer cells was achieved at all concentrations of MSCFLT used ($P < 0.001$ at ratio MSCFLT/Hela cells of 1:16, ANOVA). There was a cell ratio-dependent effect (Fig. 3*A*). This experiment underestimates the true killing capacity of MSCFLT cells as the seeding ratios do not account for any proliferation of cancer cells compared with MSCFLTs before the addition of doxycycline.

TRAIL-expressing MSCs kill cancer cells by TRAIL induction of the extrinsic apoptosis pathway. A TRAIL antibody with some ability to neutralize the bioactivity of TRAIL was added to the MSCFLT and Hela cell cocultures. The antibody was used at a dose to give maximal neutralizing effect (250 ng/mL; ref. 23). The amount of MSCFLT-induced death and apoptosis was significantly reduced with this antibody (38.03 ± 0.49% compared with 50.67 ± 3.8%; $P < 0.001$, ANOVA) but not back to baseline (11.48 ± 1.49%; Fig. 3*B*). We found that our doxycycline-induced MSCFLTs were potent inducers of death and apoptosis of Hela cells, with a larger proportion of apoptotic and dead cells in comparison with maximal doses (200 ng/mL) of recombinant soluble TRAIL (50.67 ± 3.8% compared with 27.50 ± 0.70%; $P < 0.001$, ANOVA; Fig. 3*B*).

The caspases are a family of closely related enzymes crucial to apoptosis. zVADfmk is a cell permeable, pan-caspase inhibitor. Application of this compound to the 1:1 cocultured MSCFLTs and Hela cells caused a 51.6% reduction in death and apoptosis (26.5 ± 0.7% compared with a DMSO-treated control 54.8 ± 3.0%; $P = 0.003$, t test) confirming the importance of caspases in the mechanism of TRAIL-induced cell death (Fig. 3*C*).

To confirm that the mechanism of MSCFLT-induced cancer cell death is via the extrinsic pathway, Hela cancer cells were retrovirally transduced with a *dnFADD* construct or an empty vector (18). The dnFADD consists of the death domain that binds to the TRAIL receptor but not the domain responsible for caspase-8 recruitment and the triggering of apoptosis. We observed a significant reduction ($P = 0.018$, t test) in death and apoptosis of Hela cells transduced with *dnFADD* after coculture with activated MSCFLT cells (Fig. 3*C*). This data present strong evidence that MSCFLT cells induce apoptosis via the extrinsic pathway.

MSCs migrate toward some tumor cells. *In vitro* Transwell experiments showed the ability of MSCs to home toward tumors. A549, MDAMB231, and Hela cancer cell cultures were used to attract MSCs, with benign fibroblast 293T cells and medium alone used as controls. There was significantly increased migration to the MDAMB231 cells; 250.4 ± 0.8 cells per field compared with 98.6 ± 9.3 cells to 293T and 57.6 ± 7.6 toward the medium ($P < 0.001$, ANOVA). There was no significantly increased migration toward the A549 (92.0 ± 7.1) and Hela (81.0 ± 2.1) cells (Fig. 4*A*).

To examine if MSCFLTs could be traced to metastatic tumors, we used a lung metastasis model. Intravenously injected MDAMB231 cells produced lung metastases in all of 20 NOD/SCID mice. These tumors were visible at day 10 post-injection and grew to large metastases by day 30 (Fig. 4*B*). DiI-stained MSCFLTs were injected at day 10 and shown histologically to preferentially localize to lung

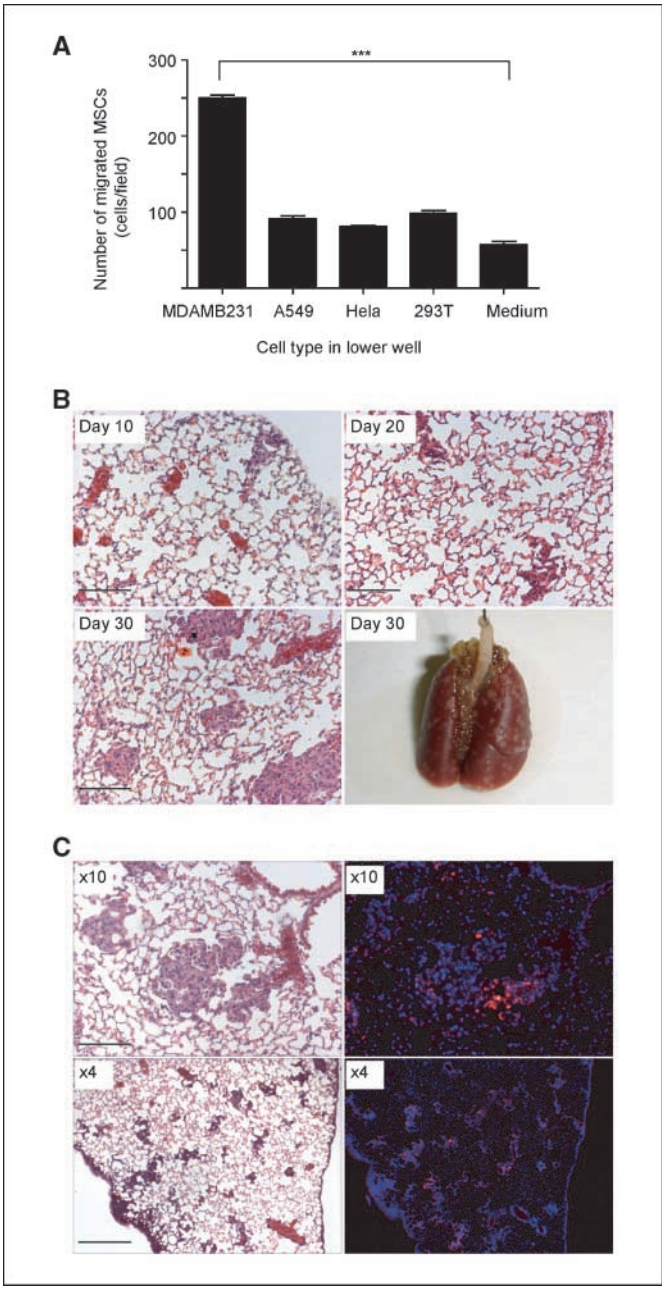

Figure 4. MSCs migrate to some cancer cells *in vitro* and preferentially engraft *in vivo*. *A,* Transwell migration studies showed an increased number (per microscopic field) of MSCs migrating through the Transwell membrane toward MDAMB231 cells but not toward other (A549 and Hela) cancer cell types compared with control 293T cells or medium alone. ***, $P < 0.001$. *B,* H&E showing representative lung metastases post–intravenous injection of MDAMB231 cells into NOD/SCID mice at days 10, 20, and 30 and a macroscopic picture at day 30. *Bar*, 20 μm. *C,* DiI-labeled MSCFLTs (*red*) injected intravenously at day 10 and shown to localize to lung metastases on fluorescent microscopy with DAPI nuclear counterstain with H&E contiguous sections from day 30 harvested lungs (magnification, ×10; *bar*, 20 μm and magnification, ×4; *bar*, 60 μm).

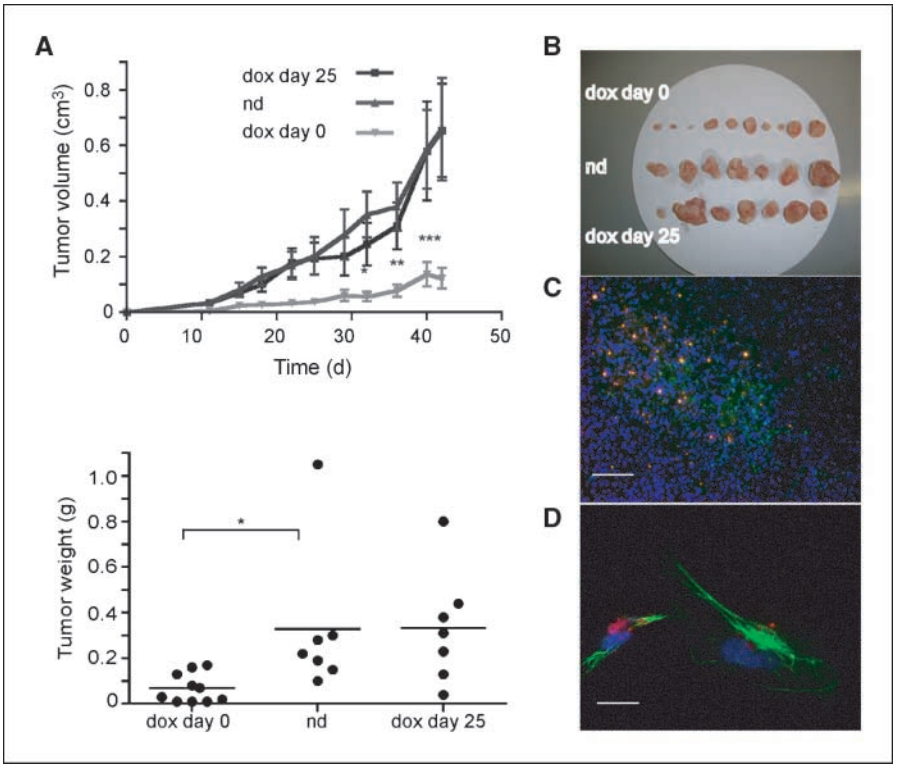

Figure 5. TRAIL-expressing MSCs reduce the growth of subcutaneous tumors. *A,* doxycycline treatment of subcutaneous tumors composed of mixed MDAMB231 cells and MSCFLT cells from day 0 led to a decreased size and weight (*, $P < 0.05$; **, $P < 0.01$; ***, $P < 0.001$) of the tumors compared with untreated mice. There was no reduction in tumor growth if TRAIL was activated at day 25. *B,* macroscopic appearance of the tumors. *C,* TUNEL staining (*green*) showed areas of tumor apoptosis localized with areas of MSCFLTs (DiI, *red*) within the tumors in mice treated with doxycycline from day 0 (DAPI nuclear counterstain, *blue*). *Bar,* 25 μm. *D, ex vivo* single-cell digestion and culture showed DiI-positive (*red*) cells with MSC morphology that costained with vimentin (*green*; DAPI, *blue*). *Bar,* 3 μm.

metastases (Fig. 4*C*). DiI-stained fibroblasts were not detected in the tumors or in the lungs 10 days after injection (data not shown). These histologic data show that MSCFLTs preferentially engraft and are maintained in the *in vivo* tumor environment compared with surrounding lung parenchyma, whereas fibroblasts are not.

TRAIL-expressing MSCs reduce subcutaneous tumor growth in mice. Two million MDAMB231 cells were coinjected with 0.75 million MSCFLT cells and the *TRAIL* transgene was activated with the addition of doxycycline at day 0 or 25 or never, with tumors harvested at day 42. A recent study has shown that coculture of MSCs with MDAMB231 cells did not alter the tumor growth (24). In our study with transduced MSCs, activation at day 0 resulted in a significantly reduced tumor size (0.12 ± 0.12 cm^3 versus 0.66 ± 0.49 cm^3; $P < 0.001$, two-way ANOVA) and weight (0.07 ± 0.06 g versus 0.33 ± 0.33 g; $P < 0.05$, Kruskal-Wallis); however, there was no change in the tumor growth when *TRAIL* was activated after the tumor had already become established at day 25 (Fig. 5*A* and *B*). TUNEL staining of excised tumors showed areas of apoptosis colocalized with DiI-labeled MSCFLT cells (Fig. 5*C*). The subcutaneous tumors were excised and digested to a single-cell suspension. Confocal microscopy of the *ex vivo* DiI-labeled cells included cells of MSC-type morphology and showed vimentin staining (Fig. 5*D*). A separate experiment injected transduced MSCFLTs into established tumors. Similar to late activation of coinjected cells, the late injection of MSCFLT cells into established tumors and activation of *TRAIL* at this later stage was unable to alter the growth of the tumors (Supplementary Fig. S2).

Systemic delivery of TRAIL-expressing MSCs reduces and can eliminate lung metastases. Intravenously injected MDAMB231 cells were used to produce lung metastases in NOD/SCID mice. MSCFLTs were then used as an intravenous combined cellular and gene therapy with delivery at days 7, 14, 21, and 28 (Fig. 6*A*). At day 35, tumor metastases were found in all mice (8 of 8) without MSCFLT and all mice with MSCFLT without the use of doxycycline (8 of 8). In the MSCFLT plus doxycycline arm, 3 of 8 mice were tumor-free ($P = 0.032$, χ^2; Fig. 6*B*). In addition to the elimination of metastases with MSCFLT plus doxycycline, the lung weight ($P < 0.01$, ANOVA), which serves as a correlate for metastases load, was also significantly reduced in all of these mice. Similar results were achieved when metastases numbers per lung area was used as an endpoint ($P < 0.001$, ANOVA; Fig. 6*C*). Three mice had to be excluded from this latter analysis as the lungs did not inflate during the fixation procedure. MSCFLT cells delivered to control mice without doxycycline were unable to clear the metastases in any mice but did have less metastases per area ($P < 0.001$, ANOVA) and a lower lung weight ($P < 0.05$, ANOVA) than the untreated mice. Doxycycline treatment, however, produced a further significant reduction ($P < 0.05$, ANOVA; Fig. 6*B* and *C*). In a subsequent experiment, TRAIL and GFP were both shown to be expressed *in vivo* by MSCFLT with immunohistochemistry when mice were harvested 2 days after treatment with MSCFLT and doxycycline (Fig. 6*D*; primary antibody controls showed no staining; data not shown). *TRAIL* mRNA derived from the lungs of these mice was also increased (Fig. 6*D*).

Discussion

The ability of TRAIL to lead to tumor apoptosis and death without affecting normal cells makes it an extremely exciting molecule for tumor therapy. Here, we have shown that MSCs can be engineered to express TRAIL under the sensitive control of the Tet-On inducible system. These cells were able to kill cancer cell lines *in vitro* via the extrinsic death pathway to a higher degree than recombinant protein. *In vivo*, we show that TRAIL-expressing MSCs reduce the growth of early subcutaneous tumors, whereas, in a systemically delivered metastasis model, these cells reduced

metastases but most significantly eliminated metastases in three mice.

We used MSCs as vectors of delivery due to observations that they appear to home to, or at least engraft preferentially, within tumors. MSCs also make an attractive therapeutic tool as they are widely acknowledged to be immunoprivileged. Theoretically, future cell therapies using allogenic MSCs could be used in patients without the use of prior immunomodulation (25). Alternatively, with the ease of harvest, culture, and infection of MSCs, the use of autologous cells may also be realistic.

It is important to consider the possible direct effects that MSCs may have on disease. Some studies have suggested intrinsic antineoplastic properties of these cells, with improvements in Kaposi's sarcoma (2) and subcutaneous breast tumor models (26). Various mechanisms have been proposed for these effects, including Akt inhibition (2), nuclear factor-κB down-regulation (27), and the Wnt pathway (26). Conversely, MSCs have also been associated with a tumor-promoting effect in certain models, including increased growth and metastasis in colonic (28) and breast (24) subcutaneous tumor models. In our subcutaneous tumor model, we did not see an increase in lung metastases when the tumor cells were coinjected with MSCs. Furthermore, MSCs in our lung metastasis model appeared to have an antineoplastic effect.

To our knowledge, this is the first study that uses MSCs as a vector for a lentiviral delivery of a gene therapy for cancer. We used a lentivirus in view of their significant advantages over other vector systems. Adenoviral vector expression is transient and often produces a significant host immune response, whereas retroviruses may cause incorporation errors. Lentiviral vectors are less likely to cause insertional mutagenesis as the promoter can be modified extensively. Furthermore, they have the ability to stably transduce both dividing and quiescent cells (29), which is a further significant advantage when using stem cells that are often quiescent or slow-growing. Finally, our construct incorporates the Tet-On system allowing us to both turn on and, through withdrawal of doxycycline, off the protein expression, attractive in the view of possible

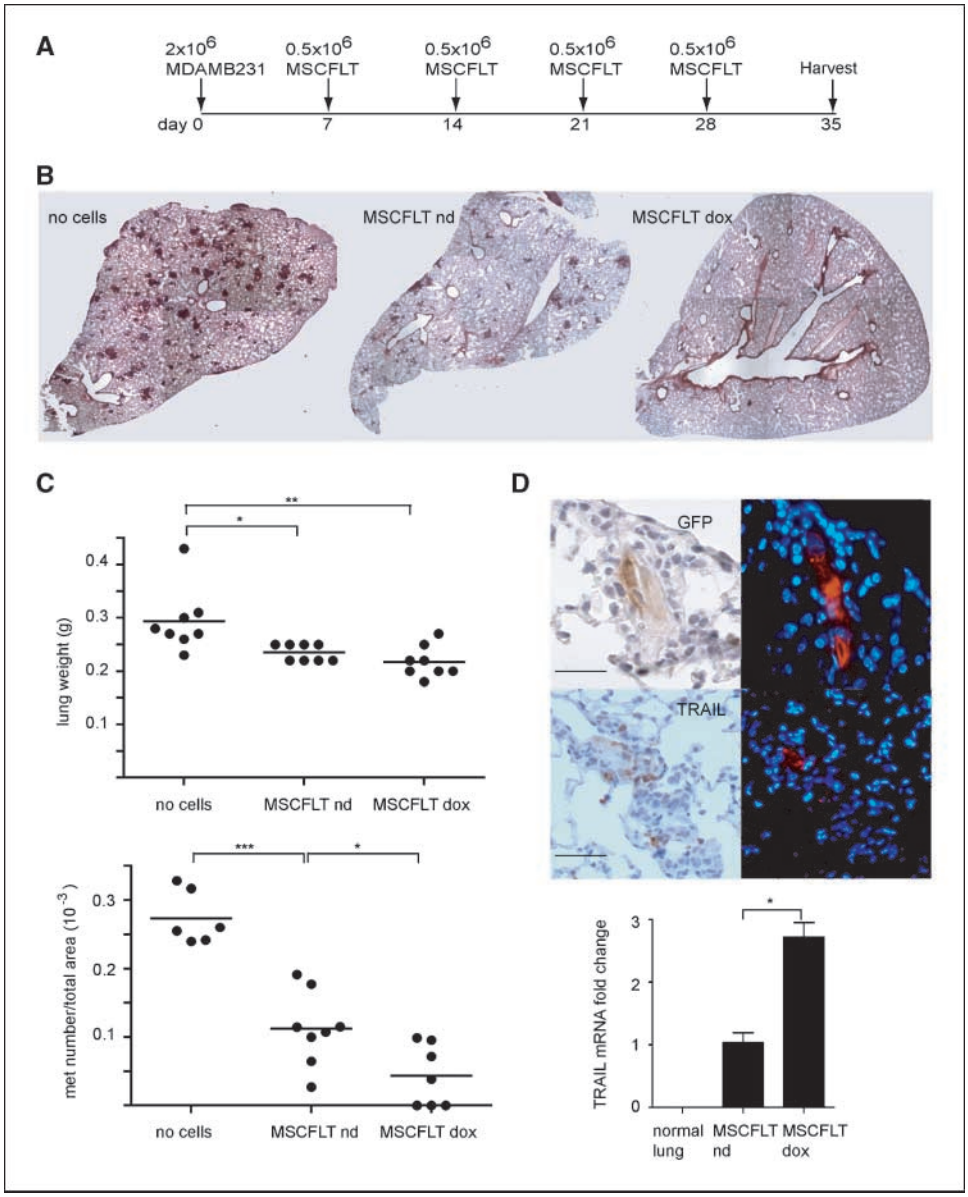

Figure 6. TRAIL-expressing MSCs reduce the growth of lung metastases. *A,* 2 million MDAMB231 cells were injected intravenously at day 0 followed by delivery or no delivery of MSCFLT cells at days 7, 14, 21, and 28 with or without doxycycline. *B,* representative histology of lung lobes in the three experimental groups. Metastases remained, but were reduced, after injection of MSCFLT without activation of the *TRAIL* construct, whereas *TRAIL* activation of MSCFLTs eliminated metastases in 3 of 8 mice ($P = 0.03$). *C,* reduction in lung weight and metastases (*met*) number per lung area with the use of MSCFLTs both with and without doxycycline treatment. There was a further significant reduction between activated MSCFLTs compared with inactivated. ***, $P < 0.001$; **, $P < 0.01$; *, $P < 0.05$. *D,* immunohistochemistry showing cells expressing GFP (*bar*, 5 μm) and TRAIL (*bar*, 10 μm) and consecutive immunofluorescence sections showing these cells also express DiI. There is an increase in *TRAIL* mRNA from lung digests treated with MSCFLT and doxycycline. *, $P < 0.05$.

longevity of using stem cells as delivery vehicles in disease. Clinically, treatment could be timed to chemotherapy or radiotherapy regimes, with the expression turned off in between courses.

TRAIL is thought to operate physiologically in the immunosurveillance against tumors. Administration of a neutralizing anti-TRAIL antibody or the use of *TRAIL* knockout mice showed the increased susceptibility of TRAIL deficient mice to TRAIL-sensitive tumors and metastases (30–32). TRAIL-expressing MSCs in this study may act in a similar way, replacing the deficient immunosurveillance systems in the NOD/SCID mice leading to tumor cell destruction and prevention of metastasis. The property of metastasis prevention would be ideal as an adjuvant therapy in the treatment of many patients with solid organ tumors, who remain at significant risk of future metastatic disease despite primary tumor resection and chemotherapy and radiotherapy. Identifying these patients is now becoming a reality with the use of highly sensitive and specific molecular and cytologic techniques, which allow the detection of very small numbers of circulating tumor cells in the blood and bone marrow (33, 34), which could be amenable to MSC-directed TRAIL therapy.

The use of targeted TRAIL therapy could be widely applicable to many different cancers. Despite some cancers being resistant to the effects of TRAIL, an additive effect has been shown with the concomitant use of TRAIL with other antineoplastic agents that act at different positions in either intrinsic or extrinsic apoptotic pathways. For example, the down-regulation of Bcl-2 (35) or the DNA damage caused by chemotherapy can increase the effects of TRAIL therapy in various *in vivo* models (36–39).

One of the limitations of our study is the model used for the *in vivo* experiments. With the aim of future translational therapeutics, we used human cancer xenograft models, human MSCs, and human *TRAIL* constructs. It is important to consider that human *TRAIL* has only 65% homology to murine *TRAIL* (9), and there are also differences in the receptors in mice and humans. In the mouse, only one death-inducing receptor with homology to DR5 has been discovered in addition to two decoy receptors (mDcTRAILR1 and msDcTRAILR2; ref. 40). Consequently, the effects of TRAIL on the normal murine cells may be different to the response of normal human cells.

In summary, we describe, for the first time to our knowledge, the use of TRAIL-expressing MSCs for the reduction and, in some cases, elimination of metastatic disease in a murine lung metastasis model. We believe that this therapy may have an important future therapeutic role in preventing metastatic recurrence in patients.

Disclosure of Potential Conflicts of Interest

No potential conflicts of interest were disclosed.

Acknowledgments

Received 12/12/08; revised 2/19/09; accepted 3/20/09.

Grant support: This work was partly undertaken at University College London Hospital/University College London, which received a proportion of funding from the Department of Health's National Institute for Health Research Biomedical Research Centres funding scheme.

M.R. Loebinger is a Medical Research Council UK Clinical Training Fellow. S.M. Janes is a Medical Research Council Clinician Scientist.

The costs of publication of this article were defrayed in part by the payment of page charges. This article must therefore be hereby marked *advertisement* in accordance with 18 U.S.C. Section 1734 solely to indicate this fact.

We thank Dr. Dominique Bonnet, Dr. Susana Aguilar, Prof. Geoff Laurent, and Dr. Rachel Chambers for helpful comments on experimental design and Dr. Laura Bazley for technical assistance.

References

1. Jemal A, Siegel R, Ward E, Murray T, Xu J, Thun MJ. Cancer statistics, 2007. CA Cancer J Clin 2007;57:43–66.
2. Khakoo AY, Pati S, Anderson SA, et al. Human mesenchymal stem cells exert potent antitumorigenic effects in a model of Kaposi's sarcoma. J Exp Med 2006; 203:1235–47.
3. Menon LG, Picinich S, Koneru R, et al. Differential gene expression associated with migration of mesenchymal stem cells to conditioned medium from tumor cells or bone marrow cells. Stem Cells 2007;25:520–8.
4. Nakamizo A, Marini F, Amano T, et al. Human bone marrow-derived mesenchymal stem cells in the treatment of gliomas. Cancer Res 2005;65:3307–18.
5. Studeny M, Marini FC, Dembinski JL, et al. Mesenchymal stem cells: potential precursors for tumor stroma and targeted-delivery vehicles for anticancer agents. J Natl Cancer Inst 2004;96:1593–603.
6. Studeny M, Marini FC, Champlin RE, Zompetta C, Fidler IJ, Andreeff M. Bone marrow-derived mesenchymal stem cells as vehicles for interferon-β delivery into tumors. Cancer Res 2002;62:3603–8.
7. Xin H, Kanehira M, Mizuguchi H, et al. Targeted delivery of CX3CL1 to multiple lung tumors by mesenchymal stem cells. Stem Cells 2007;25:1618–26.
8. Kim SM, Lim JY, Park SI, et al. Gene therapy using TRAIL-secreting human umbilical cord blood-derived mesenchymal stem cells against intracranial glioma. Cancer Res 2008;68:9614–23.
9. Wiley SR, Schooley K, Smolak PJ, et al. Identification and characterization of a new member of the TNF family that induces apoptosis. Immunity 1995;3:673–82.
10. Ogasawara J, Watanabe-Fukunaga R, Adachi M, et al. Lethal effect of the anti-Fas antibody in mice. Nature 1993;364:806–9.
11. Nagata S. Apoptosis by death factor. Cell 1997;88: 355–65.
12. Ashkenazi A, Pai RC, Fong S, et al. Safety and antitumor activity of recombinant soluble Apo2 ligand. J Clin Invest 1999;104:155–62.
13. Walczak H, Miller RE, Ariail K, et al. Tumoricidal activity of tumor necrosis factor-related apoptosis-inducing ligand *in vivo*. Nat Med 1999;5:157–63.
14. Aguilar S, Nye E, Chan J, et al. Murine but not human mesenchymal stem cells generate osteosarcoma-like lesions in the lung. Stem Cells 2007;25:1586–94.
15. Chan J, O'Donoghue K, de la Fuente J, et al. Human fetal mesenchymal stem cells as vehicles for gene delivery. Stem Cells 2005;23:93–102.
16. Barde I, Zanta-Boussif MA, Paisant S, et al. Efficient control of gene expression in the hematopoietic system using a single Tet-On inducible lentiviral vector. Mol Ther 2006;13:382–90.
17. Kagawa S, He C, Gu J, et al. Antitumor activity and bystander effects of the tumor necrosis factor-related apoptosis-inducing ligand (TRAIL) gene. Cancer Res 2001;61:3330–8.
18. Janes SM, Watt FM. Switch from $\alpha_v\beta_5$ to $\alpha_v\beta_6$ integrin expression protects squamous cell carcinomas from anoikis. J Cell Biol 2004;166:419–31.
19. Janes SM, Ofstad TA, Campbell DH, Watt FM, Prowse DM. Transient activation of FOXN1 in keratinocytes induces a transcriptional programme that promotes terminal differentiation: contrasting roles of FOXN1 and Akt. J Cell Sci 2004;117:4157–68.
20. Legg J, Jensen UB, Broad S, Leigh I, Watt FM. Role of melanoma chondroitin sulphate proteoglycan in patterning stem cells in human interfollicular epidermis. Development 2003;130:6049–63.
21. Abayasiriwardana KS, Barbone D, Kim KU, et al. Malignant mesothelioma cells are rapidly sensitized to TRAIL-induced apoptosis by low-dose anisomycin via Bim. Mol Cancer Ther 2007;6:2766–76.
22. Zhang X, Zhao P, Kennedy C, et al. Treatment of pulmonary metastatic tumors in mice using lentiviral vector-engineered stem cells. Cancer Gene Ther 2008;15: 73–84.
23. Matthews N, Neale ML. Cytotoxicity assays for tumour necrosis factor and lymphotoxin. In: Clemens MJ, Morris AG, Gearing AJH, editors. Lymphokines and interferons, a practical approach. Oxford: IRL Press; 1987. p. 221.
24. Karnoub AE, Dash AB, Vo AP, et al. Mesenchymal stem cells within tumour stroma promote breast cancer metastasis. Nature 2007;449:557–63.
25. Chen XC, Wang R, Zhao X, et al. Prophylaxis against carcinogenesis in three kinds of unestablished tumor models via IL12-gene-engineered MSCs. Carcinogenesis 2006;27:2434–41.
26. Qiao L, Xu ZL, Zhao TJ, Ye LH, Zhang XD. Dkk-1 secreted by mesenchymal stem cells inhibits growth of breast cancer cells via depression of Wnt signalling. Cancer Lett 2008;269:67–77.
27. Qiao L, Zhao TJ, Wang FZ, Shan CL, Ye LH, Zhang XD. NF-κB downregulation may be involved the depression of tumor cell proliferation mediated by human mesenchymal stem cells. Acta Pharmacol Sin 2008;29:333–40.
28. Zhu W, Xu W, Jiang R, et al. Mesenchymal stem cells derived from bone marrow favor tumor cell growth *in vivo*. Exp Mol Pathol 2006;80:267–74.
29. Kyriakou CA, Yong KL, Benjamin R, et al. Human mesenchymal stem cells (hMSCs) expressing truncated soluble vascular endothelial growth factor receptor (tsFlk-1) following lentiviral-mediated gene transfer inhibit growth of Burkitt's lymphoma in a murine model. J Gene Med 2006;8:253–64.
30. Takeda K, Smyth MJ, Cretney E, et al. Critical role for tumor necrosis factor-related apoptosis-inducing ligand in immune surveillance against tumor development. J Exp Med 2002;195:161–9.
31. Cretney E, Takeda K, Yagita H, Glaccum M, Peschon JJ, Smyth MJ. Increased susceptibility to

tumor initiation and metastasis in TNF-related apoptosis-inducing ligand-deficient mice. J Immunol 2002;168:1356–61.
32. Takeda K, Hayakawa Y, Smyth MJ, et al. Involvement of tumor necrosis factor-related apoptosis-inducing ligand in surveillance of tumor metastasis by liver natural killer cells. Nat Med 2001;7:94–100.
33. Riethdorf S, Wikman H, Pantel K. Review: Biological relevance of disseminated tumor cells in cancer patients. Int J Cancer 2008;123:1991–2006.
34. Lang JE, Hall CS, Singh B, Lucci A. Significance of micrometastasis in bone marrow and blood of operable breast cancer patients: research tool or clinical application? Expert Rev Anticancer Ther 2007; 7:1463–72.
35. Kock N, Kasmieh R, Weissleder R, Shah K. Tumor therapy mediated by lentiviral expression of shBcl-2 and S-TRAIL. Neoplasia 2007;9:435–42.
36. Ucur E, Mattern J, Wenger T, et al. Induction of apoptosis in experimental human B cell lymphomas by conditional TRAIL-expressing T cells. Br J Cancer 2003; 89:2155–62.
37. Jin H, Yang R, Fong S, et al. Apo2 ligand/tumor necrosis factor-related apoptosis-inducing ligand cooperates with chemotherapy to inhibit orthotopic lung tumor growth and improve survival. Cancer Res 2004;64:4900–5.
38. Ray S, Almasan A. Apoptosis induction in prostate cancer cells and xenografts by combined treatment with Apo2 ligand/tumor necrosis factor-related apoptosis-inducing ligand and CPT-11. Cancer Res 2003; 63:4713–23.
39. Naka T, Sugamura K, Hylander BL, Widmer MB, Rustum YM, Repasky EA. Effects of tumor necrosis factor-related apoptosis-inducing ligand alone and in combination with chemotherapeutic agents on patients' colon tumors grown in SCID mice. Cancer Res 2002;62:5800–6.
40. Lawrence D, Shahrokh Z, Marsters S, et al. Differential hepatocyte toxicity of recombinant Apo2L/TRAIL versions. Nat Med 2001;7:383–5.

British Journal of Cancer (2008) 98, 380 – 387

www.bjcancer.com

Squamous cell cancers contain a side population of stem-like cells that are made chemosensitive by ABC transporter blockade

MR Loebinger[1,4], A Giangreco[2,4], KR Groot[1,4], L Prichard[1], K Allen[3], C Simpson[3], L Bazley[3], N Navani[1], S Tibrewal[1], D Davies[3] and SM Janes*[,1]

[1]Centre For Respiratory Research, Rayne Institute, University College London, 5 University Street, London WC1E 6JJ, UK; [2]Keratinocyte Laboratory, Cancer Research UK, Cambridge Research Institute, Robinson Way, Cambridge CB2 0RE, UK; [3]Flow Cytometry Laboratory, Cancer Research UK, London Research Institute, 44 Lincoln's Inn Fields, London WC2A 3PX, UK

Cancers are a heterogeneous mix of cells, some of which exhibit cancer stem cell-like characteristics including ATP-dependent drug efflux and elevated tumorigenic potential. To determine whether aerodigestive squamous cell carcinomas (SCCs) contain a subpopulation of cancer stem cell-like cells, we performed Hoechst dye efflux assays using four independent cell lines. Results revealed the presence of a rare, drug effluxing stem cell-like side population (SP) of cells within all cell lines tested (SCC-SP cells). These cells resembled previously characterised epithelial stem cells, and SCC-SP cell abundance was positively correlated with overall cellular density and individual cell quiescence. Serial SCC-SP fractionation and passaging increased their relative abundance within the total cell population. Purified SCC-SP cells also exhibited increased clonogenic potential in secondary cultures and enhanced tumorigenicity *in vivo*. Despite this, SCC-SP cells remained chemotherapeutically sensitive upon ATP-dependent transporter inhibition. Overall, these findings suggest that the existence of ATP transporter-dependent cancer stem-like cells may be relatively common, particularly within established tumours. Future chemotherapeutic strategies should therefore consider coupling identification and targeting of this potential stem cell-like population with standard treatment methodologies.
British Journal of Cancer (2008) **98,** 380 – 387. doi:10.1038/sj.bjc.6604185 www.bjcancer.com
Published online 22 January 2008

Keywords: stem cell; squamous cell carcinoma; side population; ATP-binding cassette transporters

Translational Therapeutics

Stem cells are present in many tissues where they function to maintain appropriate homeostasis and differentiation as well as regulate tissue responses to injury and infection (Watt and Hogan, 2000; Janes *et al*, 2002). These cells are capable of self-renewal, have a relatively undifferentiated phenotype, exhibit high proliferative potential, and are multipotent (Griffiths *et al*, 2005). In adult tissues, stem cells tend to divide infrequently and many exhibit an intrinsic resistance to environmental toxins or chemotherapeutic agents (Giangreco *et al*, 2002; Zhou *et al*, 2002; Hirschmann-Jax *et al*, 2004).

Traditionally, stem cell pollutant resistance has been identified on the basis of efficient Hoechst 33342 dye efflux (Goodell *et al*, 1996). Drug-resistant stem cells, termed side population (SP) cells, have been identified in a growing number of tissues including bone marrow, pancreas, muscle, brain, and lung (Goodell *et al*, 1996; Lechner *et al*, 2002; Giangreco *et al*, 2003; Summer *et al*, 2003; Kondo *et al*, 2004; Oyama *et al*, 2007). This SP phenotype is dependent on ATP-binding cassette (ABC) transporter activity, as ATP inhibitors such as verapamil and reserpine block dye efflux (Goodell *et al*, 1997; Zhou *et al*, 2001; Scharenberg *et al*, 2002). In particular, the ABC transporter ABCG2/BCRP1 appears critical to maintain this phenotype as Abcg2 knockout mice lack SP cells and are particularly sensitive to chemotherapeutic agents such as mitoxantrone (Zhou *et al*, 2002).

In addition to normal tissues, recent evidence suggests that some cancers also contain a population of stem-like, pollutant-resistant cells (Passegue *et al*, 2003). Cancer stem or stem-like cells, which exhibit increased chemotherapeutic drug resistance, have been found within acute myeloid leukaemia (Wulf *et al*, 2001; Reya *et al*, 2003), breast, and brain solid tumours (Al-Hajj *et al*, 2003). Recently, several cancer cell lines have been identified that contain a subpopulation of chemotherapeutic-resistant, cancer SP cells including the rat glioma line C6, human breast cancer line MCF-7, rat neuroblastoma line B104, and the human adenocarcinoma cell line HeLa (Kondo *et al*, 2004). Cancer SP cells have also been identified *in vivo* within 65% of human neuroblastoma tumours (Hirschmann-Jax *et al*, 2004). These repopulate both SP and non-SP cell types, indicating their multipotent differentiation potential (Hirschmann-Jax *et al*, 2004). They also express numerous ABC transporter proteins, providing them with increased drug resistance (Hirschmann-Jax *et al*, 2004). Finally, it appears that following chemotherapy, cancer SP are uniquely capable of producing drug-insensitive secondary tumours (Passegue *et al*, 2003). On the basis of these observations, cancer SP cells are increasingly considered to be potential cancer stem cells (Hadnagy *et al*, 2006; Giangreco *et al*, 2006).

*Correspondence: Dr SM Janes;
E-mail: s.janes@ucl.ac.uk
[4] These authors contributed equally to this work.
Revised 27 November 2007; accepted 11 December 2007; published online 22 January 2008

Aerodigestive squamous cell carcinomas (SCCs) frequently exhibit chemotherapeutic resistance and increased metastatic potential following unsuccessful cancer treatment. We, therefore, wished to determine whether SCC cell lines contained SP cells, and, if so, whether these displayed cancer stem cell characteristics. We now describe the presence of an SCC-SP cell subset whose abundance was positively correlated with increasing cell confluence and quiescence. These cells exhibited characteristics of cancer stem cells including increased growth, multipotent differentiation, and a capacity for *in vivo* tumorigenesis.

MATERIALS AND METHODS

Tissue culture

H357, SCC4, SCC13, and SCC15 cell lines, derived from patients with advanced SCCs, were cultured in complete FAD medium (Sugiyama *et al*, 1993). The culture medium (FAD + FCS + HICE) consisted of one part Ham's F12 medium and three parts Dulbecco's modified Eagle's medium, supplemented with 10% fetal calf serum (FCS), 0.5 μg ml^{-1} hydrocortisone, 5 μg ml^{-1} insulin, 10^{-10} M cholera toxin, and 10 ng ml^{-1} epidermal growth factor (HICE). The culture medium was changed every 2 days.

Fluorescence-activated cell sorting

Cells were harvested at 70% or full confluence, washed, and resuspended at 1×10^6 cells ml^{-1} in FAD medium and incubated at 37°C for 10 min. Cells were labelled with 5 μM Hoechst 33342 (Sigma, St Louis, MI) for 15, 30, 45, 60, 75, 90, 105, 120, and 135 min at 37°C to determine the required incubation time. As the size of the SP was found to be stable from 30 min, all subsequent staining was carried out for 45 min at 37°C. The cells were counterstained with 5 μg ml^{-1} propidium iodide (Sigma) to label dead cells, which were excluded from the analysis. Fluorescence-activated cell sorting (FACS) was performed using a MoFlo High-Performance Cell Sorter (DakoCytomation, Denmark). For SP analysis, at least 1×10^5 total events were collected, and all subsequent analysis was performed using FlowJo software (Tree Star Inc., Ashland, Oregon). For cell cycle status analysis following Hoechst 33342 efflux, ethanol-fixed cells were stained with 50 μg ml^{-1} propidium iodide in the presence of RNase A (50 μg ml^{-1}) and analysed with a FACS-Calibur flow cytometer. The Watson Pragmatic model was applied to determine cell cycle. All flow cytometry experiments were repeated to confirm consistency. A representative plot is shown for each profile.

Colony-forming assays

In all, 200 SP and non-SP H357 cells were seeded per six-well plate and cultured for 14 days. Colonies were washed, fixed using 3% paraformaldehyde (BDH), and stained with Rhodanile Blue overnight. Colonies of two or more cells were counted using an Olympus CK2 inverted phase-contrast light microscope. Abortive colonies were defined as colonies that contained fewer than 32 cells according to the system described by Jones and Watt (1993). A large colony was defined as greater than 32 cells per colony. All experiments were performed in triplicate. In mitoxantrone dihydrochloride (Sigma) dose–response assays, 200 H357 cells were plated per well of a six-well plate and cultured in the presence of 0, 1, or 10 ng ml^{-1} of mitoxantrone for 3 days. After a further 14 days, the cultures were fixed, stained, and counted. In mitoxantrone and verapamil assays, 300 H357 cells were plated per well of a six-well plate, cultured in the presence of 0, 1, or 10 ng ml^{-1} of mitoxantrone ± verapamil hydrochloride 100 μM (Sigma) for 7 days, and, subsequently, grown for a further 7 days in the absence of drugs.

Proliferation assay

A total of 1000 H357 cells were plated per well and cultured in complete FAD medium. Cells were harvested at days 2, 4, and 8, and cell number counted by haemocytometer. Each H357 cell population and time point were analysed in triplicate.

Quantitative RT-PCR

cDNA synthesis (random hexamers + Superscript II; Invitrogen, Paisley, UK) and subsequent quantitative RT-PCR (QPCR) was performed using 1 μg of total RNA isolated from freshly sorted or serially passaged H357 SP, non-SP, and parent cells as indicated in text. Human gene-specific, predesigned, and inventoried probes were purchased from Applied Biosystems, Foster City, CA, TaqMan QPCR analysis was based on the $\Delta\Delta C_t$ relative mRNA abundance method and normalised to β2-microglobulin expression. At least two samples per sort parameter were assayed using an ABI7900 real-time PCR machine (Applied Biosystems).

Subcutaneous tumour model

Six-week-old, male NOD/SCID mice purchased from Harlan (Bicester, UK) were used for the experiments. All mouse studies were performed in accordance with British Home Office procedural and ethical guidelines. Animals were housed in pathogen-free conditions with filtered air, and autoclaved food and water was available *ad libitum*. H357 SP(1) and G2(1) cells (both sorted and passaged once to expand cell numbers) were suspended in sterile PBS at a concentration of 1×10^7 cells ml^{-1}. A total of 200 μl of the suspension containing two million cells was injected subcutaneously in the left flank with a 29G needle. Tumours were measured every 3–5 days with callipers, and the volume calculated as $4/3\,\pi r^3$, where r is the estimated radius.

Statistics

Student's *t*-, Student–Newman–Keuls, and Mann–Whitney statistical tests were carried out using SigmaStat. Data are expressed as means ± s.e.m. Data not in normal distribution were log transformed prior to statistical testing.

RESULTS

Squamous cell carcinomas contain an ABC transporter- and cell density-dependent side population

Several tumours and tumour cell lines maintain a population of chemotherapeutic and pollutant-resistant cells with characteristics of stem-like SP cells (Hirschmann-Jax *et al*, 2004; Kondo *et al*, 2004). To determine whether SCCs might also contain a subpopulation of drug-resistant SP cells, four 70% confluent SCC cell lines were incubated in 5 μM Hoechst 33342 dye and analysed by FACS. Cell confluence was verified by cell cycle analysis (Figures 1A–C). A characteristic SP fraction was detected in all four cell lines examined and was stable after 30 min dye incubation as determined by time course analysis (15–135 min, SP examined every 15 min; not shown). Overall, SCC-SP abundance varied between each cell line examined from 0.076% (SCC15) to 0.47% (H357) (Figures 1D–F and Table 1). All SCC-SP populations were reserpine sensitive, indicating their dependence on ABC-type transporter activity (Figures 1G–I).

We next wished to examine whether a cancer's cellular density or cell cycle status influenced SCC-SP cell abundance. We therefore cultured H357 cells to 100% confluence prior to Hoechst dye incubation (Figure 1J). On average, increased cellular density or

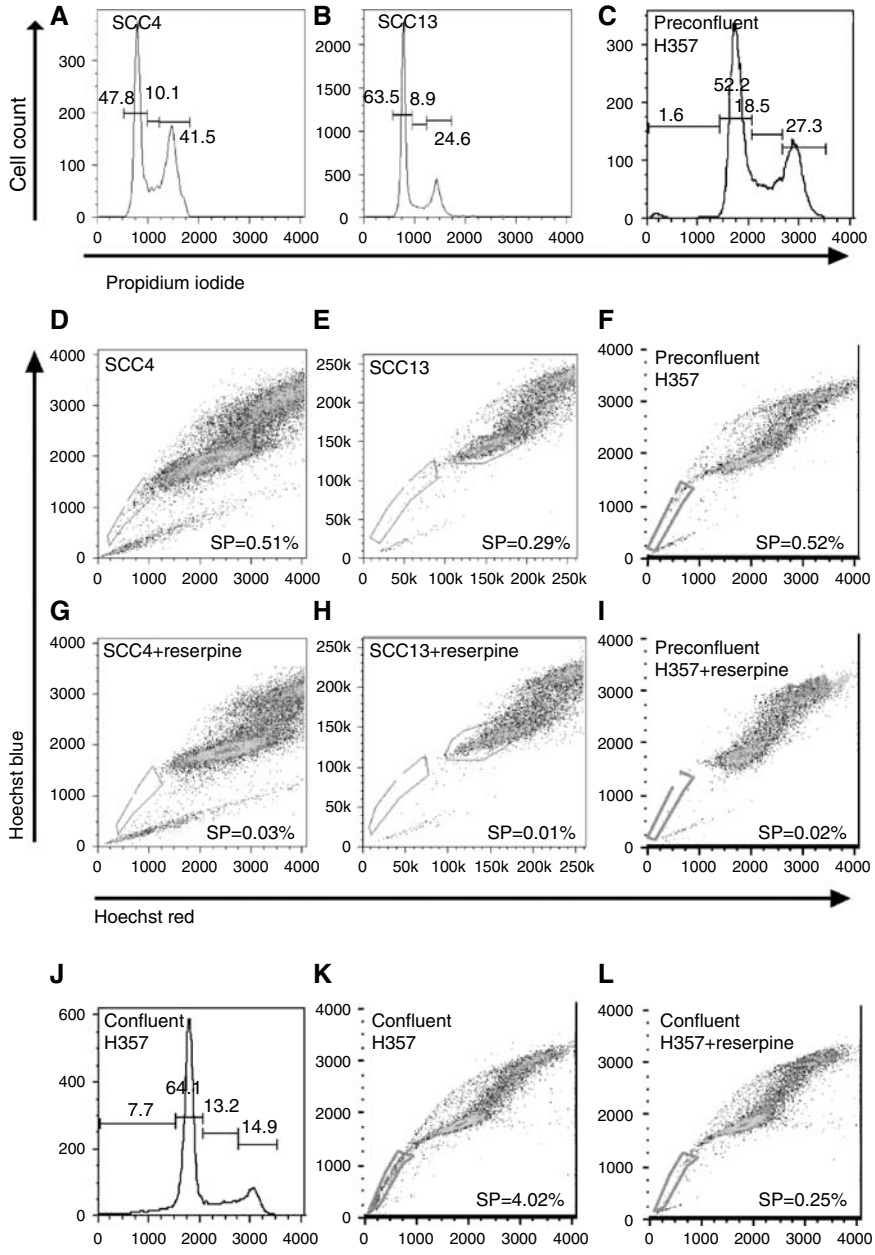

Figure 1 Squamous cell carcinomas contain an SP that varies with cell confluency. Seventy percent confluent SCC4, SCC13, and H357 SCC cells were stained with propidium iodide staining profiles, highlighting the relative percentage of S-phase cells as an indication of cell confluence (**A**–**C**, **J**). The cells were incubated in Hoechst 33342 prior to analysis by flow cytometry (**D**–**F**). The SP was compared between subconfluent (70%) (**F**) and confluent (**K**) cell populations with reserpine controls (**G**–**I**, **L**).

Table 1 Summary of average SCC SP cell abundance

Cell line	Average % of SP	s.d.	Minimum/maximum % of SP	No. of replicates
H357	0.470	0.160	0.25/0.63	4
SCC4	0.385	0.177	NA	2
SCC13	0.270	0.028	NA	2
SCC15	0.076	0.063	NA	2

NA = not applicable; SCC = squamous cell carcinoma; SP = side population. SP analysis performed at 70% cell confluence.

reduced proliferation increased the H357 SP cell population from 0.47 ± 0.16 to $4.53 \pm 0.61\%$, or nearly 10-fold ($n = 4$, Figures 1K and L).

SCC-SP cells express epithelial stem cell markers

To ascertain whether SCC-SP cells exhibited an enhanced stem cell-like phenotype, we isolated and serially propagated H357 SCC-SP cells as indicated in Figure 2A. Using QPCR, we examined the expression of known epithelial stem cell genes including chondroitin sulphate proteoglycan 4 (CSPG4/MCSP; Legg *et al*, 2003), tumour suppressor of lung cancer 1 (TSLC1; Morris *et al*, 2004; Tumbar *et al*, 2004), integrin β1 (ITGB1; Jones and Watt, 1993), and keratin 15 (KRT15; Liu *et al*, 2003). Serially propagated SCC-SP cells (SP(3)) expressed significantly more CSPG4/MCSP and TSLC1 than parent H357 cells but did not express increased levels of either KRT15 or ITGB1 (Figure 2B). In freshly isolated, unpassaged SP(1) cells, only TSLC1 expression was significantly enriched relative to parent cells (data not shown). Altogether, these

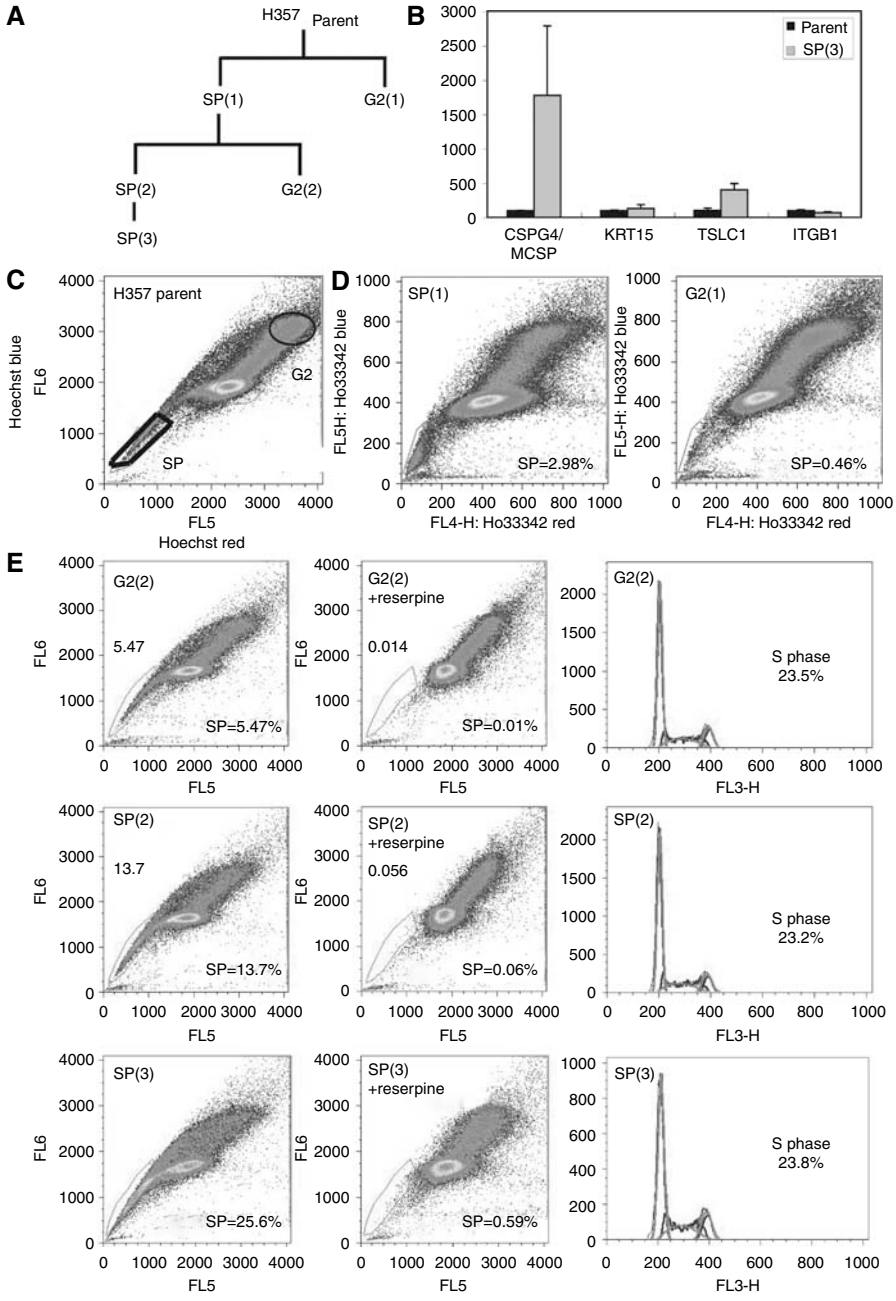

Figure 2 Squamous cell carcinomas containing SP cells express stem cell markers and are selectable. (**A**) Schematic of H357 cell populations isolated following successive rounds of FACS analysis. (**B**) Relative mRNA abundance of epithelial stem cell markers chondroitin sulphate proteoglycan 4 (CSPG4/MCSP), tumour suppressor of lung cancer 1 (TSLC1), integrin β1 (ITGB1), and keratin 15 (KRT15). (**C**) FACS analysis of Hoechst 33342-stained parental H357 cells with sorted areas marked SP and G2. (**D**) FACS analysis of Hoechst 33342-stained cell populations isolated from (**C**). (**E**) G2(2) and SP(2) cells were stained with Hoechst 33342 and analysed in the presence or absence of reserpine. Side population size is increased in SP(2) cells and further in SP(3) cells, suggesting that the SP phenotype is selectable. Propidium iodide staining indicates equivalent levels of confluence and cell viability.

data indicate that SCC-SP cells but not parent H357 cells resemble epithelial stem cells.

Serial SCC-SP cell propagation enhances SP cell abundance

We next wished to examine whether isolated and *in vitro* expanded H357 SP cells were capable of repopulating secondary SP and non-SP populations. Parent H357 cells were therefore labelled with Hoechst 33342 dye and sorted into two populations termed SP(1) and G2(1) based on their relative blue/red fluorescence intensity (Figure 2C, schematic Figure 2A). The G2 grouping reflected each cell's relative position in the cell cycle (that is, G2 phase; Figure 2C). Following *in vitro* expansion, G2 cells reproduced both an SP and non-SP cell population in similar proportions to those of the parent population (0.46%, Figure 2D). In contrast, SP(1)-sorted cells produced greater numbers of drug-resistant SP cells relative to both parent and G2 populations (2.98%; Figure 2D).

On the basis of our observation that SCC-SP cell expansion leads to an enrichment of drug-resistant cells, we wished to determine whether further SP cell propagation might continue to increase SP cell abundance. H357 SP(1) cells were therefore re-sorted into

SP(2) and G2(2) fractions; SP(2) was additionally expanded and fractionated into an SP(3) population (see schematic, Figure 2A). Under these conditions, the ABC-dependent drug-resistant SP fraction increased dramatically within both SP(2)- and G2(2)-sorted subpopulations compared to the original parent cells (Figure 2E). Further SP(2) fractionation to SP(3) increased the SP fraction to 25.6% of total cells, an increase of approximately 50-fold from the original parental population (Figure 2E). These percentages were confirmed with a repeat experiment (data not shown).

SCC-SP cells express ABCG2 and ABCC1 type ABC transporters

On the basis of the observation that SCC-SP purification enriched the relative SP abundance in secondary cultures, we wished to examine whether SP cells also contained elevated ABC transporter expression relative to parent and non-SP cells. Results of QPCR analysis revealed that both parent and freshly sorted SP(1) but not G2 cells expressed ABCG2(BCRP1) and ABCC1(MRP1) transporters (Figure 3A). Expression levels were not significantly different from those of independently isolated haematopoietic SP stem cells (HSC (SP), Figure 3A). There was additionally no significant difference in either ABCG2 and ABCC1 expression when serially propagated SP(3) cells were compared with parent SCCs (Figure 3B). We were unable to detect ABCB1/MDR1 expression in any SCC cell lines examined. Overall, these results suggested that ABC transporter mRNA expression does not directly determine SP cell abundance.

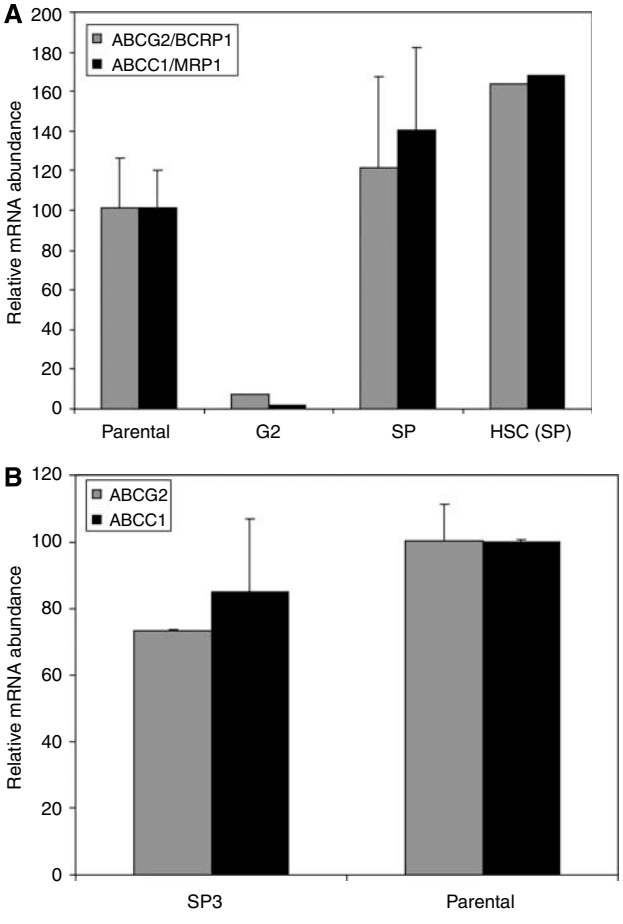

Figure 3 Quantitative RT-PCR of SCC populations. (**A**) Unpassaged SP(1) and G2(1) cells show differential expression of ABCG2 and ABCC1 transporter proteins. SP(1) levels are equivalent to parent and haematopoietic stem cells. (**B**) Highly selected SP(3) cells have equivalent expression to parent cells.

SCC-SP cells exhibit stem cell-like characteristics *in vitro*

One of the principal characteristics of epithelial stem cells is enhanced *in vitro* clonogenicity and growth. To examine whether SCC-SP cells exhibit enhanced *in vitro* proliferation, 1000 parent, SP(1), and SP(3) cells were cultured for 2, 4, and 8 days. Both SP cell populations grew significantly more rapidly than parent cells (Figure 4A). SP(3) cells also exhibited significantly faster growth rate 8 days postplating than SP(1) cells, indicating a serial enrichment in SCC-SP proliferative capacity (Figure 4A). The data

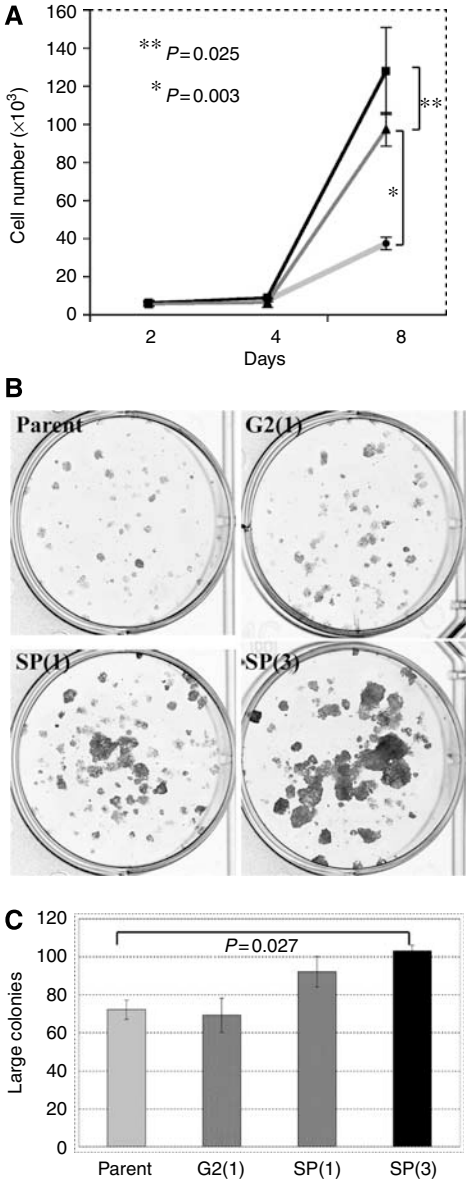

Figure 4 Side population cells have higher proliferation rates and greater clonogenic ability. (**A**) 1000 parent H357, SP(1), and SP(3) cells were plated and the total cell numbers counted at days 2, 4, and 8; SP(3) (squares), SP(1) (triangles), parent (circles). (**B**) Analysis of clonogenicity of H357 cell populations. (**C**) Quantitation of large colony numbers from clonogenicity assays shown in (**B**). Assays were set up in triplicate. Error bars indicate s.e.m.

shown are representative of two proliferation assays performed in triplicate.

We also examined the clonogenic potential of SCC-SP cells as an indicator of their individual proliferative capacity. Parent, G2(1), SP(1), and SP(3) H357 cells were plated in triplicate and cultured at clonal density for 14 days (Figure 4B). Results revealed significant increases in large colony formation uniquely within both SP(1) and SP(3) populations but not G2 cell populations when compared with parent cells (Figures 4B and C). These findings were especially evident following serial SP cell propagation (SP(3); Figures 4B and C).

SCC-SP cells exhibit stem cell-like characteristics *in vivo*

To test for *in vivo* tumorigenic potential, we compared the tumour formation capacity of H357 SCC-SP and non-SP cells. We subcutaneously injected two million SP(1) cells ($n=6$) or two million G2(1) H357 cells ($n=6$) into the flank of NOD/SCID mice and allowed these to grow for 49 days. In accordance with previous attempts to grow H357 cells in an *in vivo* model (Jones *et al*, 1996; Janes and Watt, 2004), none of the G2(1) cell grafts produced tumours (Figures 5A and B). Interestingly, three out of six SCC-SP-sorted and -engrafted cell populations did produce subcutaneous tumours with an average volume of 0.038 cm^3 (Figures 5A and B). Human SCC cell contribution to tumours and active cell proliferation were confirmed by H&E and Ki67 staining (Figures 5C and D). To our knowledge, this is the first demonstration of the ability of an H357 cell population to produce tumours *in vivo*, strongly suggesting that our SCC-SP contains a unique population of cancer stem-like cells.

Stem-like SCC-SP cells are chemotherapeutic resistant but sensitised by verapamil

Our observation that SCC-SP cells expressed both ABCG2 and ABCC1 multidrug transporters and exhibited elevated Hoechst 33342 efflux indicated that these cells likely possessed resistance to cytotoxic chemotherapeutic drugs including mitoxantrone. To assess SCC-SP and parent cell mitoxantrone sensitivity, 200 cells were cultured in the presence of 0, 1, and 10 ng ml^{-1} mitoxantrone for 3 days followed by 14 days culture in mitoxantrone-free media. Results indicated that both SP(1) and SP(3) were significantly more resistant to 10 ng ml^{-1} mitoxantrone treatment and capable of maintaining large colony formation in comparison with parent cells (Figure 6A). All cells appeared resistant to 1 ng ml^{-1} mitoxantrone in agreement with previous ABC transporter expression data (Figure 3A).

To investigate whether the addition of ABC-dependent transport inhibitors might block mitoxantrone resistance and restore chemotherapeutic sensitivity, parent and SP(3) cells were cultured at clonal density in the presence of 1 ng ml^{-1} mitoxantrone alone or in combination with verapamil for 7 days followed by 7 days in the absence of both drugs. We found that both parent and SP(3) cells that previously exhibited full resistance to 1 ng ml^{-1} mitoxantrone were dramatically growth inhibited following verapamil treatment (Figures 6B and C). These data suggest that verapamil-dependent ABC transporter inhibition blocks efficient SCC-SP mitoxantrone efflux, thereby restoring chemotherapeutic drug sensitivity to this previously resistant and aggressive tumour stem cell-like population.

DISCUSSION

The present study is the first to identify a Hoechst 33342 effluxing cell SP in several SCC cell lines that exhibits properties consistent with cancer stem or stem-like cells. The abundance of this SCC-SP varied between different SCC cell lines, and appeared highly dependent on both cellular density and proliferation status. As expected, SCC-SP cells expressed several previously characterised multidrug effluxing ABC-type transporters and were resistant to the chemotherapeutic agent mitoxantrone. SCC-SP cells also expressed elevated levels of the epithelial stem cell genes MCSP and TSLC1 relative to parent H357 cells. Importantly, we demonstrated that SCC-SP cells may be chemosensitised following the inclusion of ABC transport inhibitors. This finding may suggest novel approaches to cancer treatment, which could include the specific targeting of cancer stem cells.

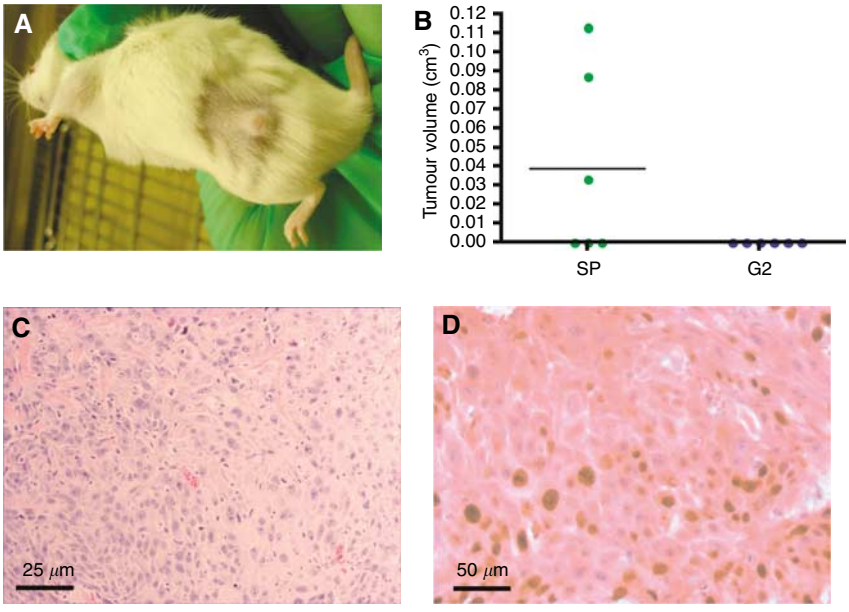

Figure 5 Squamous cell carcinomas containing SP cells are tumorigenic *in vivo*. (**A**, **B**) Three out of six NOD/SCID mice grew subcutaneous tumours following injection of two million SCC-SP(1) cells compared with no SCC G2(1) cell-derived tumours ($n=6$). (**C**) H&E confirmed SCC and (**D**) Ki67 staining demonstrated high cell proliferation.

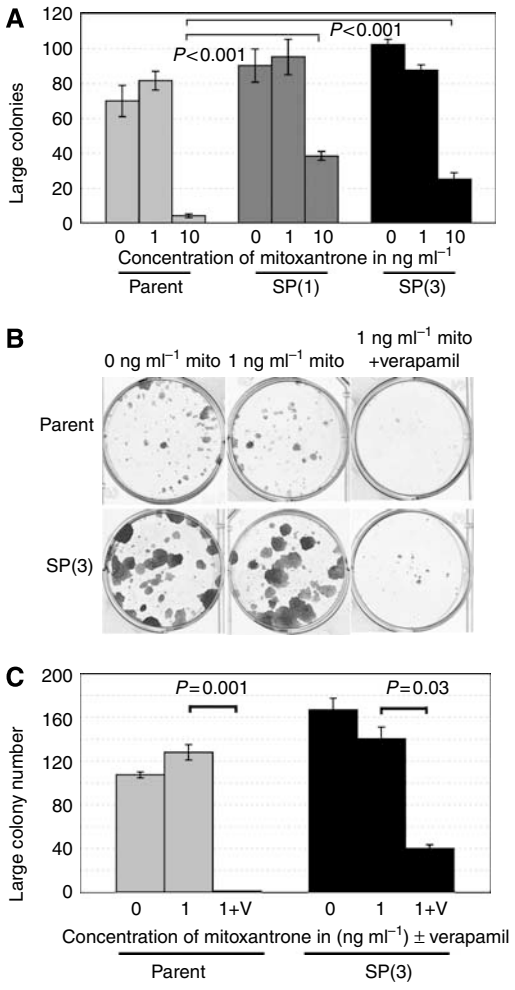

Figure 6 Side population cells have an increased level of resistance to mitoxantrone but are sensitised by concurrent ABC transporter blockade. (**A**) Analysis of stem cell colony numbers in clonogenicity assays of parent, SP(1), and SP(3) cells in the absence or presence of mitoxantrone at 1 or 10 ng ml^{-1}. Cells were grown in the drug for 3 days and grown for a further 14 days in the absence of the drug before analysis. Assays were performed in triplicate. Error bars indicate s.e.m. (**B**) Parental and SP(3) cells were grown in 0 or 1 ng ml^{-1} mitoxantrone ± verapamil for 7 days and, subsequently, grown for a further 7 days in the absence of drugs and clonogenicity analysed. (**C**) Quantitation of large colony numbers from (**B**). Assays were set up in triplicate. Error bars indicate s.e.m.

Our observation that SCC-SP abundance is cellular density or confluence dependent has not been previously described. This observation may partially explain differences reported between several laboratories studying SP cells and highlights the importance of considering cell confluence when examining SP cells *in vitro*. It is also possible that these cellular density effects might contribute to the relative 'stemness' of cancer cells contained within an *in vivo* tumour microenvironment. For example, infrequently proliferating cells within well-established tumours might be able to divert increased resources towards maintaining this chemoresistant or stem cell-like phenotype.

Previous studies of cancers *in vitro* and primary tumours *in vivo* have shown that SP cells are uniquely capable of generating both SP and non-SP cell fractions. This data have been used to suggest that SP cells are multipotent 'cancer stem cells' (Hirschmann-Jax *et al*, 2004; Kondo *et al*, 2004). In the current study, we find that serial SCC-SP cell propagation selects for cells that generate an increased SP cell abundance while maintaining multipotent differentiation. This is in contrast to non-SP (G2) cell populations, which could only produce secondary cultures similar to the original parental H357 cell line. We therefore believe that our SCC-SP cells uniquely represent a cancer stem or stem-like cell population.

In addition to stem cell-like properties in SCC-SP cells including multipotent differentiation and high *in vitro*/*in vivo* growth capacity, we have also now shown that SCC-SP stem cell-like cells are rendered chemosensitive using simple ABC transport inhibitors including verapamil and reserpine. This finding is significant, as it has recently been observed that many cancers maintain subpopulations of stem-like cells, which are chemotherapy insensitive and uniquely maintain tumour regrowth capabilities (Bonnet and Dick, 1997; Al-Hajj *et al*, 2003; Passegue *et al*, 2003; Hirschmann-Jax *et al*, 2004; Singh *et al*, 2004; Patrawala *et al*, 2006). Thus, it is increasingly important that cancer treatments target and eradicate putative cancer stem cells to halt clinical tumour recurrence. Intriguingly, early combinatorial therapy experiments demonstrated an effective synergistic therapeutic effect using verapamil plus mitoxantrone administration in the treatment of ovarian cancer (Tsuruo *et al*, 1985; Hendrick *et al*, 1991). Whether or not this *in vivo* chemosensitisation occurred via similar mechanisms to those described in our current study is not known, although clearly these findings highlight the need for more research into this potentially combined therapy.

ACKNOWLEDGEMENTS

We thank YC Gary Lee for his advice with statistical analysis. This work was started at the Cancer Research UK London Research Institute in the laboratory of Fiona Watt. None of the authors has any financial relationship with any commercial entity that has any interest in the subject of this paper. MRL is an MRC clinical training fellow. AG is the recipient of a Marshall Sherfield Fellowship and NIH fellowship. SMJ is an MRC clinician scientist. This work was partly undertaken at UCLH/UCL, which received a proportion of funding from the Department of Health's NIHR Biomedical Research Centres funding scheme.

REFERENCES

Al-Hajj M, Wicha MS, Benito-Hernandez A, Morrison SJ, Clarke MF (2003) Prospective identification of tumorigenic breast cancer cells. *Proc Natl Acad Sci USA* **100:** 3983 – 3988

Bonnet D, Dick JE (1997) Human acute myeloid leukemia is organized as a hierarchy that originates from a primitive hematopoietic cell. *Nat Med* **3:** 730 – 737

Giangreco A, Groot KR, Janes SM (2006) Lung cancer and lung stem cells: strange bedfellows? *Am J Respir Crit Care Med* **175:** 547 – 553

Giangreco A, Reynolds SD, Stripp BR (2002) Terminal bronchioles harbor a unique airway stem cell population that localizes to the bronchoalveolar duct junction. *Am J Pathol* **161:** 173 – 182

Giangreco A, Shen H, Reynolds SD, Stripp BR (2003) Molecular phenotype of airway side population cells. *Am J Physiol Lung Cell Mol Physiol* **8:** 8

Goodell MA, Brose K, Paradis G, Conner AS, Mulligan RC (1996) Isolation and functional properties of murine hematopoietic stem cells that are replicating *in vivo*. *J Exp Med* **183:** 1797 – 1806

Goodell MA, Rosenzweig M, Kim H, Marks DF, DeMaria M, Paradis G, Grupp SA, Sieff CA, Mulligan RC, Johnson RP (1997) Dye efflux studies suggest that hematopoietic stem cells expressing low or undetectable levels of CD34 antigen exist in multiple species. *Nat Med* **3:** 1337 – 1345

Griffiths MJ, Bonnet D, Janes SM (2005) Stem cells of the alveolar epithelium. *Lancet* **366:** 249 – 260

Hadnagy A, Gaboury L, Beaulieu R, Balicki D (2006) SP analysis may be used to identify cancer stem cell populations. *Exp Cell Res* **312:** 3701 – 3710

Hendrick AM, Harris AL, Cantwell BM (1991) Verapamil with mitoxantrone for advanced ovarian cancer: a negative phase II trial. *Ann Oncol* **2:** 71 – 72

Hirschmann-Jax C, Foster AE, Wulf GG, Nuchtern JG, Jax TW, Gobel U, Goodell MA, Brenner MK (2004) A distinct 'side population' of cells with high drug efflux capacity in human tumor cells. *Proc Natl Acad Sci USA* **101:** 14228 – 14233

Janes SM, Lowell S, Hutter C (2002) Epidermal stem cells. *J Pathol* **197:** 479 – 491

Janes SM, Watt FM (2004) Switch from {alpha}v{beta}5 to {alpha}v{beta}6 integrin expression protects squamous cell carcinomas from anoikis. *J Cell Biol* **166:** 419 – 431

Jones J, Sugiyama M, Speight PM, Watt FM (1996) Restoration of alpha v beta 5 integrin expression in neoplastic keratinocytes results in increased capacity for terminal differentiation and suppression of anchorage-independent growth. *Oncogene* **12:** 119 – 126

Jones PH, Watt FM (1993) Separation of human epidermal stem cells from transit amplifying cells on the basis of differences in integrin function and expression. *Cell* **73:** 713 – 724

Kondo T, Setoguchi T, Taga T (2004) Persistence of a small subpopulation of cancer stem-like cells in the C6 glioma cell line. *Proc Natl Acad Sci USA* **101:** 781 – 786

Lechner A, Leech CA, Abraham EJ, Nolan AL, Habener JF (2002) Nestin-positive progenitor cells derived from adult human pancreatic islets of Langerhans contain side population (SP) cells defined by expression of the ABCG2 (BCRP1) ATP-binding cassette transporter. *Biochem Biophys Res Commun* **293:** 670 – 674

Legg J, Jensen UB, Broad S, Leigh I, Watt FM (2003) Role of melanoma chondroitin sulphate proteoglycan in patterning stem cells in human interfollicular epidermis. *Development* **130:** 6049 – 6063

Liu Y, Lyle S, Yang Z, Cotsarelis G (2003) Keratin 15 promoter targets putative epithelial stem cells in the hair follicle bulge. *J Invest Dermatol* **121:** 963 – 968

Morris RJ, Liu Y, Marles L, Yang Z, Trempus C, Li S, Lin JS, Sawicki JA, Cotsarelis G (2004) Capturing and profiling adult hair follicle stem cells. *Nat Biotechnol* **22:** 411 – 417

Oyama T, Nagai T, Wada H, Naito AT, Matsuura K, Iwanaga K, Takahashi T, Goto M, Mikami Y, Yasuda N, Akazawa H, Uezumi A, Takeda S, Komuro I (2007) Cardiac side population cells have a potential to migrate and differentiate into cardiomyocytes *in vitro* and *in vivo*. *J Cell Biol* **176:** 329 – 341

Passegue E, Jamieson CH, Ailles LE, Weissman IL (2003) Normal and leukemic hematopoiesis: are leukemias a stem cell disorder or a reacquisition of stem cell characteristics? *Proc Natl Acad Sci USA* **100:** 11842 – 11849

Patrawala L, Calhoun T, Schneider-Broussard R, Li H, Bhatia B, Tang S, Reilly JG, Chandra D, Zhou J, Claypool K, Coghlan L, Tang DG (2006) Highly purified CD44+ prostate cancer cells from xenograft human tumors are enriched in tumorigenic and metastatic progenitor cells. *Oncogene* **25:** 1696 – 1708

Reya T, Duncan AW, Ailles L, Domen J, Scherer DC, Willert K, Hintz L, Nusse R, Weissman IL (2003) A role for Wnt signalling in self-renewal of haematopoietic stem cells. *Nature* **423:** 409 – 414

Scharenberg CW, Harkey MA, Torok-Storb B (2002) The ABCG2 transporter is an efficient Hoechst 33342 efflux pump and is preferentially expressed by immature human hematopoietic progenitors. *Blood* **99:** 507 – 512

Singh SK, Hawkins C, Clarke ID, Squire JA, Bayani J, Hide T, Henkelman RM, Cusimano MD, Dirks PB (2004) Identification of human brain tumour initiating cells. *Nature* **432:** 396 – 401

Sugiyama M, Speight PM, Prime SS, Watt FM (1993) Comparison of integrin expression and terminal differentiation capacity in cell lines derived from oral squamous cell carcinomas. *Carcinogenesis* **14:** 2171 – 2176

Summer R, Kotton DN, Sun X, Ma B, Fitzsimmons K, Fine A (2003) Side population cells and Bcrp1 expression in lung. *Am J Physiol Lung Cell Mol Physiol* **285:** L97 – L104

Tsuruo T, Kawabata H, Nagumo N, Iida H, Kitatani Y, Tsukagoshi S, Sakurai Y (1985) Potentiation of antitumor agents by calcium channel blockers with special reference to cross-resistance patterns. *Cancer Chemother Pharmacol* **15:** 16 – 19

Tumbar T, Guasch G, Greco V, Blanpain C, Lowry WE, Rendl M, Fuchs E (2004) Defining the epithelial stem cell niche in skin. *Science* **303:** 359 – 363

Watt FM, Hogan BL (2000) Out of Eden: stem cells and their niches. *Science* **287:** 1427 – 1430

Wulf GG, Wang RY, Kuehnle I, Weidner D, Marini F, Brenner MK, Andreeff M, Goodell MA (2001) A leukemic stem cell with intrinsic drug efflux capacity in acute myeloid leukemia. *Blood* **98:** 1166 – 1173

Zhou S, Morris JJ, Barnes Y, Lan L, Schuetz JD, Sorrentino BP (2002) Bcrp1 gene expression is required for normal numbers of side population stem cells in mice, and confers relative protection to mitoxantrone in hematopoietic cells *in vivo*. *Proc Natl Acad Sci USA* **99:** 12339 – 12344

Zhou S, Schuetz JD, Bunting KD, Colapietro AM, Sampath J, Morris JJ, Lagutina I, Grosveld GC, Osawa M, Nakauchi H, Sorrentino BP (2001) The ABC transporter Bcrp1/ABCG2 is expressed in a wide variety of stem cells and is a molecular determinant of the side-population phenotype. *Nat Med* **7:** 1028 – 1034